Additive Manufacturing: Multi Material Processing and Part Quality Control

Pedersen, David Bue

Publication date:
2013

Document Version
Publisher's PDF, also known as Version of record

PhD dissertation

Additive Manufacturing

Multi Material Processing and Part Quality Control

Author
David Bue Pedersen

Committee
Assoc. Professor
Torben Anker Lenau

Research Engineer
Jan Lasson Andreasen

Assoc. Professor
Enrico Savio

For fulfillment of the degree
Doctor Philosophiæ

November 2012

Dept. of Mechanical Engineering
The Technical University of Denmark

To my Mother and Father

Acknowledgement

I owe thanks to Professor Hans Nørgaard Hansen, my supervisor and head of section, formally for being my daily mentor. More important to me, I would like to warmly and informally thank Hans for always having believed in me. Always entrusted me to follow my intuition. Dear Hans. You have given me the room to explore the paths that have lured off the trail and towards exiting academic adventures. I want to thank you for reinforcing me in the choices I have taken, and the decisions that I have made. Even when you knew that my brilliant ideas was not as bright as I thought them to be.

My thanks goes to Professor Leonardo De Chiffre. You as my supervisor, have given me room to explore my own ideas. You have had faith in that I possess the ability to work independently, and you have but reinforced me in my strives.

Thank you Jakob Skov Nielsen. We have always been academic sparring partners, sharing ideas and knowledge. Today, you have become a personal friend of mine. Thank you not least for all the lunches (burgers) we have shared.

Thank you Finn Paaske Christensen. You are the senior of our department. I write this with the most loving intent. You have been there to always sermon classical virtues of traditional Mechanical Engineering. Your never diminished appetite toward new technologies has inspired me. You have also learned me a few indecencies, that an aspiring scientist such as myself have never heard before.

A warm thanks to all my students that I have supervised. Thank you Anders Ravn Jørgensen, Christian Deverell Pedersen, Daniel Vestergaard Nielsen, Greta D'Angelo, Henrik Juul Spietz, Jannik Dipo Knudsen, Jes William Hickman, Kristine Munk Jespersen, Marta Perez,Paw Møller, Rune Garbers Born, Simon Bjørn Thordal, Simon Rabbe, Thomas Lind Madsen, Tobias Maduro Nørbo and Troels Nandrup-Bus

A special thanks goes to: Aminul, Arne, Ask, Claus, Fabio, Fan, Finn, Giovanna, Giuliano, Greta, Guido, Jakob, Jan, Kenneth, Linn, Matteo, Michaela, Nikolaj, Pia, Rene, Stefania, Simone, Ugo, Ulrik, Vivi-Ann and Yang

Abstract

English

This Ph.D dissertation, ⌜*Additive Manufacturing: Multi Material Processing and Part Quality Control*⌟, deal with Additive Manufacturing technologies which is a common name for a series of processes that are recognized by being computer controlled, highly automated, and manufacture objects by a layered deposition of material. Two areas of particular interest is addressed. They are rooted in two very different areas, yet is intended to fuel the same goal. To help Additive Manufacturing technologies one step closer to becoming the autonomous, digital manufacturing method of tomorrow.

Vision systems

A paradox exist in the field of Additive Manufacturing. The technologies allow for close-to unrestrained and integral geometrical freedom. Almost any geometry can be manufactured fast, efficiently and cheap. Something that has been missing fundamental capability since the entering of the industrial age. Now, with the geometrical freedom given back to the designer and engineer, a technology stale-mate keep us from benefitting from this freedom. Parts can easily be designed and manufactured beyond the capabilities of all common industrial measurement and verification methods, the designer and engineer is left to design parts that from a geometric metrology point of are view possible to verify the tolerances of. A proposal of a method for altering the stale-mate to a check-mate is given. An inline vision system is developed that allow for verification of parts of a complexity that leave the only industrial alternative to the field of CT scanning. The background knowledge to develop such system is synthesized from an analysis of existing additive manufacturing processes and vision systems. The system is implemented and benchmarked throughout the scope of this Ph.D dissertation.

The proposed inline vision system has been put through several tests against sev- eral additive manufacturing systems. Till now the system has proven to be up to the task of reconstructing geometries otherwise only possible by CT scanning. The system outcompeted a reference CT scan of a large metal part by to an indisputable degree. The system finally showed promising results when applied indirectly to reconstruct geometries from a DLP system. In general, the system has a potential for being implemented in different AM machines and processes and provides traceable measurements of the complex parts. As the technology of inline layered reconstruction of

additively manufactured parts has just been proposed within this thesis, the technology is at a dawning level, and there is an abundance of open questions to be answered and much yet to be investigated. It is impossible but leaving this part of the project open-ended. What is to hope is that future research will tie these ends with the emerge of a fully developed system.

Additive Multi Material Manufacturing

Additive Manufacturing share close family bonds with CNC machine tools. State-of-the-art CNC machine tools of today are multi-axis hybrid machines. A bend of lathes, mills, grinders in one platform. If history repeat itself, hybrid additive manufacturing machines will emerge as the field evolve. It is sought to fuel this, by developing a flexible multi material manufacturing platform that will permit fundamental research towards a second generation additive manufacturing system that truly will be a universally applicable manufacturing machine. A desktop sized factory. Not merely the development of such machine is undertaken, also examined is the possibility to additively manufacture complex electromechanical systems, as a step towards being able to autonomously additively manufacture readily functional complex products. Based upon a synthesis of the applicability for each industrially accepted additive manufacturing process, the platform deemed most suitable was selected. The result was an Open and fully customizable FDM based multi material platform. The design solicit flexibility and the ability to alter the platform to conform to a multitude of experiments involving multi-material extrusion. The resultant platform is also able to reproduce itself and as such future generations of the platform can efficiently be iterated through. Two generations of this platform was realized within the scope of this project.

To empathize why, and how versatile the prospect of multi-material platforms is, a set of subsystems that can be realized by multi-material manufacturing using FDM extrusion has been conceived. A functional battery is built using multi material extrusion. Composites that allow for the additive manufacturing of electrical conductors and resistors are engineered. A proposed method for additive manufacturing of linear actuators is assessed and proved promising. It is proposed that a library of additively manufacturable subsystems are built as a part of a knowledge sharing network. This systems library can over time grow to an extend where it is applied in the same manner as traditional engineering elements such as ball bearings, nuts, screws, washers, guide-rails, wires, batteries, electrical components and their like are used today.

Dansk

Denne Ph.D afhandling, ⌜*Additive Manufacturing: Multi Material Processing and Part Quality Control*⌟, omhandler additive fremstillingsmetoder, hvilket er en familie af processer der er kendetegnet ved at de er computerstyret, de drager nytte af en høj grad af automation, og de fremstiller emner lagvis ved addition af materiale. To områder af særlig interesse er addreseret i denne afhandling. De er begge forankret i to meget forskellige områder, men tjener fælles formål. At styrke additive fremstillingsteknologier, og føre dem et skridt tættere på at blive morgendagens autonome digitale fremstillingsmetode.

Vision systemer

Der eksisterer et paradox blandt de addtive fremstillingsmetoder. Teknologierne giver tilnærmelsesvis ubegrænset geometrisk frihed. Kan en geometri visualiseres, kan den fremstilles. Denne mulighed har ikke eksisteret siden før den industrielle revolution. Nu, med muligheden tilbage til designeren, bliver han forhindret i at anvende den nyvundne frihed på grund af en teknologisk stopklods: Geometrisk kontrolmåling. Det er muligt at fremstille emner der er så komplekse at de mest udbredte og tilgængelige målemetoder ikke kan håndtere kontrolmåling. Der forslåes en ny metode til at løse denne problemstilling. Et vision system overvågende den lagdelte fremstillingsproces der muliggør verifikation af emner der er så geometrisk komplekse at kun industriel CT scanning er et reelt alternativ. Udfra en syntese af de industrielt anvendte additive fremstillingsprocesser og industrielt tilgængelige måleteknikker, dannes rammerne for udviklingen af et fleksiblet og portabelt vision system.

Vision systemet udsættes for en række forsøg hvor dets egenskaber til korrekt at inspicere, opmåle og geometri-gendanne emner der fremstilles på flere forskellige type additive fremstillingsmaskiner. Systemet testes i et scenarie op mod en industriel CT scanner, og det viste sig at vision systemet producerede en mere korrekt gengivelse end CT scanneren. Et sådant resultat spår lovende for inline overvågning og opmåling af emner fremstillet på additive fremstillingsmaskiner.

Additiv Multi Materiale Fremstilling

Additiv Fremstilling deler familiebånd med CNC bearbejdnngsmaskiner. Moderne CNC bearbejdningscentre er multi-akesede hybrid maskiner der tillader

en lang række bearbejdningsprocedurer såsom fræsning, drejning og slibning i éen og samme enhed. Idet der er et nært bånd mellem additiv fremstilling og CNC bearbejdning, spåes det at historien vil gentage sig selv, og at fremtidens additive fremstillingsmaskiner vil udvikle sig til at blive hybrider. Denne evolusion ønskes styrket ved udviklingen af en multi-materiale platform. En syntese over industrielt udbredte additive fremstillingsmetoder viser hvor egnede de forskellige processer er til at håndtere en bred palette af materialer. Udfra denne syntese, besluttes det at multi materiale platformen skal basere sig på det princip der hedder FDM. Resultatet af udviklingsforløbet blev en fleksibel, parametrisk og let opgraderet platform der udvikledes i to generationer.

For at fremhæve styrken ved additiv multi materiale fremstilling, drages en parallel til nutidens standard-elementer. De komponenter som produktionsvirksomheder har outsourcet produktionen af, såsom kuglelejer, skruer, møtrikker, skiver og linære føringer. Det foreslåes at et digitalt system-bibliotek danner rammerne for en udvikling af standard-systemer der kan realiseres ved multi materiale fremstilling. Således anvendes den additive multi materiale platform til fremstilling af at funktionelt batteri, elektriske lederbaner og elektriske modstande. Endeligt foreslåes og valideres en metode for additivt at femstille lineære aktuatorer. Såfremt det forslåede digitale system-bibliotek kommer til verden, vil det i fremtiden være muligt, direkte fra CAD designværktøjer, at plukke standardstystemer til den designopgave der arbejdes på.

To the reader

Dear reader. This dissertation contains the written tale of my efforts during my studies in the field of Additive Manufacturing. My studies has been made possible by the Ph.D programme at the Technical University of Denmark and was carried out at the Department of Mechanical Engineering from the 1'st of november 2009 to the 31'st of september 2012. My research topic, Additive Manufacturing, is a branch of technologies that in the popular press has been labelled 3D printing. A branch of technologies which amongst experts is seen as a propellant for technology into the next era of industrialization. For the last three years I have enthusiastically been engulfed into these technologies, and been thrilled by the opportunity to research in such a fast-paced and technologically advanced field. I have on occasion from my concerned Mother and Father been pledged to take care and not to cave in. A concern to which I have answered in self realization, that what I do is not something that I look upon as tedious work, but something that I have embraced as a lifestyle. The life of the scientist. I hope that when you read my dissertation, you will feel this enthusiasm though my written word, and I hope that you will find the reading experience as joyous as I have enjoyed to write down my tale of science. The dissertation is flavored by the two topics of my research. Two noticeably different topics that both share one common goal. To enforce the Additive Manufacturing technologies so that these become even stronger competitors in the field of manufacturing engineering. I have taken great care to structure my dissertation, with which I hope you will not relate my words to the ciphered codex of the Voynich Manuscript[1]. A structure that I hope will leave you with a thorough understanding of what I have undertaken during the last three years. When I embarked out on my postgrad journey towards becoming a Doctor Philosophiæ, I had the privilege with my advisor to formulate the very framework of this research project. For that I am very obliged. I believe it is reflected by my excitement to my field of research, and I hope that you upon reading my dissertation will have understood why I find Additive Manufacturing such an interesting field. It is for me a palette of technologies that turn Science Fiction into Science Fact.

David Bue Pedersen
November 2012

Contents

List of Figures

Introduction

Background

Vision Systems

Vision Based Reconstruction

Multi Material Additive Manufacturing

Multi Material Platform Design

Systems for Additive Multi Material Manufacturing

List of Tables

Background

Vision Systems

Multi Material Additive Manufacturing

Multi Material Platform Design

Systems for Additive Multi Material Manufacturing

Symbols and Abbreviations

Background

Abbreviations

ABS Acrylonitrile Butadiene Styrene, page 39

CAD Computer Aided Design, page 29

CAT Computer Aided Tomography, page 62

CGI Computer Generated Imagery, page 30

CMM Coordinate Measuring Machine, page 62

CNC Computer Numerical Control, page 29

CT Computerized Tomography, page 62

DLP Direct Light Projection, page 37

HDPE High Density Poly Ethylene, page 47

LOM Laminated Object Manufacturing, page 37

MEMS Micro Electromechanical system , page 53

NC Numerical Control, page 29

PA-12 Poly Amide - 12, page 47

PC Poly Carbonate, page 39

PEEK PolyEtherEtherKetone, page 47

PLA Polylactic Acid, page 39

POM Poly Oxy Methylene, page 47

PS Poly Styrene, page 47

SLA Stereo Lithography, page 37

SLM Selective Laser Melting, page 37

SLS Selective Laser Sintering, page 37

T_g Glass Transition Temperature, page 57

UV Ultra Violet, page 60

Symbols

A CAT/CT scan slice system matrix, page 70

b CAT/CT scan slice raw data, page 70

b_i Total attenuation of X-rays passing through a sample, page 68

C Centre of a circle in 3D space, page 31

$E_{1-2,..,2-3}$ Face edges, page 32

F_n Facet n, page 32

I_0 X-ray intensity before passing through a sample, page 68

I_i X-ray intensity after passing through a sample, page 68

M The number of X-ray measurements within a scan slice, page 70

n_F Face normal, page 32

P Points on the boundary of a circle in 3D space, page 31

r Radius of a circle, page 31

u, v Orthonormal vectors in a 3D space, page 31

V_{1-3} Face vertices, page 32

x x=X_{image}, page 70

X_{image} An NxN matrix of constant attenuation coefficient, discretizing a CAT/CT scan slice., page 70

Vision Systems

Abbreviations

DSLR Digital Singe Lens Reflex. - A type of digital camera with interchangeable lenses., page 77

Background Visible surrounds of the cross-section of part in the image plane, page 87

Foreground Visible cross-section of part in the image plane, page 87

Symbols

P A point cloud which is being evaluated for noise., page 95

$P_{i,j,k}$ A point in the point cloud P, which is presumed to be noise., page 95

·⁚A brief introduction to Additive Manufacturing. About the intent of this dissertation and about how the dissertation is structured. ⁚·

1 Introduction

Additive Manufacturing is a common name for a series of processes that are recognized by being computer controlled, highly automated, and manufacture objects by a layered deposition of material. Additive Manufacturing, a fairly new palette of manufacturing technologies have since 1989 had an annual growth rate of 32%. [2, p. 132] and is predicted to be one of the main driving forces towards an era of digital manufacturing. The palette of processes, in common tongue affectionately designated ⌜*3D printers*⌟, is regarded upon by many as science fiction turning science fact. Machines that to some extent already can an universally will be able to procure any object, any one thing that can be imagined. Today, readily finished products (restrained to one material) can be built directly on additive manufacturing equipment. Tissue Engineering using Additive Manufacturing allow organs and tissue to be Additively manufactured from the patients own living cells. ⌜*3D printers*⌟ in conjunction with a 3D scanner becomes a 3D photocopier Amazing is that geometries can be made by additive manufacturing to a complexity and level of detail so high, that not even highly advanced industrial measuring techniques can measure and verify the geometrical freedom given.

1.1 Statement of intent

With a field of technology in such rapid growth, there are many open ended questions awaiting to be answered, and many areas of the field to which research will fuel development and immediately impact the industry. Two areas of particular interest is addressed within the scope of this Ph.D dissertation. They are rooted in two very different areas, yet is intended to fuel the same goal. To help Additive Manufacturing technologies one step closer to becoming the autonomous, digital manufacturing method of tomorrow.

Due to the nature of the the research divided into two separate topics, the dissertation has been structured as such. Figure 1.1 show the structural composition of the report. A joint introduction and background chapter form the foundation for two separate discussions. The first is regarding geometric verification of very complex additively manufactured geometries by means of a novel vision system.

The last, is the a discussion of additive multi material manufacturing.

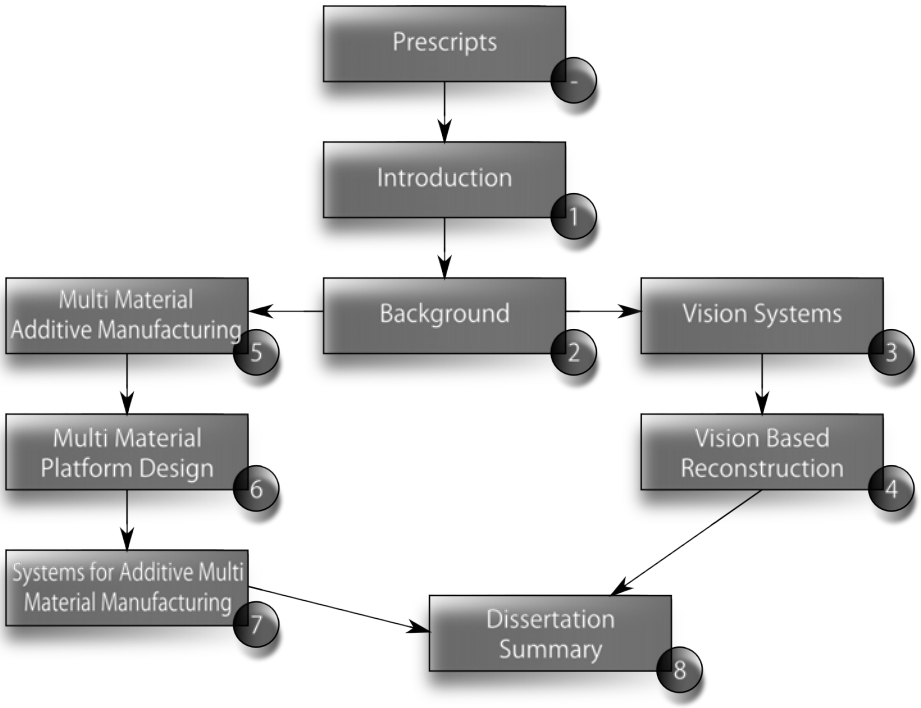

Figure 1.1: *Dissertation structure,* 1 *to* 8 *showing chapter index.*

Multi material manufacturing

It is sought to develop a flexible multi material manufacturing platform that will permit fundamental research towards a second generation additive manufacturing system that truly will be a universally applicable manufacturing machine. A desk-top sized factory. Not merely the development of such machine is undertaken, also examined is the possibility to additively manufacture complex electromechanical systems, as a step towards being able to autonomously additively manufacture readily functional complex products.

Geometric verification of very complex additively manufactured geometers.

It is a paradox that Additive Manufacturing technologies allow for close-to unrestrained and integral geometrical freedom. Almost any geometry can be manufactured fast, efficiently and cheap. Something that has been missing fundamental capability since the entering of the industrial age. Now, with the geometrical freedom given back to the designer and engineer, a technology stale-mate keep us from

benefitting from this freedom. As parts easily can be designed and manufactured beyond the capabilities of all common industrial measurement and verification methods, the designer and engineer is left to design parts that from a geometric metrology point of view possible to verify the tolerances of. A proposal of a method for altering the stale-mate to a check-mate is given. An inline vision system is developed that allow for verification of parts of a complexity that leave the only industrial alternative to the field of CT scanning. The method is implemented and benchmarked throughout the scope of this Ph.D dissertation.

1.2 Problem definitions

The research has been highly interdisciplinary and an abstraction between said multi material manufacturing and vision system has been introduced throughout the three years of research and within this dissertation. As such, there are two distinct problem definitions. The dissertation is structured so that a common point of origin is set with a background chapter addressing the state-of-the-art of the additive manufacturing field as a whole. From the common origin, the dissertation split to two branches presented in serial. First is the development of the vision system which is introduced in chapter 3. A detailed motivation and problem definition is here given. After a conclusion to the numerical development the sequel is given. This is the testing of the vision system, addressed in chapter 4.

The second branch presented, directly follow the development of the vision system. Additive multi material manufacturing is synthesized and a problem definition of this branch is stated in chapter 5. The motivation for, and the considerations given to the design a flexible multi material platform is here given. Following the development of the multi material platform, is a closing chapter that address different additively manufacturable electromechanical and thermoelectromechanical systems that is regarded as possible to manufacture using the developed multi material platform.

⁘ A presentation of the family of Additive Manufacturing technologies, the information age as a driving force for intelligent processing and manufacturing. From Computer aided Design and Manufacturing to Verification and Control. ⁘

2 Background

Since entering the Industrial Age, a consistent effort has been put into optimizing a demanding industry-driven global society. Processing and Manufacturing has been two prevalent sectors that have been fueled by this effort throughout two centuries. Today, well intro the third Industrial Revolution of equal impact, the Information Age, Manufacturing Engineering boast a high level of process automation by employing Computer Aided Design (CAD), process simulation, and Numerical Control (NC) schemes for material processing.

2.1 Numerical Control

Numerical Control is a term describing machine tools instituted as automatons. Design of the first NC machine tool was initiated by the Massachusetts Institute of Technology in July 1949.[3] The development project was known as ⌜*The development of a system applicable to machine tools for controlling the position of shafts in accordance with output of a computing machine*⌟ and the first complete automatic control system for a three-axis milling machine was assembled during 1952. Due to the then high cost of computers, special, dedicated punch-card based machines was used to interpret numerical commands to physical movement of axis. No later than 1959 does NC meet CAD. This happens with the development of one of the earliest CAD systems called DAC-1, for ⌜*Design Augmented by Computer*⌟[4]. Released in 1963 DAC-1 form the foundation for the growth and prosperity of the Computer Numerical Control Systems (CNC) that today have outcompeted manually operated machine tools used for production.

2.2 Describing Geometrical Shapes

Numerous methods for describing three-dimensional geometrical shapes exist. From classical isometric methods employing sectional two-dimensional drawings, over textured wireframe meshes to Engineering CAD software. Wireframe meshes are

widely used in Computer Animation and can be sculpted as a virtual clay in Computer Generated Imagery (CGI) software. Engineering CAD software employes underlaying mathematical and physical models to describe a geometrical shape, and it's corresponding mechanical and physical properties.[5][6]

2.2.1 Isometric and 2D Orthographic Projection

Classical engineering employ a two dimensional Orthographic Projection often supported by an isometric 3D representation to describe three-dimensional structures. A method that is largely superseded by 3D CAD in mechanical engineering yet still has limited employment in the field of construction engineering, where floor plans are still created as two-dimensional CAD models.

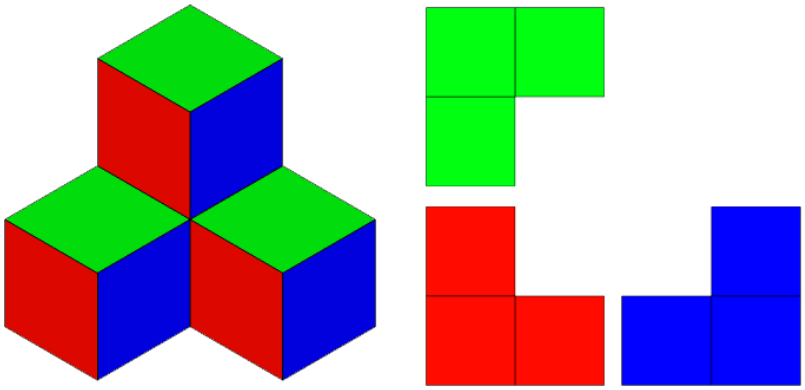

Figure 2.1: *Orthographic Projection (right) and Isometric Representation (left) of a 3D geometry*

Figure 2.1 illustrates how a three-dimensional shape can be Isometrically described as a three-dimensional sketch and by Orthographic Projection by three two-dimensional representations of the top, front and right hand side.[7] The Isometric and Orthographic method of describing geometrical shapes however fast and easy to employ, impose many limitations to the sketch artist. Intricate shapes quickly become impossible to precisely represent by isometric means. In classical construction engineering this has been solved by the architect providing the entrepreneur with additional shaded sketches of three dimensional structures such as ornaments, stucco and facade decorations. It was then up to the entrepreneur to appoint a sculpting artist which by means of creative skill would complete the physical product overlapping the grey-zones of limited geometrical information with the artists own interpretation of the sketch provided by the architect.

2.2.2 Computer Aided Three-Dimensional Representation

Three-dimensional representation of geometries has emerged thanks to CAD, as previously described in section 2.2 on page 29. Different approaches to CAD modeling exist. These governed by the following major distinguishable characteristics:

- Mathematically defined geometries
- Wireframe based geometries
- Solid feature geometries
- Freely defined geometries

Mathematically defined geometries

Mathematical defined geometries are geometries, where shapes are defined from exact mathematical descriptors. A circle as simple shape in Euclidean geometry can be defined in 3D space by the following.[8] Let u and v be two orthonormal vectors in the plane that is containing the circle that is to be described. Let the parameter t vary from 0 to $2 * \pi$ Points along the bound of the circle can be pointwise described; either as a vector equation or by it's components. The vectored equation will be:

$$P = C + r * cos(t) * u + r * sin(t) * v \tag{2.1}$$

The corresponding equation written out in its components will be:

$$\begin{aligned} P_x &= C_x + r * cos(t) * u_x + r * sin(t) * v_x \\ P_y &= C_y + r * cos(t) * u_y + r * sin(t) * v_y \\ P_z &= C_z + r * cos(t) * u_z + r * sin(t) * v_z \end{aligned} \tag{2.2}$$

where C is the centre of the circle in 3D space, P is the points on the boundary of the circle in 3D space and r is the radii of the circle. The main strength of approaching three dimensional representation based upon mathematics is that that there is no resolution based losses which will be the case for wireframe meshes. The closer the spectator approach the surface of a wireframe mesh, the coarser will the geometry appear, whereas the spectators viewpoint, matters nothing for a mathematically defined geometry.

Wireframe based geometries

Unlike Mathematically defined geometries, wireframe based geometries suffer from having a fixed resolution. This set a distinct limit to which extent operations such as rescaling can be applied to a geometry. Example rescaling features beyond the wireframe mesh resolution is futile. Wireframe based geometries however have certain strengths that validate their existence. (They play a key role as a file format used within the field of Additive Manufacturing, section 2.2.3)

Wireframe meshes are surfaces described intersecting by polygons.[9] Most polygon based formats use another Euclidean geometry as their base geometry for the individual faces of a surface. This being the triangle.

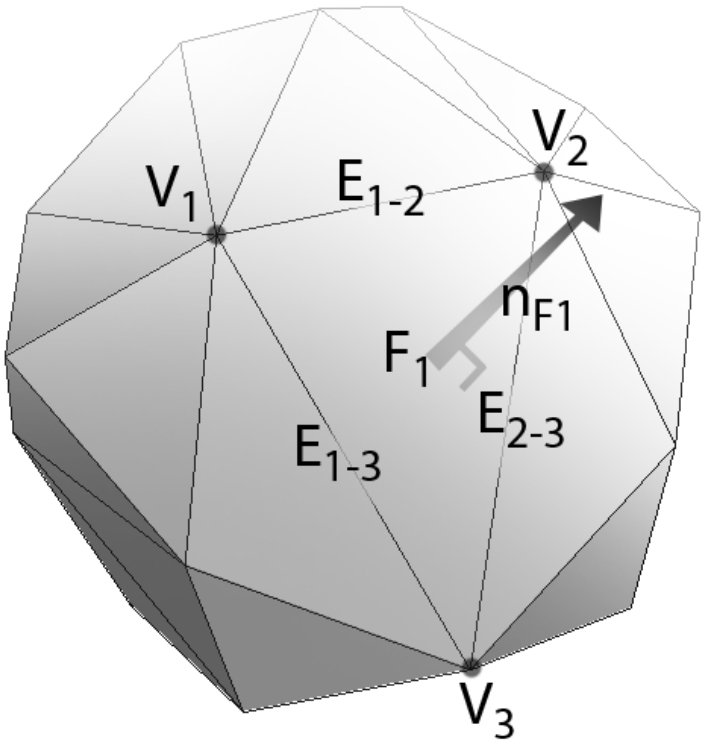

Figure 2.2: *Wireframe mesh of an icosidodecahedron. One face has been given labels*

In a triangulated mesh, each face is constructed by three edges that is described by three vertices. Each face has a normal vector describing which direction is outward. Several facets form a surface by sharing least one edge with a neighboring facet.[9] Figure 2.2 show a highlighted facet in the wireframe mesh of an icosidodecahedron. V_{1-3} enumerate the vertices of face F_1. E_{1-2} to E_{2-3} enumerate the face edges.

Most CAD and Computer Aided Manufacturing[1] suites require a geometry to be described by a non-manifold mesh. A manifold mesh is a mesh where there is at least one case of three or more faces sharing the same edge. Furthermore most CAD and CAM suites does not allow any faces to be self-intersecting with the mesh. This is the situation where the mesh collide with itself. When least two mesh elements intersect. Common for manifold and self-intersecting meshes are that neither mesh can describe an exclusive, finite surface. This will result in a failure trying to perform finite element analysis of such meshes, as well as cause unwanted artifacts in visualization front ends.

Solid feature geometries

Solid defined geometries are geometries consisting of closed surfaces forming hulls. These geometries are the most commonly used geometries in CAD for engineering applications. A complex part consist of several sub-geometries often referred to as features. Each feature, forming a closed hull is looked upon as a solid chunk of material This makes it possible to assign the entire geometry solid attributes such as density, and mechanical properties such as tensile strength. For describing solid feature geometries,[10] each feature is normally described as a mathematically defined feature as shown in section 2.2.2 on page 31.

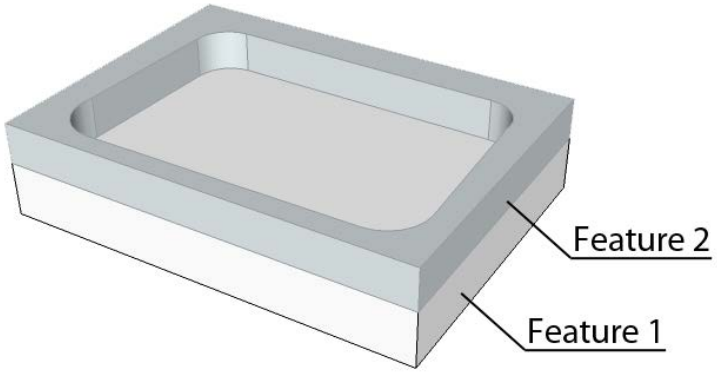

Figure 2.3: *A geometry consistent of two extruded mathematically defined features.*

Features can be manipulated individually affecting only locally the combined geometry. An illustration of this can be seen in figure 2.3. Feature operations such as cutouts, joining, and grouping is often implemented in commercial engineering CAD software.

Most engineering CAD software suites allow for assembling several geometries to a virtual model of a product. This virtual assembling allows the engineer to visualize the entire system that is being designed, and help as a tool to identify

[1] Abbreviated CAM

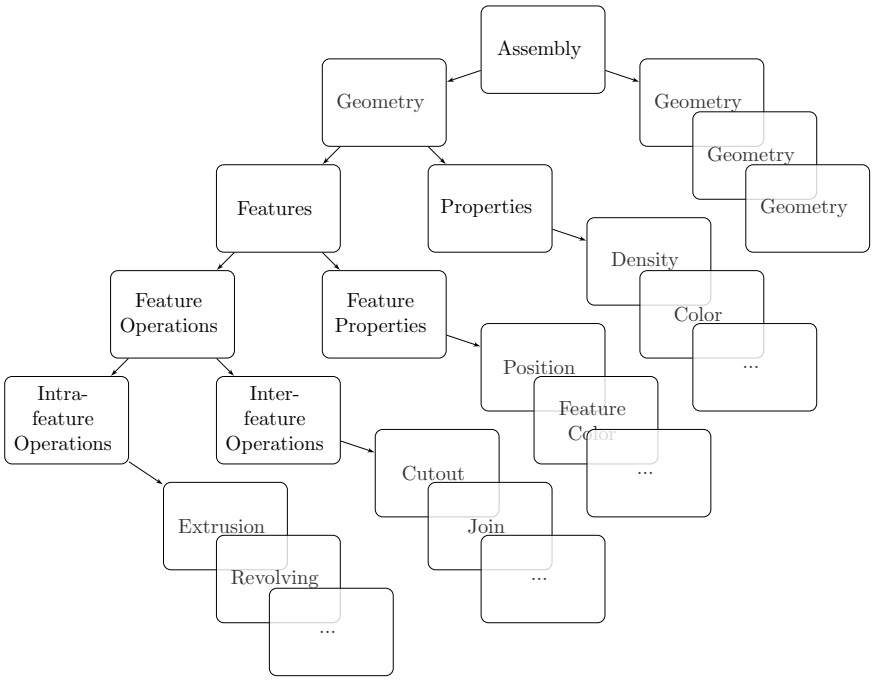

Figure 2.4: *Relation-tree of a CAD assembly.*

design errors as early as in the detailing process. There is therefor a relation-tree spanning from assembly, over geometries and features, till the inter- and infra-feature operations. The relation tree can be outlined as seen in figure 2.4.

Being a strong design tool in the field of engineering, modeling with solid feature geometries however impose limitations that makes complex three dimensional design a crippling task. Since every feature in a geometry beyond the graphical user interface[2] must be defined as a set of mathematical relations, free-form modeling is limited. Commercial engineering CAD softwares often foster an interactive modeler, a GUI allowing for the definition of operations the operations shown in the relation tree on figure 2.4 such as Extrusion and Revolving. 2.4

Other engineering CAD softwares are minimalistic and behaves as a renderer that compiles a script into a 3D geometry. OpenSCAD, as such is well known. This mimic the behavior of software compilers where a script such as C, C++ or fortran is compiled to an assembly. The minimalistic user interface is visible in figure 2.5 on the facing page

Freely defined geometries

Unlike defining geometries by means of mathematics, wireframe meshes allows for much more flexible modeling methods. The term freely defined geometries are

[2] Abbreviated GUI

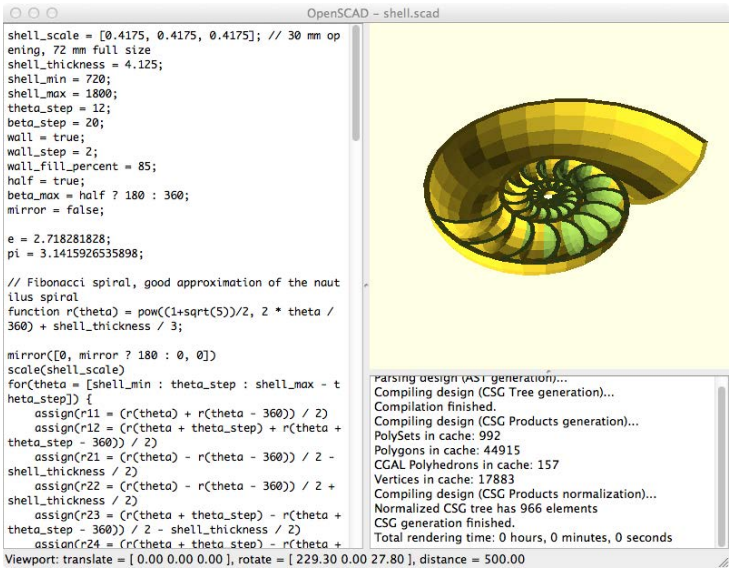

Figure 2.5: *OpenSCAD. A minimalistic mathematical CAD modeller*

geometries that can be modeled without the limiting factors that is imposed by feature-based modeling. It is a free-form modeling method where a wireframe mesh define either a surface or a hull which can be sculpted as virtual matter. The method allows for close-to unrestrained design-freedom where the wireframe mesh can be shaped in a manner similar to when an artist sculpt clay. The method is not bound by a feature-tree such as with feature-based modeling. 2.4 on the preceding page However, other limitations is imposed by the designer. Whereas feature-based modeling relies on underlaying mathematical definition of each shape that contribute to the geometry, free-form modeling of wireframe meshes loose its concise dimensioning related to a global coordinate system. Another limitation when modeling wireframe meshes is the mesh resolution. The number of faces that define the mesh is crucial to how detailed small features on a geometry can be. This is handled by having a non-uniform mesh resolution and by increasing the number of faces as the level of detail of the model is increased.

The workflow of creating a complex three-dimensional geometry that would be close-to impossible to model in an engineering CAD environment can be seen in figure 2.6 on the following page. The artist start with a simple cube defined by 8 faces (1). The mesh resolution is increased uniformly and the shape is sculpted by pushing and pulling the virtual matter into a geometry that very coarsely resemble the shape of a head (2). Again the mesh resolution is increased. (3) This time however the artist manually redefines the mesh. This to allow a non-uniform remeshing to occur so that an increased polygon-count is only available where needed. A uniform remeshing would put unnecessary memory and cpu load to the workstation computer. The remeshed geometry is once again sculpted to closer

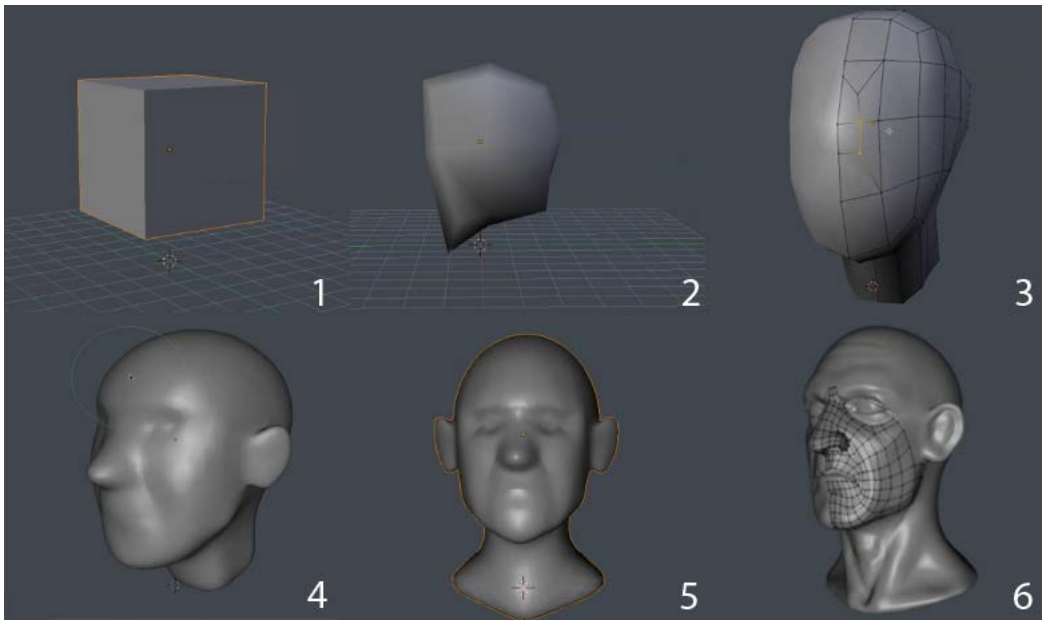

Figure 2.6: *Sculpting a wireframe mesh.*

resemble a human face (4). Another manual remeshing and sculpting iteration can be seen in (5). Finally the detailed sculpt of the head with its underlying mesh can be seen in (6). Working with wireframe meshes in this manner closely resemble how an artist factually work with clay. A mass of clay is shaped into a coarse head. More clay is added where needed to form details. This correspond to a manual remesh. Observing the artist work, he continues to locally add more and more detail. This by adding more and more clay, up till the sculpture is completed.

Direct wireframe mesh manipulation as a detailing tool in the world of mechanical engineering is limited. The methods described in this chapter however has their justification when working with reverse engineering. 3D scanning, CT/-CAT scanning and CMM probing create point clouds that can be meshed into wireframes. When either method is applied in the field of mechanical engineering, knowledge in wireframe mesh manipulation becomes crucial in processing and product development.

2.2.3 3D geometries in Additive Manufacturing.

The de-facto standard used in the field of Additive Manufacturing is a faceted file format, describing geometries as wireframe meshes comprised of triangles. The format is called .STL and is an abbreviation of Stereolithography, which is an additive manufacturing process developed by 3D systems. The stereolithography process and its origin is described in the impending sections.

Being a mesh-based format, the 3D representation of geometries in the .STL

format has a finite resolution and as such it is common practice to create geometries using engineering CAD software employing mathematically described geometries, whereby the STL file is exported from. This allow for the designer to export a geometry that meet the requirements set to the resolution by the tolerances of the manufactured part.

The American Society for Testing and Materials committee F42[11] has proposed to introduce a revised file-format standard within the field of additive manufacturing. The format, STL 2.0, is intended to be revised to suit state-of-the-art additive manufacturing technologies. It is proposed to be a format that aside geometry can describe other properties linked to the geometry. Amongst these are color textures in order to allow for additive manufacturing of color-textured structures. The STL 2.0 format however is not fully evolved as of year 2012, and the implications the introduction of this standard will have to the field of additive manufacturing is yet to be known.

2.3 Additive Manufacturing Processes

Additive Manufacturing technologies emerged under the anterior name, Rapid Prototyping. As of 2009 the ASTM international Standards Worldwide subcommittee F42.91[12] all layered, additive processing methods now fall under the category of Additive Manufacturing. The earliest technologies, Stereo Lithography (SLA) and Laminated Object Manufacturing (LOM) provided little more than prototypes that could be used as showpieces, having weak structural strength. LOM structures was manifested as paper models, and SLA structures was manifested in brittle acrylates, inferior to engineered thermopolymers.[13]. Today the Additive Manufacturing technologies has matured into a palette of technologies that yield structurally strong parts with high dimensional accuracy. Especially Selective Laser Melting (SLM) succeeding the Selective Laster Sintering (SLS) technology, as well as Stereo Lithography (SLA) and its derivative, Direct Light Projection (DLP) are processes suitable for producing parts of a quality that allow for the processes to be integrated in production chains. Noticeably is the hearing aid industry where SLA is employed to make custom-fit hearing aid shells and the medical industry employ interring for medical implants. [14]

Irrespective of the specific Additive Manufacturing processes it is noteworthy to point out that these processes are of a family sharing common process similarities. They are based upon adding material to a workpiece, starting from an empty build-surface. They are layered process methods. They are numerically controlled. Furthermore the various Additive Manufacturing processes share process relations.[2, Appendix C] These has been arranged in a schematic order, illustrated in figure 2.7 on the next page.

The palette of Additive Manufacturing technologies can be branched out in two major categories, related to how material is bonded to a structure. These

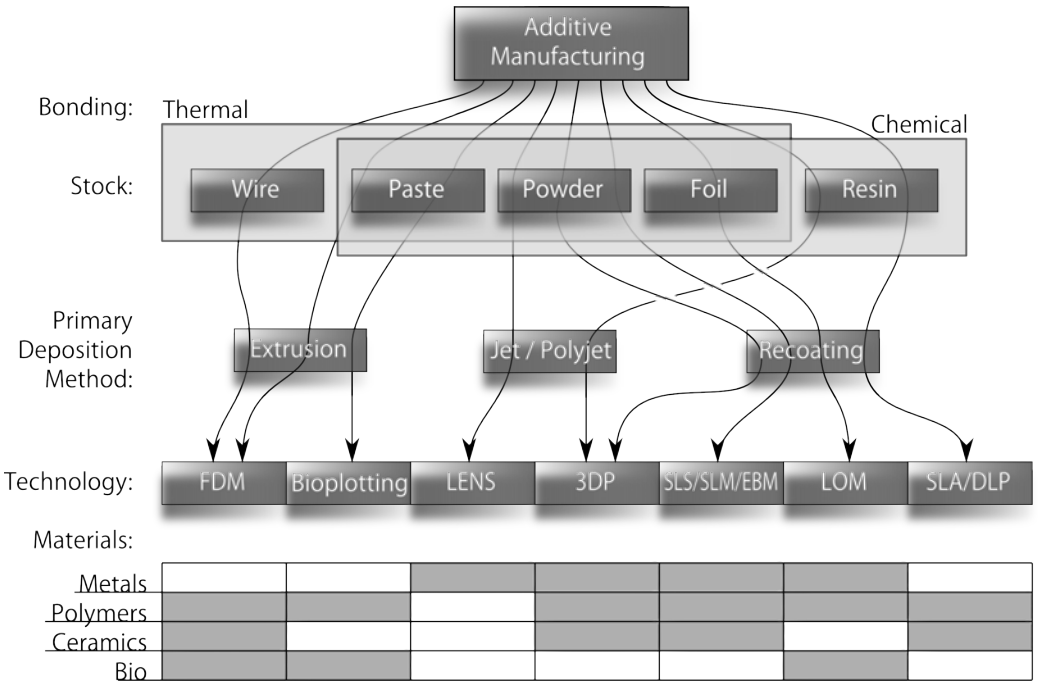

Figure 2.7: *Additive Manufacturing Process Branches*

two categories are Thermal and Chemical. Technologies falling into the thermal category use a thermal process to additively form structures, whereas technologies falling into the chemical technology use a chemical reaction to additively form structures. Five main categories of stock or feed material is used within AM Technologies. These are Wire-feed, Paste, powder, foil and photo-initiated resins. The five different types of stock material is deposited within the different AM technologies by three classes of primary deposition units; By point-wise extrusion, By point-wise or multi-point ejection from a jet- or a polyjet-system resembling inkjet cartridge systems[15], or by coating/re-coating the entire build plane with a powder or a photo-initiated resin. At the fourth level of the technology-tree, the specific technologies are listed, and what materials they operate with; Fused Deposition Modelling (FDM) allow for extrusion of thermo-polymers, ceramics, thermo-polymers based composites and biological material; Bioplotting allow for deposition of biological material in a similar fashion to FDM; Laser Engineered Net Shaping (LENS) allow for selectively spray-coating of metals; Selective Laser Sintering, Melting (SLS/SLM) & Electron Beam Melting (EBM) allow for sintering or melting of a powder, either thermoplastic, metal or ceramic, in a powder-bed; Laminated Object Manufacturing (LOM) allow for contour tracing and layered manufacturing of metal, polymer and paper foil; Stereo Lithography (SLA) & Direct Light Projection (DLP) allow for selective curing of photo-initiated polymer resins and composites with ceramic fillers. All of the mentioned technologies will

be discussed in the following sections:

2.3.1 Fused Deposition Modeling

Fused Deposition Modeling is the numerically controlled additive fabrication of structures by thermo-plastic extrusion from a material deposition unit. The process bears resemblance to 3-axis CNC machine tools with the major distinction that material is added contrary to be removed by a material removal unit. The process was initially invented by Steven Scott Crump and published in 1992 under the US patent #5121329 as a ⌜*Apparatus And Method For Creating Three-Dimensional Objects.*⌟ [16] The patent describe a workflow from CAD model to 3D object that resemble the workflow for 3-axis CNC machine tools. A CAD model is processed to an instruction sequence for the FDM machine. These instructions, in the form of tool-chains, control the FDM platform in a scheme where flowable solidifiable material is locally and sequentially extruded to from the structure described by the CAD model. The invention by Steven Scott Crump led him to found the company Stratasys Inc, which is the oldest company manufacturing FDM flavored Additive Manufacturing machines. The expiration of the patent by Steven Scott Crump led to a sale of more than 20,000 low-cost personal FDM machines in year 2011.[2, p. 253] Open Hardware derivatives of FDM have been in existence since 2005.[17]

The basic working principle of FDM is shown in figure 2.8 on the following page. A thermo-polymer is passed by a numerically controlled wire-feed mechanism into a hot extrusion system. The extrusion system which is temperature controlled by the numerical controller melt the thermo-polymer and extrude it as a find strand of material. The extrusion nozzle is traversed relative to the workpiece by a cartesian 3-axis movement system that weave the structure up, layer by layer. As the strand of extrude is still above liquidus temperature when the strand get in contact with the structure, the strand partially remelt the previous layer to form a bond.

Commonly used thermo-polymers applied to the FDM principle is Polylactic Acid (PLA)[2, p.191], Acrylonitrile Butadiene Styrene (ABS) and Poly Carbonate (PC).[2, p. 79] Some FDM platforms use a dual extrusion system where PLA is used as support material as it can be removed by softening in hot tap water.[2, p. 111] FDM has its advantages and disadvantages. These are listed in table 2.1 on page 41. Filament for FDM machines come in a variety of colors. If proprietary stock material is not used, any color applicable for Injection Molding can be used to color the filament wire. Filament wire is cheap compared to stock material for other Additive Manufacturing processes. Changing material is a simple task done by pre-eating the extrusion unit, reversing the filament through the feed mechanism, inserting new filament, and flushing the extrusion unit by forwarding a short length of wire. Maintenance is low. The cartesian axis have a service interval comparable with any other cartesian platform. The extrusion unit can clog from burn-ins building up within the extrusion unit, or from foreign debris introduced as inclusions within the filament wire, or from being dragged in with the

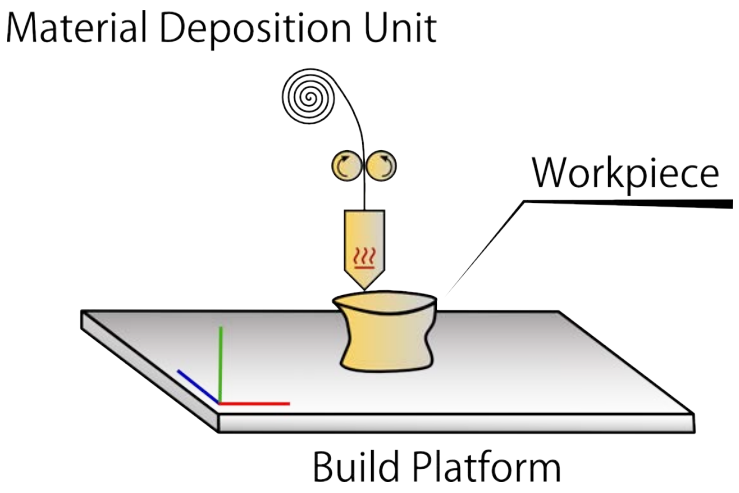

Figure 2.8: *Fused Deposition Modelling*

filament. Thin, shelled structures are built comparably fast with respect to other AM processes, as the FDM process extrude material in a point-wise manner. Thin layers below 0.1 mm can be reached, superseding other AM processes. The FDM system can be left unattended, as fault detection is easily registered, and should a machine fault occur, the extruder tool chain is always moving the extrusion unit farther away from to workpiece, rendering collision risks immaterial. The FDM process expose the operator to a comparably hazardous environment. Unlike AM processes involving fine powders and volatile photo-initiated monomers, the toxicity from the FDM process is limited to the fumes generated from melting and extruding the polymer filament. This puts the FDM process in the same toxicity category as other thermo-polymer oppressing machines such as Injection Molding machines. Finally the FDM processes have a relatively small footprint. The machines can make use of but does not require any kind of external installations such as fume cabinets, cleaning stations or other post processing equipment. Disadvantages of the FDM process is that visible seams can be seen in-between layers. If the processing material is ABS, chemical polishing with acetone can reduce the visibility of the seams. If the extrusion unit is paused within a build-job, heat will be dissipated into the workpiece, forming visible defects. Residual thermo-polymer material may also build up, as the extruding unit dependent on the specific FDM machine can tend to sludge. Since structures are formed free-standing, support structure may be needed to support overhangs. If the structure is hulking, exhibiting large cross-sectional areas, build times increase dramatically. In the interface of layers, FDM structures exhibit weak sheer strength, as the interface is reliant on the topmost strands of extruded filament remelting and adhering to the previous. By the same adhesion mechanism, structures can be found delaminating to the touch, or from thermal stresses, if operational temperature of the extrusion unit is low. ABS in particular tend to delaminate from the build-platform during

Table 2.1: *Fused Deposition Modelling - Advantages and Disadvantages*

Advantages	Disadvantages
Filament comes in a variety of colors	Visible seam between layers
Filament is cheap	Defects form at discontinuous extrusion
Material Change is easy	Structures may require support
Maintenance Costs are low	Layer build time depend on area
Shelled parts are produced fast	Weak strength in sheer between layers
Layer heights below 0.1 mm	Low extrusion temperature can
System does not need supervision	cause delamination between layers
Low toxicity of fumes and materials	Thermal stresses can make structures
Compact machine footprints	curl off the build platform

operation.

2.3.2 Bio Plotting

Bio Plotting is a novel process used for tissue engineering.[18] Bio plotting set high standards for sterile environment, and biocompatibility of structures made by this process. Bio plotting is a derivative of the FDM technology where stock material is handled in sterile cartridges and deposited by extrusion. Unlike traditional FDM, Bio Plotting employ a pressurized air source to press out viscous pastes from up to 5 cartridges of different materials.[18] As such, the process is highly specialized for applications within the medical industry, and will not be addressed further.

2.3.3 Laser Engineered Net Shaping

Laser Engineered Net Shaping is a thermal process invented by Sandia National Laboratories.[19] LENS is a powder-based method for fabrication of structures directly from CAD solid models by cladding with a laser beam. A metal powder is carried by an inert gas in a contracting cone-shaped flow. In the centre of the conical powder stream, a high powered laser beam is projected. At the focal plane of the laser, the powder stream, laser beam and workpiece coincide.

The powder is melted and cladded to the surface of the workpiece. A graphical representation of this can be seen in figure 2.9 on the following page. A list of advantages and disadvantages of the LENS process can be seen in table 2.2 on page 43. LENS has three major advantages. The first is that the powder-fed laser nozzle can be controlled in a variety of control schemes. 3D cartesian movement, 4D with a rotary stage, and even in articulated 5D patterns by an industrial robot, allowing for truly freeform, however still layered deposition of material. Metals used by the LENS process are stainless steel alloys (316, 304L, 309, 174), maraging steel (M300) and titanium alloy(6AI-4V).[19] The powder particles will

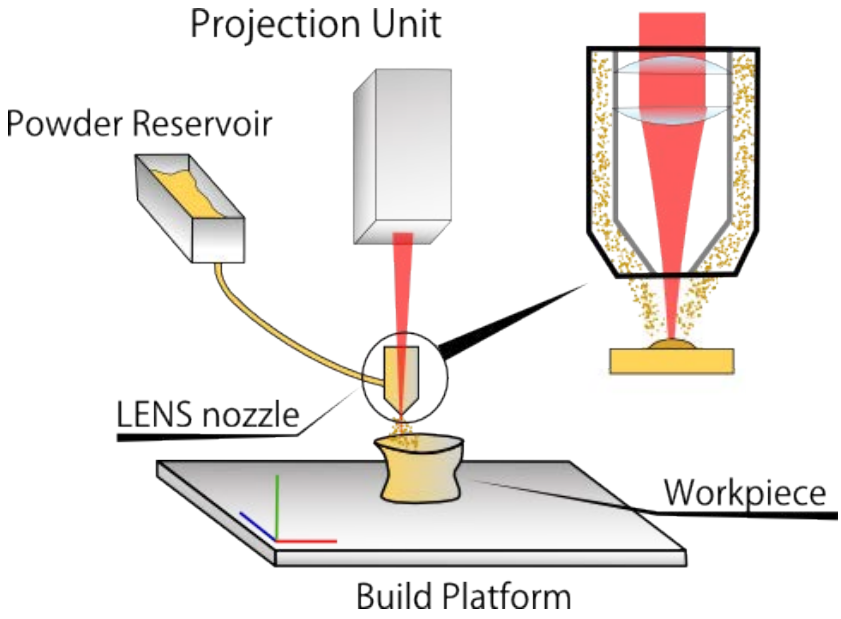

Figure 2.9: *Laser Engineered Net Shaping*

liquify as they reach the focal area of the laser beam, and ballistic be cladded to the workpiece. This spray of molten metal, clad to a fully dense layer when it adhere to the workpiece. As a result of this, structural strength of LENS made parts are unprecedented,[19] and is the second of the primary advantages of the process. Finally the LENS technology can be applied to more than pure Additive Manufacturing. It can be used to add wear-resistant coatings to existing parts, and as a mean to existing parts. Typical repair application is of mechanical equipment with moving parts that need rebuilding due to wear. Titanium components in the aerospace industry is a primary actor in this field.[20] Not only titanium parts are sought to be repaired in this manner. Also the service time of gas turbine components in Inconel 718 steel alloys is extended by LENS based repairing. Disadvantages to the LENS technology is that if a flexible system for both exclusively Additive Manufacturing, cladding and repair jobs is wanted, the LENS technology set high requirements to the operator skill, requires an advanced control scheme, and may require a 4D or 5D control system of the nozzle. Furthermore the powder particle size used within the process can prove hazardous, as the powder is finely grained and has a high density. This can impose a health risk if inhaled. Another drawback is that the LENS process require an expensive high-powered laser. To gain full flexibility of the process, this laser is preferably fiber coupled or fiber laser based, which increase the system cost further. Finally, as structures are built free-standing, support structure may be needed for complex structural shapes.

Table 2.2: *Laser Engineered Net Shaping - Advantages and Disadvantages*

Advantages	Disadvantages
Ability to build fully dense shapes	Articulated control scheme requires expensive industrial robotry
Mechanical properties similar to or better than traditional processing methods	Powder particle size can result in a hazardous work environment
Allow for articulated nozzle movement	Reliant on expensive laser technology
Can be used for repair and surface cladding of traditionally manufactured parts.	Complex structures will require support as parts is produce free-standing

2.3.4 Three Dimensional Printing

Three Dimensional Printing is a commonly misinterpretation of the name Additive Manufacturing. However there are indeed a process branch within Additive Manufacturing that convey this name. It is a non-thermal powder based technology which employ an inkjet cartridge to deposit a binder liquid to Plaster of Paris, to form a solid structure. As this powder based technology indeed employ inkjet technology it can boast the name 3D printing without denounce. Another technology based upon inkjet technology is the direct deposition of photo-initiated resins to a build platform bathed in UV light. Whereas this technology is known in the field of Additive Manufacturing merely as ⌜*Inkjet*⌟ it is however included in this section as the mechanism at which the resin is deposited employ the same principle as that of true 3D printing.

Resin

Additive Manufacturing by Resin Based Inkjet share process similarities to both LENS, FDM, SLA/DLP and 3D printing. The process involve cartesian control of an inkjet cartridge over a free-standing workpiece at times supported by a specific support material sharing similarity to FDM. The process clad material in its liquid state to the workpiece as with LENS. The cladded material is cured by a UV light source as curing is handled by SLA/DLP. The way material is cladded to the workpiece is by employing inkjet technology as with the binder material in 3D printing. The working principle is illustrated in figure 2.10 on the following page

Resin is fed from a reservoir to the inkjet cartridge or print head. Material is ejected at high velocity, cladding onto the surface of the workpiece. A curing flash, or in derivate systems, a continuous light source cure the cladded layer. The printhead moves one layer up, and the process repeat itself until the structure is formed. The processing material in inkjet systems are the same as with SLA/DLP. Originatively resins was baste upon brittle acrylates, however mod-

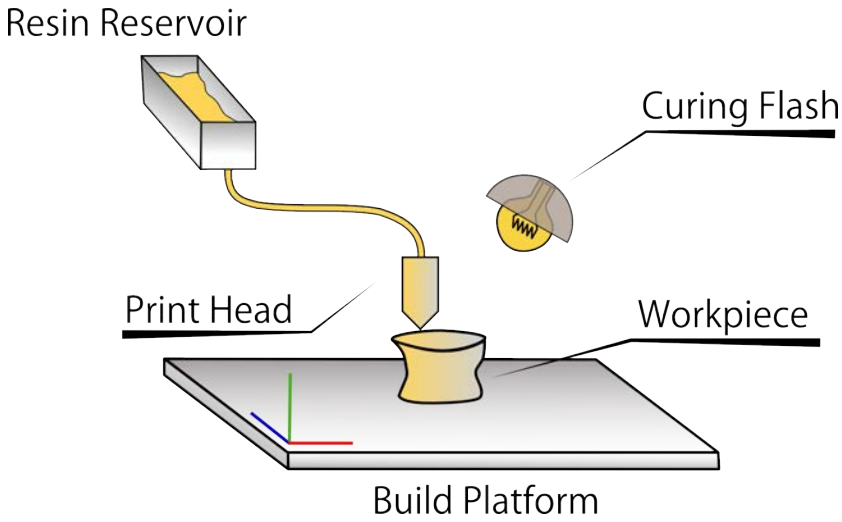

Figure 2.10: *Resin Based Inkjet Printing*

ern epoxy-based UV initiated resins allow for material properties ranging over High Temperature materials, Bio-Compatible materials, ABS-like, Transparent, Rigid Opaque, Polypropylene-like, and Rubber-like.[21] Strengths and weaknesses of Resin based Inkjet is listed in table 2.3 on the next page. Two of the key strengths of the technology is ultra-fine layer heights, and resolution in the traverse directions of the inkjet print head. Employing known technology from 2D printing allows the technology to reach the same deposition accuracy within layers as the deposition accuracy of photo-printers.[21] Resin based inkjet printing offers a versatile material choice in terms of mechanical properties as listed above. Even more interesting is that some platforms allow to graduate these properties within structures. This allow for ex. rubber-like buttons to be directly integrated in a hardened case, for prototypes and products built using resin based inkjet printing. Noticeable disadvantages is that since UV curable resins are used, mechanical properties can change over time if parts are not carefully and correctly post processed after manufacturing. Relatively low build speeds is a tradeoff from the high resolution that can be achieved. Office friendliness is accentuated as an advantage and a disadvantage alike. This can be regarded as an acquisitive statement that can be disputed by the office friendliness of UV-initiated photo monomers. Spite a versatile choice of materials exhibiting versatile mechanical properties, the exact chemical composition and hence necessitate chemical and mechanical information needed to ensure product quality in manufacturing engineering is rendered opaque from trade-named resins. Finally, little to no overhang can be produced without imperforate underlying support. This reduce build speed further and lead to added waste generation from the process.

Table 2.3: *Resin based Injet printing - Advantages and Disadvantages*

Advantages	Disadvantages
Less than 16 micron layers	Photo initiated resins can alter
High resolution in traverse	mechanical properties over time
direction due to inkjet technology	Relatively low build speeds
Versatile material choices	Office Friendliness can be arguable
Some platforms can graduate	Proprietary resins elude chemical
mechanical properties within	composition by vague description of
build jobs	functional properties
Rinsable support structures	Most parts need surrounding support
Marketed as Office Friendly	as the inkjet print head cannot
	deposit material if there is
	any kind of overhangs

Powderbed

The MIT patented Powderbed Based 3D Printing technology is the name of origin for the exhaustive misapplication of the term ⌜*3D printing*⌟ as a descriptor for Additive Manufacturing processes. Patented in 1995 is a technology described to be a powder-bed based layered manufacturing method that selectively bind the powder using a binder liquid. [22] One year after the patent was filed, zCorporation obtain an exclusive license to market and develop 3D printing. Development efforts result in the launch of the z402 3D printer in 1996 which by the time it reached the market was embraced as the fastest additive manufacturing platform by a margin of 5-10 times.[23, c.6.] All current additive manufacturing platforms developed and marketed by zCorporation is based upon the rehydration of Plaster of Paris. Figure 2.11 on the following page is used to describe the working principle. The machines from zCorporation build structures within a powder-filled build chamber. As the process start, the build-chamber is empty and the build platform is fully extended. A thin layer of plaster is deposited to fully coat the build platform after which the plaster is selectively rehydrated by means of an inkjet print head. Once the cross-section of the structure has been rehydrated, the build platform is lowered into the build chamber, the build surface is recoated and the process repeats itself. zCorporation has continued to develop their inkjet based 3D printing technology since 1996 and now offer plaster based machines that can produce structures in full-depth colors by allowing a secondary inkjet CMYK color cartridge dye the periphery of each cross-section of the structure. Furthermore zCorporation has developed powders that are suitable for printing molds for indirect manufacturing of metal parts by casting.

Advantages and disadvantages to powder based 3D printing can be found in table 2.4 on page 47. The technology has up till recently had one unique and

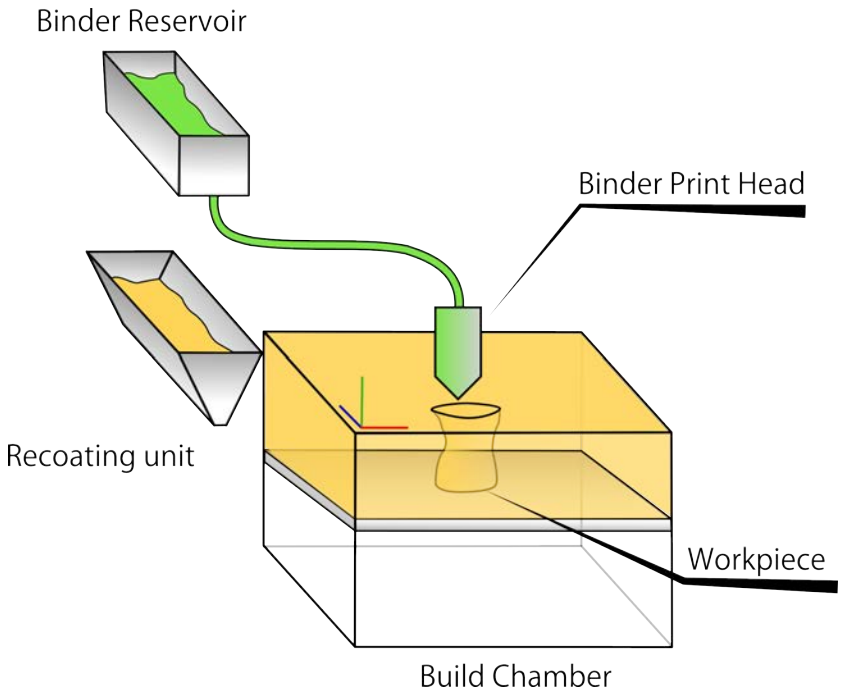

Figure 2.11: *Powder Based 3D printing*

novel advantage over any other existing additive manufacturing methods. That is the ability to manufacture structures with colored surface textures. This ability is popular as it allow for physical cross-sectioning mechanical product assemblies in full color for visualization. Similarly in the architectural field, this feature is used while making physical models of buildings, interior and exterior decorations and landscapes.[24] Other advantages are that due to the working principle of the technology, structures are fully emerged in a chamber of plaster. This render support material unnecessary. The technology exhibit high build speeds, where the build time of each individual layer is comparable with industrial-grade paper inkjet printers. The stock material is cheap in comparison to other additive manufacturing processes, and finally the capability to indirectly manufacture metal structures by casting. This last advantage is also of key importance as machines for true additive manufacturing in metal alloys are in the highest price-range of all the additive processes. A disadvantages that structures in plaster are comparably weak to all other additive manufacturing processes. This can be circumvented by infiltration of the plaster structures by acrylates, such as cyanoacrylate. Infiltration add a post processing step to the technology, and protective means must be taken to avoid volatile fumes. Furthermore dry particles of plaster are not to be inhaled, yet very light and if particles get airborne, they will be suspended in air for long periods of time, with the ability to travel long distances, polluting nearby work surfaces within the room where the machine reside. This makes plaster based 3D

Table 2.4: *Powderbed based 3D printing - Advantages and Disadvantages*

Advantages	Disadvantages
Structures are self-supported	Structures are fragile and
Build speeds are high	serve better as display items
Stock material is cheap	than functional items
Can texture structures in	Plaster powder is very light
full-depth colors	and can be carried far as
Can be used for indirect	airborne clouds
manufacturing of metal parts	Surfaces appear porous and
by casting	will give continiously give
	off powder by the touch

printing a dirty process in comparison to many other additive manufacturing processes. Finally the surface of plaster structures that has not been post processed by infiltration, appear porous in the surface structure, and will continuously give off powder when handled. The porous surface structure will when the technology is used for casting produce a surface replication in the casting that resemble that of sand-mold based casting.

2.3.5 Selective Laser Sintering, Melting, and Electron Beam Melting

Selective Laser Sintering, Melting and Electron Beam Melting are three derivatives of the same principle for manufacturing parts from a powder. The technologies are based upon machine designs that resemble that of powder based 3D printing and can be seen in figure 2.12 on the following page. Structures are built on a build platform in a build chamber. Layer-by-layer the build surface is coated by a powder, and a high-energy beam is used to bond the powder to a solid. The SLS technology[25] exist in two flavors. Polymer based SLS and Metal based SLS. The polymer based SLS machine use a finely grained thermo-polymer granulate as build material. The temperature of the build chamber is elevated close to the sinter-temperature of the granulate, and a laser beam of moderate intensity is used to selectively sinter the powder to a solid. As the temperature of the powder within the heated chamber is already close to the sinter-temperature, little to no thermal stresses are accumulated as the structure is built. This renders support material unnecessary. Nylon-grade Poly Amide-12 (PA-12) is accountable for ≈95% of all supply materials for polymer SLS machines[26], though other thermo polymers are also available as SLS powders. These are Poly Ether EtherKetone (PEEK), Poly Carbonate (PC), Poly Oxy Methylene (POM), Poly Methyl Meth Acrylate (PMMA), Poly Styrene (PS) and High Density Poly Ethylene (HDPE).[26]

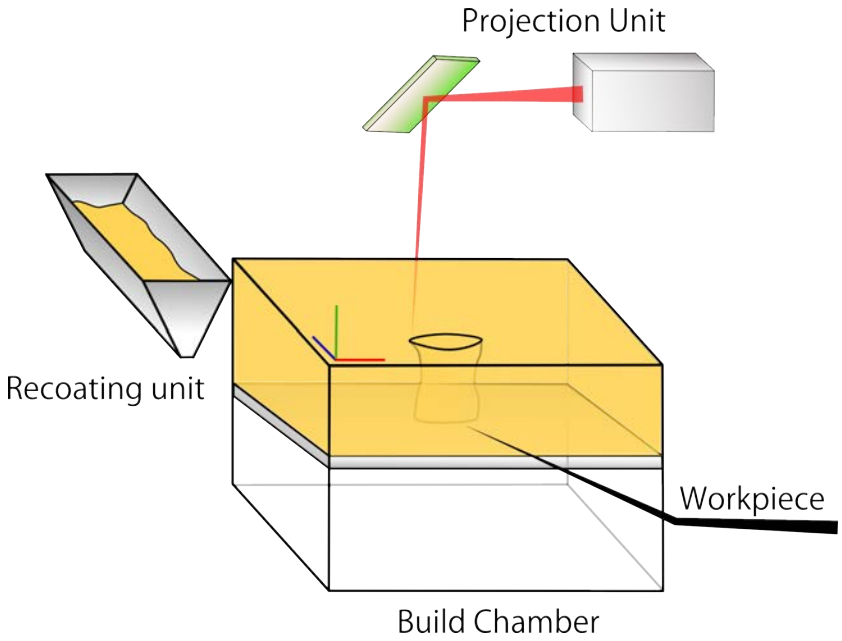

Figure 2.12: *Selective Laser Sintering and Melting*

Metal based SLS and SLM is distinguishable from polymer based SLS by setting a demand for a protective gas to be flooded into the build chamber of the machine. This to prevent unwanted oxidation of the metal powder during sintering or melting. The metal alloys used for metal SLS, SLM and EBM resemble those used within the LENS process. It is not viable to heat the entire build chamber to a temperature close to the sinter-temperature. The lack of preheating the build chamber, result in thermal stresses accumulating within structures as they are built. Therefore both additive manufacturing by SLS, SLM and EBM require generation of support structures to minimize warp and prevent structures from curling off the build platform. Processing metals call for the need for high-powered lasers to be employed within the processes. When EBM is used, a laser as thermal energy source is replaced with an electron beam cannon. In order for the electron beam to be employed, the build chamber must be put under high vacuum which has the benefit to render protective gasses unnecessary.

Structures, whether metal or thermo-polymer based, exhibit a high degree of porosity if manufactured by SLS. As the processing powder is sintered, the individual grains of the powder remain static, no mechanical force is applied, and the powder is barely altered during the sintering process. They merely stick to neighboring grains. Structures made by either SLM and EBM are formed by elevating the powder to a temperature slightly above the melting point of the alloy. This form a local melt pool, hence providing fully dense structures with recrystalized grain structure. As a result of this it is now possible to produce parts in a range of metals that are on par with wrought materials and exceed

the properties of castings. Among the most promising materials that has recently emerged for SLM and EBM are aluminum alloys, and nickel-based superalloys. [2, p. 256]

2.3.6 Laminated Object Manufacturing

Hydronetics Helisys Inc. led by founder Michael Feygin initially started the development of a powder-bed based sintering system but later decided to shift focus to their novel approach to Additive Manufacturing. -A method for producing three-dimensional structures from stock sheet material.[27]

Laminated Object Manufacturing (LOM), is a technology originally patented by Michael Feygin in 1988[28] as an ⌜*Apparatus and Method for Forming an Integral Object from Laminations*⌟ This first patent however describing a system for manufacturing three-dimensional structures from rolls of sheet stock, resemble little the LOM machines as of today. In 1998 Michael Feygin et al. filed another US patent where the terminology "LOM" was now used. This patent by the title ⌜*Laminated Object Manufacturing System*⌟ describe a fully evolved LOM platform that resemble today Laminate-based AM units. LOM was initially produced exclusively by Hydronetics Helisys Inc. with Feygin as company president. Prior to the development of the LOM technology, Helisys put effort into a SLM-like platform. However, after the formulation of the LOM technology as a patent, Helisys changed focus to the sole development of LOM.[27]

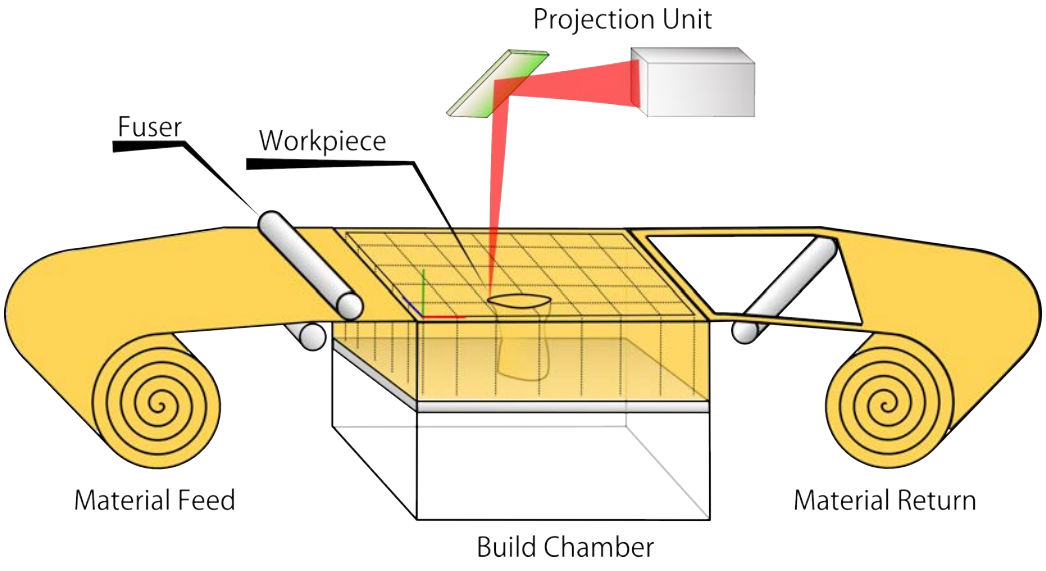

Figure 2.13: *Laminated Object Manufacturing*

The working principle of LOM is very similar to the working principle of SLS. Structures are built in a chamber fully brimmed by surrounding stock material,

hereby rendering support material superfluous. A laser is employed to form each cross-section. Unlike SLS, stock material come in sheets or fed endless by rolls. Stock material was initially limited to paper, giving parts the mechanical properties, look and feel as laminated plywood. The first commercialization of LOM used a roll of paper with a backing of thermo-activated adhesive. The machine resembled the principal sketch in figure 2.13 on the previous page A sheet of stock paper was advanced over the build chamber. A CO_2 laser cut the contour of the cross-section through the paper, and serrated the surrounding brim of paper in a checker-board pattern for subsequent eased removal. This shown as a dashed pattern on the top layer. Finally a fuser unit shaped as a roller was used to bond each successive layer.[2, p. 71] Many attempts to improve LOM has been seen in the industry. Some has been to use metal and polymer foil as improved processing materials. Some has been focusing to lower the machine costs by replacing the CO_2 laser with a swiveled mechanical knife. A novel machine from Mcor Technologies allow full-color models to be produced. Some employing ultrasonic welding of metal foils to replace thermo-based glueing.[2, p. 71-72]

The LOM process has been assessed by the process advantages and disadvantages, listed in table 2.5 on the facing page. One of the primary advantages of LOM is fast build speeds. When using paper or polymer based LOM, the build speed is governed by the bulk sheet thickness, and the paper fusing mechanism. The paper forward mechanism and the contour-tracing by scanner mirrors in negligible. When employing metal foil based LOM, the build speed is reduced to the the ultrasonic welding of sheets. Paper and polymer based LOM use a chemical bonding agent to bond laminae, hence no thermal stresses are induced into the structures built. When employing paper as a build-material especially in combination with a system employing a mechanical swiveling knife to trace contours, machine cost is relatively low, and build-material costs are unprecedented. As the only Additive Manufacturing process employing paper as a build material, LOM can be very environmentally friendly, allowing for a complete recycling of the manufactured parts, either as recycled paper or as composting. Finally, since there is no user-configurable parameters involved in the manufacturing process, most LOM machines are as easy to operate as most common 2D paper printers.

LOM possess a set of disadvantages, many of which is induced by the paper based laminae itself. Paper based laminates at best provide the same material properties as wood as a construction material. Hence industrial application is very limited. Post processing is a time-consuming tedious manual process which involve breaking the structure free of the serrated bulk comprised of blocks of brimmed laminae. For intricate details this must be dine by delaminating the serrated block with a scalpel and pliers, layer-by-layer. Some structures will not be producible because the bulk of brimmed material cannot be removed from the part at all. This is mainly for complex internal geometries. The process exhibit a high level of material waste. Though governed by how compact several parts can be packed within the build-envelope, if producing individual parts ad hoc, material

Table 2.5: *Laminated Object Manufacturing - Advantages and Disadvantages*

Advantages	Disadvantages
Relatively fast build speeds. Structures does not need support. Paper and Polymer LOM does not introduce stresses in stuctures. Supply material can be as cheap as photo-copy paper. Environmentally friendly - Paper models can easily be recycled. Ease of use - The process is very tolerant and nearly as easily operated as a 2D paper printer.	Paper LOM produce parts that are not suitable for manufacturing engineering purposes. Post processing is a tedious manual process where serrated laminate material is removed by delamination Material waste. The entire build envelope will be filled with laminate irellevant of build size

waste is superseding any other additive manufacturing process.

2.3.7 Stereo Lithography

Stereo Lithography (SLA) is if any, the Father of Additive Manufacturing. As described in section 2.3 on page 37, SLA was the very first Additive Manufacturing process to see the light of dawn. SLA was commercialized in 1988 by 3D systems. [2, p. 72] Coined by a US patent from 1986 by Charles W. Hull [29], 2 years older than LOM, stereolithography was the introductory additive manufacturing technology. Unlike LOM which has seen a steady decline in use since it's early introduction, SLA is still a process in favor by the industry, and a technology that has spun process derivatives such as resin based inkjet printing and direct light projection systems. One of the key catalysts for SLA to prosper where LOM did not, is through material development which has lead to new resins for SLA that vast supersede the acrylate based resins originally employed. As with resin based inkjet printing, which spun from SLA process, modern resins are as strong as injection molded thermo-polymeric relatives. The same resins are used as described in subsection 2.3.4 on page 43. Modern epoxy-based UV initiated resins span in material properties ranging over High Temperature materials, Bio-Compatible materials, ABS-like, Transparent, Rigid Opaque, Polypropylene-like, and Rubber-like.

The working principle of SLA is somewhat different than that of resin based inkjet printing. Structures are built on a platform submerged into a photo-initiated resin. A laser light source trace the contour and core of a layered object model at the level of resin a vat. As the light initiate polymerization, the layer is formed. The elevation of the build platform is lowered one layer, a wiper blade aid the resin to recoat the preceded layer, and the process repeat itself. SLA share some

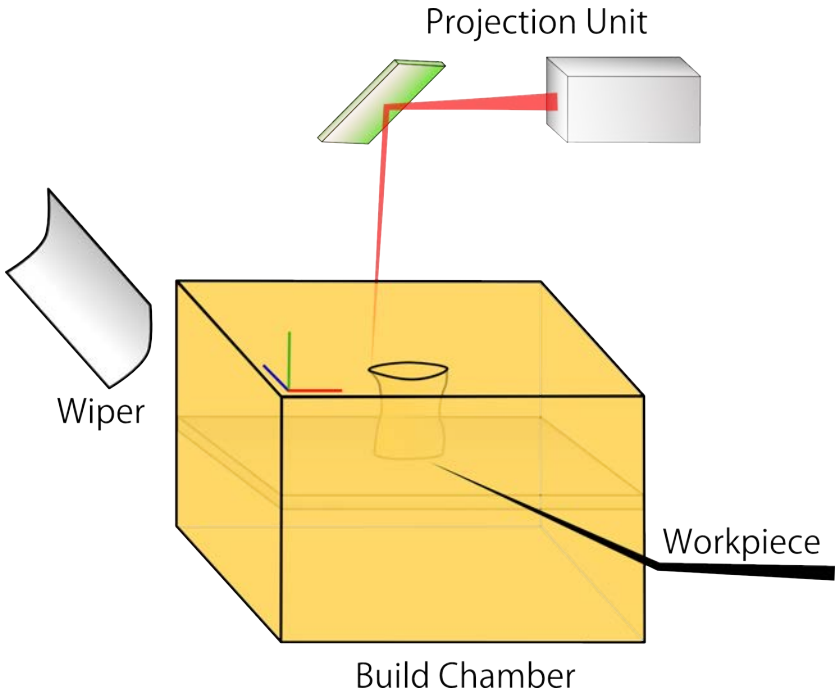

Figure 2.14: *Stereo Lithography*

of its advantages and disadvantages with the resin based inkjet printing and direct light projection. These, listed in table 2.6 on the next page. SLA can boast the same vertical and horizontal resolution as resin based inkjet technologies, and the material choice is as versatile. Furthermore the technology is well anchored within the industry and is accepted as being an efficient, accurate process producing parts at commercial production grade. One key advantage is that SLA machines can be found with impressively large build volumes. Materialize LC offers SLA services on a proprietary SLA machine, the Mammoth SLA which has a build envelope of 2100x700x800 mm. [30] Of disadvantages is that photo initiated resins can alter their mechanical properties over time. This is prevalent of post-treatment of structures has not been yielded a complete photo initiation of the resin. As with DLP and resin based inkjet printing, the commercial resins elude the consumer as to what chemical components are present. This is not favorable in commercial production by SLA, as the exact chemical composition and hence mechanical and environmental behavior of the SLA manufactured parts are not explicitly known. Finally unlike resin based inkjet printing of resins, it is impossible to add a support material of another composition than the stock resin. This limit support structures to be built in the same material as the part itself. This add complexity to the post-processing since the support must be removed leaving minimal scarring in the surface of the structure where the support is broken off. One final disadvantage is related to the working principle of SLA and the cost of photo initiated resins.

Table 2.6: *Stereo lithography - Advantages and Disadvantages*

Advantages	Disadvantages
Less than 16 micron layers	Photo initiated resins can alter
High resolution within layers	mechanical properties over time
Versatile material choices	Proprietary resins elude chemical
Proven and reknowned	composition by vague description of
technology anchor SLA to	functional properties
to a stable market share.	Most parts need surrounding support
Inustrially available SLA	which can only be created in the same
machines provide large	material as the part.
build envelopes at high resolution	Maintaining the level of resin within
	the machine vat can be costly

The principle is based upon a vat of photo initiated resin. This vat as stated, can be as large as above one cubic meter. Whenever a part has been built and subsequently removed from the build platform, the resin level within the vat falls. It is then needed to add in additional resin to reach the operational level of the machine, corresponding to the focal length of the optical system. With resins cost anno 2002 averaging $200 USD per kilogram.[31] and resin costs still found at this cost, [2, p. 153] today, large quantities of capital is bound within the resin vat. Contamination of the resin is a risk that is connected with a major capital loss.

2.3.8 Direct Light Projection

The last technology to be addressed is the Direct Light Projection (DLP) systems. These systems share a strong process resemblance to SLA. DLP is based upon the SLA principle, and emerged from the development of strong DLP video projection units vastly exceeding the light emission of traditional LCD based projection units. A DLP projection unit is used to expose a photo-initiated monomeric resin to solidify thin-film layers at a pixel-by-pixel level. A traditional LCD projector typically has a brightness of 200-300 cd/m^2 luminance with a minimum luminance for black pixels of 1 cd/m^2 [32] The typical luminance is low for photo-initiated curing of resins and the fact that light is still penetrating the LCD mask for black pixels makes traditional LCD based projectors less suitable for photo-initiation of resins. DLP based projector masks however employ a micro-electromechanical system (MEMS) comprised of a tillable mirror array to allow for ⌜*true blackened*⌟ pixels. DLP based projectors deliver a much higher contrast with a maximal luminance of above 2600 cd/m^2 and minimum luminance of 0.04 cd/m^2 for black pixels. It is therefore the development of the DLP projection technology that drives the development of DLP based resin technologies within the field of Additive Manufacturing.

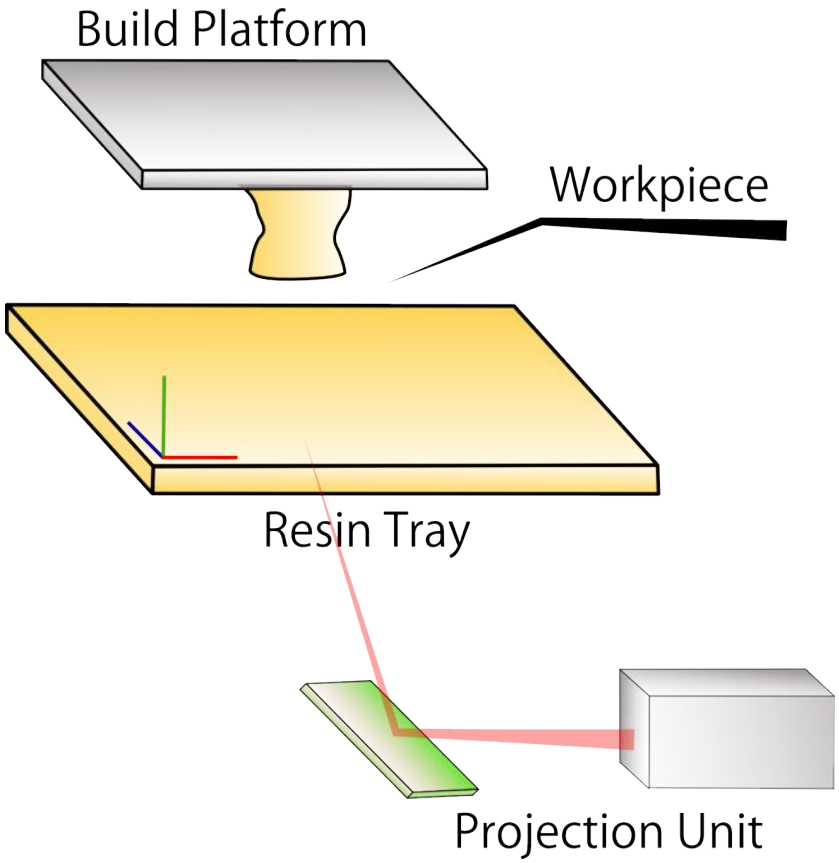

Figure 2.15: *Direct Light Projection*

DLP based AM machines operate by a principle that can be described as an inverted SLA setup. The setup can be seen on figure 2.15. Resin is not kept in a vat, but a shallow transparent tray. As the build progress, the build platform is elevated out of the tray instead of submerged into a vat as for SLA. A projection unit based upon a DLP projection unit reside underneath the tray, and expose an entire build-layer concurrently. All resin in-between the build platform and the transparent bottom of the tray will cure. Once exposed the build platform is elevated one layer, and the low pressure generated underneath the cured layer will drag in resin from the shallow tray to the vacancy formed by the elevation. Hence a recoating unit is not needed. The DLP unit will expose next layer and the process repeat itself the the entire structure is formed.

Table 2.7 on the next page show general advantages and disadvantages to DLP systems. Build resolution of DLP based resin systems is for some equipments amongst the best in industry. General resolution down to 5 micrometers has been achieved using DLP technology by TNO Research Group.[33] As DLP is a derivative of SLA, the DLP initial development of the technology has been fast-

Table 2.7: *Direct Light Projection based systems - Advantages and Disadvantages*

Advantages	Disadvantages
Less than 16 micron layers.	Photo initiated resins can alter mechanical properties over time.
High resolution within layers.	Proprietary resins elude chemical composition by vague description of functional properties.
Experimental machines reach 8 micron accuracy superseding SLA.	Most parts need surrounding support which can only be created in the same material as the part.
Versatile material choices.	Added force to support structure can deform supported surfaces.
Resemble SLA and as such process development has been accelerated.	Machine resolution is invert proportional to the build envelope as DLP units has a fixed resolution and is tailored to the DLP projector market rather than the AM market.
Platform investment is very cheap in comparison to SLA.	
Contrary to SLA little resin is kept in the build tray.	

paced and the process share the same acceptance by the industry as traditional SLA. The heritage to SLA has also set an imprint on the materials available. A vide palette of material choices are available for DLP systems. Another prime advantage over SLA is that DLP based systems can be found much cheaper than SLA based systems. This as expensive laser technology is replaced by cheaper DLP technology. Finally one of the key advantages is that unlike SLA, there is little processing material bound in the machine to keep it operational. An amount within the resin tray sufficient to keep the build-surface of the structure fully submerged throughout the build job is adequate. Disadvantages are partly shared with SLA systems. These are that improper postcuring can lead to alteration of mechanical properties over time. That the chemical composition is vaguely known by the operator, limiting the possibilities for commercial manufacturing since mechanical and chemical properties of structures is not fully known. As with SLA, parts need support, and this support is built of the same material as the bulk structure. Further deteriorating support generation for DLP systems are that unlike SLA, there are mechanical forces acting on the structure as it is being built. These appear as the build platform is elevated, and act at the interface between structure and the transparent tray. As the platform elevates, the structure is pealed off the surface of the tray, pulling the structure. The magnitude of these forces are great at the interface between support and part, and can lead to excessive scarring as the part will remain structurally weak until subsequent post-curing. Another drawback, directly lated to the driving mechanism of the technology is that the build-resolution is invert proportional with the build envelope. DLP projection

units currently used in most DLP based additive manufacturing systems originate from the DLP image projection industry. Hence a fixed and limited pixel-array is available for generation of pixel projection patterns. If the build envelope in the horizontal direction is to be expanded this can only be achieved by expanding the projected pattern from the DLP chip by altering the optical light path. This can on some machines by done by interchanging projection lenses. The result will be that each individual pixel become larger and the horizontal resolution is decreased. It will also increase the exposure time for each layer as the light intensity is decreased with the increase in pixel size. Some DLP platforms however employ a moving gantry to allow for much exposure of much bigger areas at full resolution. An example of one such system is the Huntsman Araldite Digitals which has a spectacle of a build envelope measuring 650x370x600 mm at a resolution down to 10x10 micrometers with a layer height of 50 micrometers. [34]

2.4 Processing Materials in Additive Manufacturing

Common processing materials used within Additive Manufacturing can be described in a tree structure as shown in figure 2.16 on the facing page. Five different material stock forms and five material categories form the branches of the tree. The stock forms; wire, paste, foil, powder and resin relates to what condition the processing materials are in, when used in the various additive manufacturing processes. The material categories; biological, metals, photo polymers, thermo polymers and ceramics describe the chemical properties of the different stock materials used.

2.4.1 Materials for FDM

Starting with the thermo-polymers, these are used within the FDM and SLS and LOM processes. In FDM the most commonly used thermo-polymers are Polylactic Acid (PLA, $C_3H_4O_2)_n$)[2, p.191], Acrylonitrile Butadiene Styrene (ABS, $(C_8H_8{\cdot}C_4H_6{\cdot}C_3H_3N)_n$) and Poly Carbonate (PC, $(C_{16}H_{14}O_3)_n$).[2, p. 79]

Polylactic Acid is a bio-based polymer that can be produced from renewable resources such as starch and sugar. RTP Imagineering Plastics produce a PLA based polymer, the RTP2099 X 126211 Z, which contains 89% renewable resource content. The RTP2099 PLA has a tensile strength of 46 MPa, and a specific gravity of 1.23. PLA generally is thermally stable up to ≈ 50 C°degrees after which PLA tend to become malleable and exhibit rubber-like properties. The typical extrusion temperature is ≈ 175 C°.[35] A general description of the properties of PLA is given by Södergård and Stolt, as PLA exhibiting a crystallinity of ≈37%. The glass transition temperature is ≈60-65 °C and the melting temperature is

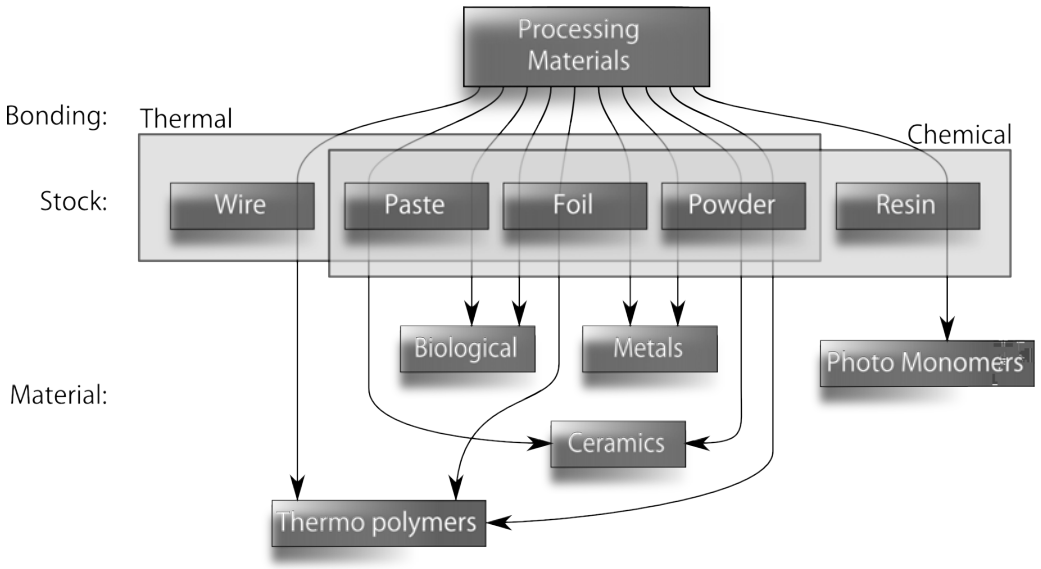

Figure 2.16: *Additive Manufacturing Material Branches*

≈173-178 °C.[36] PLA is not prone to accumulate thermal stresses during layered manufacturing by FDM extrusion.[17]

ABS is a commonly used thermo-polymer in industrial processes and dominate as processing-material in industrial grade FDM processes. ABS is unlike PLA amorphous of nature. Hence a true melting point is nonexistent. Documentation of the ABS polymer ABS-M30 used by Stratasys Inc. for FDM extrusion is exhaustive and most data relevant for processing and application is published as a white paper[37]. ABS-M30 has a tensile strength of 33Mpa, and a Glass Transition Temperature of T_g≈108 °C. The extrusion temperature is typically ≈280-300 °C for FDM application. A disadvantage with ABS over PLA is that large build-jobs can tend to curl off the build-platform of the FDM machine as internal stresses due to thermal shrinkage, that tend to accumulate within the manufactured parts.[17] Keeping the polymer structure above T_g during the entire build-job is therefore needed.

Polycarbonate is also commonly used thermo-polymer in industrial processes, yet less used in FDM processes. Like ABS it is amorphous of nature, and as ABS a true melting point is nonexistent. Documentation of the ⌜*Fortus Polycarbonate (PC)*⌟ polymer used by Stratasys Inc. for FDM extrusion is as with their ABS counterpart exhaustive documented and most data relevant for processing and application is published as a white paper[38]. The Fortus PC has a tensile strength of 57Mpa, and a Glass Transition Temperature of T_g≈161 °C. The extrusion temperature is typically >300 °C for FDM application.

2.4.2 Materials for Polymer based SLS

Selective Laser Sintering of polymers, as FDM, use thermo-polymers and thermal input to bond these to solid structures. SLS however employ granulate as processing stock material, and employ different thermo-polymers than those of FDM. Commonly used thermo-polymers can be found in figure 2.17. In the schematic representation their thermal resistance, crystallinity and their field of application is stated. The term ⌜*General Purpose*⌟ is used for those granulates where little demand is set to thermal and mechanical material properties. ⌜*Engineering*⌟ is used to describe those polymers applicable for SLS manufacturing where certain demands to either thermal resistance or mechanical properties are needed. The final category, ⌜*Advanced*⌟ is for the last class, where especially thermal properties are outspoken. The heat resistance is indicating to which temperatures the different polymers are still mechanically stable. The crystallinity is mainly linked to whether the polymer has a true melting point (highly crystalline) or whether they gradually soften as temperature is elevated[39, p. 40].

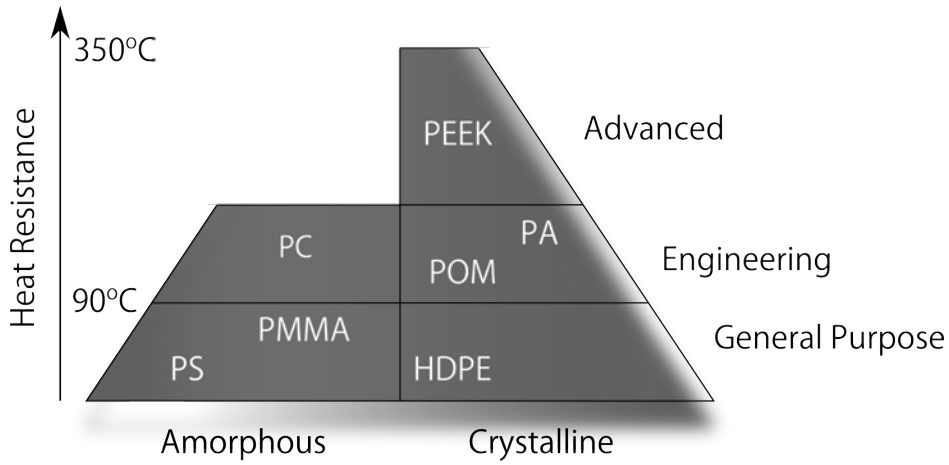

Data source: Consolidation of Polymer Powders by Selective Laser Sintering [26]

Figure 2.17: *Polymers used in SLS and their application, thermal resistance and crystallinity*

From the lower left to the upper right section of the graph is first Poly Styrene (PS, $(C_8H_8)_n$), a highly amorphous general purpose polymer, naturally transparent, and is processed at ≈180 °C. [39, p. 549]. Next is Polymethylmethacrylate (PMMA $(C_5O_2H_8)_n$), an amorphous general purpose polymer that exhibit high modulus of elastically and high strength. Processed at ≈ 200 °C and slightly

more thermally resistant than PS.[39, p. 577] High-density Polyethylene (HDPE, $(C_2H_4)_nH_2$) is unlike the aforementioned SLS granulates crystalline in nature. It is processed at ≈ 260 °C and is available wide widely differing properties which is governed by the degree of homo-and copolymerization. HDPE exhibit relatively low strength and stiffness, though high toughness and elongation at break.[39, p. 516-517] Polycarbonate (PC, $(C_{16}H_{14}O_3)_n$) is an amorphous engineering grade polymer available for SLS processing. This is seen in processing temperature of ≈ 280 °C which is comparably higher than the standard grade polymers. PC is available in any color, and color intensity, comes naturally transparent. It is very impact resistant and exhibit a high strength and stiffness in a wide temperature range from -150 to 135 °C.[39, p. 600] Following PC is Polyoxymethylene (POM, $(CH_2O)_n$) Crystalline of nature and categorized amongst the stiffest and toughest thermoplastic materials, with good slip- and wear resistance. Processing temperature is ≈ 175 °C. It is worthwhile to note that POM is diligent when it is processed, as POM decompose to gaseous formaldehyde at temperatures above ≈ 220 °C. The high strength of POM makes substitution of parts traditionally made by metals suitable. Examples are gear wheels, levers, screws, coils and fittings.[39, p. 584-585] Polyamide-12 (PA-12,$NH(CH_2)_{12}CO)_n$) is the third engineering grade thermo polymer used within SLS. This polymer is interesting as it account for 95% of all SLS parts produced[26]. It is processed at ≈ 200 °C. PA-12 is prone to absorb water and therefore must be pre-dried before processing. PA-12 exhibit hard and brittle properties just after processing. As PA-12 is allowed to reabsorb water, the polymer swell and the brittle properties are altered thus becoming less prone to cracking. PA-12 is known for good slip and wear properties, and is chemically resistant. PA soften at relatively low temperatures which makes it unsuitable for some static load-bearing applications.[39, p. 586-590] The last polymer is Polyetheretherketone (PEEK, $(OC_6H_4OC_6H_4COC_6H_4)_n$. Solemn being categorized as a polymer for advanced applications. This as PEEK has excellent chemical and thermal resistance, a high tensile strength. PEEK is processed at a high temperature of ≈ 350 °C which again reflect the polymers excellent thermal resistance. [39, p. 622-623]

2.4.3 Materials for Metal based SLS, SLM, EBM and LENS

Photo-initiated resins and thermo-polymers used within Additive Manufacturing, are often proprietary consumables sold to specific machine models, and mechanical, thermal and chemical properties are little known. It is very different with metals for SLS, SLM, EBM and LENS. An abundant variety of alloys exist and can be purchased from a variety of independent sinter-powder manufacturers. As such it can be difficult to fully cover the materials available for, and the material properties of these powders. Commonly used sinter powders are stainless steel alloys (316, 304L, 309, 174), maraging steel (M300), pre-hardened 718 steel, titanium

alloy(6AI-4V) and nickel based super-alloys, all of which has well-characterized physical properties and as such will not be discussed further.

2.4.4 Resins for photo-initiated polymerization

Initially resins used within Additive Manufacturing for SLA equipment was acrylate based, which produced brittle parts with inferior mechanical properties to most thermopolymers.[13]. Acrylates are still used within SLA, Resin based 3DP and DLP but find fierce competition from newer epoxy based resins with a higher degree of industrial applicability. [21] Exact chemical composition, mechanical thermal and chemical properties, are difficult to obtain for industrially available resins for additive manufacturing. However as either acrylates or epoxies are used, it is possible to derive what photo-initiation mechanisms are employed for these two general categories of materials. The two dominant curing methods use ultraviolet light (UV). For acrylates the mechanism is radical-curing and for epoxies the method is cationically-curing.[40] The two mechanism employ different photoinitiators. The photoinitiator in epoxies is commonly an aryldiazonium salt such as the salt phenyldiazonium tetrafluoroborate. In acrylates the photo initiator is often a carbonyl-containing compound as benzophenone.[41]

The photoinitiation mechanism for acrylates is shown in figure 2.18. Benzophenone ($(C_6H_5)C_2C{=}O$) is the photo-initiator. The double-bond in benzophenone is shattered by photons emitted in the UV spectrum and attack the hydrogen-bound radical. The activated radical and the benzophenone molecule, form $(C_6H_5)C_2C$-OH R·. Two altered benzophenone molecules react by dimerisation to $(C_6H_5)C_2C$-OH - C-HO-$(H_5C_6)C_2$ + R·. The radical attack a benzophenone ring of the acrylate monomer, shatter it open after which it polymerize with the neighboring molecule.[42]

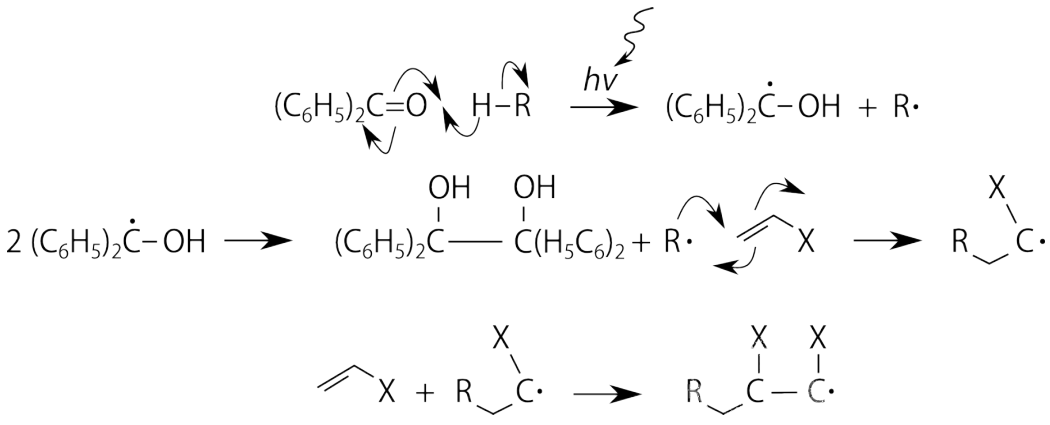

Figure 2.18: *Mechanism of photoinitiation of acrylates: Benzophenone radical photoinitation.*

The photoinitation mechanism for epoxies is shown in figure 2.19 and is based

upon diazonium salts which contain the aromatic ring-molecule benzene (C_6H_5). An UV photo-initiated reaction of phenyldiazonium tetraflouroborate (C_6H_5-($N{\equiv}N^+BF^-_4$) is initiated by the shattering of the unstable triple-bond. This cause a break-down to, fluorobenzene (C_6H_5F),nonaqueous triflouroborate salt, (BF_3) and nitrogen, (N_2). Triflouroborate is hydrated by atmospheric bound water, (H_2O), absorbed from the ambient air, and as aqueous salt, it react with the epoxide,  , by cationic ring-opening polymerization to form epoxy.[43]

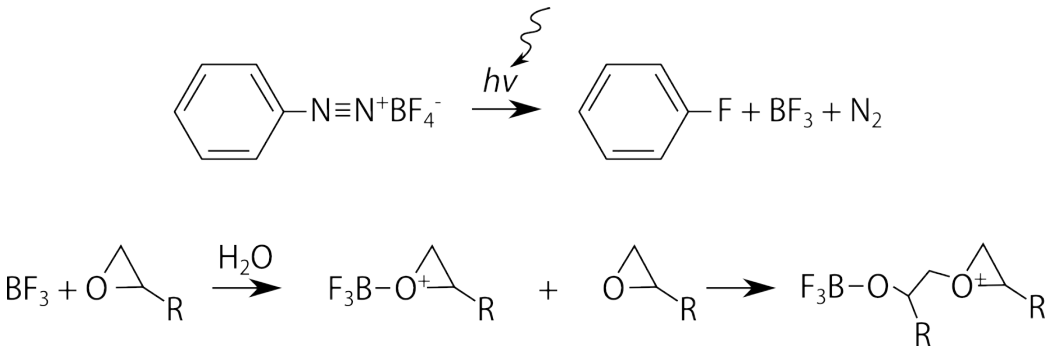

Figure 2.19: *Mechanism of photo-initiation of epoxies: Phenyldiazonium tetraflouroborate cationic photoinitiation*

The radical based photoinitation of acrylates and the cationic based photoinitation of epoxies shown in figure 2.18 on the preceding page and 2.19 are simple photoinitation mechanisms. It is important to state that commercially available photo-initiated resins contain many additives to improve the behavior with respect to influence of temperature, degradation, polymerization termination reactants and long-term stability. These are often not specified by the supplier and as such will not be addressed further.

2.4.5 Materials for powdered based 3DP

The novel material for powdered based 3DP printing is gypsum based powders. The rehydration mechanism employed follow the reaction: $CaSO_4{\cdot}\frac{1}{2}H_2O{+}3H_2O \Longrightarrow 2CaSO_4 \cdot 2H_2O + heat$ [44] Little more is to the mechanism and as such it will not be addressed further.

2.5 Systems Monitoring in Additive Manufacturing.

One key strength in Additive Manufacturing is the freedom of close-to unrestrained geometrical part design. This strength however cannot be employed to its full potential as the manufacture of geometries with great complexity is limited by

subsequent difficulties to verify their tolerances. This paradox is present for all parts containing internal and inaccessible features that cannot be handled by traditional metrology equipment such as Coordinate Measurement Machines (CMM). As Additive Manufacturing technologies are still in its prevenient state, systems monitoring is primarily oriented on a sensority level where process parameters such as material addition unit temperature, build chamber temperature, laser power and protective gas levels are monitored.

It is by the author believed that the additive manufacturing processes will benefit from a much more complex systems monitoring level. Hence one main area of focus in this thesis is the proposal of an in-line reverse engineering and 3D reconstruction system that allows for a true to scale in-line 3D reconstruction of parts that is being additively manufactured on common powder-bed based systems, such as 3D printing and Selective Laser Sintering equipment. If such systems are integrated in additive manufacturing machines it is thought to be possible not only to monitor process instabilities inline yet more interesting to verify production in a manner similar to 3D scanning and Computer Aided Tomography (CAT/CT).

Similar advanced monitoring methods has their prevalence widespread in industrialized processes Ranging from food processing over manufacturing engineering, semi-conductor manufacturing to intricate tasks such as surgery and inspection in the transportation industry.

Vision aided robots are used in livestock processing plants to ensure that cutting robots make most of the consumable resources. Vision systems ensure tasks from alignment during assembly through process inspection to metrological measurements in manufacturing. In the semi-conductor industry micro chips are inspected by vision based systems before encapsulation in polymer casings. Surgery is performed by the surgeon off-location using remote controlled utensils, aided by advanced vision technology. Inspection ranging from penetrating scanning of containers to scanning of carry-on luggage is carried out by vision systems while supervised by personnel.

The benefits of vision systems in Additive Manufacturing is of equal perspicuous magnitude. It is yet a task to be devout. Most significant it is yet to the additive manufacturing industry to stipulate a base of standards to how vision systems can aid in metrological inspection of additively layered manufactured parts. An explicit consent to such standards however will ensure that the granted geometrical freedom of additive manufacturing processes can be employed to its ambit. Proliferation of such standards by ISO standards would greatly bolster this.

2.5.1 Scanning Technologies

3D scanning (including CAT/CT) is a branched set of technologies that allow for digitalization of physical objects for generation of CGI models and CAD models. Geometrical 3D scanning is widespread as a tool for geometrical meteorology and reverse engineering. The basic working principle behind 3D scanning varies

from what underlaying method the scanning method employ. Some of the most prevalent technologies used are listed in table 2.8

Table 2.8: *3D Scanning Methods and their fundamental principle*

Method	Fundamental Principle
Tactile	Digitalizaton by touchprobe using an articulated or cartesian positioning and feedback system.
Stereo Vision	Biomimicry of triangulation by feature recognition from stereo preception.
Laser Scanning	Contour tracing from vision data aided by line-laser projected to a surface
Fringe Scanning	Contour tracing from vision data aided by a projected fringe pattern to a surface.
CAT/CT Scanning	Penetrating scanning by employing an array of X-ray emitters and detectors.

Tactile 3D reconstruction

Tactile 3D reconstruction is a method for digitalization of surface geometries by physical interaction with the specimen. This can either be by employing a cartesian robot system as is done in coordinate metrology, or by employing a pen-like device on an articulated arm that is operated by hand. Measurements tolerances are generally high, however the information density of surfaces is low, and quantified by how many times the surface has been probed by the tactile instrument.

Stereo Vision

Stereo vision is the biomimicry of stereopsis by interpretation of sensoritory vision in vertebrate animalia. Employing two cameras with a parallel viewpoint, offset a known distance, it is possible to generated a depth-image by means of feature-recognition and triangulation. Whereas triangulation is a trivial task, the applicability of stereo vision is limited by the state-of-development of feature-recognition and disparity mapping algorithms within computer vision. This render stereo vision a technology that is mainly applied for robot-vision and collision avoidance systems in the automotive industry.[45]

A preliminary assessment of the capabilities of computer stereo vision was conducted and documented in a technical white-paper by the author.[46] The investigation consisted of an implementation and experimental tests of a disparity mapping method described by Klaus et al.[47] The stereo camera setup that was use for the investigation was comprised of two we cameras fixed to a bar, and is shown in figure 2.20 on the following page. It proved possible to obtain depth maps

from this experimental system, yet as shown in figure 2.21 on the next page, the depth maps obtained was not up to par with accepted geometrical reconstruction methods.

Figure 2.20: *An experimental stereo camera system employing two high-resolution web cameras.*

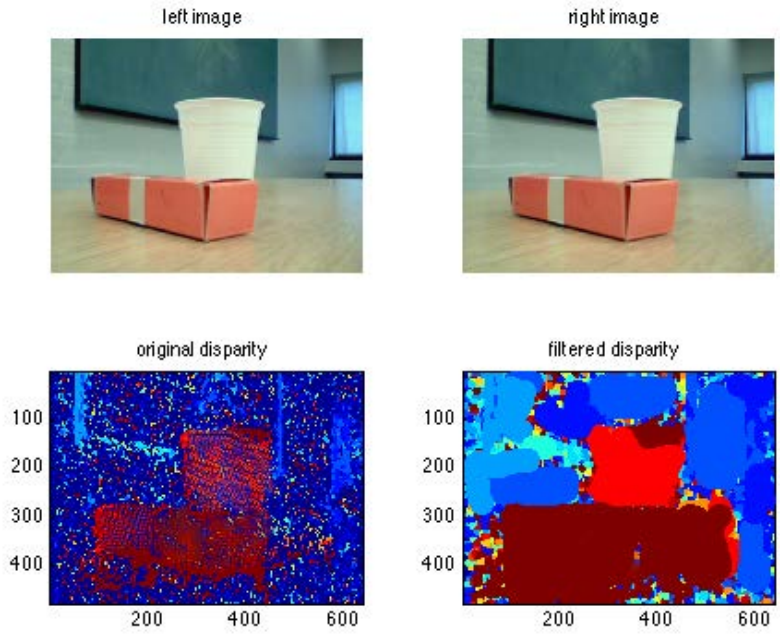

Figure 2.21: *A stereo photography and a depth map reconstruction based upon disparities.*

Laser Scanning

Laser scanning is as stereo vision based upon triangulation. If one of the two cameras in a stereo vision system is replaced by a laser source projecting a line of visible monochromatic light to an object, it is no longer needed to base triangulation measurements by complex feature detection and disparity mapping algorithms. As back-scattered laser light will clearly be distinguishable from the surroundings in the imaging plane of the camera, a simple detection algorithm can thus form the base for triangulation.[48] Industrial scanners systems often bestow several traverse and rotational axis to manipulate the perspective of the camera relative to the specimen.

An investigation similar to the stereo vision systems investigation was conducted for a rotary-table based experimental scanning system, and described in the same white-paper.[46] This experimental system relied on a turn-table to rotate objects as image series was acquired. Not relying on a line laser, the system employed discrete illumination from an angle perpendicular to the camera view angle to obtain information about the silhouette of the object to be scanned. Figure 2.22 on the following page show how images was acquired from the turntable system.

High resolution scans based from the silhouette of object was achieved. A

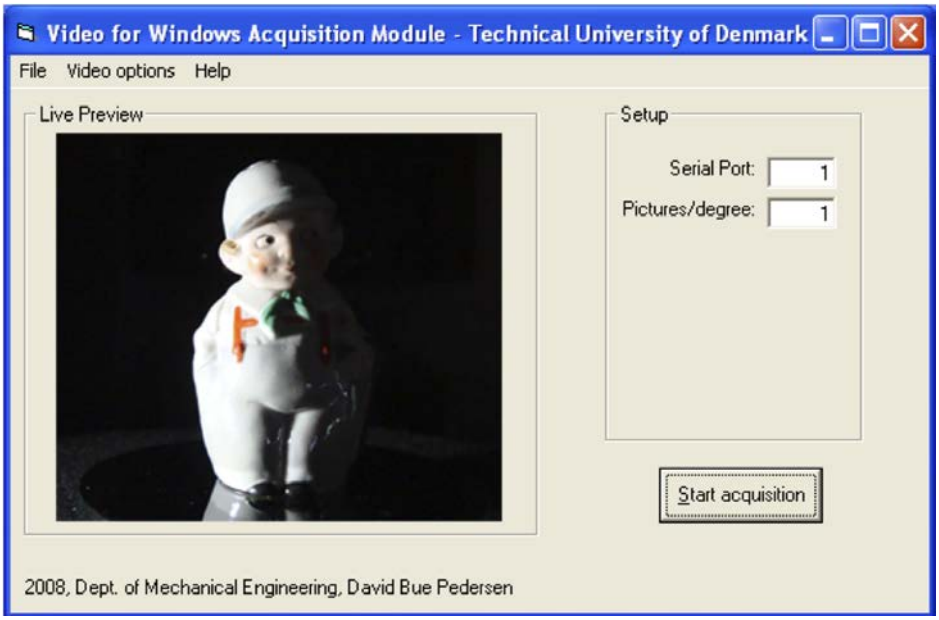

Figure 2.22: *An experimental discrete illumination scan system from a preliminary vision systems analysis.*

geometrical reconstruction of a small figurine using the experimental setup can be seen in figure 2.23 on the next page. However, this method using discrete illumination is sub-par to using line-laser based scanners. The method rely on the silhouette of the geometry, and as such certain concave surface sections cannot be detected. The experiment was yet not an effort to achieve up-par reconstruction as it was an exercise in understanding strengths and weaknesses of a method similar to line laser based 3D scanning, projected to reconstruction of additively manufactured geometries.

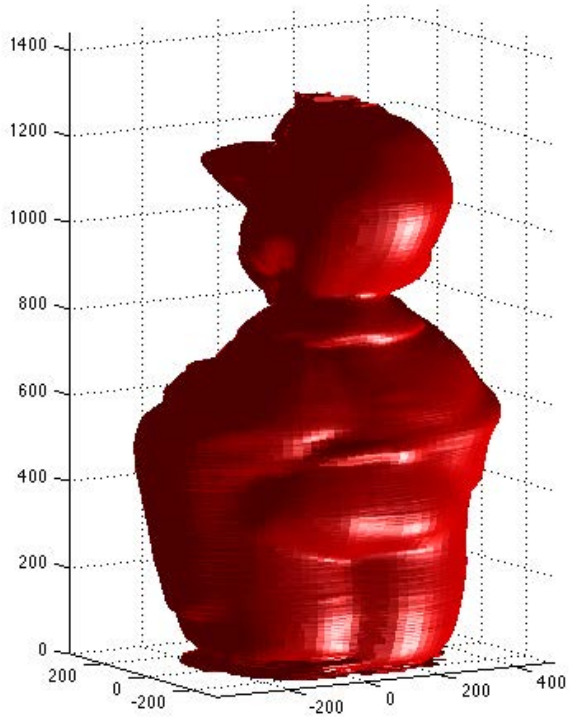

Figure 2.23: *A geometry reconstruction using discrete illumination, a principle similar to line laser scanning.*

Fringe Scanning

Fringe scanning systems is a derivative of laser scanning systems. These systems rely on a fringed pattern being projected to the object by means of a video projector. The pattern substitute the line laser and allow for geometrical reconstruction from each fringe line hereby increasing the sample rate of data points on the specimen. The basic reconstruction principle is a triangulation method.[48] As with industrial 3D scanners, most fringe based systems bestow several traverse and rotational axis to manipulate the perspective of the camera relative to the specimen.

CAT/CT Scanning

CAT/CT scanning is unlike the aforementioned methods a penetrating scanning method. This gives CAT/CT scanning the exclusive ability to be used for inspection of hidden internal geometries. CAT/CT scanning employ an X-ray emitter and sensor to determine radiation absorption through a solid body. Absorption is proportional to material density and material volume. From a scan over a specimen by emitter and sensor, it is possible generate an absorption map as an image

map. There exist many different sensor/emitter configurations. The simplest configuration is a parallel beam setup as seen in figure 2.24.[49]

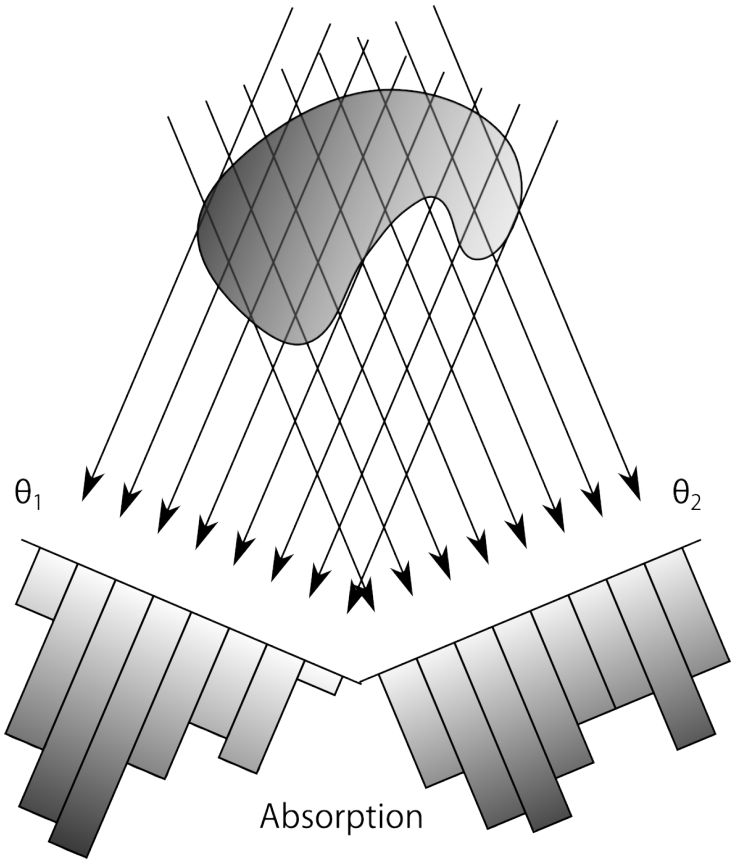

Figure 2.24: *Parallel sensor/emitter configuration at two different angles. Bars indicate absorption levels.*

Figure 2.24 represent a 2D scan-slice of a 3D CAT/CT scan. At angle θ_1 the sensor is scanned linearly at a normal to the beam propagation direction. As the sensor pass over the specimen, absorption level and position is recorded. This indicated by the bar plot at θ_1. The specimen (or emitter/sensor array) is rotated to the angle θ_2. Another linear scan-path at a normal to the beam propagation direction is made, while position and absorption levels are recorded. As each single X-ray pass through the specimen, the ray is the attenuated.[49] This can be described by formula 2.3. If the intensities before and after passing through the sample is I_0 and I_i, the total attenuation is given as b_i.

$$b_i = -log\frac{I_i}{I_0} \tag{2.3}$$

The amount of attenuation each X-ray exhibit is governed by the attenuation coefficient of the material the specimen is comprised of. Dense materials such as steels has a higher attenuation coefficient than that of polymers. A simple computational model of a series of linear scan-paths at varying angles θ (figure 2.24 on the preceding page) of a parallel sensor/emitter configuration can be achieved by assuming constant attenuation throughout the specimen. This however impose that the specimen must be of one material of uniform density. Let an NxN matrix be called X_{image}, and let it describe the image plane shown in figure 2.24 on the facing page. Let N be the hight and width of the image matrix in pixels. Given the CAT/CT scan image is already known, it is trivial to calculate the attenuation for each sensor position and rotation. The invert problem however is what need to be solved.

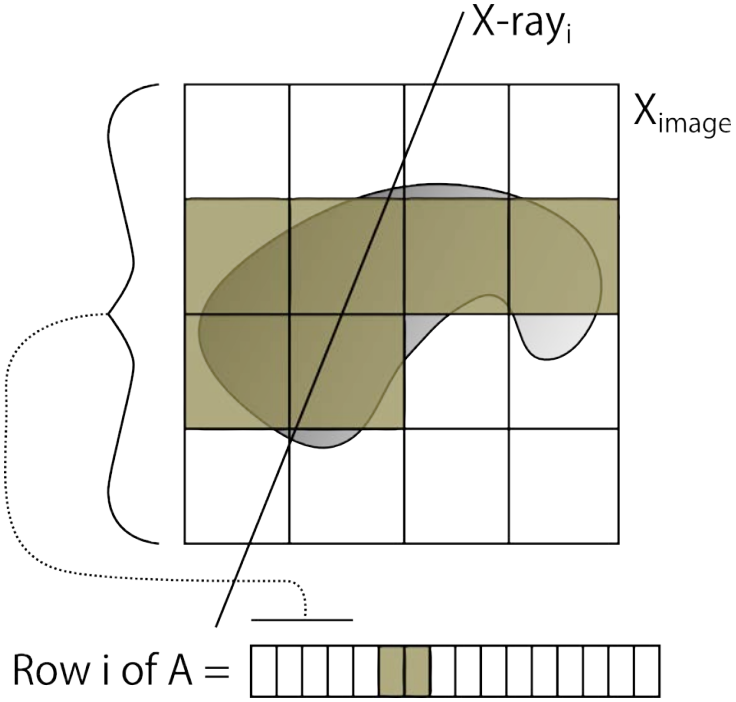

Figure 2.25: *The X_{image} image plane matrix, an X-ray, and its description in the system matrix A.*

Let M be the total number of X-ray measurements of rays with known direction and starting point. Let A be a system vector of length $NxNxM$. Let A be a row-vector, where each column of N is stacked one an after as described in figure 2.25. If the image $x = X_{image}$ is known, it is easy to set up the system matrix A from the known direction and starting point of each X-ray. Subsequently it is trivial to compute the estimated raw data, b, by $b = Ax$. The inverse problem, to reconstruct image data from A and measured raw data, b, seem equally trivial. However solving $x = A/b$ is impose complications especially when noise on the raw data, b,

is present.[50] The problem is a mathematically ill-posed problem as measurement errors will be magnified and render such reconstruction attempts useless.

Fortunately, iterative approaches can however be used to solve this ill-posed problem. One such method, the Cimmino method, can be applied in order to produce useful reconstructions. It is an iterative method that start from an initial guess, x_0, typically of the zero-image. The method use the diagonal matrix of elements defined by the norm of the rows of the system matrix, A, to weigh the calculated solution throughout each iteration. The Cimmino method has a regularizing property when applied to discrete ill-posed problems, and the high degree of parallelism of the algorithm. It is therefore suitable for implementation for multi-threaded numerical application, and it has a method known for application especially in computerized tomography.[51]

Vision systems in Additive Manufacturing as a method for enhancing build-quality and as a means of geometrical verification.

3 Vision Systems

The ability to manufacture geometries at a complexity that is unprecedented by any other manufacturing technology open up for new design and product development opportunities that can forth a leap in technology advancement that may thrust industrialism into the next industrial age of digital and autonomous manufacturing. Before this to happen, there are several barriers that need to be crossed in order to advance into the industrial frontier of manufacturing technologies. One of the most prevalent impediments is the limited ability to verify geometrical tolerance of structures which esteem the geometrical potential given by additive manufacturing processes. An assessment of available technologies for geometrical verification of complex geometries has already been given in chapter 2.5 on page 61. Now, a novel approach to geometrical verification of additively manufactured structures will be introduced.

3.1 Analysis for Generic similarities of Additive Manufacturing processes

A novel approach to geometrical verification of additively manufactured structures has been the result of an analysis of the feasibility of the proposal of a common approach to verification of additive manufacturing technologies, if these are regarded as one generic process, a process family sharing similarities, irrespective of the specific characteristic of the given sub-processes. Common denominators can be derived from the study of the additive manufacturing technologies that was given in section 2.3 on page 37. These denominators has been listed in table 3.1 on the following page for detailed assessment. Exclusively common and industrially relevant processes has been assessed. As such LENS and LOM has not been included in the chart.

Most outspoken is the similarity that all processes are additive. A structure is realized from an empty build-envelope. Second is the fact that all processes are layered. As structures are built layer-by-layer, material addition does not follow a true 3D control scheme where contours are traced in the vertical plane. As a

result, structures are defined from they layers of which they are comprised. All additive manufacturing processes that are industrially applicable have the ability to manufacture parts of geometrical tolerances that are acceptable for direct application. As such, machining allowance is typically not added to structures. If SLS or SLM is employed, some surfaces may require subsequent machining, and it is common to add allowance to certain surfaces. Some surfaces are yet left untouched. This is prevalent for hidden features which is another common denominator. All industrially applicable additive manufacturing processes retain the ability to procure hidden features within structures. Channel systems, internal functional surfaces and kin alike, are not visible from an exterior inspection of the structure. As such, these features are difficult to verify employing traditional verification methods such as tactile and optical measurement methods. Finally as all processes build structures following a $2\frac{1}{2}$D layered method, structures will accumulate residual stresses with each added layer. These stresses continuously elastically deform and warp the parts as they are built. If structural support is added to parts, a fraction of these stresses will be released during the removal of support at post processing, resulting in a spring-back effect.

From these process similarities a generic vision based geometry reconstruction method is proposed. The method will be described, demonstrated and verified in

Table 3.1: *Additive Manufacturing Technologies. - Process similarity chart.*

Similarity	Relation
Additive Manufacturing	All processes follow an additive control scheme, where a material deposition unit add material to a build-envelope being a platform or a chamber.
Layered Manufacturing	All common processes are layered processes, and as such all geometries are manifested from a $2\frac{1}{2}$D control scheme. processing scheme. (LENS being uncommon)
Functional Surfaces	It is infrequent that post manufacturing allowance is needed for additive manufactured parts. If machining allowance is accounted for most often some surfaces are left untouched. As such geometrical demands for parts are high.
Hidden Features	All common industrially applicable additive manufacturing technologies allow for the manufacture of hidden geometry that cannot easily be geometrically verified using traditional methods such as tactile scanning or 3D scanning.
Residual Stresses	All additive manufacturing processess given their layered nature will produce structures with a build-up of residual stresses.

the following sections.

3.2 Formulating a generic vision system for geometrical reconstruction in Additive Manufacturing

Given all industrially applicable additive manufacturing processes are layered, a generic geometry reconstruction method is suggested, where each layer is inspected prior to addition of the successive layers. If each layer can be characterized in a manner so that the boundaries of the layer can be found, and the machine build layer height is known, a three-dimensional model can be rendered from the accumulated data gathered during a build-job. The hypothesis is, that spite the tendency to accumulate stresses, and suffer from elastic deformations, that any structure from any additive manufacturing method exhibit during a build-job, the undeformed layers characterized by such system will yield sufficient data to assess whether defects of internal geometries are present. These being inclusions visually present from one or more of the inspected layers, the collapse of weakly supported features, and kin alike. Furthermore the hypothesis is that many additive manufacturing processes introduce so few stresses in parts, that the relaxed representation given from such system will yield a fair accuracy of reconstructed geometries. Within some processes where stress build-up is prevalent, such as with SLS and SLM, a superimposed numerical warp analysis of the relaxed geometrical reconstruction governed by boundary conditions known from the process and the geometry may yield a fair accuracy of reconstructed geometries. The latter will not be addressed within the scope of research.

Inline inspection of layers during additive manufacturing

If an inline inspection of layers during an additive manufacturing job is not to obstruct with the manufacturing process, it is proposed that such system will be a vision-based inspection system. Figure 3.1 on the next page show a principal sketch of the integration of such system on a powdered based 3DP machine. A camera vision system is positioned overseeing the build-surface of the machine. Once a layer is built, the binder print head parks outside the build envelope, to accommodate for the recoating unit to traverse over the build-surface. As this happen, a high resolution image is acquired, from which boundary information of the layer that just have been build can be extrapolated. Upon completion of succeeding layers, the imaging routine is repeated till completion of the entire build-job.

Once an entire set of images is gathered, representing each layer from within the build-job, the three dimensional geometry can be extrapolated from images of the individual layers of the build-job. In the schematic implementation in figure 3.1 on the facing page, the powderbed based 3D printing process involve wetting layers of plaster. A contrast change between wet and dry plaster is clearly visible. This

makes it possible to numerically extrapolate the boundary of the cross-section separating each deposited layer. From these data a 3D geometry can be reconstructed. Figure 3.2 on the next page depict this principle.

The intent is to parse all images of a build-job to first form a point cloud describing the geometry, second to generate a wireframe representation of the geometry where the relation between points inter- and exter-layer described. The first image must be numerically processed by a boundary detection algorithm. This algorithm determine each pixel in the image that contribute to a boundary, and store this pixel in memory. The next image will be numerically processed by the same boundary detection algorithm, and each pixel that contribute to a boundary is detected. The method involve repeating this procedure for each layer that has been built. Upon completion of the boundary detection of all image frames, a point cloud of coordinates in pixel units in the horizontal plane and layers in the vertical direction, has been generated. Next a meshing algorithm generate a wireframe mesh by meshing in-between each image layer.

Post generation, the wireframe mesh need to be corrected to world-coordinates. If the vision system is characterized it is possible to derive the length and width of each pixel in length units, and hereby convert vertical coordinates to length units. As the additive manufacturing machine build each layer at a certain height, the height of each layer is already given by the process, and can within the position-tolerances of the additive manufacturing platform be accounted for thus scaling

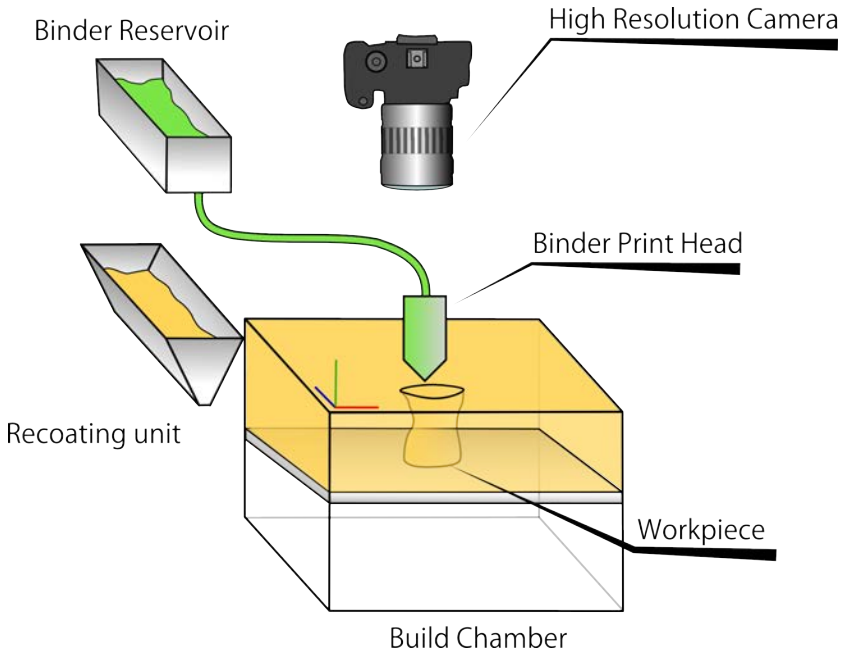

Figure 3.1: *Proposal of a system for layer inspection of additive manufacturing build-jobs*

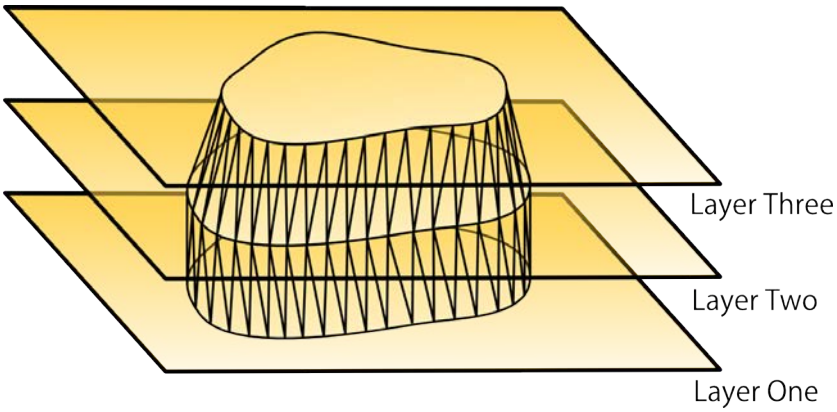

Figure 3.2: *Reconstructing the 3D geometry from layer inspection of additive manufacturing build-jobs*

the vertical height of the generated point cloud to length units.

3.3 Method implementation of a generic vision system for geometrical reconstruction in Additive Manufacturing

Given no similar methods for geometrical reconstruction of additive manufacturing has been found to be subject to similar research, development of vision systems for inline geometrical reconstruction applied to additive manufacturing was initiated at zero ground. As such is was found valuable to introduce a portable system that can be set up within a wide variety of additive manufacturing platform environments. A portable system that can serve as a proof of principle for geometrical reconstruction from layered in section of the wide palette of additive manufacturing systems in existence. Thus given the system must be portable, flexible and easy to set up it was decided to base the vision system on a digital single-lens reflex camera, commonly known as a DSLR camera. This is a professional class of digital cameras with interchangeable lenses, that allow for a high level of control of the imaging system. The ability to change lenses, and employ zoom lenses makes this class of cameras flexible to set up as a capturing system. This is of prevalence, as it can be expected that the physical frame of many additive manufacturing machines hinder an ideal positioning of the camera, let alone that a fixed camera setup integrated in an additive manufacturing machine that serve a multitude of purposes in a laboratory environment may suffer from a practical point of view from having a camera system permanently integrated into the frame. It can be expected that for some of the platforms that is sought to be investigated, that the camera must be set at an angle to the build chamber, at various distances, to optimize the use of the image frame to the build area of specific build jobs, which again will alter the focal setting and zoom of the camera lens. This makes the camera calibration which allow for conversion from pixel units to world units a procedure that must often be undertaken, and which is tedious unless an automated method is implemented.

3.4 An assessment of a DSLR camera

It is incontestably given that any vision system can but outperform its applied camera system. As such an understanding of the composition of the DSLR camera class is needed. A DSLR camera can introduce imaging distortion errors can be from manyfold sources. Any source from lens grinding affecting the beam path, through angular and translatory alignment errors as most lens arrays provide mechanically inter-positional lens elements, to the angular alignment of lenses and mirrors to the CCD chip or imaging plane affect the resultant image .

Figure 3.3 on the following page show a principal sketch of the light-path through a generic DSLR camera. Readily observable sources that loom to cause

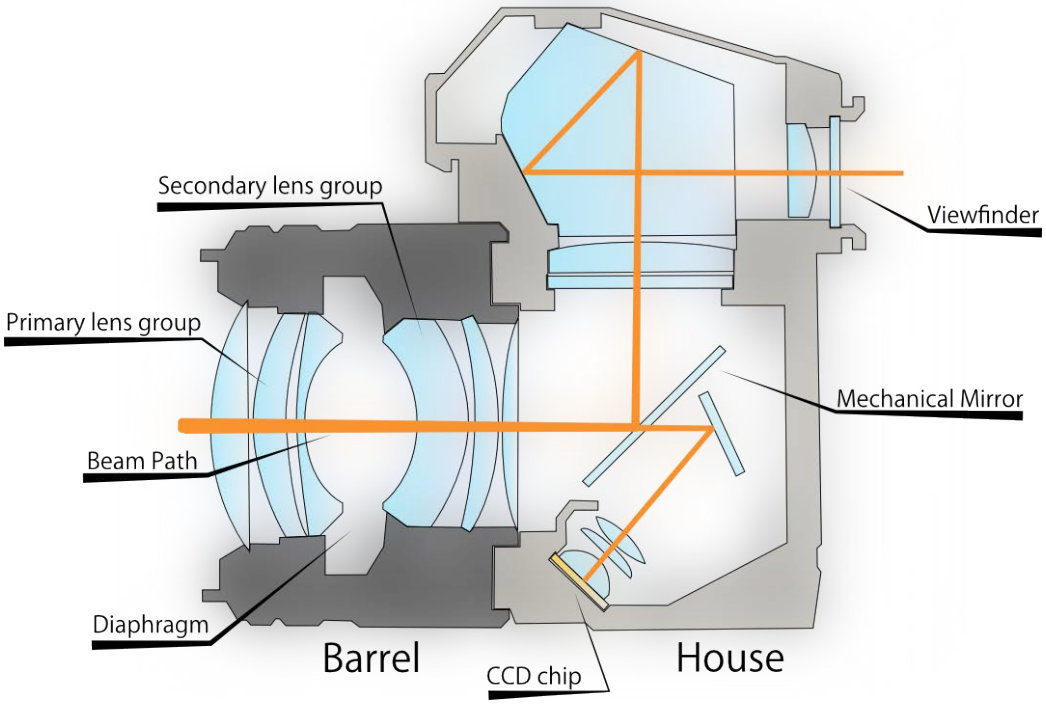

Figure 3.3: *A principal sketch of a generic SLR camera*

distortion to the image projected onto the CCD chip are classified into two major classes. Static and dynamic. Dynamic errors are to a high extent governed by the camera barrel, which is the term used to describe the interchangeable camera lens system. When the lens is adjusted for zoom and focus, or interchanged with another, the lens configuration is altered and errors superimposed through the camera system different The static errors are governed by the lens system and mirror arranged within the the camera house. An awareness of what operations are interacting with the dynamic error class is important in computer vision as any change in the camera characteristics require a recalibration of the system. As such, a DSLR camera with user configurable dynamic zoom and focus on the one side allow for flexible integration in a variety of additive manufacturing processes, yet the flexibility of zoom and focal adjustments deteriorate the robustness of a vision system. Thus camera calibration and recalibration must be carried out often.

3.4.1 Camera Calibration

Calibration is achieved based upon a series of numerical algorithms from Intel, known as ⌜*Open Source Computer Vision Library*⌟, the OpenCV, which can be included as a source code library for the development of vision related systems.[52]

These algorithms can be included in software development projects written in Matlab and C language, and gives the developer a access to a set of algorithms that is tailored for image processing and calibration. [53]citeopencv From these numerical algorithms, a model has been set up. The model is fully capable of characterizing a modern camera system. This is made possible by basing the model on the model of a pinhole camera. Superimposed to this model is model for radial and tangential distortions. These two model account for image distortions from the lenses that is not present in a pinhole camera but contribute to the distortion field of modern camera systems. From the complete camera model it is possible from any point in the image plane to calculate the corresponding point on the CCD plane within the camera and vice versa. From this model, a calibration routine can be carried out by means of a checker-board patterned plate. Images are acquired by the camera and from the distortion field of these images, the radial and tangential distortion contributions can be quantified. By calibration from multiple calibration images, the source data that form the base of for the calibration can be extended and a more concise calibration can be achieved. Once a camera has been calibrated it has been shown how the position of the camera in space can be calculated from any image of the calibration plate. This allow for the calculation of the camera position relative to the build envelope of any additive manufacturing process, and thus allow for flexible positioning of the camera in an experimental vision systems setup. Furthermore the image distortions induced from the camera can be corrected for. Once a camera system is calibrated and set up within the confines of an additive manufacturing machine, inline vision data can be gathered, undistorted and post processed.

3.4.2 Modeling a Camera

The pinhole camera model on which the calibration procedure rely is a model that form the base for determining the physical parameters of a camera based upon a series of images of a calibration pattern. The parameters can be decided into two categories, Extrinsic and Intrinsic parameters.[54] The extrinsic parameters are the qualifiers needed in order of make a transformation from the object coordinates, and world units which is defined as a cartesian coordinate system in the object space, through the camera coordinates. The intrinsic parameters are the qualifiers used to transform coordinates further onto the image plane within the camera, described as a two-axis coordinate system in pixel units. This transformation is made by employing a pinhole model based on collinearity. A point on the object is projected by in a straight line through the pinhole and further onto the image plane as illustrated on figure 3.4 on the next page.

The camera coordinate system has its origin at the projection center (x, y, z), also known as the pinhole. Its z axis standing as a normal to the projection plane marked in yellow. The camera coordinate system has the coordinates (X_0, Y_0, Z_0) with respect to the object coordinate system, (X, Y, Z), which can be defined

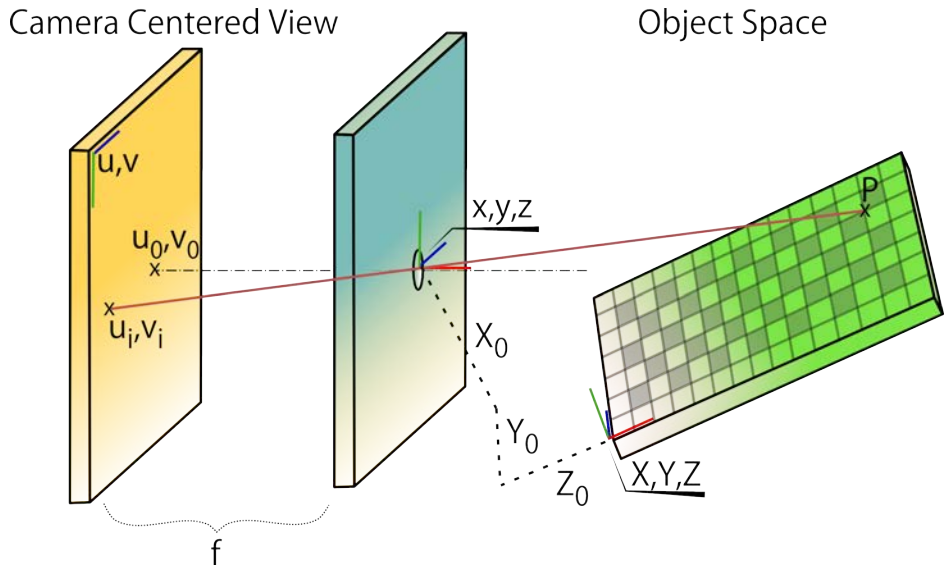

Figure 3.4: *Point projection through a pinhole*

arbitrary.

Let an arbitrary point, P, in the object space be defined with respect to the object coordinate system as $P = [X_i, Y_i, Z_i]$. It is then possible to describe the point with respect to camera coordinates by using a transformation formula based on rotation using the Euler angles ω φ and κ. A transformation function with rotational an translatory components can then be described. Let M_r be the rotation matrix given by formula 3.1:

$$M_r = \begin{bmatrix} cos\varphi cos\kappa & sin\omega sin\varphi cos\kappa - cos\omega sin\varphi & cos\omega sin\varphi cos\kappa + sin\omega sin\varphi \\ cos\varphi sin\kappa & sin\omega sin\varphi sin\kappa + cos\omega cos\varphi & cos\omega sin\varphi sin\kappa - sin\omega cos\varphi \\ -sin\varphi & sin\omega cos\varphi & cos\omega cos\varphi \end{bmatrix} \quad (3.1)$$

Transformation from object coordinates to camera coordinates can then be carried out by equation 3.2:

$$\begin{bmatrix} x_i \\ y_i \\ z_i \end{bmatrix} = M_r \begin{bmatrix} X_i \\ Y_i \\ Z_i \end{bmatrix} + \begin{bmatrix} x_0 \\ y_0 \\ z_0 \end{bmatrix} \quad (3.2)$$

Once the transfer function has been defined, the model can now be expanded to include the intrinsic parameters of the camera, so that the projection of point P can be described as a point on the image plane with the coordinates u_i,v_i. First, P will be described with the same units as those of the object space, referenced

from the principal point, u_0,v_0. Hence let $\tilde{u}_i$,$\tilde{v}_i$ denominate this position. Let formula 3.3 describe $\tilde{u}_i$, $\tilde{v}_i$. The focal length as an intrinsic parameter is used to transform the contribution of the z coordinate.

$$\begin{bmatrix} \tilde{u}_i \\ \\ \tilde{v}_i \end{bmatrix} = \frac{f}{z_i} \begin{bmatrix} x_i \\ \\ y_i \end{bmatrix} \tag{3.3}$$

Finally a transformation from object space coordinates to pixel coordinates can be performed. Hence let u'_i,v'_i describe the projection of point P on the image plane in pixel coordinates. Let D_u and D_v be transfer coefficients from object space units to pixels. It must here be noted that the direction of the secondary axis is inverted as the description of the projection of P follows the normal axis orientation in digital imaging and computer vision literature. The transformation is given by formula 3.4. Finally it can be seen that D_u and D_v is linearly dependent of the focal length.

$$\begin{bmatrix} u'_i \\ \\ v'_i \end{bmatrix} = \begin{bmatrix} D_u \tilde{u}_i \\ \\ D_v \tilde{v}_i \end{bmatrix} + \begin{bmatrix} u_0 \\ \\ v_0 \end{bmatrix} \tag{3.4}$$

With a complete description of the pinhole model written in code, it can be address how radial and tangential distortions can be modeled. The pinhole model serves as the foundation which then is expanded with a modeling of radial and a tangential distortions. Radial lens distortion which is when the point P is distorted in a radially manner in the image plane,[55] can be approximated by formula 3.5. Let k_1, k_2, ... be radial distortion coefficients and r_i be defined as $r_i = \sqrt{\tilde{u}_i^2 + \tilde{v}_i^2}$

$$\begin{bmatrix} \delta u_i^{(r)} \\ \\ \delta v_i^{(r)} \end{bmatrix} = \begin{bmatrix} \tilde{u}_i (k_1 r_i^2 + k_2 r_i^4 + ...) \\ \\ \tilde{v}_i (k_1 r_i^2 + k_2 r_i^4 + ...) \end{bmatrix} \tag{3.5}$$

Depending of the degree of distortion, several coefficients may be needed to compensate, however in most cases two coefficients are satisfactory. [54] With radial compensation added to the model, tangential distortion can be addressed. This is when the centers of curvature of the lenses in the optical path are not perfectly collinear. This type of decentered distortion yield both a tangential and radial distortion component[54]. Where the radial component of lens misalignment will be handled by formula 3.5 as a sum of all radial distortion components in the image field, the tangential component needs to be singularly addressed. Let p_1 and p_2 be be the coefficients for tangential distortion. The tangential component is then described by introducing formula 3.6.

$$\begin{bmatrix} \delta u_i^{(t)} \\ \\ \delta v_i^{(r)} \end{bmatrix} = \begin{bmatrix} 2p_1 \tilde{u}_i \tilde{v}_i + p_2 (r_i^2 + 2\tilde{u}_i^2) \\ \\ p_1 (r_i^2 + 2\tilde{v}_i^2) + 2p_2 \tilde{u}_i \tilde{v}_i \end{bmatrix} \tag{3.6}$$

With the pinhole model, and the compensation for radial and tangential distortions identified, it is merely needed to merge the three partial models to one complete, which accurately allows for compensation and calibration of any camera in a computer vision scheme. This is given from formula 3.7

$$\begin{bmatrix} \delta u_i \\ \delta v_i \end{bmatrix} = \begin{bmatrix} D_u(\tilde{u}_i + \delta u_i^{(r)} + \delta u_i^{(t)} \\ D_v(\tilde{v}_i + \delta v_i^{(r)} + \delta v_i^{(t)} \end{bmatrix} + \begin{bmatrix} u_0 \\ v_0 \end{bmatrix} \tag{3.7}$$

3.4.3 Undistortion of Frames

Undistortion of image frames employ the the pinhole model with the superimposed radial and tangential distortion components given from 3.7 in reverse. When the calibration routine has yielded the internal parameters of the camera, the model is used to undistorted frame to compensate for any lens errors in the optical path. In order to demonstrate the capacities and the potential of the model, a calibration scenario is illustrated. The calibration performed in the following is that of a Canon EOS 1000D with a EFS 18-55mm f/3.5-5.6 IS kens kit. A series of 20 frames has been taken of a 9x7 checker-patterned plate with 30mm^2 checkers. A Camera Calibration routine has been performed and the accumulated error from the lens kit characteristics and those of the camera house have been found. First, all frames are parsed through the detection algorithm, as shown on figure 3.5 on the next page.

Subsequently the image calibration routine is run, which yields the qualifying parameters of the camera. Once calculated the model can now be used in reverse to calculate the camera position in space. Hereby the camera extrinsic can be illustrated by a three-dimensional plot where for each frame, the camera position in space relative to the checker-pattern. This illustrated in figure 3.6 on page 84.

By means of the radial and tangential distortion contributions, it is possible to visualize the entire distortion model with the three plots shown in figures 3.7 and 3.8 on page 85 and 3.9 on page 86. The first showing the tangental contribution to the distortion of images, the second showing the radial contribution to the distortion of image taken with the camera, and the third showing the accumulated distortion.The gradient lines seen in the distortion plots show the length in pixels of the vectors that indicate pixel-shift. It can hence be seen that in the corners of the imaging plane, that for the complete distortion model, a pixel shift of as much as 80 pixels is detected. By using the complete distortion model as an overlay to any photograph taken at the cameras current configuration, a pixel shift can be performed to undistorted that frame. This will result in a frame that can be regarded as linear to scale.

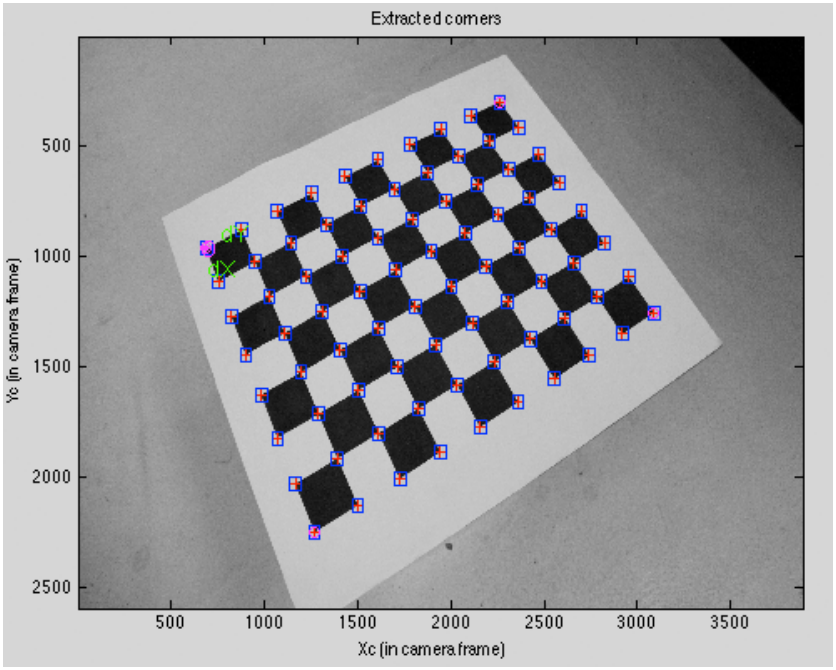

Figure 3.5: *An image parsed through the detection algorithm*

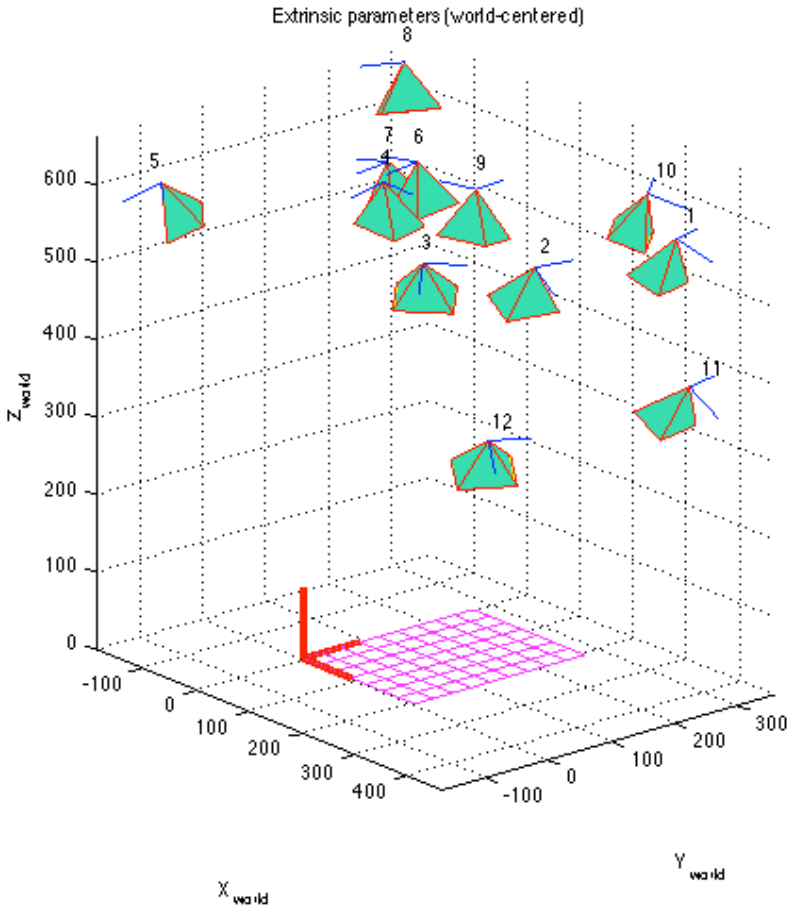

Figure 3.6: *Camera extrinsic*

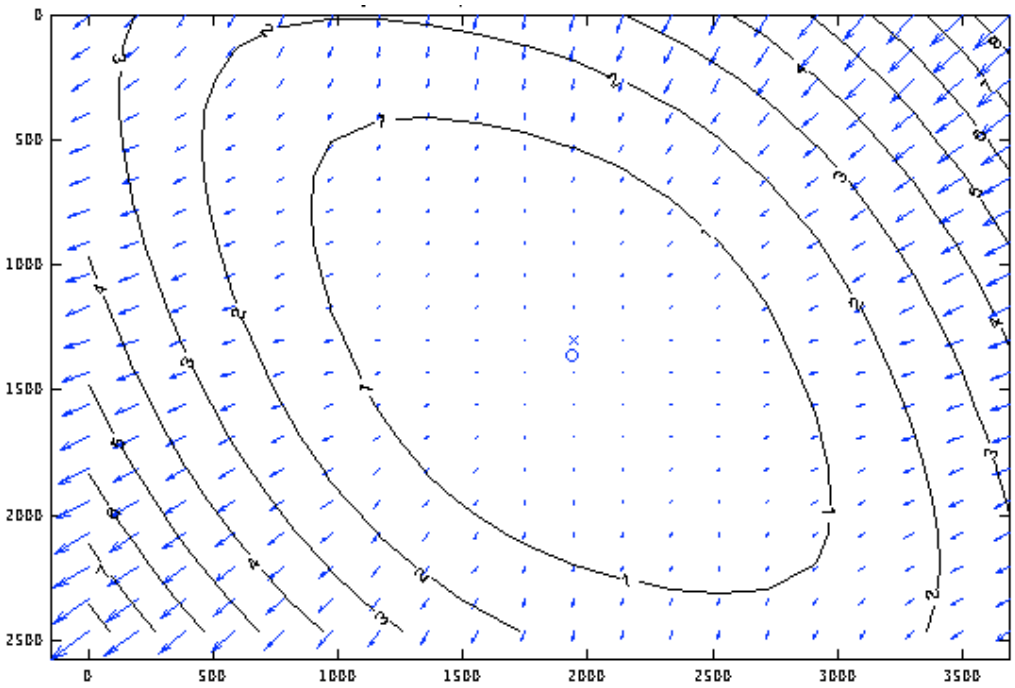

Figure 3.7: *Tangential Distortion Component*

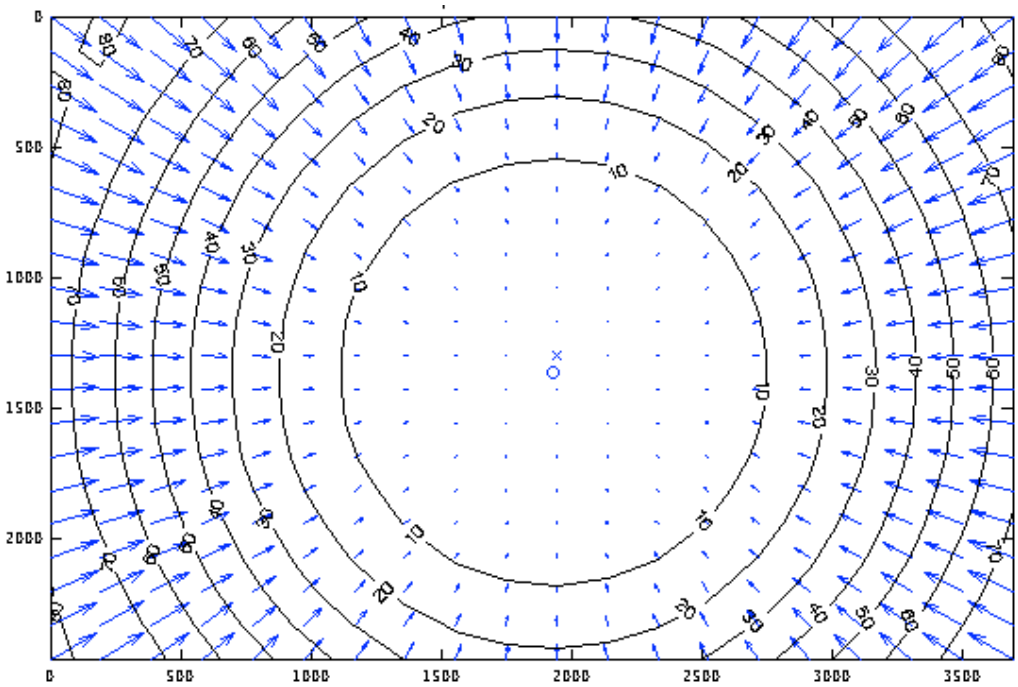

Figure 3.8: *Radial Distortion Component*

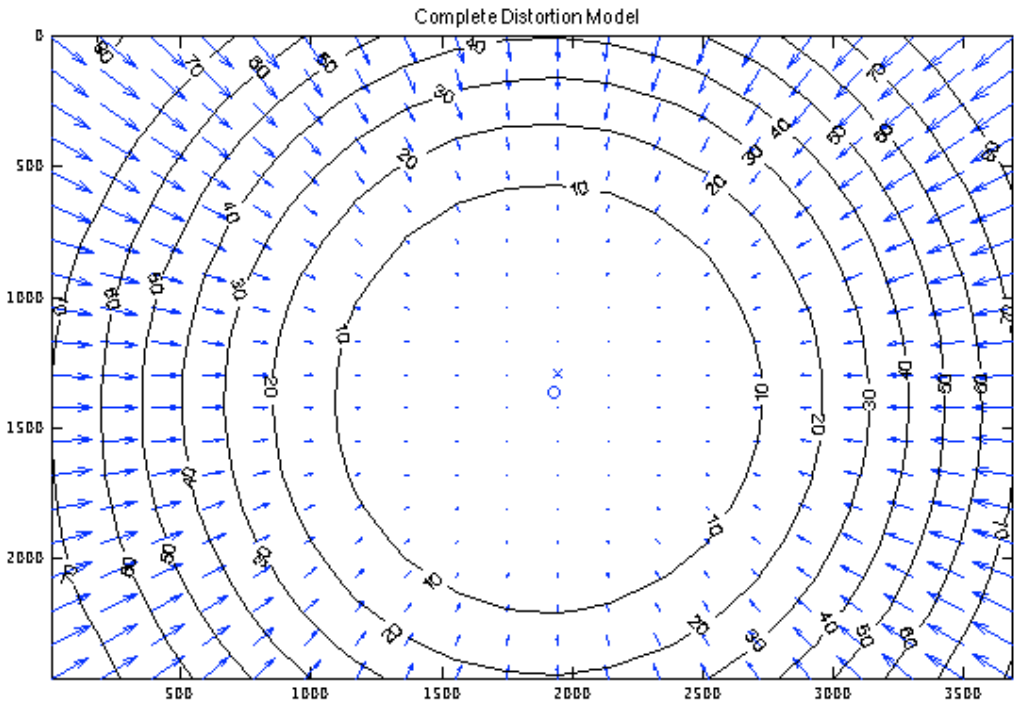

Figure 3.9: *Complete Distortion Model*

3.5 Geometry reconstruction from layered boundary detection

As concluded in section 3.2 on page 74, it is a trait for all common additive manufacturing processes that they employ a 2.5 dimensional manufacturing principle. Layers are added upon layers to form a three-dimensional structure comprised of thin-walled sections describing the boundaries of the structure, at their given section height. Solving the challenge of geometrically verify extremely complex structures that any additive manufacturing process, can be envisioned as to verify each individual layer after it has been deposited, thus still accessible and visible. If each layer of a structure is imaged by a vision system before additional layers are built on top, it is possible with numerical algorithms to reverse engineer the geometry from its cross-sections. With a calibrated vision system it will be possible to reconstruct a true-to scale three-dimensional model of the structure. In order to analyze the possibility for vision system integration in a variety of additive manufacturing processes, flexibility is of precedence. A fundamental criterion to make this system flexible is a rugged detection algorithm that allow for the extraction of features from the layered image data, hereby ensuring system compatibility with a variety of additive manufacturing processes. As such, different approaches to extract features from the layered image data has been implemented, tested, and forms an integral part of the post processing engine of the system. Any combination of the implemented methods can be superimposed to facilitate a composite feature detection method tailored to the process.

In the following section, the terms ⌜*Foreground*⌟ and ⌜*Background*⌟is introduced. The foreground is the visible cross-section of the manufactured part in the image plane. The background is the remainder.

3.6 Numerical feature detection

Predominantly feature detection must accurately locate the cross-section of parts in the build envelope of an additive manufacturing process with high precision, while decimating noise to a minimum influence. Secondary is a requirement that the feature detection engine form a computational aspect must be efficient. Therefore computation time and algorithm memory footprint is added to the requirements set to the post processing engine. An initial assessment of valid feature detection methods used in the field of computer vision lent thee candidate approaches, These are segmentation, edge detection and thresholding. The factual difference between these three methods, are illustrated in figure 3.10. Here, an image from a vision system in an SLM process for the base for a feature detection, and as seen the three methods gives a varying approximation of what part of the image is structure and which part is background.

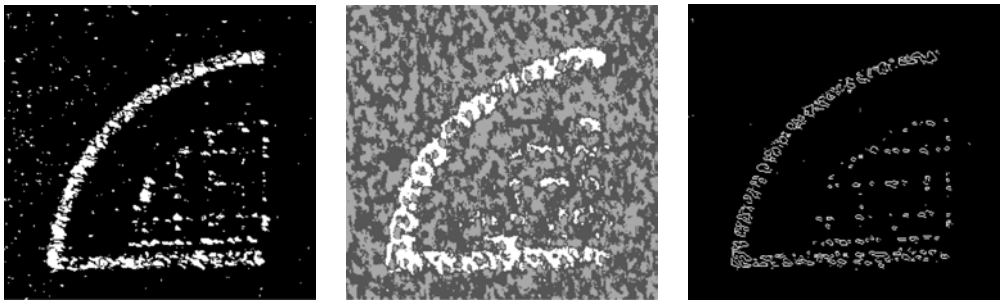

(a) *Threshold based feature detection*

(b) *Segmentation based feature detection*

(c) *Edge detection based feature detection*

Figure 3.10: *Numerical Feature Detection*

3.6.1 Edge detection

Edge detection is one of the most famous methods for feature detection. The implementation used here, is employing the Sobel operator by Irwin Sobel, 1964 and presented in 1968[56]. Edge detection using the Sobel operator is a discrete differentiation method, to yield an approximation to the size of the gradient at a moving mage point. The gradient images are binarized based on threshold and return edges found within the image The Sobel edge detection method has been found to perform poorly with some datasets where the background is found in a narrow range of intensity values, while the foreground of the part itself contains pixel intensities spanning over the histogram of the image. From an algorithmic aspect, this result in the Sobel edge detection exhibit a tendency to find structures inside the foreground, over the edge between the part and the background. This can be seen in (c) of figure 3.10. This method through benchmarking poorly in the SLM case study may yet be applicable to other additive manufacturing processes where both background and foreground visually is relatively uniform. Histogram based threshold detection works equally well in this case. Although known as a fast algorithm when convolution is optimized, edge detection using the Sobel operator was found to be slower than the histogram based algorithms addressed in the succeeding sections.

3.6.2 Segmentation

Segmentation is implemented using a method called ⌜*k means segmentation*⌟. It is a common image segmentation method characterized by taking k random samples from an image to then define the intensities of these as cluster centers. The remaining image pixels are assigned to a cluster by minimizing the distance to the centre. The algorithm now define a new centroid of the cluster. This is defined by calculating the mean of the pixel intensities. This iterative method is repeated until stopped.[57] The segmentation seen in subfigure (b) of figure 3.10 has been

stopped after three iterations. As with the edge detection method, the *k means* method does not yield a good segmentation of the sample image. Ideally the image would be divided into a uniform background and foreground. However, other additive manufacturing processes may show suitable for this feature detection method, and yield proper segmentation. From an algorithm execution speed point of view, the method arrogate computational resources from its iterative structure. A less demanding approach is histogram based thresholding which is the next method to be addressed.

3.6.3 Histogram based Thresholding

Histogram based feature detection was found to be successful in detecting features in image sets, irrespective of the additive manufacturing method from which the images originate. This was found to be caused by the background irrespective of the process is distributed over a narrow band of pixel color intensities. This can be seen readily in the image histograms as shown in figure 3.12 where the localized peak indicate the frequency of the pixel intensities for the red, green and blue color channel. It was found that if the background was targeted over the foreground, the background proved far easier to locate and decimate. The resultant detection of the foreground can be seen in subfigure (a) of figure 3.10. Though noise is prevalent, the histogram based thresholding method yield a detection of the foreground unprecedented by the preceding methods. Two different algorithms have been implemented for thresholding of slice images. The former is Otsu's method. This method which dividee images into foreground and background classes. This is done through the agency of maximization the between class variance. A non-adaptive thresholding mechanism has been included which require the operator to deduct an initial threshold estimate.

3.6.4 Otsu's Method

Otsu's method[58] was presented in 1979 in IEEE Transactions on Systems, Man, and Cybernetics. It is today a proven and widely applied methods for image segmentation and was the first of the feature detection methods implemented within this research project as a Matlab model later to be rewritten in Ansi C to speed up execution. The method attempt to divide a source image into a background and a foreground class. This is done by minimizing the within class variance. This can mathematically be described as in formula 3.8. σ_W is the within class variance. The probability of belonging to the foreground is given by ω_0 and the probability of belonging to the background is defined by ω_1, where σ_0 and σ_1 are the respective variances.

$$\sigma_W^2 = \omega_0\sigma_0^2 + \omega_1\sigma_1^2 \tag{3.8}$$

It is computationally demanding to calculate the variances. Therefore, to avoid this, it is possible to maximize the between class variance instead. This is done by introducing the class means, defined by μ_0 and μ_1, as well as the total mean, μ_T. The introduction of these is given by formula 3.9 and introduced into an algorithmic structure as of figure 3.11.

$$\sigma_B^2 = \omega_0(\mu_T - \mu_0)^2 + \omega_1(\mu_T - \mu_1)^2 = \omega_0\omega_1(\mu_1 - \mu_0)^2 \tag{3.9}$$

Otsu's method was found to perform very well for subsets of images. The method distinguished itself by returning a threshold adapted to the image, thereby reducing the need for homogeneity. This mean that uneven exposure in source images such as from uneven lighting or shadows induced by flash photography are not obstructing the feature detection. Such encountered exposure issues can be dealt with from meticulous camera setup and from image preconditioning, and is always preferable over relying on a robust image processing algorithm.

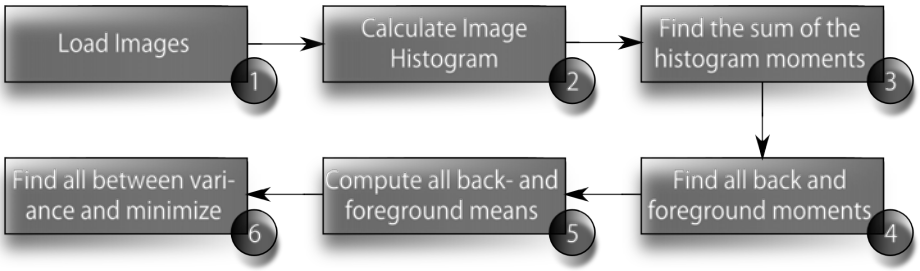

Figure 3.11: *Algorithmic structure of Otsus thresholding method*

Otsu's method was implemented as an algorithm processing the source image as subsets. The algorithm divide the source image into fragments from which a threshold for each segment is computed. This is an efficient method as there for most of the source images encountered are significant contrast between foreground and background in every fragment. Subsetting can be implemented natively or by applying heuristic methods as eg. looking for variations in the mean intensity in the proximity of the subset border, assuming the border of the image to entirely be comprised from background pixels. This method has yielded promising feature detection, and accuracy is expected to be increased by an improved accuracy of binarization of images. Using an approach given by C.J Solomon and T.P. Breckon, [59] to obtain a uniform background using tophat transform was attempted, though the background becomes more uniform this approach was prone to generate a pronounced granular background, generating significant thresholding noise.

Some limitations was found from applying Otsu's method as a feature detection method. Otsu's method is a bimodal method. This impose limitations for cases where the background resides within a histogram peak and the foreground is scattered on either side of this peak. In this case the image will not be properly segmented. This is the case for the some datasets that has been encountered

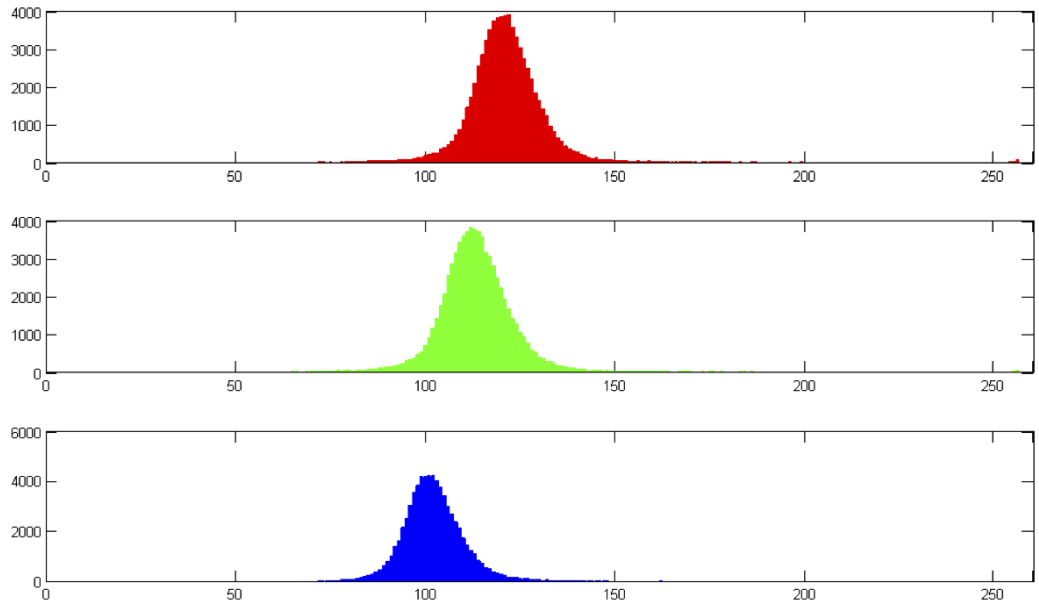

Figure 3.12: *Red, green and blue histograms for an image sample*

within the research project, generated from acquisition of image data from SLM processes. Here, due to reflections, the foreground can contain dark localized segments. Otsu's method is here prone to mistake foreground for background. In figure 3.12 Otsu's method has been applied to images from such SLM dataset as well as image sets from a DLP process. Apparent is that Otsu's method is capable of segmenting the image into classes as long as background and foreground both are uniformly placed in the histogram, as is the case with images from SLA printing. For SLM a viable solution is to deduct the mean true background intensity. As a threshold this mean background intensity can be applied to the absolute value of the foreground to unify the histogram, hereby circumventing this issue. Another known characteristic for segmentation using Otsu's method is that the method is known to segment images into classes with similar pixel count. This can be an issue when segmenting images where the background fraction is dominant. This for example if the cross-section of the part is very small. In this case the background will be segmented into two classes, ignoring the foreground. An example of these cases can be seen in figure 3.13 on the following page.

3.6.5 Assisted thresholding

To overcome the issues with thresholding images using Otsu's method an alternative approach was implemented, relying on user input to assist in correct segmenting. The method works under the assumption that the background of all images within an image set is uniform, allowing for a non-adaptive approach where a

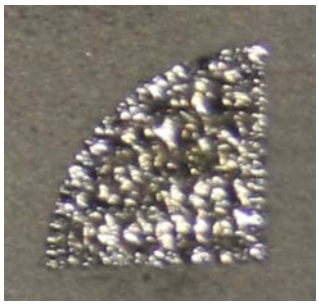

(a) *Image (SLM) showing a foreground containing dark localized reflections*

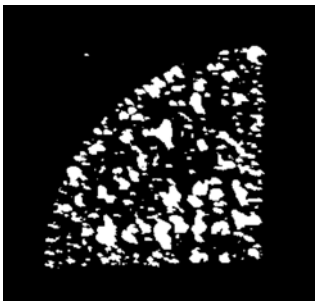

(b) *Segmented (SLM) showing holes from thresholding using Otsu's method*

(c) *Image from DLP build*

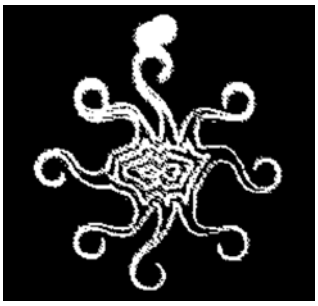

(d) *Well thresholded image (DLP) using Otsu's method*

(e) *Image with dominant background*

(f) *Poorly thresholded from dominant background*

Figure 3.13: *Otsu's method applied to different images.*

the set threshold will be applied to all images. This impose constraints in form of a proper camera setup and from image preconditioning. Furthermore all images must be acquired with the same illumination conditions. This however is a minor issue if flash photography is used, where ambient light can be negligible.

Figure 3.14 show the software flow of the implemented method. The operator is prompted to estimate the percentage of a test image that is made up of background pixels. Subsequently the red, green and blue histograms of the image are extrapolated and their global extrema are computed. Thresholds around the peaks are established and the image is binarized in a manner so that each pixel is set to background if it belongs to the subsets defined by the thresholds.. The binarized image is now displayed to the operator. If the operators estimation has yielded a good thresholding, the algorithm is applied to the rest of the images. If not, a new estimate is requested. This method was found to generate high quality thresholding of complete image sets with minimal operator labor. There are however pitfalls to be wary of. First, it is imperative that the background is dominant as it is assumed that the global extrema of the histogram is background. This has been addressed by letting a reference image only containing background be the image from which the extrema is estimated. There is a special case where there is a risk that the background span multiple extrema in the histogram. This situation has not been encountered during the research project, and therefore it has not been taken into account.

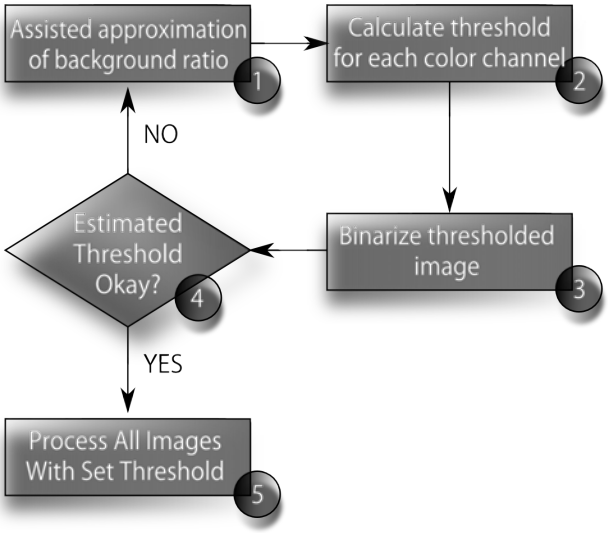

Figure 3.14: *Flow chart over user assisted thresholding*

3.6.6 Noise removal

Noise must be surveyed and dealt with. Image noise can to some extent be dealt with antecedent by ensuring a proper camera setup, proper image exposure and from image preconditioning. Nonetheless noise will inevitably subsist to some extend. Noise must be dealt with for manifold reasons. Noise can hinder proper feature detection. After feature detection of an image set a wireframe mesh sought

to be built. Noise increase computation time of the mesh, increase polygon count of the three-dimensional structure, and can render 3D reconstructions vastly larger in terms of file size than what is manageable with a workstation computer. There are three main components to noise that has been encountered throughout the reconstructive work with the vision system. Predominant in metal powder bed based manufacturing is reflections from metal powder grains that do not belong to the part. This is seen as spatially distributed noise that is dicey. This type of noise, given its random nature, is most often only of low pixel connectivity. This renders filtering trivial to a mere connectivity counting algorithm. The second source of noise that has been encountered is in the form of larger artifacts in the image frame leading to noise of a high pixel connectivity. An example to this can be a hard reflection of light from the surroundings to the build envelope, or physical artifacts visible within the image frame. Here it can be hard to numerically reckon of the artifact is indeed noise or a part of the foreground. The third noise source is a result of employing thresholding for feature recognition. Some spatially distributed noise from the imaging CCD chip and from radiation noise and radio interference[60], The thresholding algorithm will interpret some pixels in the foreground as background and vice versa. Some of the types of noise encountered while working with an SLM image set is shown in figure 3.15. Here the spatial noise from grain refections can be seen in subfigure (a). Noise as an artifact as a piece of debris in the background can be seen in subfigure (b), and noise as scattered reflections from the surface of the foreground can be seen in subfigure (c).

(a) *Noise from reflections from grains*

(b) *Noise as artifacts in the image frame*

(c) *Noise originating within the cross-section*

Figure 3.15: *Noise encountered in image data.*

Three approaches has been taken to handle noise. The first is by preprocessing image data before feature detection. This approach has involved using raster based imaging software to correct exposure, to remove gaussian noise, and to crop images to size. The second approach has been to apply low-pass filters after thresholding. This removes spatial noise of low pixel connectivity. However, some noise persist up till the generation of the three-dimensional point cloud from with

the final wireframe is generated. This lend the need to perform denoising as a post processing step.

3.6.7 Denoising in post processing

Denoising in post processing has a major advantage over denoising within image frames. This is the advantage of having access to information from succeeding and preceding layers. This open for the opportunity to look ahead and back to determine if presumed noise is subsisting between layers. Presumed noise can be assessed by quantifiers such as position, connectivity, distance to neighbors in three dimensions. This method less prone to shroud details than two-dimensional regularization of the image by means of low-pass filtering and edge aware blurring. Efficient use of qualifiers will remove as much noise possible, without loss of detail.

Several algorithms has been tested to achieve such filtering. The one that was found superior was the to create a neighborhood, excluding the coplanar neighborhood, by which the point cloud, P was traversed. The domain is traversed, and if point, $P_{i,j,k}$, is encountered, its immediate neighborhood is evaluated and the number of neighboring points is summed. If the point count is less than a set filter threshold, the point, $P_{i,j,k}$ is regarded as noise and thus removed. As the algorithm does not evaluate on the coplanar neighborhood, the virtue of this method is that it account for the fact that noise often cover connected pixies in the same image frame, yet rarely has neighbors in adjacent image frames. This due to the random spatial nature of many sources of noise.

A similar approach to account for histogram induced noise was applied. This method is closely related to the preceding, but emily a Von Neumann neighborhood. A Von Neuman neighborhood is a neighborhood that does not contain the nearest neighbor, as illustrated in a pixellated model in figure 3.16 on the following page. A sweep through the point cloud domain is carried out till a point, $P_{i,j,k}$ is found. If the neighboring point at position $P_{i+1,j,k}$ is not existing and the succeeding neighboring point in $P_{i+2,j,k}$ is, $P_{i+1,j,k}$ is set. This increase mesh connectivity. The Von Neumann neighborhood can be increased for more aggressive filtering at the risk of closing holes in the mesh that was not to be evaluated as noise.

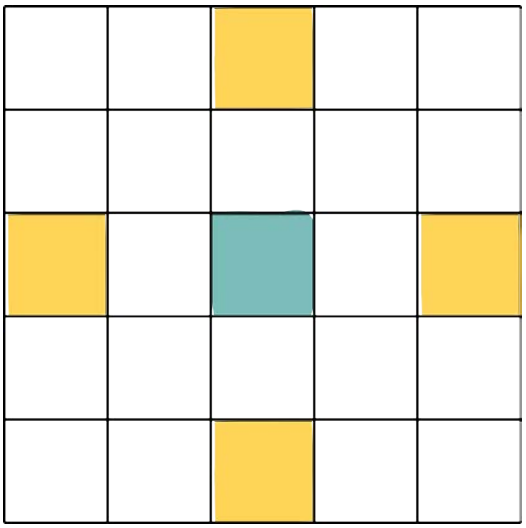

Figure 3.16: *Planar Von Neumann neighborhood. The central pixel is a non-zero pixel. The orange pixels are being tested.*

3.7 3D model construction from extrapolated image data

When features has been detected and the resultant point cloud been denoised, the factual 3D wireframe mesh can be generated. State-of-the art geometrical metrology software developers recommend the use of wireframe meshes.[61] The software GOM inspect, which is used within the scope of this research project do in fact convert point clouds to wireframe meshes before any comparison of data can be carried out. As such it is believed that the better approach is to generate the wireframe mesh based upon qualifiers related to the procedures that ultimately generate the point cloud over a generic meshing method. One such qualifier is the obvious manner by which the point cloud has been generated. From layered data. Following a meshing pattern that takes the layered nature of the point cloud into account will thus generate a more accurate mesh representation of data over a generic meshing algorithm.

The meshing of point cloud data is by far the most computationally intensive procedure performed reconstruction software. Originally implemented in Matlab, it soon became obvious that it was necessary to reimplement the meshing algorithms in Ansi C to allow for faster algorithm execution. Two meshing algorithms has been included in the post processing software. These are the Cuberille algorithm and the Marching Cubes algorithm. Cuberille was found to be the faster algorithm of the two, and the algorithm generating the smallest wireframe meshes. As the name imply though, the mesh is generated from cuboids, and as such, the resultant mesh is very voxellated in appearance. One strength of the Cuberille

mesh generation method is that loss-less edge collapse allow for significant reduction of mesh polygon count and thus output file size. How this can be achieved will be presented in the succeeding section.

The Marching Cubes algorithm was found to mesh point clouds slower than Cuberille. This is linked to the increased complexity. Whereas Cuberille generates a voxellated polygon mesh directly from an isometric consideration of the point cloud, the Marchin Cubes algorithm detect and create faces at a 45 degree angle to the cartesian reference system. The resultant mesh will as such inter-layer interpolate the surface structure at 45 degree angles. The method can be disputed by the fact that the additively manufactured parts are indeed generated layer-by-layer, and as such, an inter-layer interpolation result in information loss from the structure. This is however a trade-off that is worthwhile if the polygon count of the output mesh is to be further reduced by smoothing by external software. This can be needed for very large wireframe meshes in order to allow for these to be handled, and it was discovered experimentally that smoothing using third party utilities was in general more successful on meshes generated by Marching Cubes over Cuberille.

Common for the Cuberille and Marching Cubes is that both algorithms pass through the point cloud. If a point, $P_{i,j,k}$ is found, the immediate neighborhood is explored. If valid neighboring points are found, according to a rule-set, these are triangulated of form one or more faces. The relation between vertices that form the face, and the face normal is computed and stored. Unlike Cuberille, the marching cubes method has not been implemented with a loss-less edge collapse algorithm. This because edge-collapsing is more applicable to Cuberille over Marching Cubes.

3.7.1 Cuberille mesh generation

The algorithm implementation of Cuberille is based upon the initial algorithm description from 1979 by Herman and Liu. [62] Cuberille iterate over the point cloud. As the point cloud is describing pixellated points from the image source, the algorithm search for voxels. A distinguishment between square voxel faces and triangular mesh faces must be noted in the following. If a voxel is found from its corner connectivity, the corner indices are calculated following the enumeration pattern shown in figure 3.17 on the next page. The algorithm search for voxels that share voxels faces with the found voxel. This can be illustrated in figure 3.18. If an unshared voxel face is found, a rectangle covering the voxel face is computed. This rectangle is expanded in the coplane until no further voxels are found. When this criterion is met, the rectangle is meshed to form two coplanar triangular mesh faces sharing hypotenuse and thus sharing vertice connectivity. To avoid bifold computation, all points covered by the meshed triangles, a bitwise OR operation is flagged to set pixels. This is a parameter checked, as the algorithm preceding throughout the point cloud in search for succeeding voxel connectivity. This rectangular search pattern effectively generate a Cuberille mesh with loss-less

edge collapse where exclusively coplanar faces are joined.

Cuberille was found to impose problems if large data sets cause meshes to become excessively large. If this is the case, the coplanar decimation by edge collapsing would not sufficiently reduce polygon count, to a level where the meshes can be handled in viewer software. The attempted solution was to reduce polygon count by third party software such as filtering with Meshlab. The result from this was a mediocre due to the voxellated nature of the Cuberille mesh. To solve this, a marching cubes algorithm was implemented. The Marching Cubes method solved the mesh polygon reduction issues that was encountered by Cuberille.

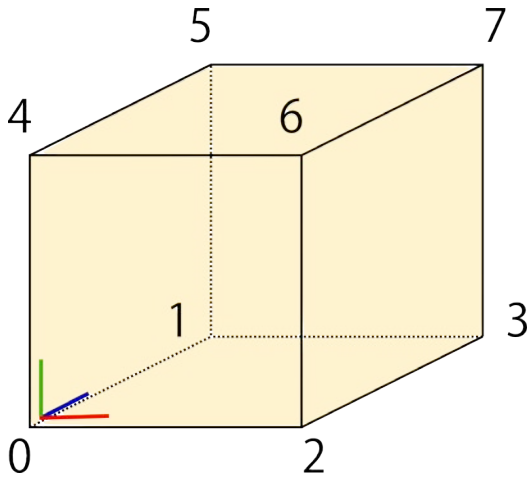

Figure 3.17: *Enumeration pattern for voxels using cuberille mesh generation*

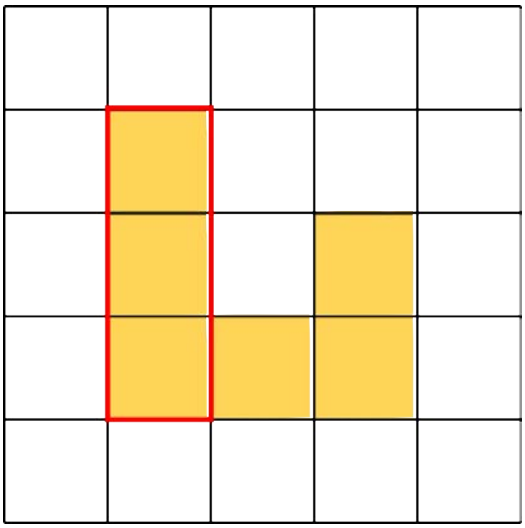

Figure 3.18: *Cuberille voxel scan: The rectangle is expanded in the coplane until no more voxels are found*

3.7.2 Marching Cubes

Marching Cubes is an algorithm by Lorensen and Cline and was first published in 1987 [63]. The algorithm was introduced as a proprietary algorithm but is today public domain. The native Marching Cubes algorithm make use of a density function as the algorithm crawl the point could domain. A simpler implementation of same algorithm can be applied to data derived from binary images, as it is the case for this application case. Since a reconstruction from planar feature detected to mesh is carried out, an exploit can be introduced. As with Cuberille, this implementation of the Marching Cubes algorithm iterate over the point cloud. As the point cloud is describing pixellated points from the image source, the algorithm search for said voxels. There are but 256 permutations of how a plane can intersect a voxel. These can be decimated to 15 permutations if one account for symmetry. Figure 3.19 on the following page illustrate these 15 permutations. As the domain of the point cloud is traversed by the algorithm, each of the intersection permutations is tested for and faces are rendered accordingly to polygonize the point cloud. Rendering is only carried out if said permutation is located either as a edge or a voxel face. This is recorded as a bit mask to a variable to avoid bifold computation. Algorithm execution time for Marching Cubes was found inferior to Cuberille. Thus spite the implementation proved slower than Cuberille but solved the mesh polygon reduction issues that was encountered by Cuberille.

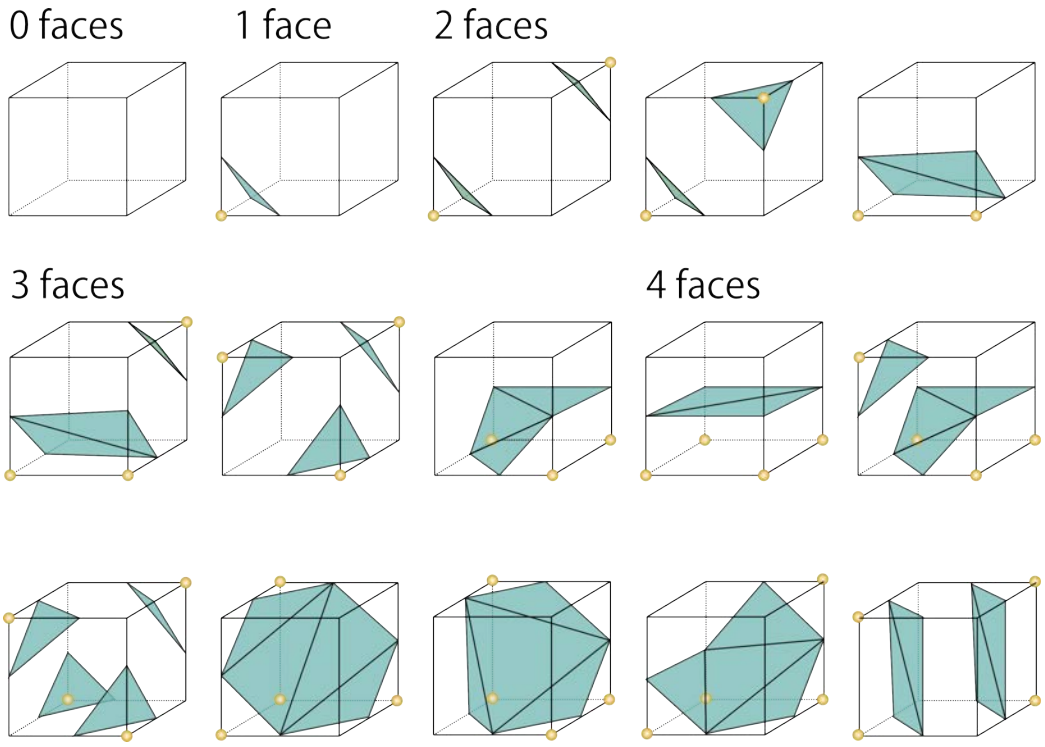

Figure 3.19: *Marching Cubes: The 15 permutations of possible intersections of a plane through a voxel*

3.7.3 A preliminary thresholding and meshing test

The thresholding, denoising and meshing system will be tested extensively in chapter 4. A preliminary test of here presented to display the result from the procedure of feature detection through denoising to meshing. Example here given is from two consecutive layers from a build-job from an SLM machine. The structure is the support structure for a part, and has been chosen as the source images as they include a complex structure with internal features. Figure 3.20, frame (a) show the resultant mesh from applying feature detection, denoising and meshing. Some noise persist from the denoising algorithms, but fragmented and with a low polygon count relative to the main components they can be removed from the wireframe mesh by handling in third party software. Here the open source utility Meshlab v1.3.0b[64] was used and perform well to remove the remaining noise components. The resultant mesh can be seen in the figure frame (b).

Large image set generate large data throughput. An analysis was carried out to show the computational runtimes on a standard workstation computer. The major machine specifications was a 2.26 Ghz Intel Core 2 Duo processor, 4 GB 1057 Mhz DDR3 RAM and a 256 GB OCZ Octane solid state disk storage unit. Otsu's method was used to extract features and the Cuberille mesh generation

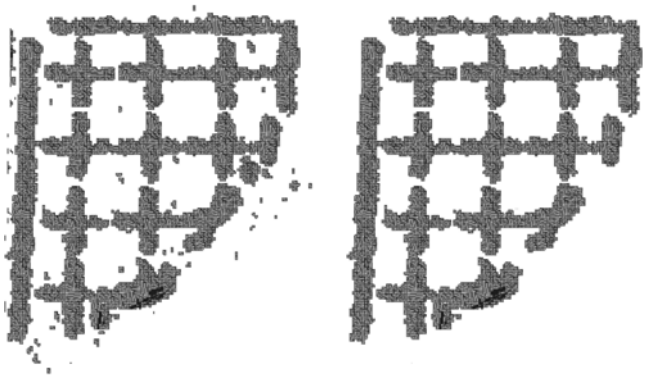

(a) *Output from feature detection, denoising and meshing of two layers from a build job*

(b) *Removal of noise by means of small-component removal using Meshlab v1.3.0b*

Figure 3.20: *Meshing between two images from a test image set and removal of noise in Meshlab.*

Table 3.2: *Run time proportions of time spent on feature detection, meshing and file output. The data source is a 150 Mb SLM image set.*

	Total	Thresholding	Meshing	Input Output	Initialization and Housekeeping
Runtime(s)	16.9	1.5	1.9	4.0	9.5
Percentage	100%	8.7%	11.2%	23.7%	56.4%

algorithm was used. The source image set was 150 Mb of bitmap data. The resultant computing time and major contributions to this can be seen in table 3.2.

3.8 Conclusions on the vision system implementation

The novel, numerical architecture for a vision system for inline monitoring of additive manufacturing processes has been proposed in section 3.1 on page 71 and developed in the precedent chapter. Three main constituent to the architecture exist. These are numerical camera calibration, two dimensional feature detection and three dimensional wireframe meshing. The architecture has been developed on the fundamental basis of flexibility. The applied numerical engine must allow for post processing of a variety of image sets gathered from a variety of additive manufacturing systems. This set demands to the image calibration routines. A

vision system with fixed optics in a fixes setup may need calibration only once, which can be achieved from a simple manual calibration. A system with dynamic optics applied to an impermanent setup do require calibration each time changes are imposed to the system. With the base in a DSLR camera, the optical system has been synthesized in section 3.4 on page 77 where the various parameters that impose camera recalibration has been identified.

Numerical Camera Calibration

The numerical camera calibration is the first the three constituents that is addressed. Calibration is achieved by means of the application of a series of numerical algorithms from Intel, bundled into an algorithm library. These algorithms can be included in the source code written in Matlab and C language, and gives the developer a set of algorithms that is tailored for image processing and calibration. From these numerical algorithms, a model has been set up. The model is fully capable of characterizing a modern camera system which is described in chapter 3.4.2 on page 79. This is made possible by basing the model on the model of a pinhole camera. Superimposed to this model is model for radial and tangential distortions. These two model account for image distortions from the lenses that is not present in a pinhole camera but contribute to the distortion field of modern camera systems. From the complete camera model it is possible from any point in the image plane to calculate the corresponding point on the CCD plane within the camera and vice versa. From this model, a calibration routine can be carried out by means of a checker-board patterned plate. Images are acquired by the camera and from the distortion field of these images, the radial and tangential distortion contributions can be quantified. The method is described in chapter 3.4.3 on page 82 By calibration from multiple calibration images, the source data that form the base of for the calibration can be extended and a more concise calibration can be achieved. Once a camera has been calibrated it has been shown how the position of the camera in space can be calculated from any image of the calibration plate. This allow for the calculation of the camera position relative to the build envelope of any additive manufacturing process, and thus allow for flexible positioning of the camera in an experimental vision systems setup. Furthermore the image distortions induced from the camera can be corrected for. An case study of this is given in section 3.4.3 on page 82. Once a camera system is calibrated and set up within the confines of an additive manufacturing machine, inline vision data can be gathered, undistorted and post processed. Post processing by two dimensional feature detection can be carried out.

Feature detection

Feature detection is the first step toward generating a three dimensional representation of the two-dimensional images captured from the vision system during

a build job from any given layered additive manufacturing process. A set of demands was outlined in section 3.6 on page 87. Predominantly feature detection must accurately locate the cross-section of parts in the build envelope of an additive manufacturing process with high precision, while decimating noise to a minimum influence. Secondary is a requirement that the feature detection engine form a computational aspect must be efficient. An initial assessment of valid feature detection methods used in the field of computer vision lent thee approaches, These are segmentation, edge detection and thresholding. All methods has numerically been implemented in order to allow for the better of the three methods to be applied to any given dataset. Section 3.6.1 on page 88 describe the way that edge detection was implemented using the Sobel edge detection method. This method was deemed to perform poorly on some imagesets such as test images from an SLM process where edge detection within the foreground was a prevalent issue.

Another method, the *k means segmentation* method was implemented. Described in 3.6.2 is the assessment of this method. It is a common image segmentation method characterized by taking k random samples from the source image from which segmentation is performed. Ideally the source image will be divided into distinct binarized foreground and a background. From an algorithm point of view this method was found heavier than its counterparts given its iterative nature.

The third feature detection method implemented was histogram based thresholding. This implementation was described in section 3.6.3 Histogram based feature detection was found to be successful in detecting features in image sets, irrespective of the additive manufacturing method from which the images originate. This was found to be caused by the background irrespective of the process is distributed over a narrow band of pixel color intensities. As such, main effort was put into evolving this method. Two methods was applied to threshold images. Otsu's method, which is an adaptive method and a user assisted thresholding method.As described in section 3.6.4 on page 89, Otsu's method was found to perform well if applied to subsets of the source image. The adaptive nature of the algorithm handled well under conditions where the background was gradiented from uneven light conditions an from cast shadows. The method however proved limited in the capability of segmenting images where the background fraction is dominant. Therefore a suggested assisted derivative of this thresholding method was implemented. This method let the operator overrule the adaptive threshold estimated by Otsu's method. The implementation, described in section 3.6.5 on page 91 vas found to be the best performing candidate of all tested methods, and as such it form the base for most reconstructions generated within this research project.

Noise

Noise will always be met in the realm of computer vision and image processing. Noise can originate from a variety of sources, and must be surveyed and dealt with

accordingly. Some image noise can be dealt with antecedent by proper camera setup, image exposure and image preconditioning. Some noise will spite these efforts inevitably subsist. It is sought to vigorously find and deal with for manifold reasons. Noise can obstruct feature detection. Noise increase computation time during mesh generation. Noise increase polygon count of the three-dimensional structure. Noise was classified into three main components in section 3.6.6 on page 93. These are spatially distributed noise, random of nature, and most often only of low pixel connectivity. Second is noise from larger artifacts in the image frame, having a high pixel connectivity. This type of noise may be recognized as foreground, and not filtered due its large size. The third noise source is a the noise induce by the nature of the feature detection algorithms that may have been employed.

Noise has been attempted to be removed by pre-processing image data prior to feature detection. This partly remove noise, yet noise may prevail through this step. Therefore a post processing step was added to remove noise from an analysis of the three-dimensional domain. Post processing has a major advantage over denoising within images. Information from succeeding and preceding layers allow the noise removal algorithm to look ahead and back to determine if presumed noise is subsisting between layers. Quantifiers such as position, connectivity, distance to neighbors in three dimensions are used to pinpoint noise and efficient use of qualifiers will allow for the removal of as much noise possible, without loss of detail. Neighborhood base and Von Neumann neighborhood based noise removal in three dimensional space was applied will good results.

3D mesh generation

With image feature detected, and noise reduced by noise removal algorithms, a three-dimensional representation of the image set is available as a point cloud, and can principally be analyzed using metrology software. It was brought to attention that some state-of-the art geometrical metrology software developers, such as GOM in force the use of wireframe meshes. Generic meshing can here be carried out. This is not found ideal as meshes can be generated based upon the knowledge of how the point cloud has come to exists; by a layered analysis. As such it is believed that the better approach is to generate the wireframe mesh based upon qualifiers related to the procedures that ultimately generate the point cloud over a generic meshing method. Two similar algorithms for doing so was implemented. The Cuberille mesh generation method and the Marching Cubes mesh generation method. Cuberille, implemented as described in section 3.7.1, iterate over the point cloud searching for voxel patterns. If found, the points are described as wireframe cubes. In order to lossless reduce the Cuberille generated mesh, coplanar faces are decimated. Cuberille generate wireframe meshes that are true its the two-dimensional reference features, and is the best algorithmm of the two in order to concisely describe the two-dimensional features as a three-

dimensional mesh. Cuberille however was found to impose problems if meshes are excessively large. If this is the case, the coplanar decimation by edge collapsing would not sufficiently reduce polygon count, to a level where the meshes can be handled in viewer software. The attempted solution was to reduce polygon count by third party software such as filtering with Meshlab. The result from this was a mediocre due to the voxellated nature of the Cuberille mesh. To solve this, a marching cubes algorithm was implemented. The implementation, described in section 3.7.2 provide smoother mesh surfaces, and is based upon a search pattern of the permutations of the possible intersections of a plane through a voxel. The implementation proved slower than Cuberille but solved the mesh polygon reduction issues that was encountered by Cuberille.

Testing the numerical vision system architecture

A preliminary test of the thresholding, denoising and meshing system has been given prior to the presentation of extensive tests in chapter 4. The preliminary test display the result from the entire workflow of feature detection through denoising to meshing. Two consecutive layers from a build-job from an SLM machine is processed from image data to wireframe mesh. The mesh contain little noise that is decimated using Meshlab, and the reconstruction yield information from both external and internal geometries. In the succeeding chapter the vision system will be tested in several environments ranging from powdered based systems to resin based systems. The reconstructive capabilities of the vision system will be assessed using geometrical inspection software, and the vision system is put through its paces to prove its worth.

Testing the proposed numerical geometry reconstruction method, and assessment of results

4 Vision Based Reconstruction

With a numerical implementation of all the subroutines required in order to calibrate a camera system, perform reconstruction by segmentation of boundaries, noise removal and wireframe meshing, several case studies on several additive manufacturing platforms has been carried out. This in order to provide evidence to the validity of the approach. Initial tests was performed on a non-thermal powdered based 3DP machine. Subsequently tests was carried out on an SLM platform to quantify the errors introduced by reconstruction from relaxed layers to a part deformed by residual thermal stresses. Finally the validity of the method with respect to resin based platforms was assessed by implementation on a DLP based additive manufacturing platform. Challenges here was to distinguish between photo-cured resin and liquid photo-initiated monomer, as there is no visible distinguishment from the camera perspective between these two states.

4.1 Pilot study - Vision integration to a 3DP powderbed platform

A pilot study was carried out on a powdered based 3DP platform, the ZPrinter 310 plus from zCorporation. The choice to implement the vision system on this platform has been governed by the fact that the 3DP platform itself is highly suited for implementation of a first version of the 3D reconstruction system. The ZPrinter, building structures in plaster($CaSO_4$) and employ a standard inkjet print head to deposit a binder liquid on the flat surface of a powder bed. This cure the plaster, and leave the surface contrasted where binder liquid has been deposited. After one layer has been selectively treated with binder liquid, the powder bed is lowered, a new layer of powder is evenly distributed, and the process repeats itself. The following is derived from a publication at the 7'th International Workshop on Micro Factories, Daejeon, Korea, by the author.[65] In order to assess the performance of the 3D reconstruction method, the part shaped as a hole-plate shown on figure 4.1 on the next page has been chosen as the geometry for verifying the method. This choice is governed from hosted knowledge from work on calibration artifacts

for optical coordinate metrology. [66][67] A hole-plate from a geometrical metrology point of view can yield information about global and local deviations of the 3DP machine and of the reconstruction method itself, and is therefore considered very well suited. In this study the lateral performance is investigated. Hence the geometry has been printed in the 3DP printer resting flat in the build chamber.

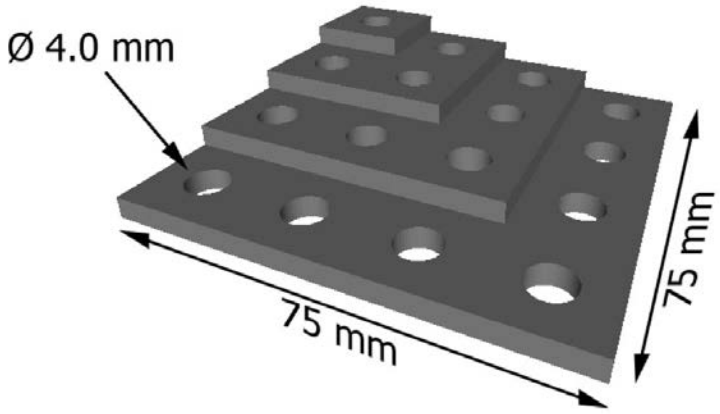

Figure 4.1: *Test geometry for pilot study of the vision system. A stepped hole-plate baed upon hosted knowledge from calibration artifacts.*

4.1.1 Pilot study - Additive Manufacturing of a test artifact

The geometry has been built with a resolution of 300 x 450 dpi (118 x 177 dpcm) in lateral resolution and of 0.875 mm vertical resolution (according to the machine specifications). It is noteworthy that the manufacturer's specifications are identical to the resolution of the print head itself in lateral direction and the resolution of the build plate actuator in the vertical resolution. The parts produced on the equipment will have tolerances deteriorated in comparison to these specifications. This is due to mechanisms such as missing guide rail tolerance compensation in the lateral direction, and not least due to process specific mechanisms such as bleed effects that occurs during the rehydration of the processing material, which has a plaster($CaSO_4$) base. During the print job, the vision system monitoring the build process will acquire one image for each layer and stores these for numerical post treatment. The camera uses was a Canon EOS 1000D with a EFS 18-55mm f/3.5-5.6 IS lens kit. One such image can be seen in figure 4.2 on the facing page It is here clearly visible how the bonding agent darkens the color of the $CaSO_4$ powder and the part is easily distinguished in contract level from the surrounding loose $CaSO_4$ powder. It is this contrast difference that is detected by the boundary detection algorithm used to post-treat the image data.

4.1.2 Pilot study - Geometry reconstruction

Upon acquisition and mesh generation, the reconstructed geometry can be studied. The raw reconstruction wireframe mesh is shown in figure 4.3 on the next page

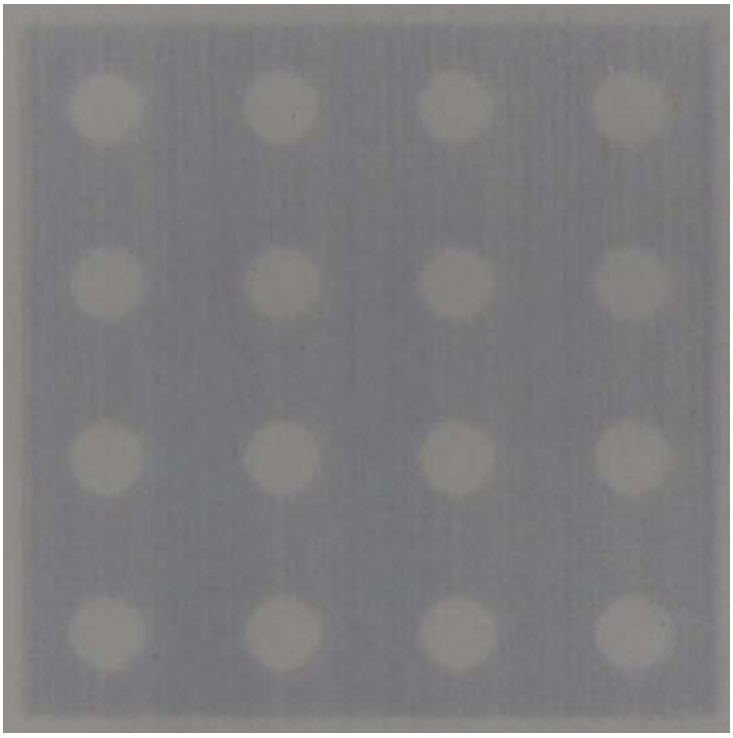

Figure 4.2: *One layer of the build of the test geometry, acquired by the vision system.*

The reconstruction of the test geometry has a resolution of 180x180 microns in the lateral given from the camera pixel resolution and of 875 microns in the vertical resolution given from the 3DP platform build-stage, governed by the machine build layer thickness.

4.1.3 Pilot study - Geometry inspection

The reconstructed model was correlated with the original CAD file. This was done by superimposing the original CAD file on the reconstruction as seen in 4.4 on page 111.

Hereby any divergence between the two models can be observed. Black color indicates the bounding CAD model over the geometrical reconstruction, white and grey colors indicate where the geometrical reconstruction proves larger or smaller with respect to the CAD file. No tolerance has been applied to this comparison, and the assessment is merely relative as the intent of this study was in an effort to pros

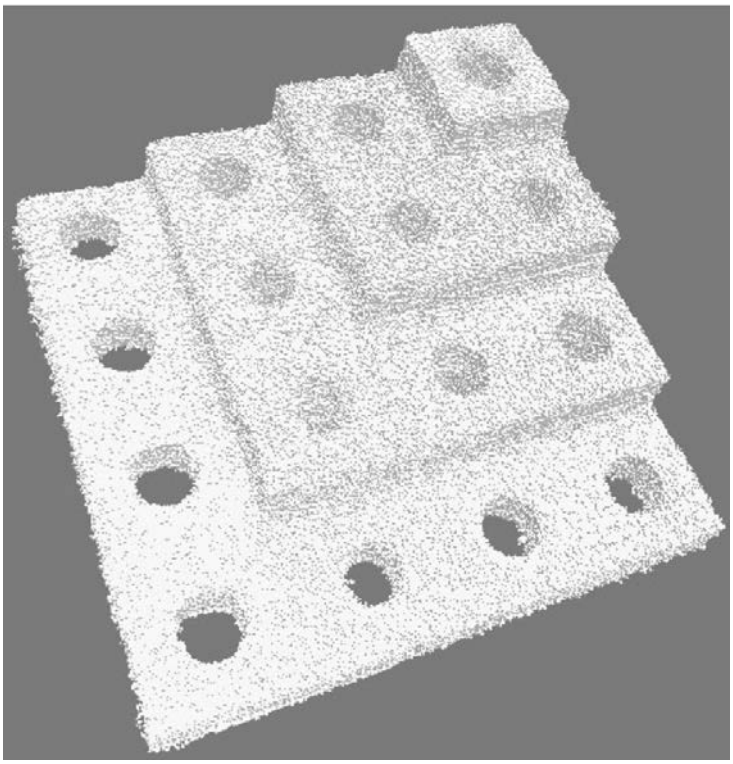

Figure 4.3: *Reconstructed 3D geometry from images acquired by the vision system.*

the feasibility of the vision based reconstruction procedure. Figure 4.4 on the next page shows that the main lateral dimensions of the reconstruction of the printed part and the CAD model is in agreement. It can be seen that the reconstruction indicates that all corners on the printed part has a rounding and is not sharp as on the CAD model. Close to the centre of the part it can be observed that the hole diameters of the reconstructed model are smaller than on the CAD model. Along the side walls of the steps it is visible that the reconstructed model exceeds the dimensions of the CAD model. Finally the reconstructed model indicates that the vertical height of the printed part is larger than the height of the CAD model. In order to investigate whether the reconstruction of the part is in agreement with the part itself, a comparison between the part and the reconstruction has been made. The printed part can be seen on 4.5 on page 112. On figure 4.5 on page 112 it can clearly be observed that the side walls of the steps have a grainy structure protruding from the wall face. This corresponds to what was observed on 4.4 on the facing page.

A close inspection of local features was conducted. Inspection of the holes of the reconstructed geometry to the CAD file was carried out. In the following, an examination of the upper left hole of the geometry as it is shown in figure 4.4 on the next page, corresponding to the farthest hole on figure 4.5 on page 112 is

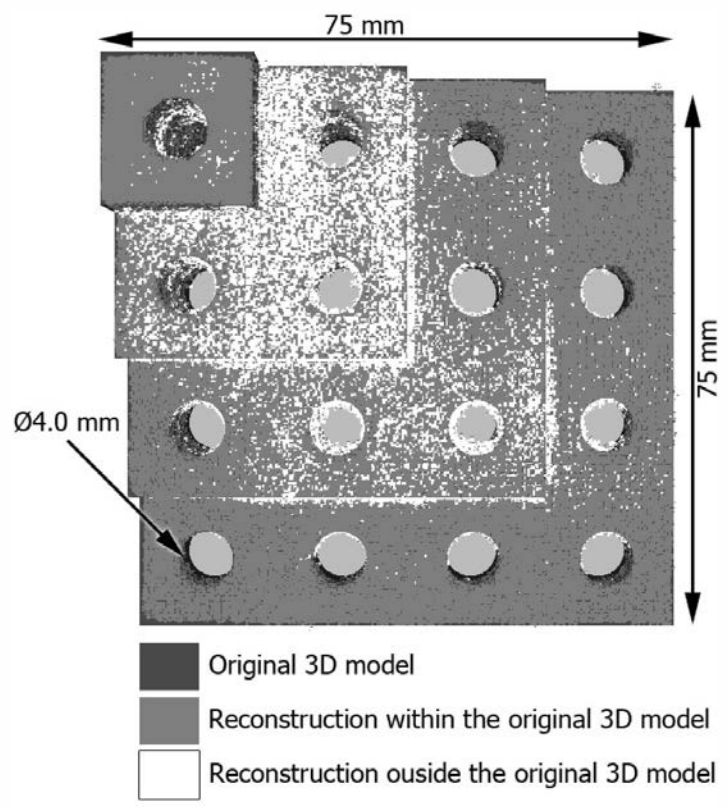

Figure 4.4: *Reconstructed 3D geometry superimposed to the original CAD file.*

presented. From figure 4.4, displaying the comparison of CAD file and the geometrical reconstruction it can be observed that burrs are present within the examined hole. This observation is verified by studying the additively manufactured part and comparing the hole shape with the reconstructed model. Figure 4.6 on page 113 clearly shows an agreement. The burrs that were detected by superimposing the CAD model on the reconstructed model is in fact also present on the part itself. Quantification of magnitude of these defect was not assessed within the preliminary study, however the tendencies observed on the geometrical reconstruction and the actual part are in conformity. It is furthermore noticed on 4.6 on page 113 that the corners of the side walls are not sharp but rounded. This was also observed during the analysis of the reconstructed geometry against the CAD model.

Finally it can be observed in the comparison between the reconstruction and the CAD model, from figure 4.4, that the holes in the centre of the part seemed to appear smaller. From a process point of view this is expected to be plausible. A common observed cause to diminishing internal features during additive manufacturing by the specific 3DP process, is a bleeding effect. The term bleeding is used to describe the phenomena that binder liquid will bleed from the deposited area out into the surrounding unhydraded $CaSO_4$ powder. This phenomenon occurs to

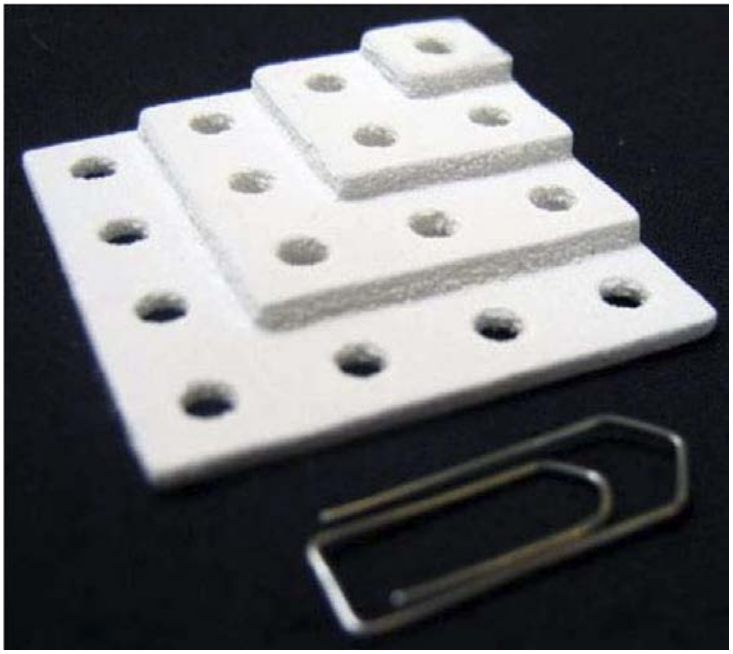

Figure 4.5: *The test artifact produced by additive manufacturing of the test geometry.*

a greater extent in the vicinity of the centre of a part than at the edges. Believed merely to be caused from the humidity within the core of the structure will be greater near the centre of the structure where much binder has been applied, than at the boundary of the part. Hence bleeding is most prevalent within the central holes. The question that remains is whether the bleeding phenomenon visible on the geometrical reconstruction is to be found on the manufactured structure. Figure 4.7 on the next page compares two of the central holes on the part with the observations done in the CAD model analysis.Again the CAD model analysis shows a correlation with the printed part. The hole diameter is slightly in smaller near the centre of the part, and hence this observation is also correct.

4.1.4 Pilot study - Conclusive summary

The results gathered from the pilot-study, have successfully proven the viability of the vision system developed and its integrated on the first candidate, an industrial powdered based 3DP platform. The system proved its capability to autonomously collect geometrical information of each manufactured layer in-line with the process, and to subsequently produce a full 3D reconstruction. The quality of our 3D geometrical reconstruction method has been verified by visual comparison. All deficiencies that can be observed on the target part are deficiencies that also can be observed on the geometrical reconstruction. It was possible to detect internal

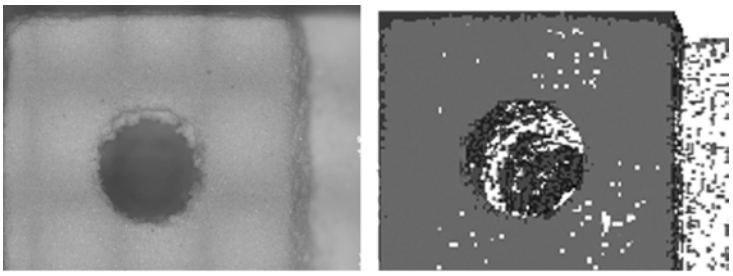

Figure 4.6: *Comparison of burrs observed on the reconstructed geometry in respect to the CAD model and additively manufactured part.*

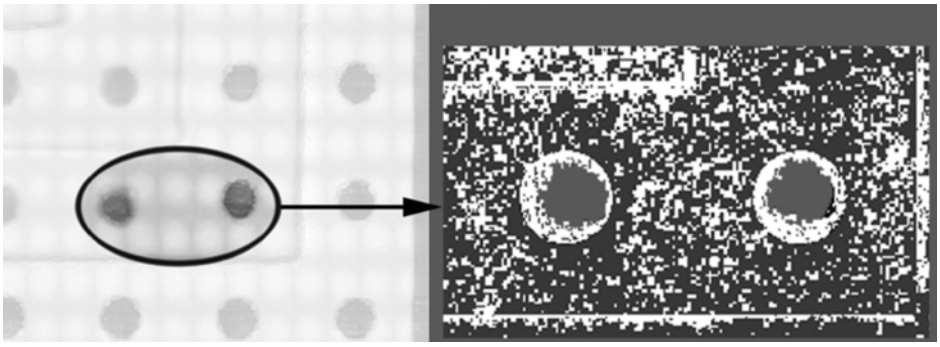

Figure 4.7: *Bleed effect visible on the printed part and reconstruction.*

deficiencies within the holes of the test artifact produced from the CAD geometry, as well as observing process specific effects such as the bleed effect. This fueled confidence in that it will be possible to expand the method to form the base for absolute geometrical measurement, part verification and tolerance control. Early-stage results, of this quality results left the impression that it is possible to lift tolerance control of complex AM parts up to a level that meets industrial standards. This of course requires the system to be calibrated and establishment of traceability is crucial. Quantitative analysis of parts and comparison of results obtained with the vision system and reference measurements are thus the immediate next steps in the investigation. There are some obvious pitfalls that have to be bridged, such as the previously discussed build-up of stresses in the parts which again leads to distortion. (section 3.1 on page 71) These will not be detected when the individual layers of the part are being measured during the build process, however the following results will provide an indicator as to how prevalent these are disturbing the reconstructive capabilities of the vision system.

4.2 Absolute 3D reconstruction using a calibrated camera.

From a successful pilot study, the succeeding efforts was channeled toward demonstrating the absolute geometry reconstruction capabilities of the vision system. The following is derived from a publication at the 16th European Forum on Rapid Prototyping and Manufacturing, Paris, France, by the author. [68] This publication address the the paradox that additive manufacturing technologies provide the industry with close-to unrestrained geometrical freedom of part design. A freedom that is being taken away from the industry from a lack of methods for absolute and precise geometrical verification of the manufactured parts. The paradox puts the AM technologies at a position where they can be employed to solve otherwise impossible design issues, yet the industry will not embrace the technologies as long as dimensional tolerances cannot be verified. It can be regarded as a technological stale-mate. The publication befall from the succeeding effort in demonstrating absolute geometry reconstruction capabilities of the vision system and validates this as an in-line reverse engineering and 3D reconstruction method that allows for a true to scale in-line 3D reconstruction of parts that is being additively manufactured on 3DP based powder-bed based systems. A system that since pilot tests evolved into a system that can fully and accurately describe additively manufactured parts in a 3D format that resembles 3D scans, yet with all internal geometries represented.

A vision system based on a high-resolution digital single-lens reflex (SLR) camera and a remote triggering interface consisting of a micro switch and a trigger controller circuit powered by an ARM7 micro-controller has been integrated to the powder feed and distribution system of the 3DP printer. The camera is a Canon EOS 1000D with a EFS 18-55mm f/3.5-5.6 IS lens kit. This allows for autonomous collection of images of the individual slices of a build job as it is being printed. The implementation can be seen in figure 4.8 on the next page.

While in progress or after finalizing a print job, the collection of 2D-slice images can be processed using a purpose-built numerical post treatment algorithm to reconstruct the 3D geometry of the printed part. The camera system itself is calibrated by means of the camera calibration method given from section 3.4 on page 77. A checker-board patterned plate that is socketed in the confines of the build chamber of the 3DP platform An image is acquired, and for the purpose of numerical compensation of the relative size given from the tele-settings of the camera objective as well as perspective, skewness, and distortions originating from lens imperfections in the optical system. Image acquisition and numerical post-treatment of the undistorted image sets from the calibrated camera system follow the procedure from section 4.1.3 on page 109.

Figure 4.8: *Vision system integration in a z310 plus 3DP machine. Showing a digital SLR camera on a tripod with an external flash unit mounted to the frame of the 3DP machine, and an integrated triggering wired extending from the camera.*

4.2.1 Quality control of the geometrical reconstruction

Upon completion of the 3D reconstruction has been, the resultant mesh, stored in the .STL file format, is ready to be used for assessment of part quality control. As a wireframe mesh the file can be imported into commercially available or open source mesh manipulation, verification and metrology utilities. Meshlab v1.3.0b[64] has been used to filter unwanted artifacts, primarily by filtering shells of a low pixels count away as these shells represent noise stemming from image noise resulting in falsely detected as boundaries by the numerical post processing algorithm. Figure 4.9 on the following page show a detailed view of a cluster of noise induced artifacts that will be removed by filtering of low polygon shells.

As the preceding pilot analysis has already showed that the methods ability to detect defects and artifacts on AM built parts. Hence weight is put on the efforts of quantifying the accuracy of the method. For this, GOM Inspect V7 SR2, a metrology software freely available by GOM Optical Measuring Techniques, has been used to perform mesh-to-mesh analysis of 3D geometries. The analysis covers comparative examination between the initial CAD model and a reconstruction from the inline monitoring system. Furthermore comparative analysis between an optical 3D scan of the octachord and the reconstruction from the inline monitoring

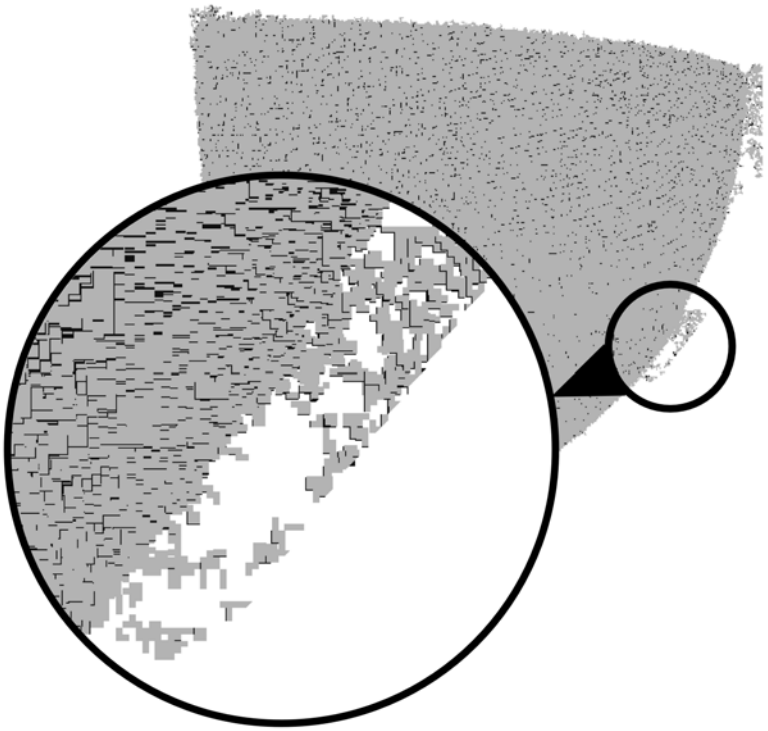

Figure 4.9: *A detailed view of a cluster of noise induced artifacts that will be removed by filtering of low polygon shells*

system is performed in order to quantify the absolute accuracy of the system.

4.2.2 Results of the geometrical reconstruction

The geometry seen in figure 4.10 on the next page has been chosen as specimen for verification of the method. The geometry is an octachord shell of a sphere that has been chosen based upon its concomitant resemblance with a spherical calibration artifact on the curved surface and a cartesian coordinate system on the adjacent orthogonal corner. This allows for vertical as well as lateral quantification of reconstruction accuracy as well as retaining traceability to a spherical calibration artefact. The octachord has been built with a resolution of 300 x 450 dpi (118 x 177 dpcm) in lateral resolution and of 0.875 mm vertical resolution (according to the machine specifications). This correlates to a mesh resolution of 0.085 x 0.056 x 0.875 mm. It is significant as with the pilot test to underline that the manufacturer's specifications in lateral resolution is identical to the resolution of the print head itself. The resolution of the build plate actuator is defining the vertical resolution. Geometries produced on the equipment will have tolerances

deteriorated in comparison to these specifications.

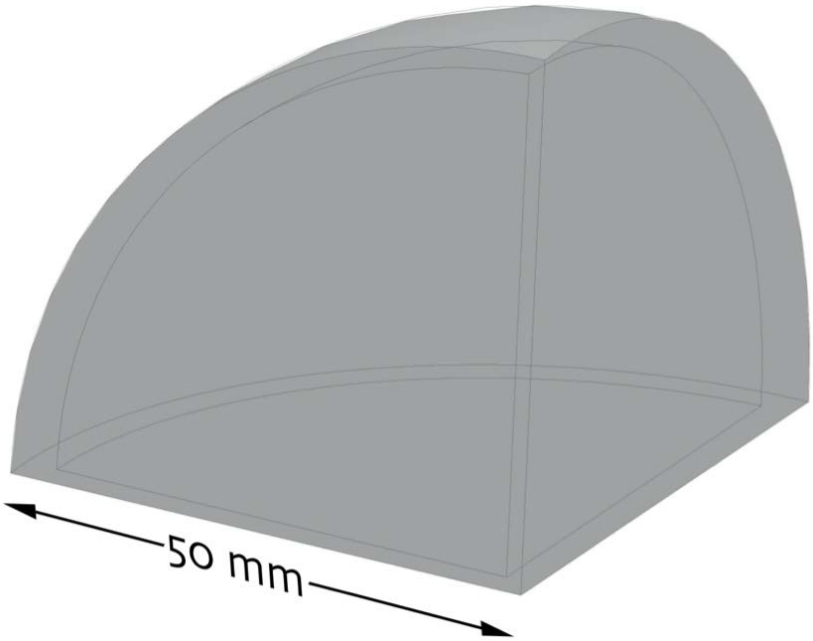

Figure 4.10: *Test geometry - An octachord of a sphere.*

As the octachord is being built, the vision system monitors the process. For each layer 3 high-resolution flash-assisted images are taken and numerically superimposed to produce a median image with reduced gaussian noise. The camera flash serves the role of exposing the layer to light that is several hundred times the intensity of the ambient light, hence ensuring an even exposure of each image. A circular polarization filter is used to reduce of flash-bounce. This will ease subsequent post processing. Upon data acquisition the image set is corrected by superimposing the calibration matrix generated from the image calibration routine. From the resultant image set, a reconstruction is created. The reconstruction of the octachord generated in this analysis consist of $39 * 10^6$ vertices. Inspection of the wireframe mesh was carried out in the geometrical inspection software, GOM Inspect V7 SR2. The GOM Inspect software is specifically designed for comparative analysis of wireframe meshes. First presented is a comparison between the reconstructed geometry and the original CAD model. The following results shows the divergence between CAD model and reconstruction as a color map.

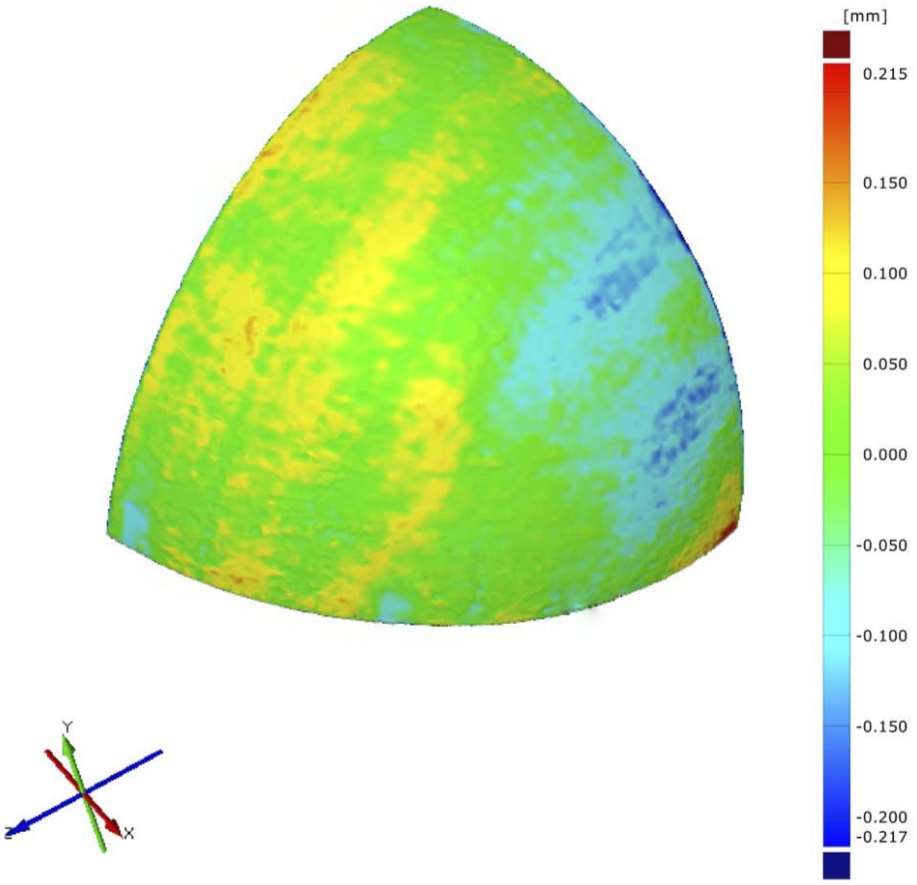

Figure 4.11: *Test geometry - An octachord of a sphere, front view.*

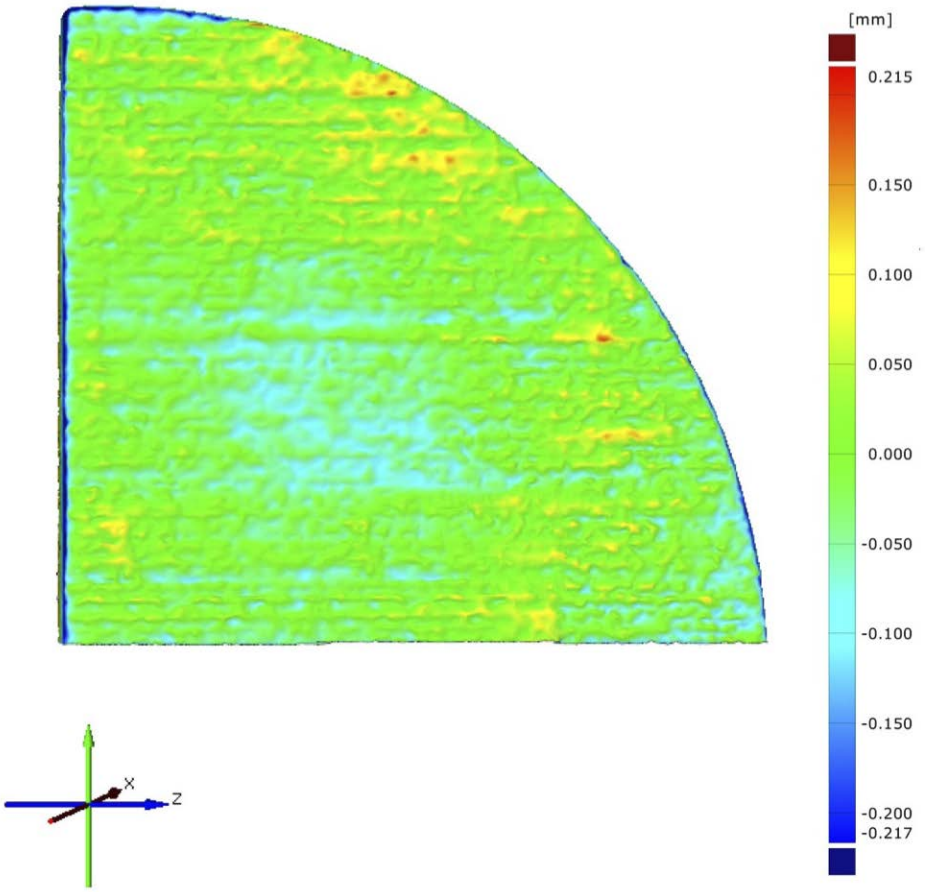

Figure 4.12: *Test geometry - An octachord of a sphere, right view.*

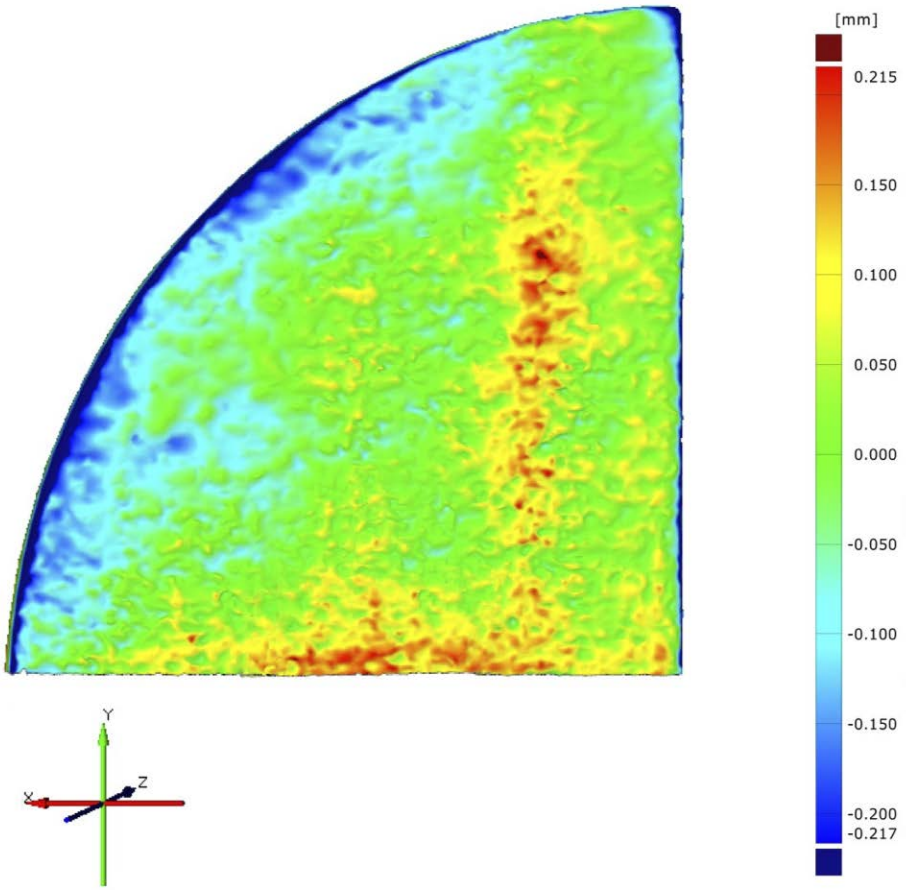

Figure 4.13: *Test geometry - An octachord of a sphere, back view.*

The reconstructed geometry and CAD model has been aligned using a common coordinate pre-alignment followed by a globally least divergence fit which is a standard alignment method supported by the GOM Inspect software. Figure 4.11 on page 118 shows a divergence as high as two tenths of a millimeter from a viewpoint showing the spherical part of the reconstruction compared the CAD model. Divergence as high as ±0.2 mm are visible and dominant in the right side of the octachord. Divergence of a similar magnitude can be seen from the side views in illustration 4.12 on page 119 and 4.13 on the facing page which show the planar surfaces of the octachord with most excessive divergence seen on illustration 4.13 on the preceding page.

This side of the octachord has been aligned as a normal to the gantry of the printer. It is this direction where the largest deterioration in print quality can be expected as the accumulated position accuracy here is the sum of the lateral axes of the machine. In order to quantify the contributions to the divergence it is needed to verify the reconstructed model against a reference measurement. This will visualize whether the divergence is a result of actual geometrical errors innate to the print process or whether these are due to inaccuracies from the geometrical reconstruction method. To perform this analysis a 3D scan of the octachord has been performed on a 3Shape Q640 line-laser based optical scanner. Traceability of this scanner is maintained, and it has been verified against a spherical calibration artifact.[69] A Ø15 mm calibration sphere (form deviation of 1 micrometer) was scanned and a deviation between the measured and calibrated diameter was found to be of the order of less than 10 micrometers. Figure 4.14 on the following page shows the divergence gradient map for the analysis of the 3D reconstruction with respect to the 3D scan. It clearly shows that there is a general agreement of the two methods within ±0.02 mm. The grey artifact in the lower centre, is a piece of wax fixing the specimen on the 3D scanner turntable. Figure 4.15 on page 123 and figure 4.16 on page 124 show a similar agreement however with slightly larger divergence. The mean divergence between the two geometries is calculated to 0.026 mm.

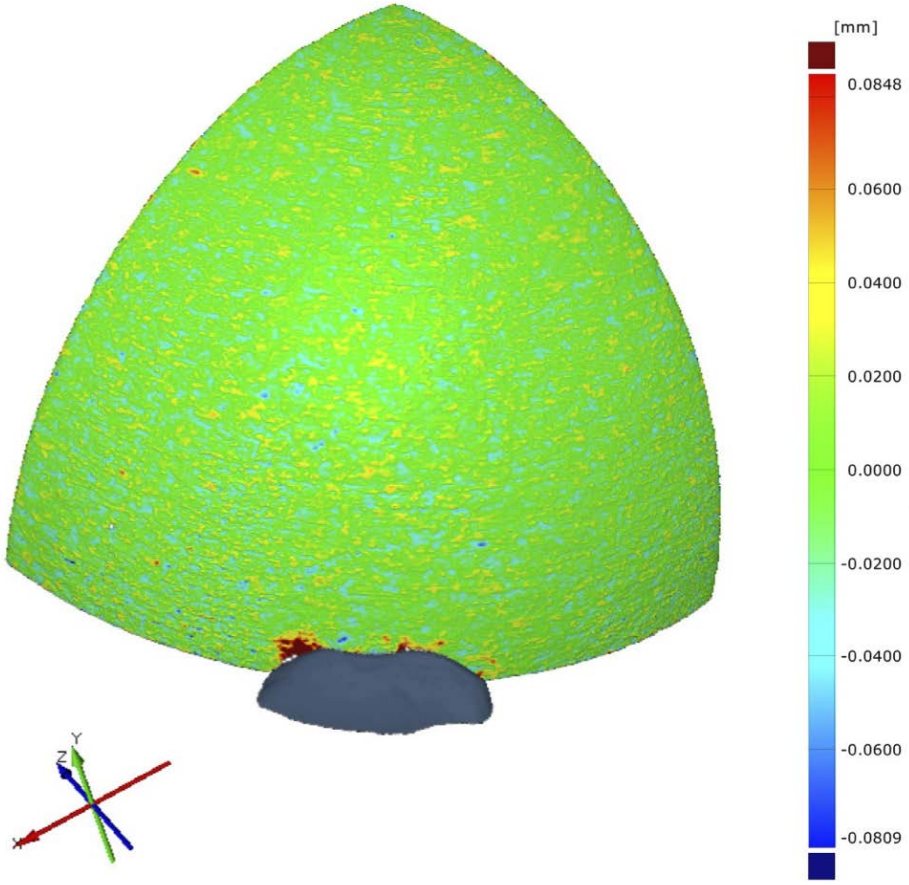

Figure 4.14: *Test geometry - An octachord of a sphere, front view.*

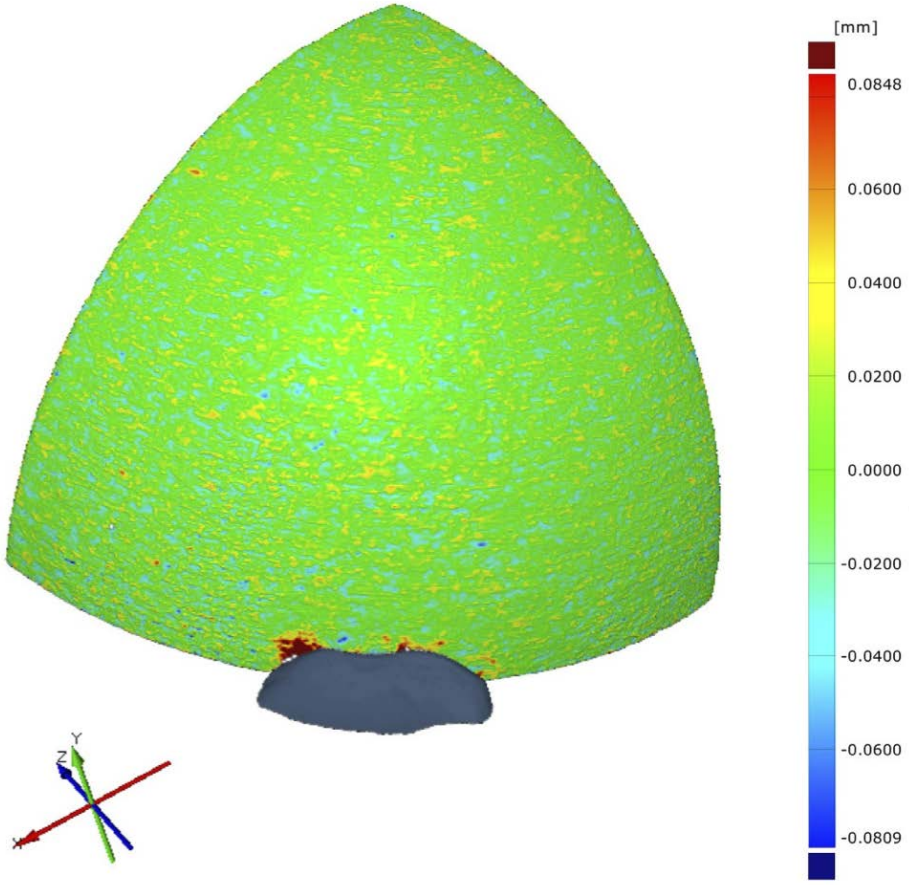

Figure 4.15: *Test geometry - An octachord of a sphere, right view.*

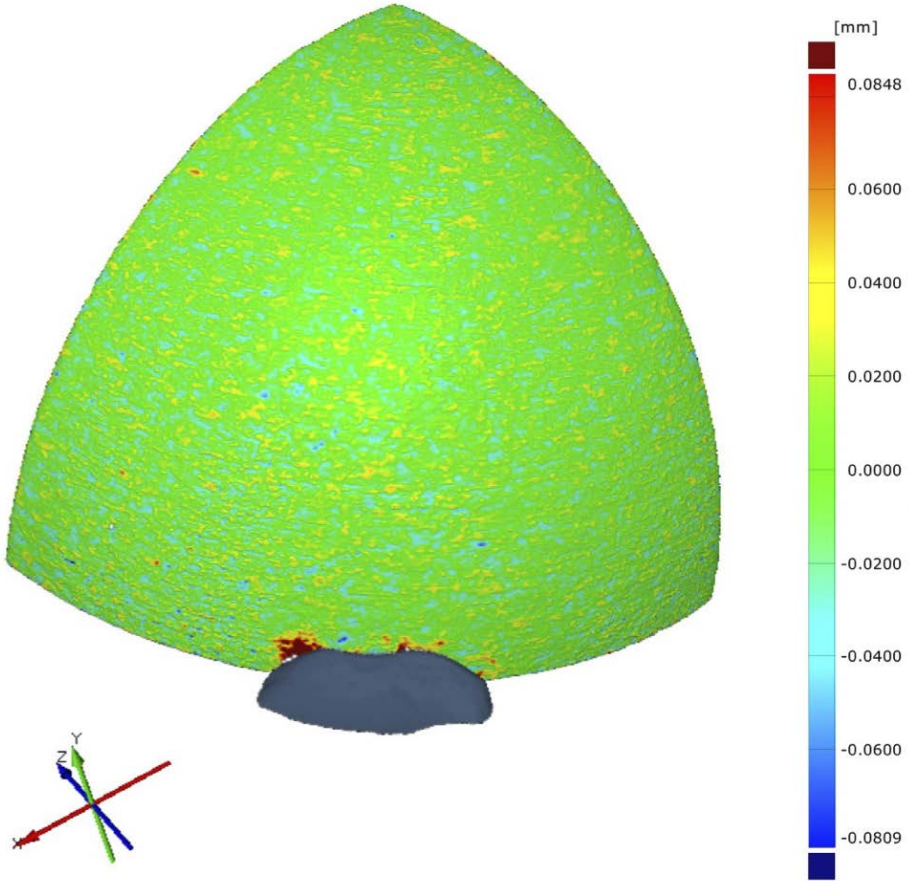

Figure 4.16: *Test geometry - An octachord of a sphere, back view.*

4.2.3 Absolute reconstruction - Conclusive summary

The vision system implemented on the z310 3DP platform from zCorporation was tested with a well defined geometry. Deviations of ±0.2 mm between physical object and CAD model were observed. This sounds reasonable taking into account the resolution of the printer and the influences of the process as discussed previously. It is quite surprising that the vertical resolution of the printer seems to influence the result in a minor way. The absolute accuracy of the setup was verified by scanning the printed physical object on a separate instrument, and good agreement was found (within ±0.026 mm). The resolution of the independent scanner as well as its calibration (based on Ø15 mm calibration sphere) was of the same order of magnitude as the calculated deviations. This could pose a potential challenge, and therefore it should be investigated further by employing a more accurate reference measurement. For the current geometry this will not give any problems. Nevertheless, the current setup is giving reliable and reproducible results and by employing a proper calibration setup, traceability can be ensured. The potential of the system to be used with more complex geometries is yet to be tested. In particular, measurement uncertainty should be determined for example based on a comparison principle. This however will not be addressed within the context of this research project at research is focused on a fundamental level.

4.3 Challenging the reconstructing vision system

The two studies of the pilot test from section 4.1 on page 107 and the absolute geometrical verification from section 4.2 on page 114, both relied on the high geometrical stability and little buildup of stresses from a non-thermal additive manufacturing process. Furthermore the verification relied on a distinct contrast difference between the cross section of the structure and the surroundings to allow for boundary detection. The non-thermal 3DP process however is not of the most adopted additive manufacturing processes within the industry. The two favored industrial processes for direct additive manufacturing are SLS/SLM and SLA/DLP,[2, p. 48-67] which challenge the reconstructing vision on either aspect.

4.3.1 Absolute 3D reconstruction from a thermal process

SLS/SLM as thermal processes are prone to introduce stresses to parts as they are built, resultantly imposing deformations. To assess how this impact the reconstructive capabilities of the vision system, a series of tests was carried out to determine the validity of reconstruction from the relaxed contour of each manufactured layer. The powdered based 3D printing process that was used within the pilot test and the test of absolute reconstruction capabilities share process simi-

larities to SLS/SLM machines. As previously stated in section 2.3.4 on page 45, 3D printing process is a powdered based process where a powdered stock material is selectively hydrated by means of an inkjet cartridge. The platform construction of an SLS/SLM machine is nearly identical to that of the 3D printing process. In section 2.3.5 on page 47 the working principle of these machines are described. SLS/SLM likewise employ a powdered stock material, and selectively bond this to a solid, the main difference is that the bonding occur as a sinter or melting process by means of a high-powered laser source.

Given the close process resemblance, the vision system was set up following the same methodology as with the former experiments involving the 3D printing platform. The camera employed was a Canon EOS 1000D with a EFS 18-55mm f/3.5-5.6 IS lens kit. The additive manufacturing platform used for this test is a Realizer SLM 250 with a build chamber if 250 x 250 x 300 mm. The build layer height setting used within tests was 20 micrometer, and the laser beam diameter was 45 micrometer. The camera was calibrated, and the build-job monitored by the vision system, sampling each layer built. One sampled layer can be seen in figure 4.17 on the next page. It is evident that a clear contrast distinguish parts from stock metal powder. Three parts were subject to test. The first part was a hole plate similar to the plate that formed the base for the pilot test in section 4.1 on page 107, the CAD file measuring 50 x 50 mm in the vertical direction. The second part was an octachord of a sphere with a radius of 10 mm. The third part was a hollow cube, core built with lowered thermal laser input, to assess whether defect stemming from laser power instability can be observed by means of the vision system. Inspection of the wireframe meshes was carried out in the geometrical inspection software, GOM Inspect V7 SR2. Reference measurement has been carried out using the same scanner that was employed to assess the absolute reconstruction capabilities of the vision system in section 4.2.2 on page 116.

The spherical geometry and hole plate form the base for verification of the performance of the reconstruction method. First, the hole plate will be addressed.

Verification of reconstructed hole-plate geometry from an SLM build job

Figure 4.18 on page 128 show the reconstructed geometry from the vision system of the hole-plate geometry. In order to establish a tangible perception as to how this reconstruction conform with the true geometry that has been produced by the SLM machine, a comparison against a reference 3D scan with a traceable accuracy of 10 micrometers. This comparison can be seen in figure 4.19 on page 129. Here it can be seen that the reconstruction is disputable to an extend of ±500 micrometers. This disagreement however, primarily in the positive side, is pronounced only locally as small speckles to the surface. This is inherited from residual image noise that the filtering algorithms have not been able to remove, and must be

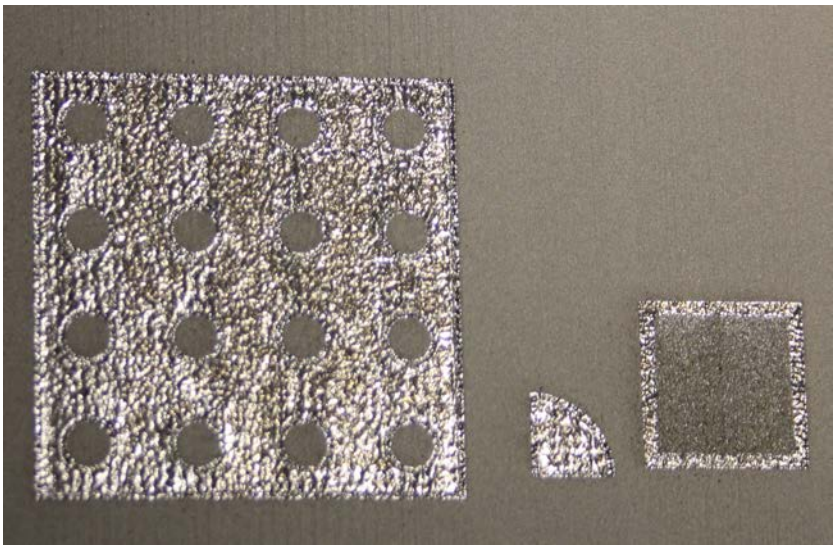

Figure 4.17: *An acquired layer from the SLM build of test geometries by the vision system.*

regarded upon, as noise that can be avoided in a process-dedicated vision system. The median divergence is of a magnitude of ±140 micrometers, supporting that a margin of performance enhancement is readily to be claimed by such process-dedicated system.

Benchmarking reconstructed geometry against CT scanning

CT scanning technologies are at present the only alternative to the vision based layered reconstruction method. As CT scanning allow for complete reconstruction of complex additively manufactured structures, a benchmark of the vision system against CT scanning has been carried out. CT scanning was performed by an industrial partner on a Zeiss METROTOM 1500 CT scanner. The scan was made from 1080 projections, with a filter of Cu 0.25mm. The resultant geometry from this CT scan is visible in figure 4.20 on page 130. As with the reconstruction from the vision system, it was the intent to compare the CT scan from the hole plate to the 3D scan of traceable accuracy from the line laser based 3D scanner. However, as given from 4.20 on page 130, the CT scan proved deteriorated to a degree where such a comparison would not yield any complacent data. Likely the reason so, is the extend of bulk material in the part structure. Identification and avoidance of artifact is a continuing challenge in CT. These can seriously degrade the quality of computed tomographic images, this to an extend to where the resultant data is rendered unusable.[70] In this case it is expected to origin from physics-based artifacts stemming from the physical processes involved in the acquisition of CT data.

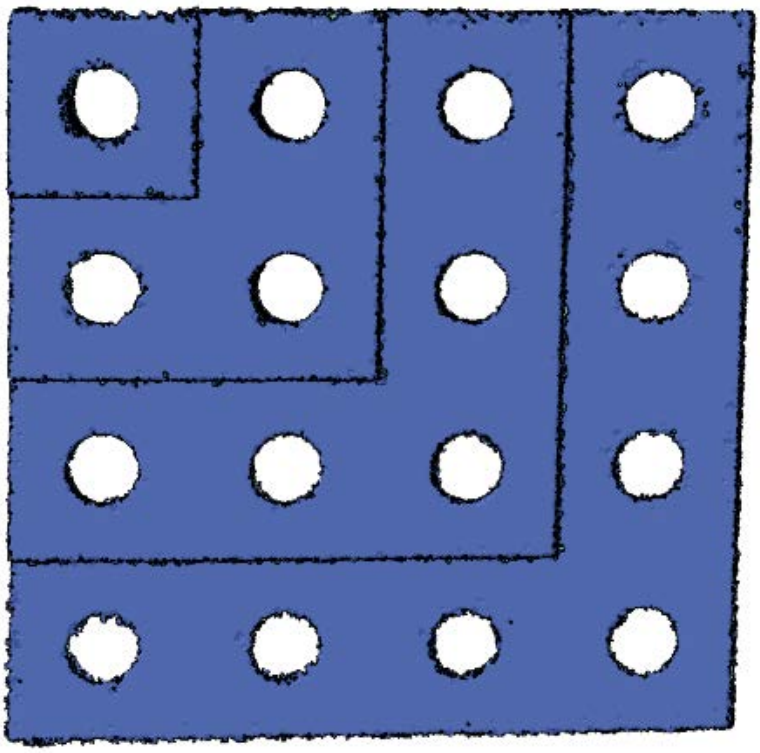

Figure 4.18: *The reconstructed geometry from an SLM build of a hole plate geometry.*

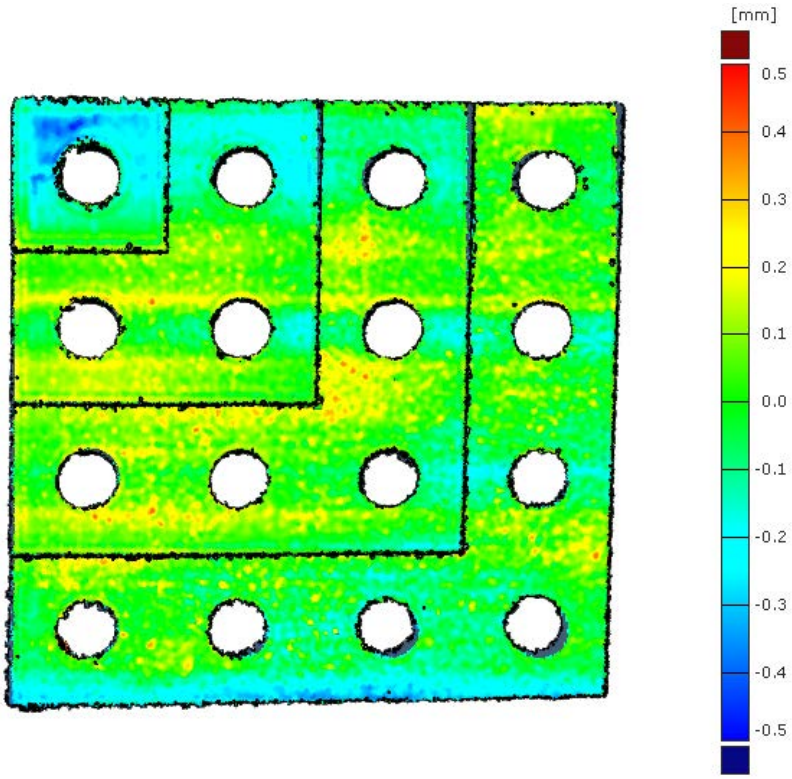

Figure 4.19: *Comparison of 3D scan and the reconstruction from an SLM build of a hole plate geometry.*

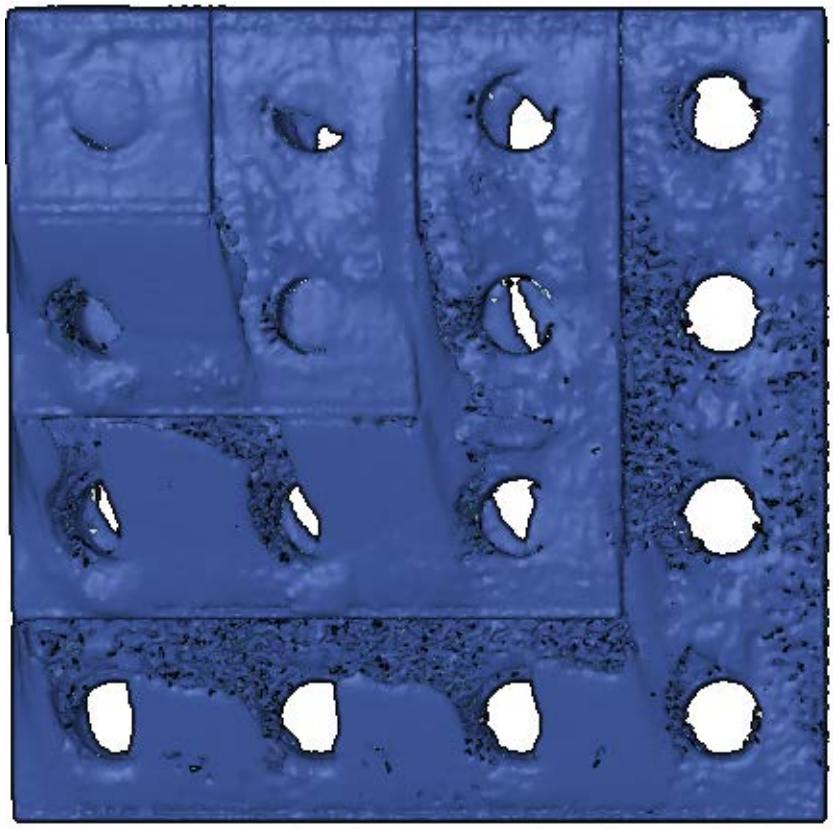

Figure 4.20: *CT scan from an SLM build of a hole plate geometry.*

4.3.2 Absolute 3D reconstruction from a resin based process

Where the challenge in terms of reconstruction from vision data in thermal processes is the alteration of layers built from their relaxed to their deformed state as stresses build up. For resin based processes the challenge is for the vision system to be able to see anything whatsoever. The vision system will be blinded from the uncured photo initiated resin having the same optical characteristics as the cured resin. Hereby distinguishment of the structural bounds within layers are impossible without interfering with the build process, by emerging the structure out the resin to acquire image data for each layer. As this level of alteration of a resin based platform will require platform alteration at a control level, and that no resin based platform allowing this is available within the research scope, an alternative proposal is made. To evaluate the build job based upon back-scattered light from the build surface. The following is derived from a publication to the Journal of Manufacturing Technology, by the author. [71] The validity of this proposal is thus demonstrated by integration of a vision system adaptation that is integrated into a DLP platform, the EnvisionTEC Perfactory MML.[72] This machine boast a high resolution in the vertical direction of down to 16 micrometer and a layer height of down to 15 micrometer. The vision system implementation indirectly capturing the layered geometry by the reflection of the projected light to the resin tray of the machine during the build job.

Vision System Alteration For Implementation To a DLP platform

The flexibility of the vision system is how it allow layered image acquisition and subsequent reconstruction to be transferred to practically any layer-by-layer manufacturing process. The Perfactory MML, is based on the principle of liquid photo-initiated polymerization, by exposure by a DLP based projection unit. The photo-initiable monomer is held within the confines of a transparent resin-tray, which is set above a projector. The build platform, the vertical axis of the machine is a flat surface to which the built structure adhere. When a build job is initiated, the build platform is submerged into the resin tray, leaving but a thin layer of monomer between the tray and the build platform. This define the layer thickness of the first layer. The projection unit expose the monomer by imaging a pixel pattern, thus hardening the cross-sectional area for the given layer. Considering all possible configurations of the machine the lateral resolution is from 16 to 60 micrometers and the vertical resolution is from 15 to 150 micrometers[72]. From experience it is known that the build platform is exposed from the projector in two intervals for each layer. The two intervals last for about 4-5 seconds each and are separated from each other with a times of less than 10 seconds. The two intervals are related to the Enhanced Resolution Module (ERM) of the platform, that consist of a $\frac{1}{2}$pixel shift in the vertical directions, for generate a surface interpolation

Figure 4.21: *Additive Manufacturing job on an EnvisionTEC MML, DLP platform.*

effect to reach a doubled resolution.

As the key challenge of the implementation for DLP is the fact that liquid monomer and the solid polymer have the same optical properties, the vision acquisition system for the Perfactory MML it is comprised to monitor the back-projected reflection of the exposure pixel mask instead of the actual object that is being built. The principle is illustrated in figure 4.22 on the facing page. The camera used for the acquisition system is a Canon EOS 1000D with a EFS 18-55mm f/3.5-5.6 IS lens kit. which is placed next to the projection unit facing up towards the resin-tray. The light from the projector is reflected at the bottom of the tray downward to the camera. This gives a back-projected image showing where the hardening process is photo-initiated by the pixel mask.

Validation of the back-projection reconstruction method referenced to tactile CMM

In order to validate the system, a series of test geometries has been built. In this series, three objects have been created in a single build job, while acquiring vision data. Figure 4.23 on page 134 show one specimen of each of the two different geometries after completion of the build job. The geometries are scaled-down versions of the test artifacts used in the preceding validation tests, the plate thus

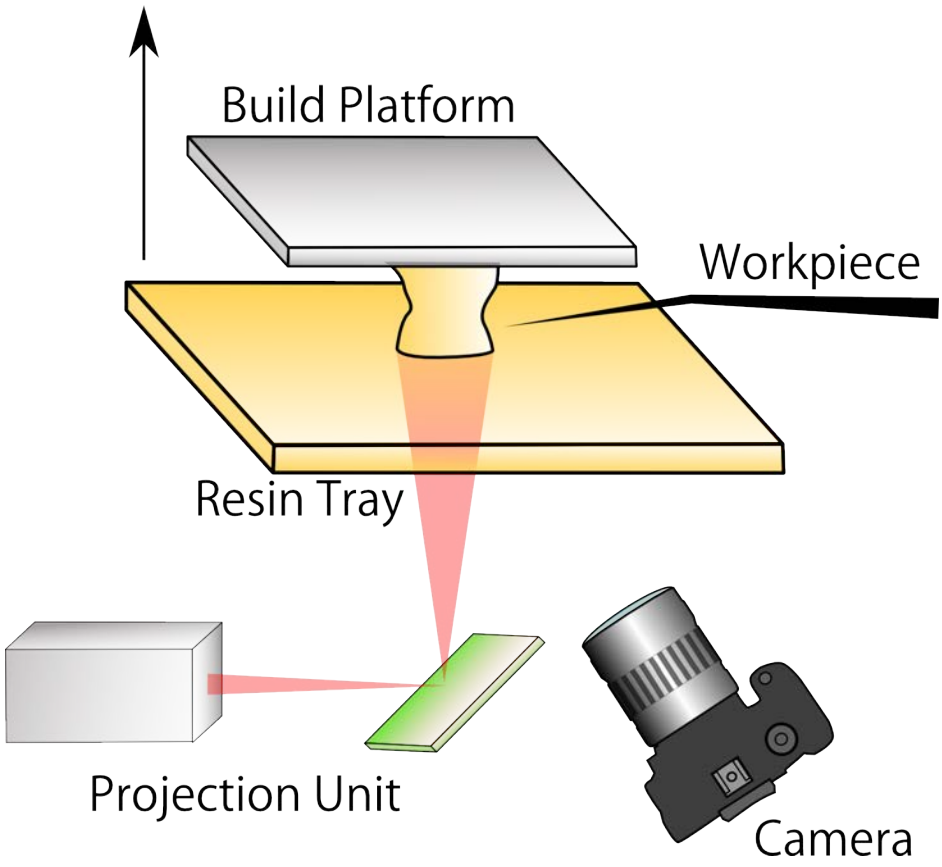

Figure 4.22: *Principal sketch of the vision system integrated in the Perfactory MML. The build platform moves in the direction of the arrow during a build job. The camera acquire the back-projected exposure pattern for each layer.*

measuring 15x15 mm and spherical octachord radii of 5 mm.

The hole plate was in this experiment forming the base to verify the image calibration by means of the hole-pattern. Calibration measurements on the physical part were performed at a Carl Zeiss 3D coordinate measuring machine of type OMC 850. Each of the 9 cylindrical holes were defined and measured as circles, given the radius and the coordinates of the center for each circle. The coordinates of the circle center points made it possible to calculate up to 36 different distances that can be compared with the images. The standard deviation of the measurements were no more than 2.1 micrometers, which is within the accuracy of the coordinate measurement machine that was employed.[71]

A comparison of the circle center point positions from the CMM measurements was now compared with image data. The position of each hole from the vision system was correlated with CMM data, and the minimum, maximum and mean difference was found. These results are presented in figure 4.24 on page 135 and

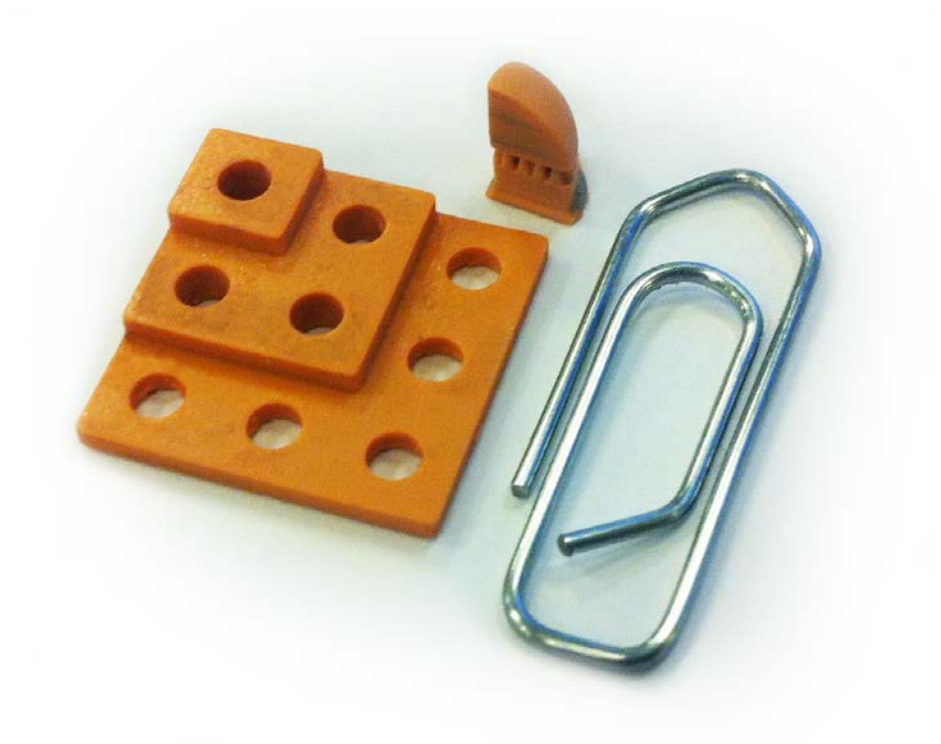

Figure 4.23: *The test objects for the validation of layered reconstruction applied to DLP. Showing a test-plate with support structure removed and a supported octachord of a sphere.*

figure 4.25 on page 136 for a total of 27 images. Combining the uncertainties of image measurements and the CMM measurements the total uncertainty of extrapolated image data of no more than 8.48 micrometer per millimeter in the X direction and 7.88 micrometers per millimeter for the Y-direction.

Validation of the back-projection reconstruction by 3D scanning

The images of each layer of the build job and the calibration factors contain all the information needed to make a 3D-reconstructions, with indicative uncertainties given from the CMM reference measurements. This is now employed to the octachord geometry of the build job. Figure 4.26 on page 137 show a comparison between the original CAD file and the reconstructed geometry. The reconstruction show good agreement with the CAD data, however it can be disputed whether the pixellated surface structure of the reconstruction given from the image set from which it has been created is an indicator that the reconstructed geometry spited calibration is too coarse to be representable for the surface.

A comparison with a 3D scan was also made, as with the preceding experiments, this was done on a traceable 3D scanner with an uncertainty of no more

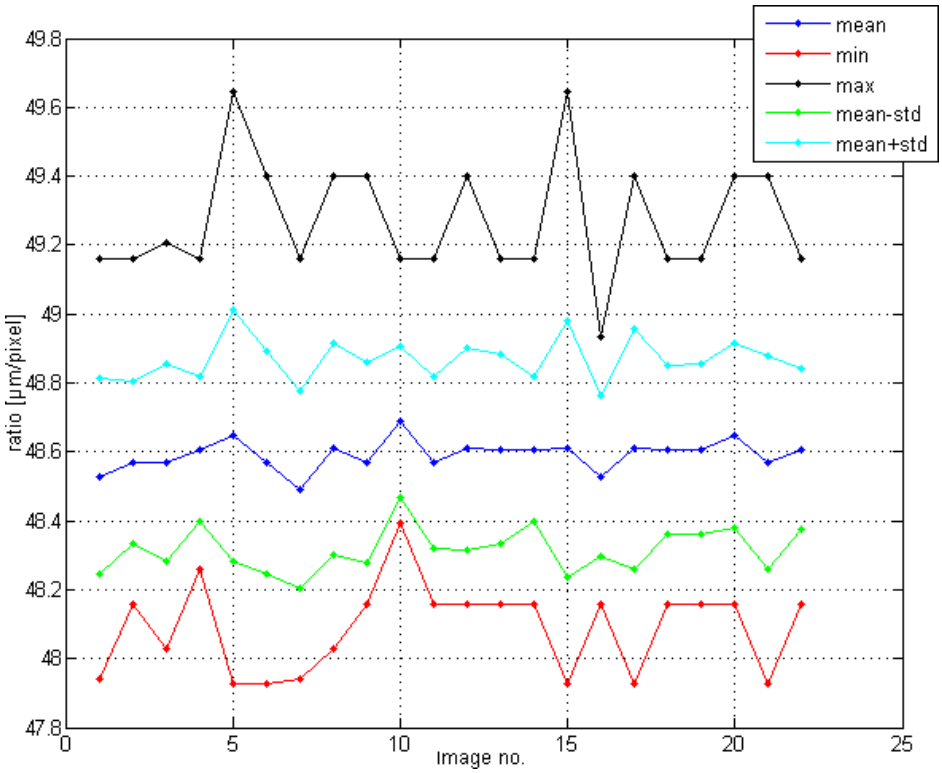

Figure 4.24: *Mean, min, max and mean ± standard deviation of the ratio between the distances in the X-direction in mm and in pixel.*

than 10 micrometers. The comparison of this scan and the reconstructed geometry can be seen in figure 4.27 on page 138. The results show good agreement, though it must be considered that the reconstruction method is not based upon measurements of the physical part as, but from the back projected pixel pattern. It can therefore be disputable if this implementation of the vision system hold true for parts affected by process-specific defects. However the 3D reconstruction of the octachord shows deviation in comparison to 3D scans of about 80 micrometer, which indicate the strong potential of this implementation. AIt is believed that the reconstruction method has the potential to become very accurate if high resolution images are obtained, it is however necessary to conduct more tests in order to verify the accuracy of the use of indirect measurements in a DLP build job

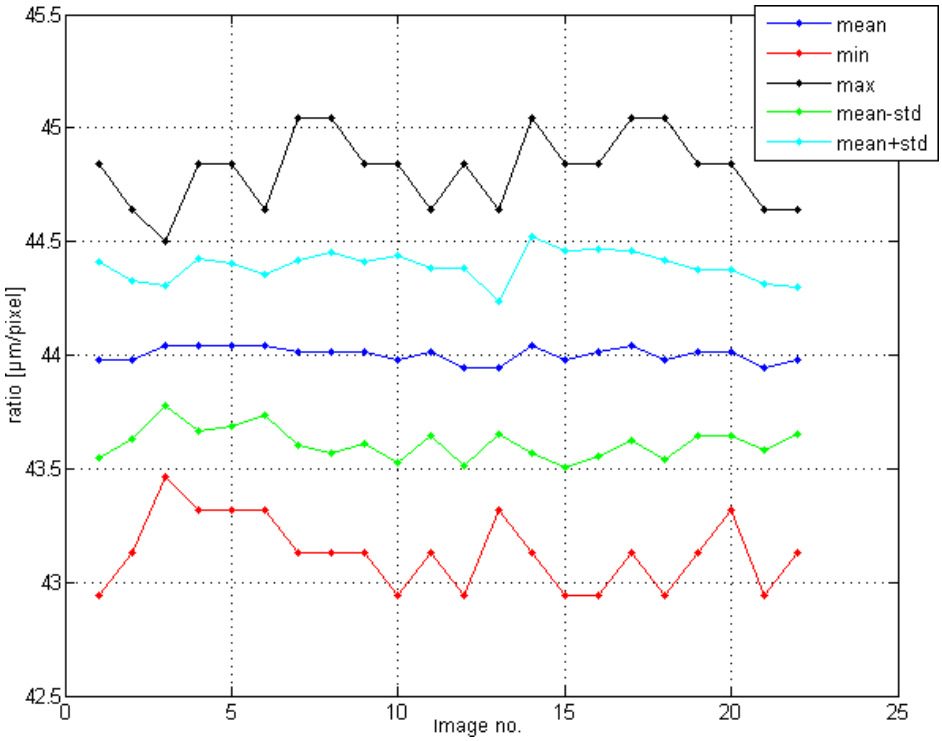

Figure 4.25: *Mean, min, max and mean ± standard deviation of the ratio between the distances in the Y-direction in mm and in pixel.*

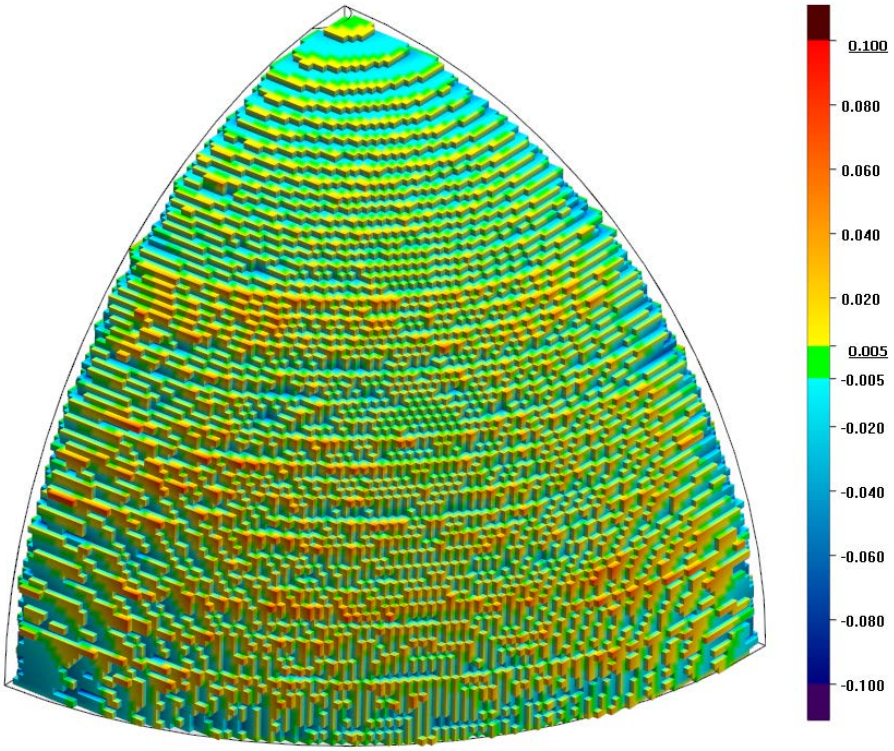

Figure 4.26: *Comparison of 3D reconstruction from the DLP machine and the original CAD file.*

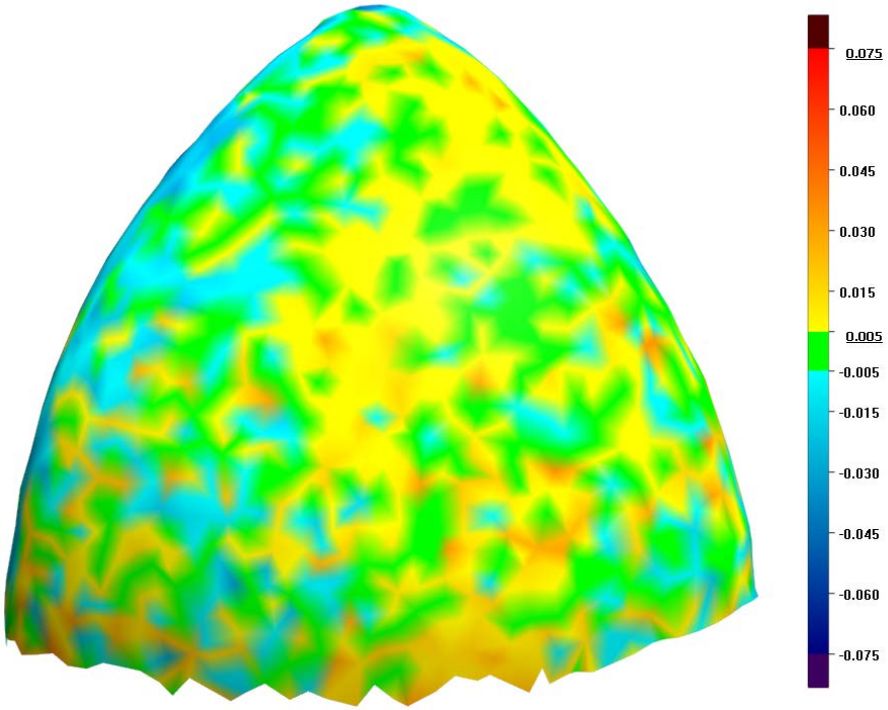

Figure 4.27: *Comparison of 3D reconstruction from the DLP machine and a reference 3D scan.*

4.4 Conclusions

The precedent chapter has been devoted to the testing to a novel, numerical architecture for a vision system for inline monitoring of additive manufacturing processes which was proposed in section 3.1 on page 71 of chapter 3 on page 71. The vision system has been subject to field tests on several additive manufacturing platforms, counting a powder bed based 3DP platform, and SLM platform and a DLP platform. A hole-plate and an octachord of a sphere was used throughout all tests.

Pilot study

The vision system was first tested in a pilot scenario, documented in section 4.1.3 on page 109. The vision system was set up with a 3DP platform from zCorporation. The choice to implement the vision system on this particular platform was governed by the fact that the 3DP platform itself was evaluated to be highly suited for a pilot test for the vision system. This because the cross-sections of bonded processing material is easily distinguishable from the background. A complete and successful reconstruction of the test geometry was generated from the vision system, and upon a comparison to the original CAD file defects was found on the reconstructed geometry that was also present on the additively manufactured part. This was furthermore the first time throughout the research project that the vision system proved its capability to autonomously collect geometrical information of each manufactured layer in-line with the process, and to subsequently produce a full 3D reconstruction. It was concluded that all deficiencies that can be visually observed on the physical part are deficiencies that also can be observed on the geometrical reconstruction. It was possible to detect internal deficiencies from the reconstruction also present on the part. Quantitative analysis of parts and comparison of results obtained with the vision system and reference measurements was not performed.

Absolute 3D reconstruction using a calibrated camera

The vision system was again benchmarked on the 3DP platform from zCorporation. This time the geometry in focus was the octachord geometry. It was built while monitored by a calibrated camera system. The subsequent analysis of the reconstructed wireframe mesh showed deviations of ±0.2 mm between the physical object and CAD model were. This was accepted as being reasonable taking into account the resolution and bleed effect which is given by the manufacturing system. The absolute accuracy of the setup was verified by accredited 3D scanning of the printed physical object and good agreement was found. The vision system was classified as giving reliable and reproducible results and by employing a proper calibration setup, traceability can be ensured.

Challenging the vision system - SLM

To challenge the vision system, two tests was carried out in order to verify how the system handle reconstruction of parts built by a thermal process and by a process where the numerical feature detection algorithms cannot rely on a distinct contrast difference between the cross section of the structure and the background to allow for high quality feature detection. First, an SLM build formed the base of a test on a thermal system. In order to establish a relation to how the resultant geometry reconstruction from the vision system conform with the true geometry, a comparison against a reference 3D scan with a traceable accuracy of 10 micrometers was carried out. The reference scan disputable the reconstruction to an extend of ±500 micrometers. This disagreement however, was primarily to the positive side, and pronounced only locally as small speckles to the surface. The median divergence was found within a magnitude of ±140 micrometers, supporting that a margin of performance enhancement is can be claimed if the speckled artifacts can be handled within the reconstruction algorithms. A reference scan with a CT scanner was attempted. The CT scan proved deteriorated to a degree where a comparison would not yield any complacent data. Likely the reason so, can be the extend of bulk material in the part structure. This proved that for the given structure, the vision system by far outperformed the CT scan to which the vision system was benchmarked.

Challenging the vision system - DLP

Where the challenge in terms of reconstruction from vision data in thermal processes is the alteration of layers built from their relaxed to their deformed state as stresses build up. For resin based processes the challenge is for the vision system to be able to see anything whatsoever. This as resin and cured material have the same optical properties. An alternative proposal is made which is to evaluate the build job based upon back-scattered light from the build surface, indirectly reconstructing the geometry. The hole plate test geometry was used to assess the camera calibration against a tactile CMM and was found to be traceable within ± 8.48 micrometers. The reconstruction of a DLP built octachord of a sphere was compared to the original CAD file and found to agree within ±80 micrometers. Agreement within ±75 micrometers with a reference 3D scan was seen.

Summary

The proposed inline vision system has been put through several tests against several additive manufacturing systems. Till now the system has proven to be up to the task of reconstructing geometries otherwise only possible by CT scanning. The system outcompeted a reference CT scan of a large metal part by to an indisputable degree. The system finally showed promising results when applied indirectly to reconstruct geometries from a DLP system. In general, the system

has a potential for being implemented in different AM machines and processes and provides traceable measurements of the complex parts. As the technology of inline layered reconstruction of additively manufactured parts has just been proposed within this thesis, the technology is at a dawning level, and there is an abundance of open questions to be answered and much yet to be investigated. It is impossible but leaving this part of the project open-ended. What is to hope is that future research will tie these ends with the emerge of a fully developed system.

·⁚*Multi Material Deposition in Additive Manufacturing as a prospect of the emerge of a electromechanical universal constructor. Synthesis of technologies and choosing a multi material platform*⁚·

5 Multi Material Additive Manufacturing

Natural evolution of production methods lead to the merge of related technologies. CNC machining which is a production method that with AM share a high level of numerical process control is illustrating this phenomenon clearly. CNC machining is no longer limited to process-dedicated machines such as 3-axis mills and lathes. Multi-axis CNC machines nowadays allow milling, drilling and turning operations to be performed within one processing machine. In an assembly line with high level of automation where, robots handle parts and partially fabricated assemblies from sub-process to sub-process, production is bordering an automaton level.Additive manufacturing however, is a branch of processing technologies in their youth. There has yet to be seen a blend of processing methods such as in the CNC world. It is however expected that in the future, multi-material production on commercial Additive Manufacturing platforms will become a reality.It is envisioned by Dr. Evan Malone[73], the founder of a multi-material printing platform known as fab@home, that a universal manufacturing machine will see its existence, a contrivance born by technology that resembled the literary invention of a Mary Poppins bag[74] , or what can be imagined as a magical box from which you can take out any physical thing. A machine that from a CAD/CAM model and by CNC control, will be able to facture any physical produce imaginable, even possess the ability to self replicate. Self replication is not a new idea. Since the dawn of civilization it has been a trait of human nature to feed the desire to create in our own image. To produce life. This desire has amid the reign of mankind been documented in philosophical texts and literature, often shrouded by mysticism. In the early years of last century however what had been a mysticism and with little foundation in science, was propelled into modern scientific acceptance by mathematician John Von Neumann. John Von Naumann recognized trivial self-reproduction methods do exist and that these could be controlled by man. Examples of such systems amongst many are crystal-like growth and template replication. These reproduction methods however serve little scientific relevance to how life evolves and does not condone the mechanisms of construction universal-

ity and evolution. Von Neumann wanted to describe self-replication as an artificial life form that can exist and evolve to a diverse variety of forms and thus possess a high level of evolvability. Neumann achieved this by introducing a universal constructor, a simulation with an abstraction layer to a physical universal assembler. The universal assembler is a device that can create matter. A such device can be envisioned as a nano mechanical device as proposed by K. Eric Drexler, that can guide molecules with atomic precision. [75] Von Neumann defined his universal constructor as a machine using 29 states.

The states constituted by means of signal carriage and logical operation, and act upon signals represented as bit streams. A 'tape' of cells encodes the sequence of actions to be performed by the universal constructor. Using a writing head (termed a construction arm) the machine can print out (construct) a new pattern of cells, allowing it to make a complete copy of itself, and the tape. [76] John Von Neumann started to formulate his universal constructor as a mathematical model in the 1940's without the aid of computers. The first implementation of his works was published in 1995 by Pesavento Umberto [77] in an article that

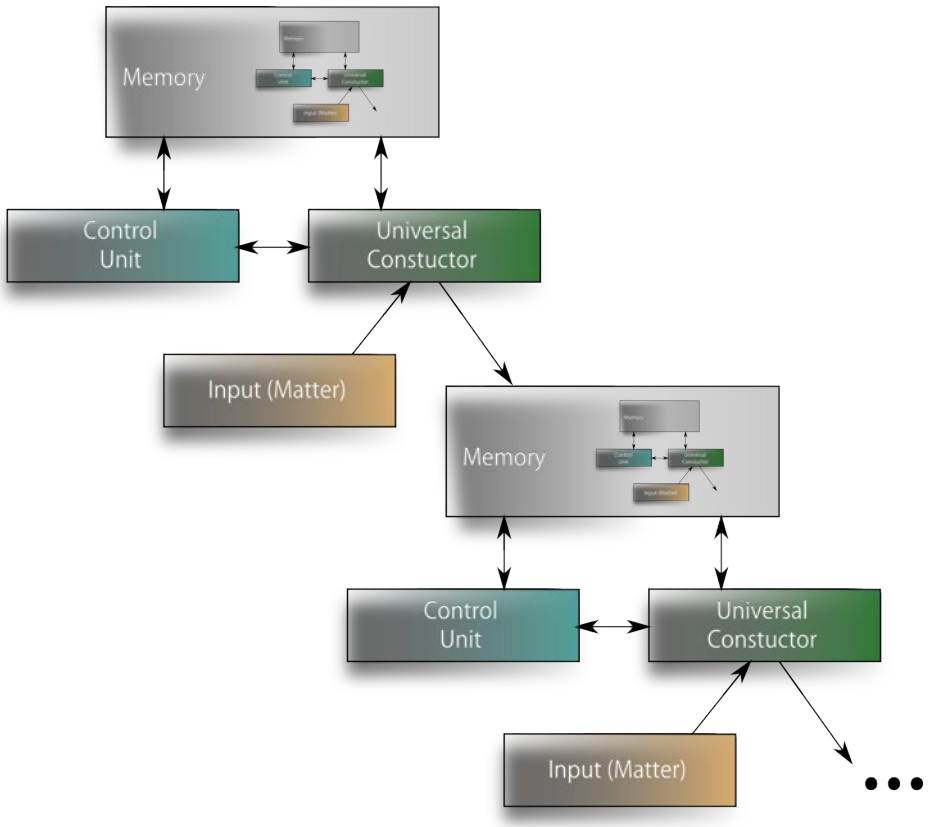

Figure 5.1: *Simplified Nobili-Pesavento replicator model structure, Incubating the third generation John Von Neumann automaton.*

describes in detail ⌜*an implementation of John von Neumann's self-reproducing machine. Self-reproduction is achieved as a special case of construction by a universal constructor.*⌟ The theoretical proof of the existence of such machines was given by John von Neumann in the early 1950s, but was first implemented in 1994, by the author in collaboration with R. Nobili. The source of this implementation, written in ANSI C, is openly distributed[1]. A simplified Nobili-Pesavento replicator model structure, Incubating the third generation John Von Neumann automaton, can be seen in figure 5.1 on the preceding page. Now, 18 years after the first numerical implementation of John Von Neumann's universal constructor, the world embrace a technology that may allow for the creation of the first coequal physical implementation. K. Eric Drexler, envisioned a device guiding molecules with atomic precision. In this dissertation the device is envisioned as a multi-material additive manufacturing machine. Hence not only does the prospect of multi-material manufacturing reveal what can best be described as a universal manufacturing platform, it may very well prove to become a worthy contender to the field of nano-technology, as to which technology will first provide a physical implementation of John Von Neumann's model. A true artificial life form shaped as an autonomous self-replicating platform.

[1] ftp://ftp.ira.uka.de/pub/cellular-automata/jvn

5.1 Motivation

Many a reason can be accentuated as a source for motivation to compel research in the field of additive multi material technologies. Three of these sources that is of particular interest in this dissertation is the medical field, the environmental field, and in the structure of commerce.

5.1.1 Tissue Engineering

A field that at current is experiencing explosive growth is the medical field of tissue engineering.[78] With a constant sector growth over the last 10 years, and commercial sales going up from $1.4 billion to $3.5 from 2007 to 2011, it is a field that is not only promising to contribute immensely to the world-wide welfare but also a field in strong financial growth which is reflected by the funding of research in this field. The annual development spendings of 2011 exceeded the sales by a small margin, yielding more than $3.6 billion worldwide. Amongst the many research fields in tissue engineering is the field of scaffolding for cell growth. The concept involve to promote cell growth of a targeted cell type to a structure that resemble a human bodily subsystem such as a blog vessel, a bone (structure) or even a complex system comprised of different cell types to allow the growth of organs.[79] Several scaffolding media is suitable for stimulating cell growth. Amongst is PLA, a biodegradable polymer which is the most commonly used synthetic biomaterial.[80] PLA is highly suited for Additive Manufacturing using Fused Deposition Modeling, hence three-dimensional scaffolds are often preferably realized by means of this process.[81]

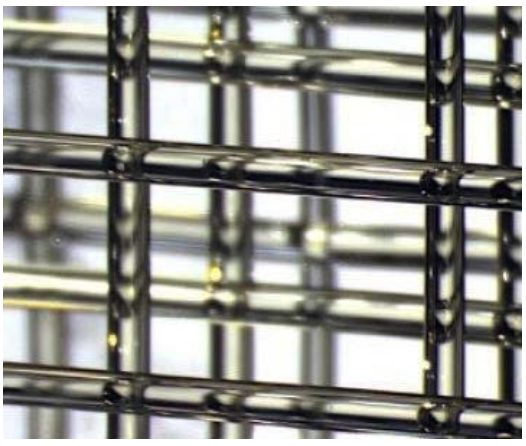

Figure 5.2: *Scaffold for Tissue Engineering made in Sugar.*
Source:[82]

Sucrose is another material used for tissue engineering applications, and adapted FDM machinery is able to realize three-dimensional structures in this material.[82]

A printed lattice forming a sugar scaffold can be seen in figure 5.2 on the facing page. By developing multi material deposition, a future prospect will be to allow for the design of much more complex scaffolds that in different sectors promote growth of different cell types, hereby making it possible to engineer much more complex structures than today.

5.1.2 Environmental Benefits of Multi Material Deposition

The prospect of advanced Multi Material Deposition systems that evolve into universal constructors, or desktop factories will allow for an entirely new way of making use of the natural resources of the Earth.[73] The environmental impact on our global ecosystem today as a result of mass production can be illustrated by visualizing the global shipping routes as of figure 5.3

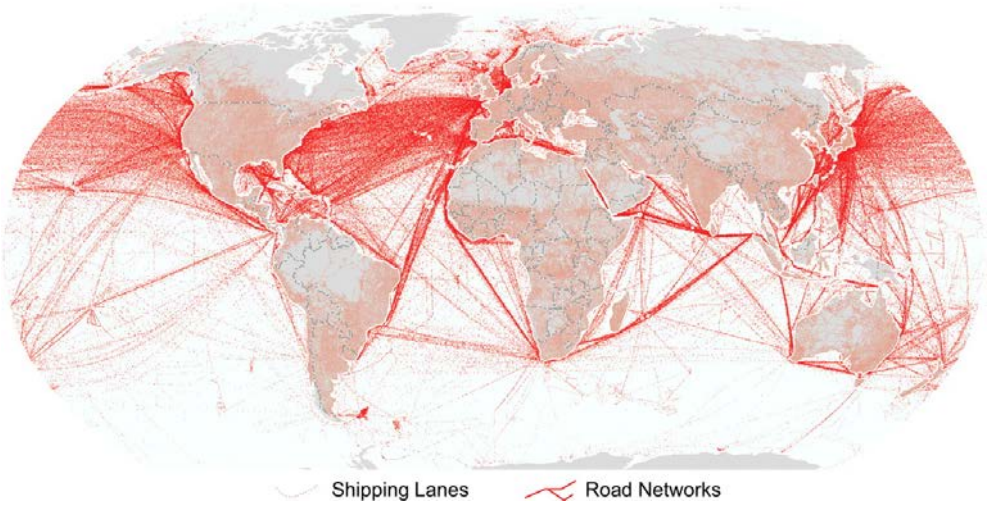

Figure 5.3: *Global Shipping Routes by Sea and Road.*
Source:[83]

It is clearly evident that the global shipping industry that support the industry with component based produce and the industrial and domestic retail industry with produce is of immense proportions. This as it is normal to find products that contain components manufactured from every continent of the world. The resulting human footprint on the Earth is prodigious. [83] Even the simplest of products we surround ourselves with is a produce of this complex logistics chain. As an example, a product containing a steel component is evaluated. Steel may be produced from ore that has been mined in one country, and subsequently shipped to another country by bulk carrier for iron extraction. In 2011 alone, a total

of 1126 million metric tones of iron ore was exported from the country of origin for extraction abroad. Excluding internal trade within the European Union, 291 million metric tones of the alloyed steel from crude iron was exported the same year. [84]

To further complicate logistics, it must be considered that once the steel has been produced it must be delivered to a production facility that turn the bulk steel into produce. Finally the sub produce need to be shipped to a centralized assembly plant where it is incorporated in the final product. Once the product is manufactured a new logistics chain start where the product is shipped from the manufacturer to the distributor and finally to the reseller.

The case scenario of steel production can be studied from a Additive Multi Material Manufacturing point of view. Today Additive Manufacturing Technologies allow for the production of steel parts, typically in powdered based systems such as Selective Laser Melting. It can be envisioned that such a platform can be modified to build parts not from readily processed steel powder but from the alloying elements that comprise steel themselves. A system where pure iron in a powder form gets mixed with other alloying elements such as carbon also in a powder form. When the powder mixture gets selectively melted, the alloying takes place in-process. A graduation of the powder blend could be controlled in-process to allow for the production of components that yield different mechanical properties in different parts of the components, providing even more flexible component design.

If this platform furthermore could handle deposition of other materials such as polymeric substances, ceramic substances and composites of these constituents, not only would production eliminate several refinement processes from natural resource to bulk material, it would also allow for production of complex products without the need of product assembly. This second generation of Additive Multi Material platforms would allow manufacturing to be decentralized. This decentralized model would allow production to order, and would not only streamline production by eliminating the need for stocking, it would also have an immensely positive impact on global pollution by cutting away most of the logistics chain.[85]

5.1.3 Benefits of Decentralized production by employing Multi Material Deposition

Todays consumption market is governed by series production in the form of mass production. This, however efficient, is a production model that does not accommodate the needs and wishes of the individual customer. As described in section 5.1.2 on the preceding page, series production of consumer products with the appertaining complex logistics chain can eventually be a thing of the past. Yet there is a larger benefit to be attained. Mass production, literarily as production to the masses, yet without the need of employing series production. With the prospect of decentralized manufacturing of consumer goods, a new era of trade will have a

chance to emerge. A Digital trading and manufacturing scenario where products can be traded as virtual products similar to how digital media is traded today. In this forecast, it can be envisioned that there is a "print-shop" in every community of the industrialized world, similar to the print shops that deliver two-dimensional printing services today. A forecast where physical products can be traded as digital media similar to how software is traded for the mobile device market by means of "application stores" such as the Apple App Store and Android Market. It can be allowed that the consumer modifies the digital product to fit the consumers need for example by using simple modular CAD environments or specifying parameters that change the appearance of the digital product, only limited by the creativity of the individual and a set of governing boundary parameters specified by the manufacturer of the digital product. Once the costumer is satisfied with the changes applied to the product, if can finally be ordered for manufacturing at the local "print shop" in a similar way as printed photos or photo books can be ordered by online service providers.

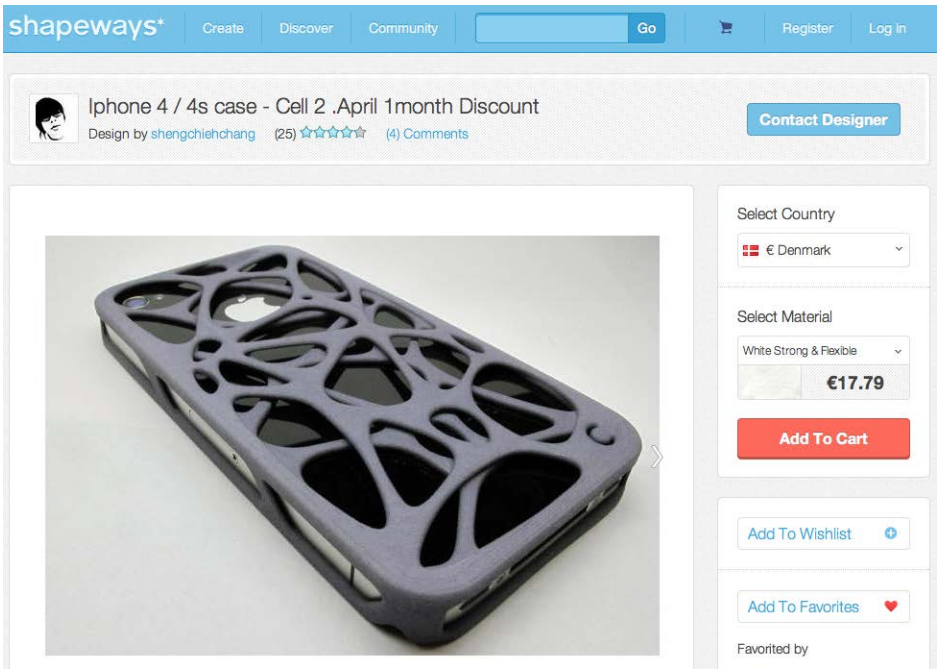

Figure 5.4: *A €17.70 iPhone case available at shapeways.com*

Business models that is based upon such a scheme already exist today, yet with the limitation of being unable to provide complex products comprised of multiple materials. Shapeways is one of the most flexible companies employing such model. It is a community driven webshop and Additive Manufacturing service provider which in structure resembles the forecast just described. Their online services can be seen in figure 5.4 and is remarkably similar to how application stores for the mobile market are run today. Many pieces of software on the application stores are

developed by individuals. Once sold the revenue is shared between the developer and the individual (or company). In the exact same manner physical products are sold on the Shapeways webstore. Individuals are the designers of the products that are available, and upon a generated sale, the revenue is shared. Not only is this production model extremely flexible, and not only is there 100% production-to-order, it is not least an effective driver of innovation as it allows anyone to start up a business merely by powering on their computer and starting to produce virtual products by CAD modeling. The individual does not need to worry about setting up a production. The individual does not need to worry about building up a consumer segment. This is all provided by the Additive Manufacturing service from Shapeways.

What is about to happen is something truly remarkable. Prior to the Industrial Revolution it was a privilege for an individual as a craftsman to earn a living by producing commodity from within their own home. Products that was tailored to suit the customer. Mass production however beneficial it has been to our modern society took away that privilege for good and worse. Since the Industrial Revolution we have all been accepting to wear shoes that does not really fit. We have all surrounded ourselves with generic products that can be found identical in millions of other homes. Additive Manufacturing and the entire Digital Production and Trade industry is about to give us that privilege back.

5.1.4 Rethinking CAD design and product development

The evolution of Additive Manufacturing through Multi Material Deposition towards a Universal Constructor, is a remote and abstract eventuation. To promote Multi Material Deposition a more current focus must be proceeded, with respect to which processes are currently evolved to what forms a suitable base for a Multi Material platform, and to what applications such a platform can fulfill in a near future.

Inspiration can be found not only amongst the present participle of interest as those listed in chapter 5.1 on page 146. A study of manufacturing engineering today yield inspiration as to how the future of Multi Material printing may evolve. Product design today evolves around standard components. Ball-bearings, nuts and washers, bolts and screws. A similar collection of Additively Manufacturable standard systems can be sought to be invented. These systems, when manufacturable, can form a digital library that can be brought forth within a CAD design environment, for the designer to pick from. Related to the systems development in chapter 7, section 7.1 on page 220, an example can be that of a subsystem forming a battery. The designer will then be able to draw a free-formed three-dimensional body within his product, to which he can assign the material property "battery". Once the product has been designed, and is being processed as a build-job in a Multi Material machine, that part of the virtual product with the corresponding

material property will be built as a functional battery, which will fit perfectly in that void of the product where a traditional battery-cell would not.

5.2 Analysis of potential Multi Material platforms and Evolution methods

To identify how an early revision of a Multi Material Platform can be manifested, a needs and requirements analysis must be performed. This to condole platform flexibility and coverage of a wide array of materials for Multi Material Deposition.

The analysis will be based upon a ranking of how applicable existing additive manufacturing technologies are in a multi-material environment. An initial assessment of existing processes and their known application in multi material deposition is listed:

- SLA and DLP
  - Process characteristics
    - Selective polymerization of a photo monomer.
    - Workpiece partially or fully submerged in a tray of substrate.
    - Commonly acrylates are used as substrate, some of which can be reinforced with ceramics.
  - Experimental platform available: ✓
  - Note on Multi Material Deposition
    - Some composite materials are available.[86]
    - Some photo monomers has been engineered to be suitable of electroless plating.[86]
- SLS/SLM
  - Process characteristics
    - Selective melting or sintering of a powder.
    - Workpiece fully encapsulated by powder substrate.
    - Commonly thermopolymers, steel, titanium and ceramics.
  - Experimental platform available: ✗
  - Note on Multi Material Deposition
    - Graduating a powder mixture from A ➠ A+B ➠ B has yielded positive results here amongst graduation from a metal to a polymer.[87]
    - Mechanical adhesion is extremely strong on sintered parts both using mechanical adhesives[88] and in tissue engineering[89] due to the porous nature of sintered parts.

·:· FDM

:· Process characteristics

· Fused point wise extrusion of a viscous matter.

· Workpiece is freestanding.

· Commonly support the extrusion of two different materials. A build material and a support material.

· Commonly thermopolymers but also sugars, wax and paste.

:· Experimental platform available: ✓

:· Note on Multi Material Deposition

· The principle of extrusion of a viscous material from a deposition unit allow for a vast amount of materials to be deposited using FDM.

· The FDM platform has already been used to realize complex multi-material structures such as solid freeform fabrication of mobile robots including the fabrication of electronics and electromechanical systems.[90]

· Completely Open Source designs of FDM platforms makes these very suitable for realization as experimental platforms in laboratory environments thanks to the work of Dr Adrian Bowyer, Senior Lecturer in mechanical engineering at the University of Bath in the United Kingdom whom founded the RepRap project, the self-replicating rapid prototyping machine project, in 2005.[17]

·:· LOM

:· Process characteristics

· Lamination of sheets of stock material, cut to contour by a laser or a mechanical knife.

· Workpiece is encapsulated in residual stock material.

· Commonly vinyl or polymer sheets.

:· Experimental platform available: ✗

:· Note on Multi Material Deposition

· A process resembling LOM where sheet metal has been joined by Ultrasonic Consolidation, a development from ultrasonic welding, has proven to allow Silicon Carbide fibers to be sandwiched in-between layers of sheet metal, where they can function as sensors, actuators and as reinforcement.[91]

·:· LENS

:· Process characteristics

- Laserwelding of a powder sprayed onto a workpiece.
- Workpiece is freestanding.
- Steel and titanium as process material.

:· Experimental platform available: ✗

:· Note on Multi Material Deposition

- Spite lack of research activity in multi material deposition using LENS, it is the powder-based process that intuitively provides the best platform for multi material deposition using a sinter-like technique. As powder is sprayed onto the workpiece, and particles that not adhere to the workpiece can be removed freely, multi material deposition of several powders can from a theoretical point of view take place without cross-contamination of the residual powder. This allow for easy powder recycling.

·:· Powder based 3DP

:· Process characteristics

- Selective bonding of a powder by means of a binder liquid.
- Some systems can color the periphery of the workpiece by means of an inkjet cartridge, producing high resolution colored parts.
- Workpiece fully encapsulated by powder substrate.
- Commonly Plaster of Paris or Foundry Sands are used as substrate.

:· Experimental platform available: ✓

:· Note on Multi Material Deposition

- Many powder based 3DP machines form 3D systems, a company formerly known as zCorporation, produce platforms that can colorize printed parts. This pigmentation is from a strict point of view a multi-material deposition.[92]
- It is possible to realize molds that allow for casting of resins an alloys such as Zinc and Aluminum by using powder based 3DP.[92]

·:· Resin based 3DP

:· Process characteristics

- Selective deposition of a liquid photo monomer by inkjet technology. Subsequent UV curing.
- Workpiece free standing
- Commonly Acrylates

:· Experimental platform available: ✗

:· Note on Multi Material Deposition

- Some systems have a double material deposition unit that can build support in a wax-like structure.[21]
- Some systems can graduate the mechanical properties by layer, from brittle ABS-like to ductile and rubbery.[21]

From the list, process characteristics that is related to the possible ease-op-adaption to multi material deposition is listed. For each platform type, there is an indicator, telling whether that platform is available in an open and experimental derivative, and finally a set of notes related to multi material deposition has been provided. Each platform pose its own challenges as to whether multi material deposition is applicable, and not one candidate stands out as being readily providing the elements needed to span over deposition of metals, polymers, rubbers, ceramics not least more exotic materials.

5.2.1 Selective Laser Activation and Direct Light Projection

Selective Laser Activation and Direct Light Projection are two derivatives of the same processing philosophy, selectively exposing a photo monomer to engage a polymerization reaction. These technologies are renowned for their high resolution deposition, which deliver unprecedented surface qualities in the additive manufacturing field. From a multi material point of view they are however imposing major challenges. SLA processes occur fully submerged in a reservoir of photo monomeric fluid. DLP occur partly submerged in a similar reservoir.

A Multi Material platform employing the SLA/DLP principle is envisioned. The major challenge of such system will be to address an evident issue of cross-contamination of monomeric fluid as the workpiece is interchanged between the reservoirs containing the two different monomeric fluids. Fluidic residue from one resin tray will be transferred with the workpiece to the other as illustrated in figure 5.5 on the facing page. This cross-contamination can be sought to be minimized by various means, such as by employing a mechanical wiper, that will scape off residual remains from the bottom of the workpiece before this is moved from one tray to the other. Yet spite great care, cross contamination cannot be completely avoided and as the resins is being diluted by contamination, their applicability as substrates will deteriorate over time.

Another concept as shown on figure 5.6 on the next page can be to allow a mixture of multiple resins to reside in the same resin tray. Each resin engineered to polymerize when exposed to different wavelengths of light. Alternatively the same base resin can be used, however with different photo-initiators and photo-inhibitors, allowing for the resin to polymerize by different mechanisms, allowing

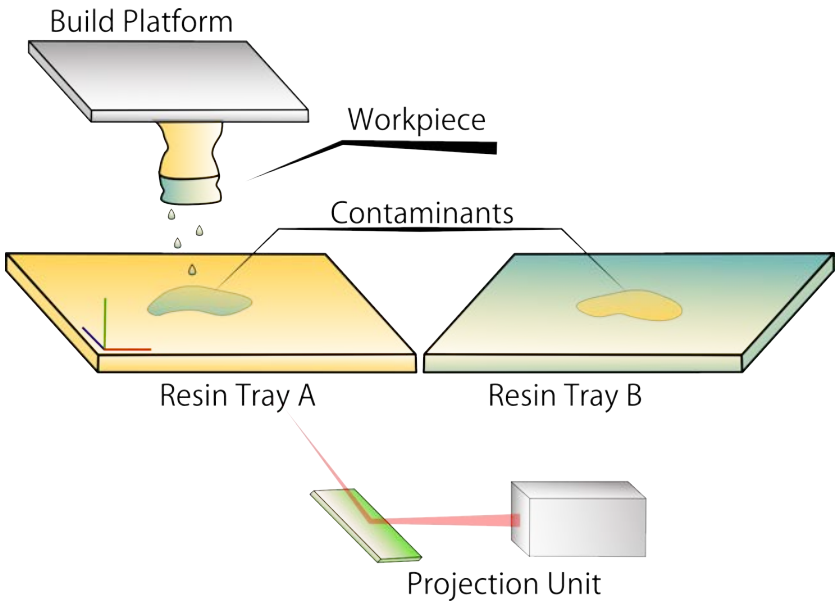

Figure 5.5: *A suggested SLA/DLP setup illustrating cross-contamination*

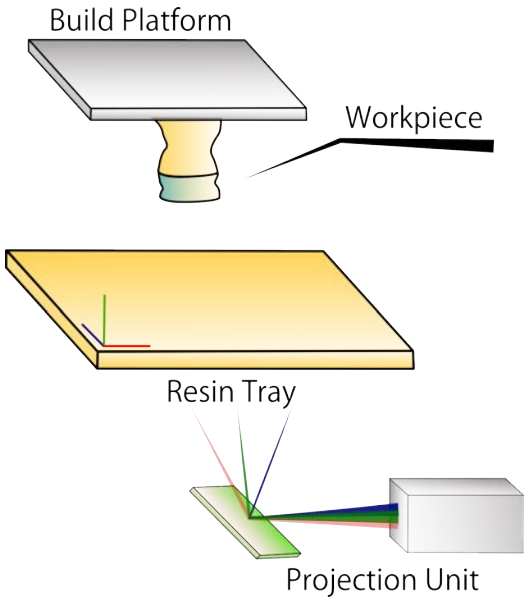

Figure 5.6: *A suggested SLA/DLP setup employing wavelength based polymerization*

for different material properties once solidified. This conceptual idea however impose its own set of challenges. If a mixture of multiple resins are mixed within the same tray, how will they interact and is it at all possible to selectively polymerize one of these at all? If possible, how can it be prevented that any of the other

resins does not get entrapped at their liquid state within the solidified structure. If a homogenous base resin is used, what material properties can be controlled by employing different photo-initiators and photo-inhibitors. How flexible is the platform in terms of the variety of resins applicable, and what mechanical, electric and electromechanical systems are possible to realize. These questions are all unanswered as of today.

5.2.2 Selective Laser Sintering and Selective Laser Melting

Selective Laser Sintering and Melting are two closely related processes merely distinguishable by the energy input from the laser source to the powder substrate. Sintering and melting of a variety of materials is possible. Ranging from metal through ceramic materials to thermo polymers the process is very versatile, however envisioning a multi material system is troublesome. A layered deposition of multiple powders has been proven [93] yet the current methods for multi material deposition result in a contamination of the residual powder that is normally recycled, leading to high levels of material waste.

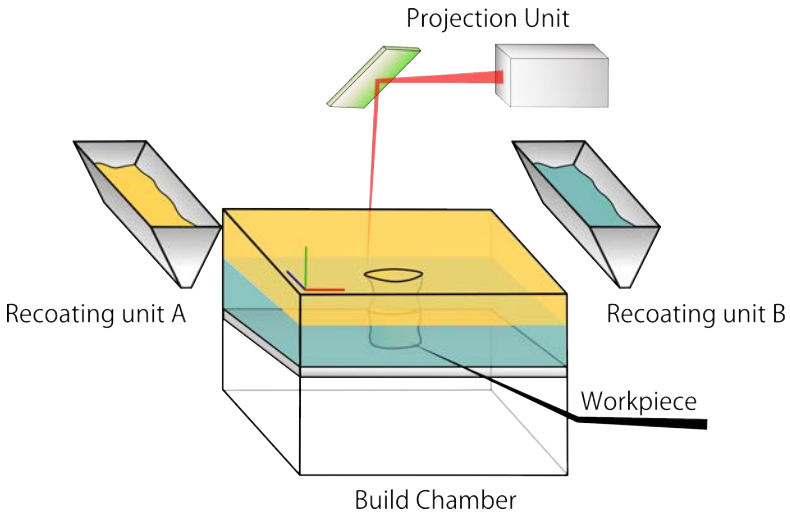

Figure 5.7: *A suggested SLS/SLM setup for multi material deposition*

The working principle of a multi-material SLS/SLM platform is illustrated on figure 5.7. The principle employ a traditional SLS/SLM design but makes use of two recoating units. Each layer is sintered or melted according to the process parameters of the powder in use. Subsequent layers can be built in another powder by setting another recoater active. Hence with SLS/SLM it is not the sintering or melting process method itself that impose challenges, it is how to isolate the different powders from each other in the build chamber.

Another drawback using SLS/SLM for multi material deposition is the fact that it is difficult, if not impossible to work with two or more materials within the same layer. Doing so would require selective powder deposition within the layer, and is a daunting thing to achieve. Nonetheless, such selective powder deposition is what occurs within a color laser printer. This is done by selectively charge a photoreceptor drum with static electricity and picking up a thin layer of toner powder from a toner hopper.

5.2.3 Fused Deposition Modelling

Fused Deposition Modelling is one of the few Additive Manufacturing processes that employ a point-wise deposition of material to a free-sanding object, typically by building parts in a thermopolymer by a heated material deposition unit shaped as an extruder nozzle, into which the thermopolymer is fed in wire form by a pinch wheel mechanism.

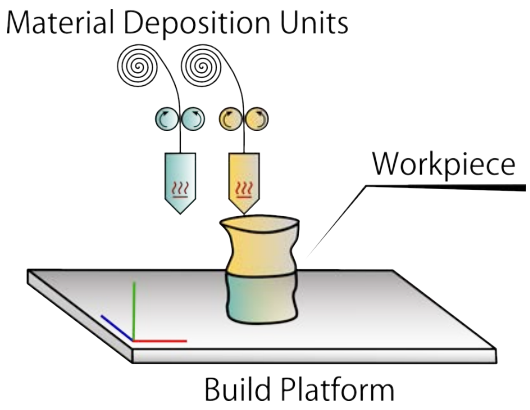

Figure 5.8: *A commonly used multi material deposition scheme for FDM*

Most industrial FDM machines already function with a dual extrusion unit, where a primary unit deposit the build material, and the secondary extrusion unit deposit a support material. Already, industrial FDM machines with multiple extruders, can print parts in different colors within the same build job. Both experimental and industrial FDM machines is exists, that can deposit material by other means than the traditional wire-fed extruder. Typically syringes are used to deposit a variety of substances, where the sole true limitation to what materials can be employed is the requirement that they have a low enough viscosity to allow for extrusion. One great advantage by creating multi-material structures by means of the FDM principle, is that it is extremely easy to deposit several different materials within the same layer.

5.2.4 Laminated Object Modeling

Laminated Object Modeling is one of the earliest Additive Manufacturing methods to emerge. The first machines employed a laser to cut contours in a paper strip, that by automation was glued to the workpiece, layer by layer. Other machines employ the same principle to cut contours in polymer foil by means of a mechanical knife.[94]

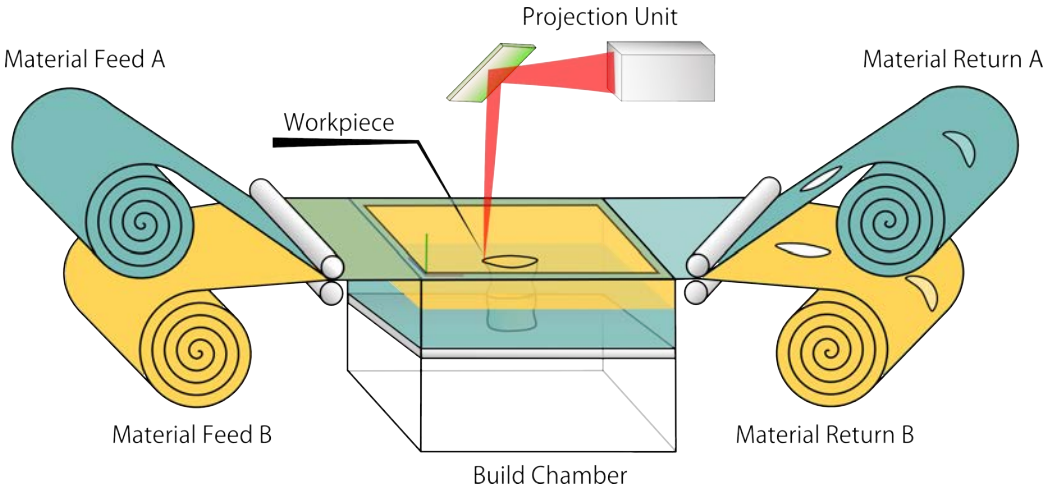

Figure 5.9: *A possible multi material LOM system*

Spite research in the related process, Ultrasonic Consolidation, where fibers are laminated in-between layers of sheet-metal, no known attempts has been made to realize a genuine multi-material platform based upon the LOM principle. Such platform however can be envisioned as given by figure 5.9

The lower part of the workpiece has been build in material A. The material has been fed through feed roller system, and the contour of the part has been traced, layer for layer. This while a window in material B has allowed access to cut and bond each layer of material A to the workpiece. Halfway through the object, the feed material has been changed to type B. This by cutting a window in material A, so that it now is material B that has access to the workpiece. The build job continues layer-by-layer. As with SLS/SLM, it is difficult to employ material A and material B within the same layer.

5.2.5 Powder Based 3D Printing

Powder Based 3D Printing and Selective Laser Sintering or Melting are related processes, distinguishable by how a powdered substrate is bonded to a solid. Whereas sintering and melting processes employ a laser as a heat source to bond the substrate, Powder Based 3D Printing employ inkjet technology to deposit a liquid binder to the powder. This can be water to plaster, where the reaction

$CaSO_4 \cdot \frac{1}{2}H_2O + 3H_2O \Longrightarrow 2CaSO_4 \cdot 2H_2O + heat$ will rehydrate and harden the powder, or simply by ejecting a glue to a powder surface. Ranging from metal for subsequent sintering in an oven through polymers[95] to ceramic materials[92], the process is as versatile as SLS and SLM, however envisioning a multi material system is equally troublesome. Current methods for multi material deposition result in a contamination of the residual powder that is normally recycled, leading to high levels of material waste.

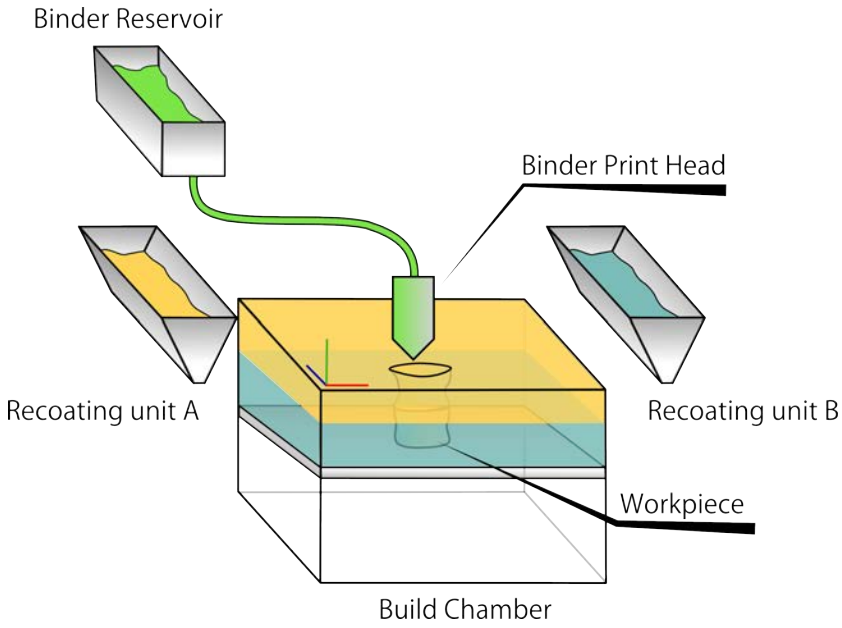

Figure 5.10: *A possible multi material powder based 3DP system*

The working principle of a multi-material powder based 3D printing platform is illustrated on figure 5.10, and closely resemble the principle of multi-material SLS/SLM previously shown on figure 5.7 on page 156. The principle employ a traditional design but makes use of two recoating units. Each layer is bonded by an inkjet print head according to the process parameters of the powder in use. Subsequent layers can be built in another powder by setting another recoater active. Hence it is not the bonding process itself that impose challenges, it is how to isolate the different powders from each other in the build chamber.

Another drawback using the proposed method for multi material deposition is the fact that it is difficult, if not impossible to work with two or more materials within the same layer. Doing so would require selective powder deposition within the layer, and is a daunting thing to achieve. Nonetheless, as with the suggested principle for multi material SLS/SLM, selective powder deposition could be achieved my mimicking the working principle of a color laser printer where a selectively charged photoreceptor drum employ static electricity to pick up a thin layer of toner powder from a toner hopper.

5.2.6 Resin Based 3D printing

As with Fused Deposition Modelling, resin based 3D printing is another of the few Additive Manufacturing processes that employ a point-wise deposition of material to a free-sanding object. Resin based 3DP however benefits from a much better deposition accuracy with a print-head that resemble that of an inkjet printer. Parts are typically built in UV hardening resins, fed from a reservoir to the printhead. Depending on the deposition strategy, the resin is either flash-cured for each layer, or continuously exposed by an UV light source throughout the build process as seen in figure 5.11

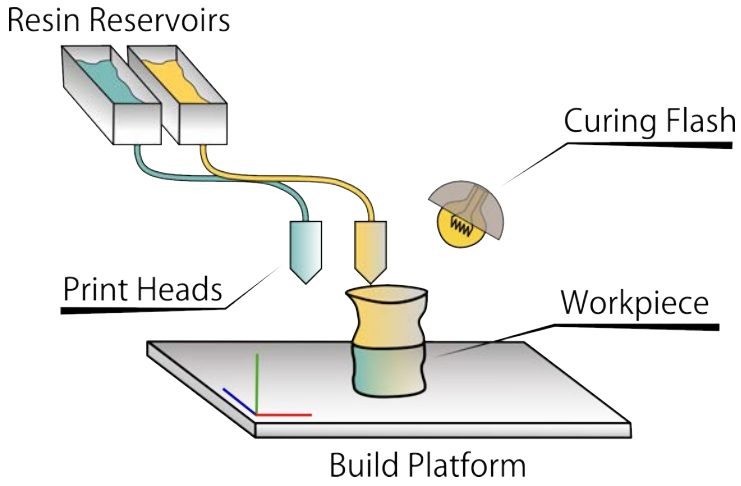

Figure 5.11: *A possible multi material resin based 3DP system*

As with FDM, most industrial resin based 3DP machines already function with a dual deposition unit, where a primary unit deposit the build material, and the secondary unit deposit a support material. Unique to resin based 3D printing, is the availability of commercial equipment that can graduate the material properties of the workpiece from rubbery and ductile to hard and brittle. This can be done within layers, and provide the ability to print systems such as hinges and clamps. Unlike FDM based machines, however, with the exclusion of some thermal 3D printing technologies, being a resin based technology, 3D printing machines are constrained to UV curing resins.

5.2.7 Assessment of platforms for multi material deposition

Many factors contribute to whether a platform is suitable for development for a multi material platform. A platform choice must be based upon a suitable technology. This can be done by systematically describe each platform based upon evaluation of a selected parameter set that describe preeminences and restrictions.

Table 5.1: *Ease of Multi Material integration*

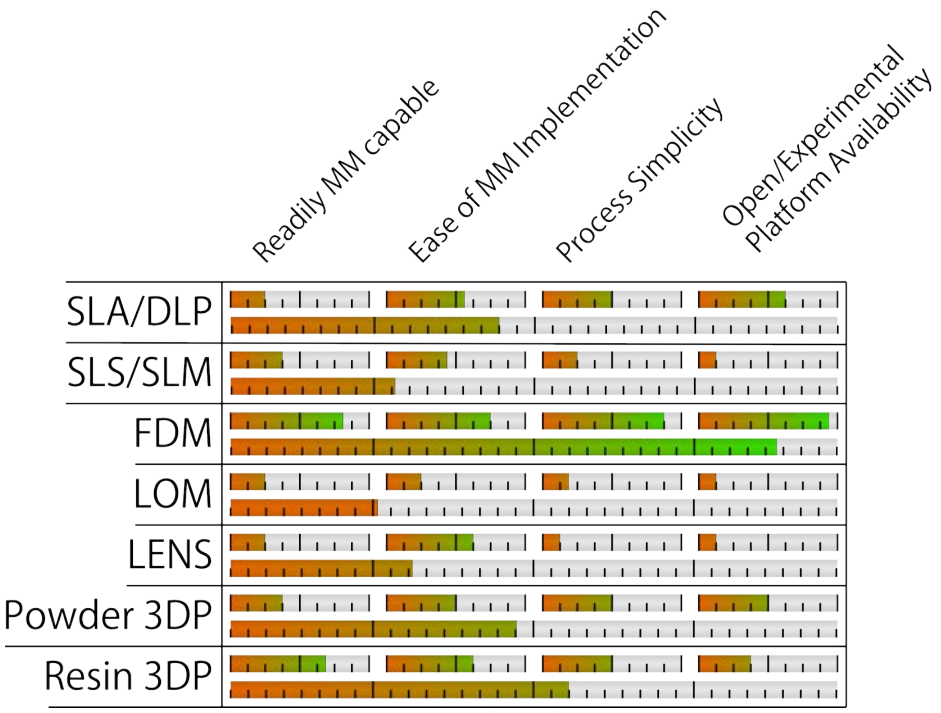

Table 5.1 show an assessment of the various platforms described in precedent sections, evaluated by a set of parameters in percentage from 0-100%. The sum of the scores in the individual parameters is indicated by an overall score that indicate the serviceability of the given platforms. One, or more of the high-scoring platforms can then be selected for further analysis. The four parameters chosen to assess the platforms, are as entities encompass several evaluation points. In order to describe these four parameters in details, they will thoroughly described.

- Readily MM capable - Whether the platform "as is" can function as a multi-material platform
  - Is the platform already being used as a commercial or experimental multi-material platform?
  - Is the platform already handling a build and a support material of different material properties?
  - Is the platform able to handle a broad variety of processing materials?
- Ease of MM Implementation - How difficult will it be to implement the Multi Material principle.

:· Are there any major obstacles in terms of material processing in one of the proposed multi material integrations?

:· Will a multi material integration require the design of several complex subsystems?

:· Will the numerical control scheme be difficult to realize?

·:· Process Simplicity - How simple the process is in general.

:· Does the process require fume protection?

:· Does processing require an inert atmosphere?

:· Will the implementation be complex to operate?

·:· Open/Experimental Platform Availability - Is there already a strong platform candidate available as Open Source and Open Hardware? This will foster an accelerated platform development.

:· Can an experimental platform be readily purchased?

:· Can an experimental platform be readily be built from open development resources?

:· Is there an active research and development community active within the given process?

Evaluation of the chosen candidates for a multi material platform deem Fused Deposition Modeling in discernible favor, as illustrated by table 5.1 on the preceding page. Several FDM-style platforms such as the fab@home platform[96], the EnvisoinTEC Bioplotter™[18] and derivatives of the Reprap project[97] already support multi-material deposition. The Fab@home platform and proper tooling for the Reprap platform[98] allow for universal extrusion of materials with a viscosity low enough to allow extrusion from a medical syringe. The FDM process principle very simple in terms of NC control and in processing parameter windows. Most prominent, the Reprap project itself[17] is one of the most successful Open Source Additive Manufacturing platforms in existence.

On a second place is Resin Based 3DP. This method as with FDM, build structures, that are free-standing, and is not in direct contact with stock substrate. Hence the risk of inter-material cross-contamination of stock materials are minimal. This makes implementation of a multi-material system easy from a material-processing point of view. There already exist machines that can graduate mechanical properties of structures,[21] so a level of multi-material implementation is already industrially available. Using ink-jet technology, the process simplicity is but outspoken, yet mass manufacturing of ink-jet cartridges for the home printing industry is widespread, and some of these cartridges has been reverse engineered, so that they can be interfaced in experimental applications. The Hewlett Packard C6602A has been reverse engineered by the Pwdr, open source platform project.

It is forked using github.[99] The Personal 3D Printer rev. 3B use cartridges from a Lexmark z715 ink-jet printer.[100] Replacing the ink with liquid photo initiated monomers allow for possibly eased development of experimental Resin Based 3DP platforms. One major concern is the availability of processing materials that can be deposited by a principe based upon Resin Based 3D printing. The processing materials must be of a viscosity and excerpt the right physical properties to be channeled through an inkjet cartridge. This may stingily limit the palette of materials that can be used within a Resin Based 3DP setup.

On a third place is Powder Based 3DP. Unlike the two cardinal candidates, being a powder-based process, cross contamination of processing stock substrates is an issue. However in-process cross-contamination does not directly impact the manufactured structures, yet recycling of powder will be perplex, strongly impairing the application of this process at a true multi-material platform. However, could powder selectively be deposited using a photoreceptor drum as suggested in section 5.2.5 on page 158, chances are that this issue can be circumvented, yet unavailingly adding to the platform complexity. A strong dividend that speak for using a Powder Based 3DP process as an experimental multi material platform is that the process itself is very similar to a traditional inkjet printer, hence there are several open experimental platform developments that can serve as foundation for a multi material platform.[99] [100]

5.2.8 Open Hardware and Open Source as evolutionary catalysts

An effective method for promoting and developing a technology is to propagate and compass it. An effective method for propagation is Open Sourcing. Open Source and Open Hardware from a corporate point of view however can be considered impairing as your technological foundation will be readily available to everyone. It is yet unarguable that all published research belong to the public domain. If this research has been carried out with Open Hardware, and following the Open Source sprit, it can from a Darwinian point of view be argued that this research will evolve faster than if carried out in corporate secrecy. It be argued that if electronic commerce systems such as Credit Card transaction systems, even the construction of Nuclear Power Plants was carried out as Open Hardware and Open Source, these platforms would be much safer in their application, as a large community with a diverge skill and mindset will have tested all worst-case scenarios. Given such approval to Open Sourcing, is a suggestive remark to consider when selecting a platform for a rapidly evolving technology such as Additive Manufacturing.

Open Source and Open Hardware is to a far extend an ideological statement, yet consider the ideological viewpoint of a corporate party. A potentially highly flexible manufacturing technology as additive multi material deposition is spoken to yield the ability to produce highly complex electromechanical systems. This form the foundation to acquiesce the technology to be a potential realization of a

self-replicating machine, the emerge of the Von Neumann Assembler, as discussed in section 5 on page 143. This render ideological arguments trivial as an external spectator will conclude that Open Source and Open Hardware will condole evolution of multi material additive manufacturing as a self-replicating species. The platform as a species will need human resources and a symbiosis between man and machine can be manifested by Open Sourcing from the very initial research. The machine-man symbiosis is a corporative model where man assist the machine with reproductive tasks ranging from trivial assembly to systems development which correspond to a biological mutation. The machine in return will provide more than just clones of itself. It will complete the symbiosis by providing man with more than just copies of itself as it can provide a vast variety of structures that serves a variety of functions not related to reproduction.

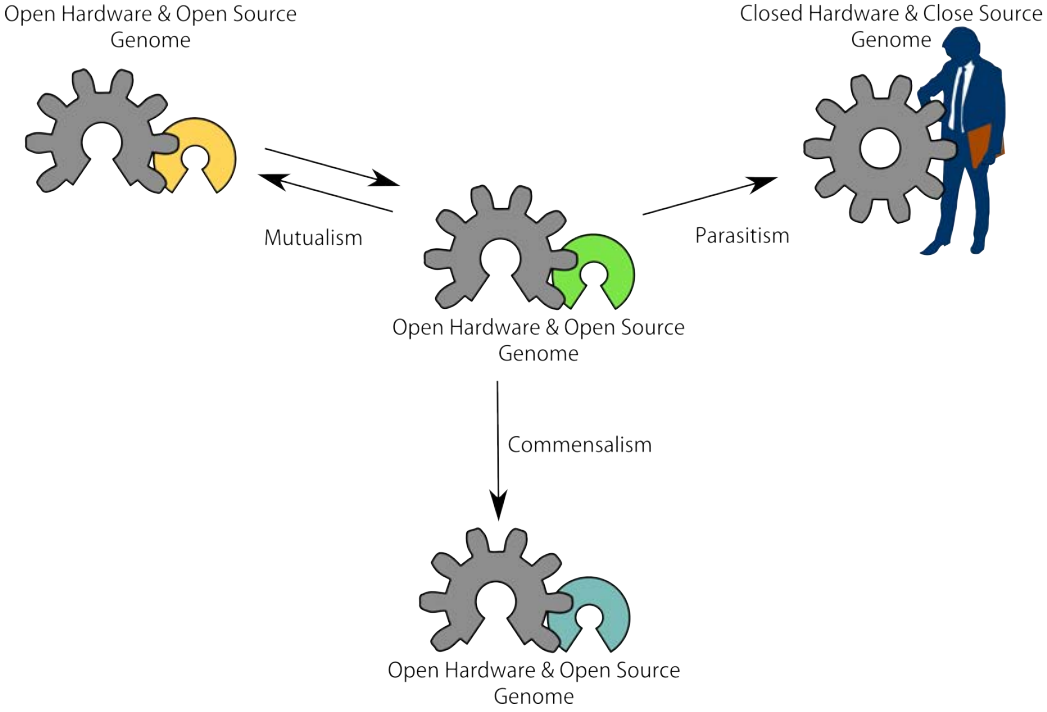

Figure 5.12: *Symbiosis in its three forms: Mutualism, Commensalism, Parasitism*

Symbiosis amongst actors can be depicted as in figure 5.12. The central genome, the host, is in symbiosis with three symbiont genomes. The symbionts represent three different classes; the mutualistic symbiont, where the host and the symbiont both benefit from the symbiosis; the parasitic symbiont that prosper from the host genome in a harmful manner; and the commensal symbiont that has come to exist from, and coexist with the host genome in a non-harmful manner.[101] Arrows indicate knowledge-flow. Two Open Source, Open Hardware projects can coexist in mutualism, where both project benefit from interaction in terms of knowledge-flow, research and development. One Open Source, Open Hardware

project can be a spin-off of another Open Source, Open Hardware project, no longer directly related and hence, only the spin-off project, being the commensal symbiont, has benefited from the host, yet not harming the host. Finally a parasitic symbiont can in a similar manner come to exist from it's Open Source, Open Hardware host, siphoning knowledge, yet this parasitic symbiont harms it's host by being Closed Sourced and turning a strain of the Open Platform proprietary.

Table 5.2: *Growth of non-commercial additive manufacturing platforms*

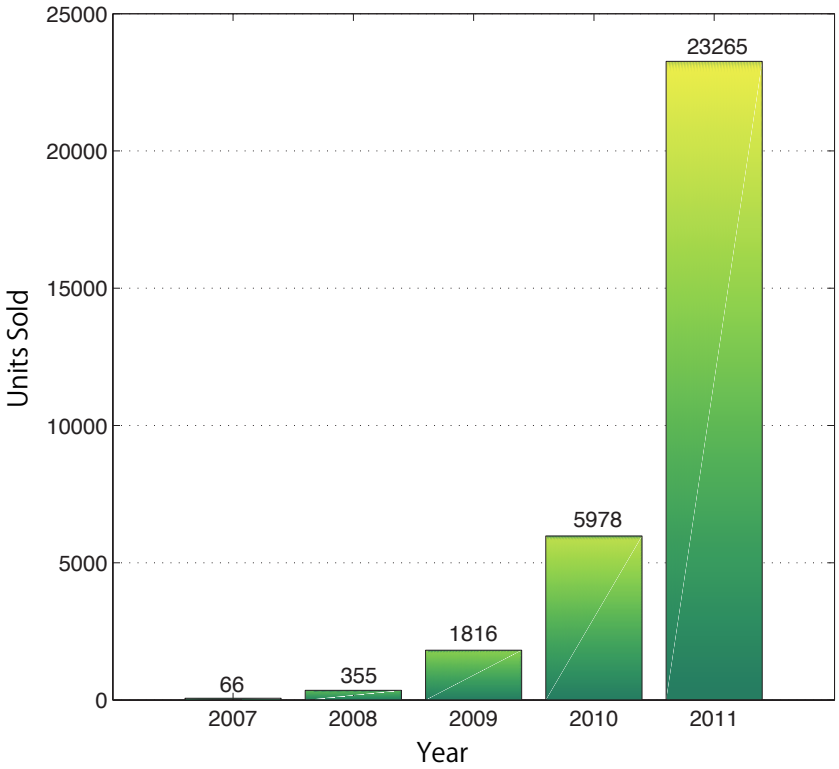

Data source: Wohlers Associates - Annual Report 2012

It can be argued that corporate actors should not fear Open Source in the first place. Corporate actors will benefit, subcontracting e.g. electromechanical systems, what subsystems cannot yet be realized by the open and replicating machine itself, not least subcontracting the matter used as stock materials for processing within the open platform. Eventually when the technology will or may become truly self-replicating, it is the machine as a species that become an asset, not just as a manufacturing tool but also as a automaton live-stock, that can be bread by the corporate business and the open source community alike.

The in brief stated above, the evolution can be considered by a Darwinian approach, by seeking answers to two trivial questions. The former being: What will

be the most numerous platform, promoting a certain technology. A self-replicating platform or a platform that need manufacturing by conventional means? The latter question: Which will be the most successful replicating technology as a species. The technology that has been manifested by Open Source and Open Hardware allowing for inter-special symbiosis with man, or the technology that is mystified by close-source, disallowing this symbiosis?

The promotion of multi-material additive deposition as an Open Source and Open Hardware technology as a species, empowered by Open University Research is a strong competitor to what technology will realize Von Neumann's Universal Assembler, simply because Darwinian game-theoretic analysis will prove this form of development to be an evolutionarily-stable stratagem. Open Source hence become a strategy to out-compete Closed Sourced and Closed Hardware genomes. In a grim scenario, attentive corporate actors may and will pursue open platforms to take advantage of what technology is readily available and close it off by turning a strain proprietary. If a Closed Source, Closed Hardware technology from one corporate business is mimicked by a competing corporate business, aside upholding copyrights, the two actors stand equally strong competing in an evolutionary race and competing for market domination. If the former is the case, that one corporate business close off an open technology, the open genome will remain equally reproductive whereas the closed strain will become less fertile, if not sterile (research halts). Hence the closed strain will be more subjectable to loose the technology race.

The Frontier of the Future will prove nature to repeat itself, where any open replicating platform will be able to reproduce. Every closed replicating platform will be able to reproduce. Every non-replicating platform will be able to produce a replicating genome. The evolutionary game theory will prove that the open self-replicator will prevail. Table 5.2 on the preceding page show the growth of non-commercial additive manufacturing platforms from year 2007 to year 201. The growth, exponential in nature, whereas the Compounded Annual Growth Rate of the field of Additive Manufacturing in year 2011 was 29.4% [2] is an indicator of the evolutionary behavior of the Open Source, Open Hardware additive manufacturing platforms, validating the darwinian game theory of the survival of the fittest.

5.3 Conclusion: Platform Choice for Multi Material Deposition

The analysis through section 5.2 on page 151 has been covering a series of key-points to determine a suitable platform for Multi Material Deposition. An analysis of a variety of existing technologies, their state of development as single-material platforms, and their suitability and availability for experimental multi material deposition has been covered. Open Source and Open Hardware as a catalyst for ongoing evolution of a multi material platform has been investigated, and different

possible technological improvements to single material platforms for the allowance of multi material deposition has been addressed.

Three candidates was picked out as possible platforms to serve as experimental multi material deposition. These in the order of appearance are Fused Deposition Modelling, Resin Based 3DP and Powder Based 3DP. The two latter proved inferior due to issues relating working principles and complexity. The Achilles' heel of Powder Based 3DP is that cross-contamination of different powders render powder recycling challenging if not prohibitive. Changing processing material within a layer is thought to be repressive, yet a solution to accomplish this has been discussed. Resin Based 3DP does not institute cross-contamination. The concern is to what materials the process will be limited to. The materials must be kept at their liquid form, with a viscosity that allow for channeling through ink-jet cartridges, greatly limiting the availability of suitable materials. Furthermore, no readily available experimental platforms are available, which encumber the implementation phase of the project, where an experimental platform must be established. The last candidate, Fused Deposition Modeling, proved most suitable for expedited implementation and bespeak of the possibility to deposit a vide palette of materials and composites. In a standard configuration, an Open Source, Open Hardware derivative of a Fused Deposition Modeling platform will be limited to extrusion of thermo polymers. Yet with a thermo polymer deposition unit, the platform can realize its own upgrades such as a universal paste extrusion tool, for deposition of any substance that can be ejected by means of a medical syringe, with or without a needle attached.[98] Finally as the FDM platform is the most numerous experimental multi material deposition platform, it allows for an effective knowledge exchange by means of community driven research. Hence the FDM platform is chosen.

Design and construction of an experimental multi material platform, tooling, electronics and software. Two generations of development is presented.

6 Multi Material Platform Design

As concluded in section 5.3 on page 166, an FDM extrusion platform has been chosen as a base for research in the field of additive multi material manufacturing. With paramount solicit on flexibility and empathy on the ability to tinker and alter the platform to conform to a multitude of experiments involving multi-material extrusion, and to efficiently lift what challenges must arise during research within this field, it has been decided to base the FDM extrusion platform upon existing stable grounds, thus deriving the experimental FDM platform from the Open Hardware and Software FDM platforms that has been around since Adrian Bowyer et. al. founded the Reprap project. With an abundance of community-driven hardware, electronics, and software derivatives of the first Open FDM platform, the Reprap Darwin, rich resources exist to fuel development of such platform.[17]

Throughout the research and development of this flexible multi material FDM platform, two systems-revisions has been made. The development of the first generation system was primarily emphasizing on the constitution of a functional FDM machine with a traditional thermo-polymer extruder. The second generation design empathized on solving issues found during implementation and operation of the first generation, as well as developing a flexible multi-material extrusion tool.

6.1 First generation design

The first generation design is based upon an existing Reprap platform derivative called the "Reprap Prusa Mendel"[102], designed by Josef Prusa. The platform design exclude controller electronics, tooling and controller software. As such, a choice between existing solutions for setting up the tooling scheme and numerical control scheme and the development of such must be chosen throughout the occurrent platform design. This with aim at the final goal, to procure a platform not merely able to function as an FDM extrusion platform, moreso allowing for multi-material deposition within a flexible setup.

6.1.1 Hardware platform

In the following, the standard platform design of the Prusa Mendel machine will be discussed. Subsequently alterations to this system will be explained. The Prusa Mendel, seen in figure 6.1 on the next page is a 3-axis cartesian robot. The robot is a frame construction, with all frame vertices and other constituent os the platform can be manufactured by means of FDM extrusion. The platform is of a parametric nature. As such the platform can be scaled to suit its application scene. The default scaling factor for the machine is at a desk-top footprint, for assembly of the frame by means of threaded M8 rods, and 8mm guide rods for linear traversing. These rods can be shortened or extended to suit the specific application of the platform. The frame rod diameter can be upscaled as well by scaling all FDM manufacturable components that comprise the platform. The drive motors used follow the NEMA size standard for stepper and servo motors[103, ch. 1-5] and hence a parametric 2:1 machine will employ M16 rods an larger motor class. The machine footprint chosen is the default size, employing M8 rods and with frame rod lengths that constrain outer machine dimensions to ≈ 400x400x400 mm. The X- and Y- axis are driven by T5 module tooth belts whereas the Z-axis is driven by spindles.[104]

Design alterations has been made in an effort to improve the machine design. The X-axis carriage by default host the filament drive mechanism for the extrusion tool. The motor driving the filament by far is the main contribution to the total mass of the carriage and extrusion system. In an effort to minimize the carriage mass, hereby allowing for faster tool accelerations during operation, the extrusion filament drive has been removed from the carriage and mounted on the frame as shown in figure 6.2 on page 172. Instead, the filament wire is fed by means of a Bowden cable to the carriage. The implications of this change is ambiguous. Reduction of the mass of the carriage will indeed allow for much faster accelerations of the carriage, however a noticeable hysteresis is imposed upon the filament drive system. Extrusion will as such not occur instantaneous when the filament drive motor is engaged, as the filament will kink and compress within the Bowden cable and hence will loiter. Stopping the extrusion will suffer from the same phenomena. This however has proven during operation of the platform to easily controllable by employing a suitable control scheme, where the filament wire is advanced rapidly at extrusion start, and reversed rapidly at extrusion stop. For the FDM manufactured drive gears of the filament drive to handle the added load from rapid forwarding and reversing the filament, the teeth of these gears has been altered to conform with a double-helical or ⌜*herringbone*⌟ geometry. This ensure that two teeth will be engaged at all times, hereby reducing wear. The second alteration to the platform is an upgrade of the linear bearings. The standard Prusa Mendel design employ additively manufactured linear bearings built in thermo-polymers as simple bushings. All linear bearings has been replaced by LM8UU linear ball-rail bearings to decrease friction. Life expectancy of these is as such extended and friction is decreased, also improving acceleration capabilities of the platform. The final

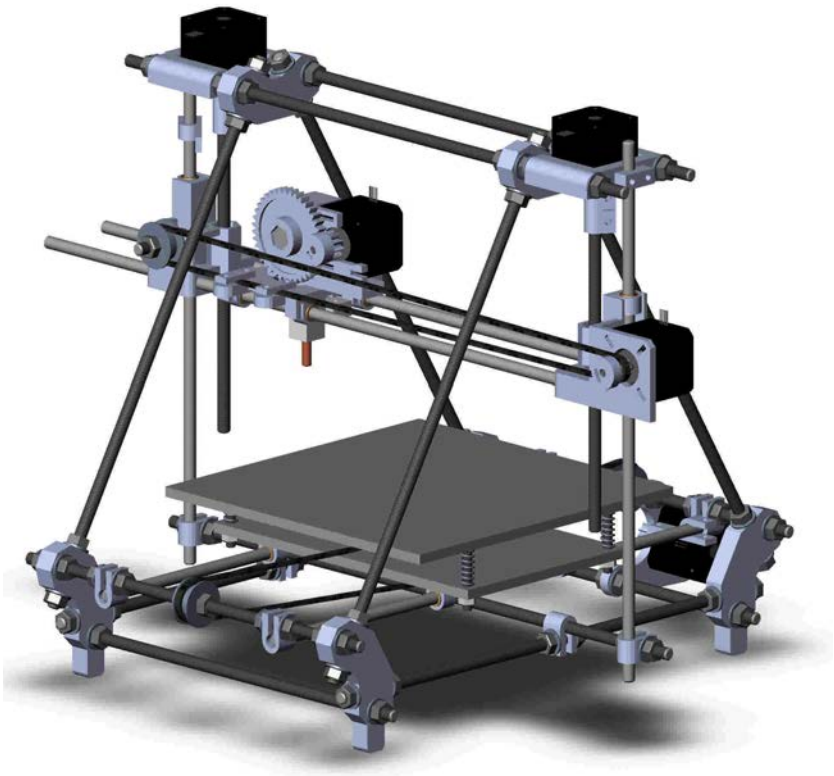

Figure 6.1: *The Reprap platform derivative, the standard Prusa Mendel machine*

change is to the Z-axis spindle motors. As seen on the original machine design in figure 6.1, the elevation of the Z-axis spindle motors are at the same level as the upper frame vertices. They attach to the Z-axis spindles by clamp-fit brackets. To ensure better alignment tolerances these brackets has been replaced by Oldham couplings and the Z-axis motors has been mounted by means of two pylons, as shown in figure 6.2 on the following page. This extend the stroke of the Z-axis of the machine ≈ by 60 mm.

6.1.2 Tooling

The tooling for the first generation system has been based upon a hot extrusion unit for polymer extrusion. Based upon the knowledge-base available within the community-walls of the Reprap project, a basic extruder design. The standard extruder for the Reprap Mendel machines employ s PTFE insulator barrel, and a heated brass nozzle. It is designed for 3mm filament wire, and has a nozzle diameter of 0.5mm. The final design of the first revision thermal extruder replace the standard reprap extruder design with an extruder with a barrel of PEEK as in

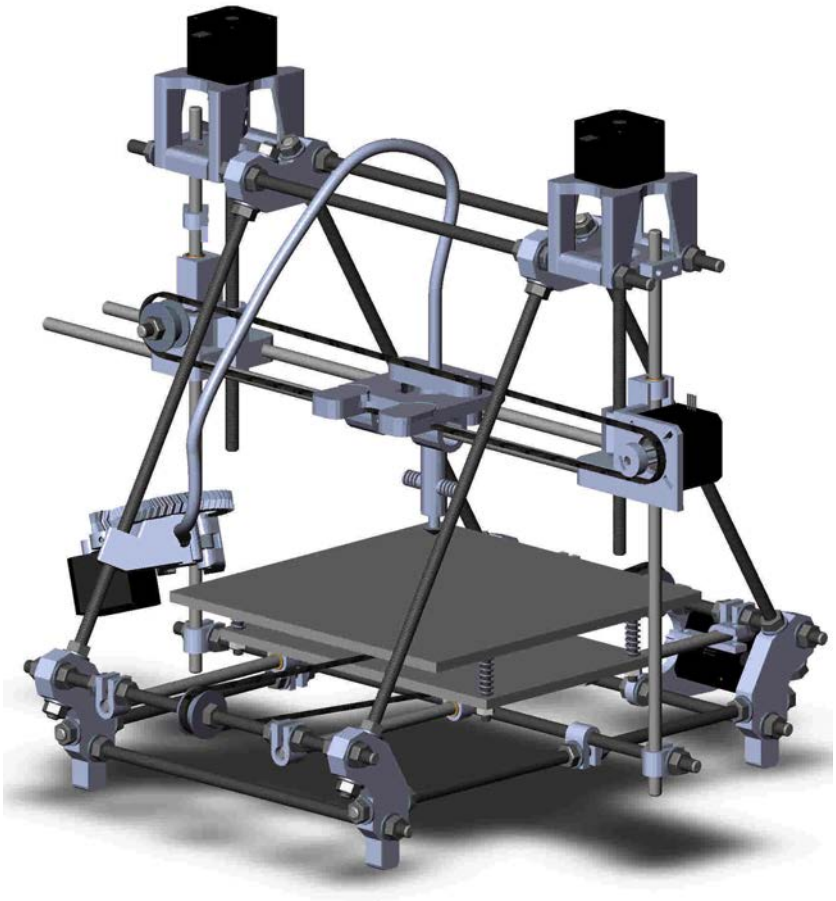

Figure 6.2: *The altered Prusa Mendel machine featuring a Bowden cable filament drive and higher Z-axis motor brackets*

figure 6.3 on the next page. A comparably good thermal insulator, yet as discussed in chapter 2.4.2 on page 58 mechanically stable at high temperatures that allow for extrusion of most common thermo-polymers. Inside the PEEK barrel is a thin internal PTFE lining. This because at high operation temperatures though PTFE is not mechanically stable, supported by the outer PEEK barrel, the PTFE lining has been tested to be able to handle the forces that may be imposed by driving the filament through the extruder. The main function of the PTFE lining is to lower friction between filament and the insulator side walls.

The brass nozzle has a creese into which a thermal sensor and a heater wire of nickel chromium alloy is wound. The heater wire and thermal sensor is fixed by ceramic paste which subsequently is thermally cured. The length of heater wire and hence the impedance of the heater wire to match $\approx 5{,}8\Omega$ so that the heater $@12V \eqsim$ will generate $\approx$ 25W, allowing the nozzle to reach 300 C°. The thermal sensor is a thermistor, a thermally sensitive resistor by which the FDM machines

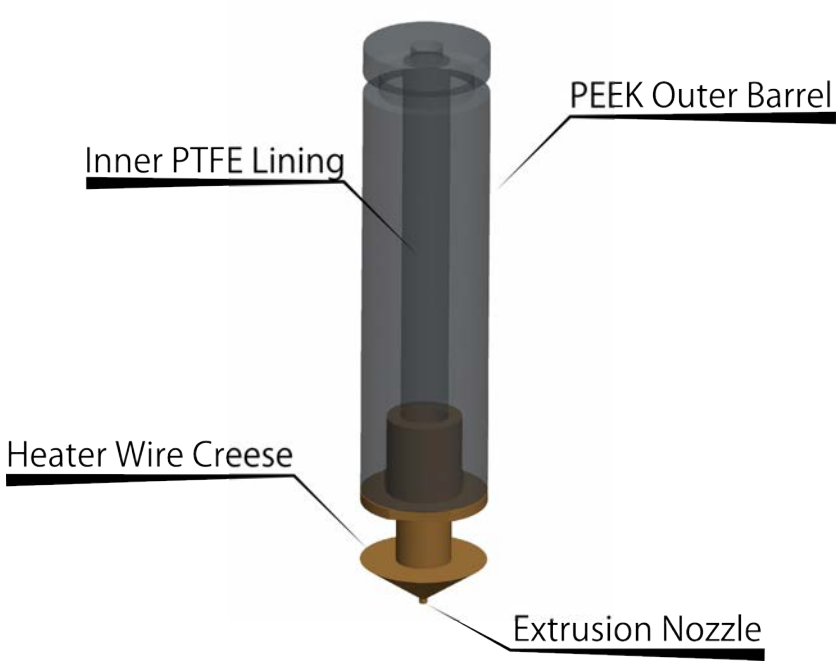

Figure 6.3: *First Revision Extrusion Unit: Showing extrusion nozzle and insulator*

electronic control system can measure the extruder temperature. The extrusion unit has been manufactured with several nozzle diameters, ranging from 0.2 to 0.5 mm. As a secondary tooling system is the build platform of the machine. The purpose of the build platform is to support structures being built. As such it is important that these structures adhere properly to the build platform. This is achieved by constructing a build platform that can be heated during operation, hereby allowing the bottom layer of polymer structures to be elevated above T_g to allow these to adhere to the build platform. The build platform is comprised by an aluminum plate, that on the rear side has a similar thermal heating system as that of the extruder unit. A thermistor sense the platform temperature, and several 25W rated power-resistors are used as heat elements. The build platform has been projected to generate 144W of thermal energy @12V ⎓, allowing it to reach 120 C°degrees.

6.1.3 Electronics

Whereas advanced controller electronics will be needed for a generic multi-material controller, this to support a variety of yet-to-be-discovered subsystems, it is ambitious to anticipate what requirements will surface. This has been considered to be addressed by two approaches. One being a modular approach, where the controller electronics are sought to be divided into interchangeable modules that can be redesigned individually to accommodate future needs. The latter to design

the electronics in a pseudo-modular approach where an abstraction layer is introduced between CAD and the staging of the electronics. Here it is aspired that the various sub-systems are designed with modularity as a preeminent characteristic, yet manifested as one entity during production. This will simplify the electronics, depreciating connectors and wiring to an extend where interchanging the entire board comes at a minimal effort and cost. The latter approach has been chosen to avoid a ruffled electronic layout, excessive wiring harness, and to minimize the risk loose wiring. This to keep the experimental platform as reliant as possible.

Speculation deferred, a list of ascertained subsystems that the electronics must enclose can procured as a requirements sheet, based upon the initial state of the hardware platform design:

·:· A central Micro Controller Unit to handle I/O routines and directing other subsystems.

Requrements:

:· Programmable using In Circuit Programming.

:· Estimated calculation speed ≈ 10 million instructions per second (MIPS).

:· Internal clock and postscaler allowing for high clock frequencies. Possibly by employing Phase-Locked Loops. (PLL)

:· Addressable UART running off the internal device clock, to allow for bidirectional communication to allow the controller electronics to serve the role as a peripheral device.

:· Least 10-bit resolution, multi-channel Analog to Digital (ADC) converter module to allow for precise analog decoding of input such as from temperature sensors.

:· Multi channel Pulse Width Modulation module, to modulate transistor logic driven high-current outputs.

:· Must operate at a positive supply level, at the potential of V_{DD} = $+5V$ ⎓.

:· Must be well-shielded against Electromagnetic Field (EMF) noise.

·:· A communications subsystem allowing for data exchange with a host computer

Requrements:

:· Must serve the role as bridge between a host computer and the micro controller.

:· Must follow a widely accepted standard such as RS232 or USB.

:· Must have an integrated clock source

:· Must have an integrated level converter on both UART and Communications BUS at V_{DD} = +5V ⎓, allowing the device to generate the required voltage levels for host communication and to power the logic circuits of the controller electronics.

:· Must be well-shielded against Electromagnetic Field (EMF) noise.

·:· A multi-channel motor controller subsystem that allow for accurate positioning of numerical axis.

Requrements:

:· A single-chip motor driver is preferred over transistor logic based control circuitry.

:· Current rating must be at least 2A@ + 12V ⎓

:· Each channel must support one bipolar or hybrid stepper motor, or one servo motor.

:· Each channel must have an isolated logical translator and power driver.

:· Communication between driver circuit and the central Micro Controller Unit must be in TTL. and with a maximum of two serial channels. This set a requirement for built-in PID controller if employing servo motor technology.

:· Current limiting technology must allow for chopping control of the motor supply lines.

:· There must be a distinct isolation between logical translator and power driver with respect to Electromagnetic Field (EMF) noise.

·:· Transistor–transistor logic (TTL) inputs for monitoring of logical hardware such as switches.

Requrements:

:· If externally driven each channel must be opto-isolated to protect the central Micro Controller Unit.

:· If internally driven, each channel must be protected against over-current.

:· Either driver mode requires a hardware based debunce filter to avoid unwanted signal chatter.

·:· Analog inputs for monitoring analog hardware such as temperature sensors.

Requrements:

:· Internally driven

:· Each channel must be protected against over-current.

:· Must include a hardware based low-pass filter to avoid unwanted signal noise.

·:· High-current outputs for driving hardware such as heat elements and direct current motors.

Requrements:

:· Circuit must be transistor driven.

:· The transistor recovery time (forward and backward) must be short enough to allow for high frequency pulse width modulation. .

:· The transistor base or gate voltage must be TTL or fully open the transistor at $+5V$ ⎓.

:· The transistor must either have a built-in fast rectifying diode or have an externally fitted, to circumvene back induced currents.

The specified requirements serve two primary purposes. One is inter-compatibility between subsystems. An example can be that the central Micro Processing Unit must be able to operate at a positive supply level, at the potential of V_{DD} = $+5V$ ⎓. This is in order for the device to be able to be powered by the communications subsystem that can provide this potential. This is also why the motor driver subsystems and the logical inputs are specified as TTL. TTL is a transistor transistor logic level standard defining a voltage between 0 to $+0.8V$ ⎓ as a logical zero and voltages between +2 to $+5V$ ⎓ as a logical ones.[105] The other purpose is to serve as a reference to compile a specifications sheet based upon the requirements, that will contain the specific integrated circuits that will be used to design the electronic controller.

Micro Controller Unit

Given the requirements, a Micro Controller Unit has been chosen from Microchip Inc. The PIC18F2620. All specifications for the device is derived from the device data sheet.[106] It is a 28 pin device, available in a surface mounted Small-outline integrated circuit (SOIC) package. It boasts Harvard Architecture of an 8 bit data bus along a 16 bit instruction bus, running at speeds up to $40MHz$. Using its internal oscillator @ $8MHz$ and enabling Phase-Locked Loops(PLL)[107], the Micro Controller can run @ $32MHz$. PLL is a method where two variables, phase and frequency of the clock signal is used to measure the phase difference. Hereby the clock frequency can be quadrupled. Instead of merely triggering on the period, but on zero-crossings and extrema throughout the clock cycle. This allow for an operation frequency @ $32MHz$ without an external clock source. The PIC18F2620 can be configured to use two Capture/Compare/PWM(CCP)modules, allowing for high-frequency pulse-width modulation. This can be employed to modulate

the output transistors at a variable duty-cycle to allow for variable mean-power draws of devices where the kinematics are not affected by the pulsed supply power source.Pulse Width Modulation can be illustrated as shown on figure 6.4.Systems that has a kinematic behavior that is not affected by high-frequency Pulse Width Modulation is for example heat elements and Direct Current motors.

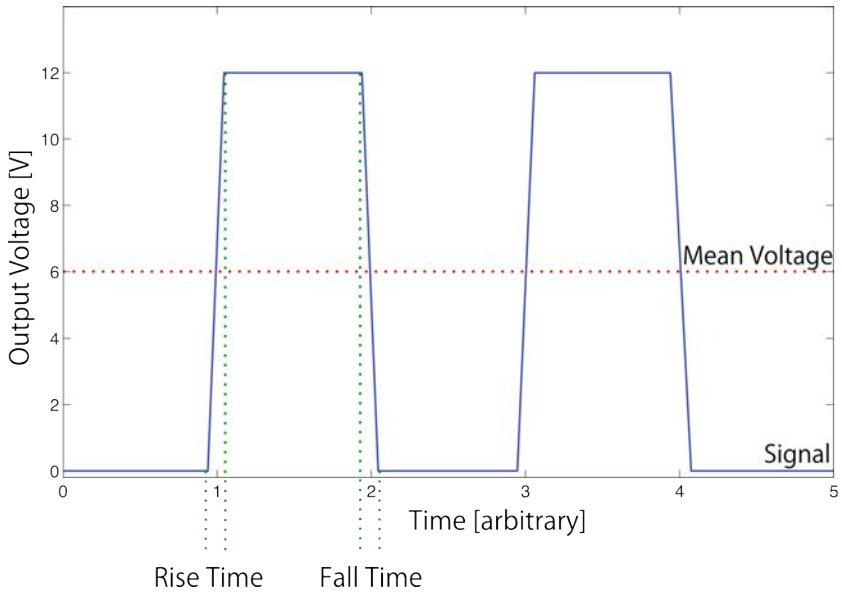

Figure 6.4: *Pulse Width Modulation of a signal*

The PIC18F2620 has a 13 channel, 10 bit Analog to Digital (ADC) converter. With a reference voltage of $+5V$ = and a 10 bit range from 0-1023 this gives a resolution of 0.0049 V. This allow for high resolution of analog input from external sensors. To accommodate communication between the Micro Controller as a peripheral device, and a Host device the PIC18F2620 comes with an Enhanced Addressable UART supporting a wide variety of protocols. RS-485, RS-232 and LIN/J2602. Of importance is that RS-232 operation can be achieved using the device's internal oscillator, so that no external clock source in needed. This allow for common serial communication to be achieved at no cost of additional circuitry. The device has a programmable memory of 32768 single-word instructions, a data memory of 2968 bytes static RAM, and a static additional static memory in terms of an EEPROM of 1024 bytes. This allow for execution of complex firmware of up to 64kb, and storage of firmware-updatable parameters such as system calibration tables that can be modified through instructions to the firmware from the user at run-time. Finally is it noticeable that this device comes at a volume cost of merely $4.06 USD.

Communications

Communication with the Central Micro Controller Unit can be imagined in several ways. It can be in terms of a physical hardware subsystem comprised of input devices such as buttons, and feedback devices such as a liquid crystal display and indicator diodes. If such an interface is to be used, a data-exchange module must be implemented, that allow the operator to transfer job-files to the electronic controller. A method for that can be by using an SD memory card. This kind of direct machine interface has the strength of providing the electronic controller board with a readily available job-file on a storage media that is directly accessible by the firmware. This means that execution of instructions found on the storage media will be possible with close-to no significant delay. This allow for smooth transition between movement of axis of the platform, and mean that the parsing of job-files can be done in an instruction-by-instruction manner. Furthermore it allow for off-line operation of the platform. A draw-back from this design is that the user-interface is fixed, and it requires hardware modifications to expand or alter the interface. This can prove cumbersome on an experimental platform, resulting in excessive time spent by implementing minor changes to the way the platform is operated. An added cost to the electronic controller board in terms of added components will be expected. Furthermore if integration of an SD card reader is to be carried out, a dedicated 4-wire connection between card reader and micro controller must be implemented for data lines alone, not counting the multiple lines needed to drive a display and user input in terms of buttons. This will occupy a substantial part of the communication pins of most common micro controllers. An alternative way to provide a suitable user interface and provide a means of data exchange can be by establishing a communication line between the controller electronics and a host computer. In this scenario the controller electronics will take on the role as a peripheral device such as any other external printer, scanner and similar. The communication line can be used not only to send instructions from job files to the controller but also to issue individual commands to the controller by means of a graphical user interface with buttons, drop-boxes and sliders, as commonly seen in desktop applications. This also means that changes in the user interface is no longer a hardware task, but can simply be done in software. This add to flexibility of the platform as entity. The solution however does not come without drawbacks. The most obvious is that communication between host and controller comes at a cost in communication delay. An entire job unless rudimentary simple to a trivial level, cannot be buffered in the memory of common micro controllers. This mean that job-data must be streamed live to the controller. If an instruction-by-instruction based communication is implemented, the controller will wait in-between instructions to receive the next. The result of this can be corrugated movement of axis and general jolting behavior of the platform. Hence an instruction buffer must be integrated in firmware, at the cost of processing resources and added code complexity. This instruction buffer allow for continuous and smooth execution of instructions when communication delay

exceed the execution time of the individual instructions. Another drawback is the fact that the platform cannot be operated as a singular entity. A host computer must be online when the platform is operated. Since the platform development is focused on procuring a flexible, experimental platform, it is thought that the latter approach is the most applicable. This because implementation of added and altered interfacing features can be handled in software alone. A bidirectional communication between a micro controller and a host computer can be established in numerous ways. The chosen micro controller support RS-232 at TTL level. RS-232 is a standard serial communication protocol widely used, it is obvious to employ this communication method. RS-232 while still used to a great extend in embedded devices, this communication protocol has seen less use in peripheral devices to workstation computers over the last decade. This as the use of serial internet modems over telephone lines by large has been phased out, and most peripherals today employ the USB1.1 or USB2.0 protocol. Hence providing the controller electronics with an RS-232 interface through a TTL to RS-232 logic level converter driver will merely produce a controller that is incompatible with most modern computers. Instead the USB protocol can be used. An efficient way of establishing communication between an RS-232 enabled micro controller unit and a host computer through USB is to employ an intermediate USB to RS-232 serial UART. A popular UART is produced by Future Techonology Devices International Itd. The FT232R USB UART IC. The following specifications is derived from the device data sheet.[108] This is a single-chip solution to establish asynchronous serial data transfer between peripheral and host. The device support transfer rates up to 3 megabit per second, and the entire USB protocol is handled on-chip. When integrated to the controller electronics, and the electronics are connected to the host by means of a USB cable, the FT232 driver chip will simply be recognized as a hardware RS-232 port, tunneling data through to the micro controller unit. Employed to establish communication between the host and the controller electronics, a communication nitrate of 115.200 bits/s is used.

Motor Control System

A motor control subsystem is an integral part of the controller electronics. This subsystem must allow for accurate motor positioning in order to drive NC axis. The two most common methods to achieve this is by either implementing a servo motor controller or a stepper motor controller. Both solutions have benefits and drawbacks. Employing servo motors require a motor controller with a current-chopping H-bridge to power the servo motor in either direction, and an encoder interpreter that can read the position of the encoder on the servo motor and regulate the output accordingly. This is often done by employing a Proportional Integral Derivative (PID) control loop feedback. [109] Dedicated integrated servo controller chips are available for miniature direct current drives, and can be integrated with the electronic controller with relative ease. Servo drives are charac-

terized by being rugged. They don't loose their position reference if they are over torqued, as the encoder will measure the true motor position. Their operation is smooth, and relatively silent in comparison to stepper motors. The numerical control of stepper motors are much simpler than of servo motors. Where a servo motor relies on a PID control loop feedback to reach and not overshoot its target position, a stepper motor as implied moves step-by-step towards their position. As a clock-work it is merely a matter of stopping the sequence once the desired position is reached. Stepper motors are widely used in instrumental applications, computer peripherals, office equipment, machine tools, robotics and electromedical applications. [110] They are known by their simplicity of their control scheme, and low cost relative to servo driven systems. The eased operation however does not come costless. Stepper motors are prone to introduce vibrations due to their uneven movement, and are known to loose torque as a function of rotational speeds. However given the low cost of stepper based systems over servo based systems, not least a much easier control-scheme, it has been chosen to base the controller electronics of the experimental multi material platform on stepper motors in an effort to reduce time. With this decision it needed to characterize how stepper motors is efficiently controlled. Vibrations can be reduced by two main control parameters. The current delivered to the stepper motor, and the stepping method. If the current drawn by the motor is limited by current chopping, the magnetic field, and hence the attraction of the rotor to the stator is reduced. This result in a smaller "kick" (FIND ANDET ORD!!!) of the rotor due to a smaller kinematic reaction. Another way is to alter the stepping sequence. The 1'st order stepping sequence is a full-step sequence where each of the four inductor circuits is toggled in turn. This resulting behavior of the motor is to turn one full step, assuming constant acceleration, reaching the angular velocity of ω_1, excerpting a force relative to the velocity when the rotor is abruptly decelerated as the magnetic fields of rotor and stator align. The 2'd order stepping sequence is a half-step sequence where the inductors of the stator is controlled in pairs. Stepping from a state where the first inductor circuit is engaged is performed by engaging the second inductor while keeping the first engaged. This result in the rotor turning half a step. Assuming constant acceleration, the rotor reach an angular velocity of $\omega_2 = \frac{\omega_1}{2}$. The corresponding deceleration force as the rotor and stator align is hence halved, decreasing vibrations. An assessment of the relation between torque and rotational speed is also to be carried out to determine whether a stepper motor control scheme is suitable. A generic graph shown in figure 6.5 on the facing page shoe this relationship.

The figure show an arbitrary relationship between torque and stepping speed of a generic stepper motor. Two curves are shown. They indicate the maximum stepping rate, at a given load before the motor loose synchronization. The Start-Stop curve indicate the torque that can applied if the stepper motor is started or stopped without acceleration at a certain speed. The zero at $\tau = 0$ is the maximum speed the motor can reach without any acceleration control The Slewing

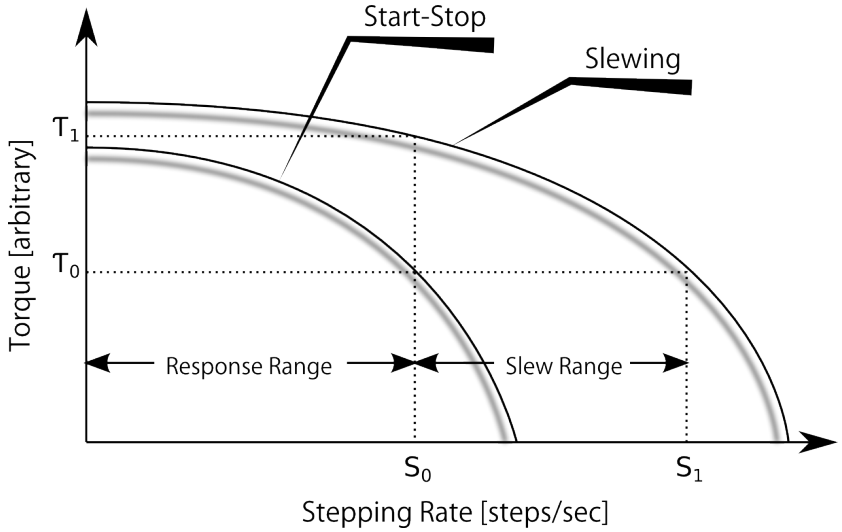

Data source: Stepper Motors - Fundamentals Applications and Design[110]

Figure 6.5: *Declination of torque as a function of stepping speed*

curve indicate the torque that can applied if the stepper motor is accelerated or decelerated in a controlled manner, or running at constant speed. Within the Response Range the stepper motor is able to accelerate from still to S_0 at a load of τ_0 in just one step. However if the stepper motor is accelerated from still, the stepper motor can reach the speed of S_1 without loosing synchronization. At the speed of S_0 the stepper motor can tolerate a load of τ_0 if the stepper motor is not accelerated, whereas at the same load, the motor can handle a load of τ_1 if the stepper is accelerated. Finally it can be noticed that at very slow speeds, there is little difference between load-handling whether the stepper motor is accelerated or not. It can be seen that without acceleration control it is possible to run a generic stepper motor at no more than half its efficiency without integration of an acceleration algorithm in the electronic controller firmware. However, since it is not of interest to run the stepper motors at high torque and at high currents due to vibration issues, it is considered that the relation between torque and stepping speed can be neglected in the specific application.

The controller electronics has been designed to employ both a current-limiting and a half-stepping control scheme to employ these two methods as means to limit vibrational noise. This is done by selecting an integrated stepper motor driver chip, that has both features built-in. The device selected is the Allegro Microsystems A3982 driver. All specifications has been derived from the device data sheet.[111] The chip comes in a 24 pin SOIC package, and allows for half stepping of bidirectional stepper motors. It has a built-in translator that is interfaced at TTL level. The translator is comprised of a set of parallel TTL communication lines.

Enable, step and direction. Direction and enable is set by a logic-level high or low. A step is carried out when a low-to-high flange is detected @ TTL level on the step input. The device can drive stepper motors at a voltage up to $+35V$ ⎓, supplied on an isolated supply line, with a supply current up to $2A$. This allow the driver to control motors up to 70W. The chip has an in-built over heat protection circuit that automatically cut power to the stepper motor if operation temperature is exceeded. With the ability to chopping control the supply current to stepper motors not least provide half-stepping is the main reasons why this device has been selected.

Modulated Power Outputs

Contrasting the specification of the micro controller logics, motor driver and communication modules, the power output module of the electronic controller board is trivial. Due to a rapid growth in markets for synchronous rectification in switching mode power supplies, the field of high speed power switching in level converters and in the emerging field of high-power controller systems for environmentally friendly electric technologies, highly efficient, high current MOSFET based transistors are abundant at a low cost. Fundamentally any logic-levet N-type MOSFET for high-powered switching applications is suitable as a pulse-width modulated transistor to drive the output channels of the electronic controller board. The IRF1324S has been chosen due to its low cost, high-speed power switching tolerance and not least the exulting capability to handle a silicon-limited current of 429A @ 24 volts, conveying up to 10.3 kW @ peak-load. All specifications has been derived from the device data sheet.[112] This in a small surface-mounted D^2PAK package. Furthermore the transistor has a built-in fast rectifying diode to dissipate reverse induced electro magnetic noise. This diode protect the transistor at reverse induced peak currents up 1636A, making the device rugged and sturdy in noisy operation conditions.

Analog and Digital Inputs

Two types of input are used with the electronic controller. These are digital and analog inputs. The digital inputs are used to handle simple on/off signals such as from mechanical switches and button. It has been chosen to include three digital inputs on the controller board. This as if a home/limit switch system is sought to be integrated on the experimental multi material platform, three channels allow for an individual switch channel per cartesian axis. The inputs are comprised by a resistor to provide high impedance signals to the micro controller, protecting its inner circuits agains over currents. In parallel there is a capacitor serving to debounce signal noise from the input signals. The three inputs are wired to bidirectional pins on the micro controller. This allow the three channels to also be used as outputs in case the electronic controller is to drive an external system that was not accounted for at development time. This can be a solid state relay, or

using two channels, a bidirectional communications line to external serial enabled circuitry.

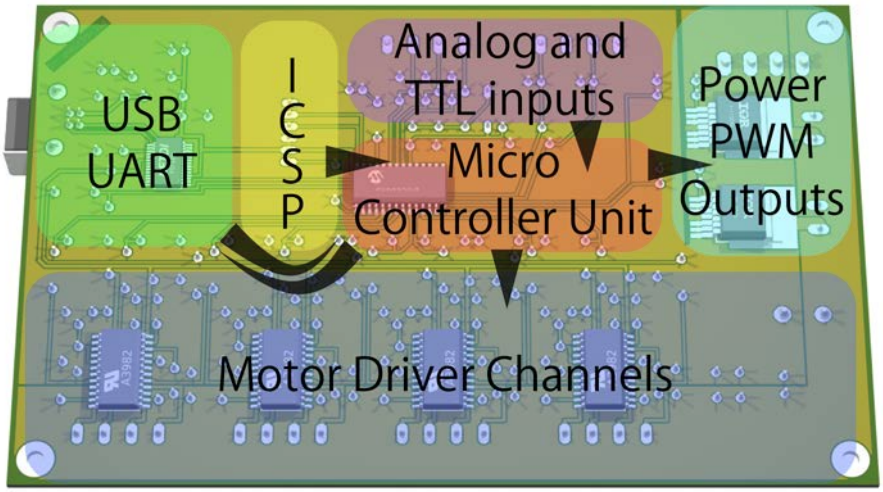

Figure 6.6: *FDM controller electronics, revision 1*

6.1.4 Embedded software

Figure 6.7 on the next page shows an operational flow chart of the Micro Controller Firmware. At boot-time a series of initialization routines is carried out. (1) The EEPROM of the micro controller is audited for calibrated machine parameters such as conversion factors from motor steps to axis movement in millimeters. If none is found, a default parameter set is loaded. Setpoint temperatures are set to zero degrees to ensure that heat elements are idling at ambient room temperature, and the 4-axis machine coordinate system is set to zero. Once the system has been initialized, the serial buffer is queried. The serial buffer (2) is a software buffer implemented to contain incoming data from the host computer. The PIC18F2620 has a hardware master serial synchronous port (MSSP) consisting of a synchronous serial port shift register, (SSPSR) of 8 bits, and a synchronous serial port buffer register (SSPBUF) into which the SSPSR register is emptied. An interrupt driven routine dumps the SSPBUF into a software buffer of a fixed size. This interrupt

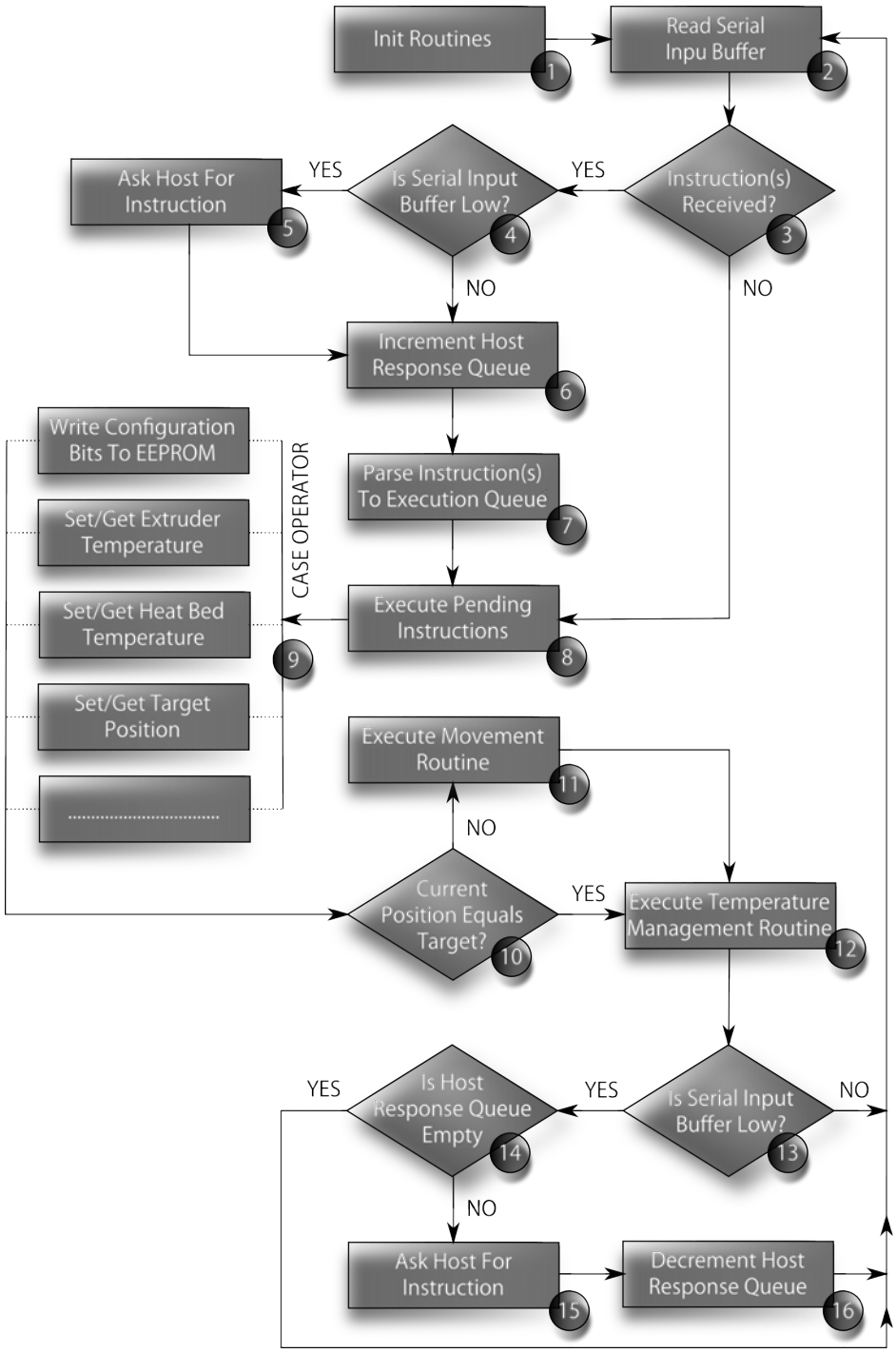

Figure 6.7: *Operational Flow Chart describing the firmware*

driven software buffer is implemented as a ring-buffer where a leading index and a tailing index indicate the current read and write bit position in the buffer. The buffer is dynamically written, and the leading index is updated upon serial data arrival. The firmware reads the software buffer (3) searching for a return character which indicate that an instruction line has been received from the host computer. If no instructions are found within the serial input buffer, the firmware proceeds to (8) If one or more instructions are found, the serial tailing index is updated to indicate what bits has been read. (4) If the serial ring buffer is low, there is room to buffer more data from the host, in the ring buffer, and the host is asked to send another instruction already before the current instruction is executed. This is done at (5) where and "OK" is returned to the host. If there is not room in the serial input buffer (6) a counter, queues the "OK" response so that this can be sent at a later point in time. This hinder further incoming data to be streamed by the host. The instruction received from (3) is now parsed, and queued to the execution buffer.(7) This is a buffer holding valid commands, that has been parsed, understood, and are now ready to be executed. If an instruction from the Execution Queue is pending to be executed (8) the instruction is looked up using a case select operator routine. The type of instruction is determined and executed. (9) The dashed box indicate a set of less interesting commands not included in the flowchart. Next the firmware compare the current cartesian position of the stepper motors with the target position that may or may not have changed by the instruction executed. If the current and target position differ (10) a movement from the current location to the target position(11) is executed. As the target position and current position now is identical, a temperature management routine is executed. (12) Heat elements are turned on or off by intercomparing actual and set point temperatures. Finally a serial input buffer routine is executed. This routine, spanning from (13) to (16) serve to either request the host computer to add to the serial buffer if there is room by first calculating the free space of the buffer (13) or to wait querying for new instructions. If there is room, then, yet only if the host is expecting an "OK" to be returned (14) another host instruction is queried (15) and the host response queue counter (16) is decremented. This will add one extra instruction to the serial input buffer per firmware iteration, until the buffer is nearly full.

6.1.5 Host software

Communication between host and controller-electronics at a protocol level is implemented as an ASCII character based protocol. The controller electronics has an implementation of a G-code flavored instruction set based on the ISO 6983 standard, and subsequently expanded to tailor the instruction set to the FDM process. This makes the electronic controller directly compatible with several Open Source utilities for generating job files from 3D files following the STL format. One such utility employed for generating job files within this research project is a utility

called Slic3r developed within the Open Source community of the Reprap platform to be cross-platform compatible and highly efficient at processing 3D structures to uild jobs.[113] Slic3r accept 3D structure in the .STL file format. This format, as described in section 2.2.3 on page 36 is the de-facto standard in the field of Additive Manufacturing. Slic3r has a simple graphical user interface that allows the operator to define machine specific parameters such as build feederate, layer height, extrusion temperature and other process-relevant parameters. The user interface can be seen in figure 6.8

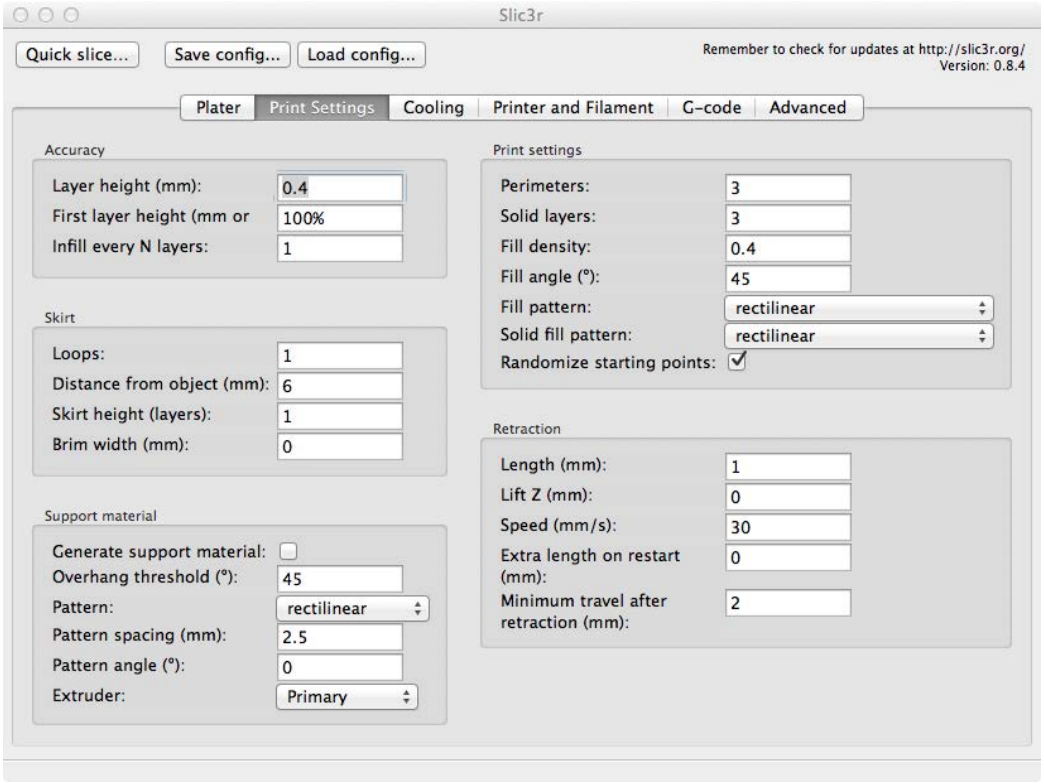

Figure 6.8: *Slic3r v.0.84 - build job generator for Open Source FDM platforms*

Once a job file has been generated there are several options to parse a job file to the electronic controller. This must be done line-by-line in a synchronous manner where a new line is passed to the electronic controller each time the electronic controller report ready to receive a command by sending an "OK\n". Initial testing has been done using a simple *nix based bash script within a shell terminal. Subsequently another Open Source cross-platform utility called Pronterface has been employed to succede the bash script in order to provide the operator with eased operation of the platform. Pronterface, seen in figure 6.9 on the facing page allow for execution of often used instructions such as movement, and temperature control, by user input to text fields and by button-clicks. Furthermore buttons with

related G-code commands can be added dynamically to extend the user interface as needed.

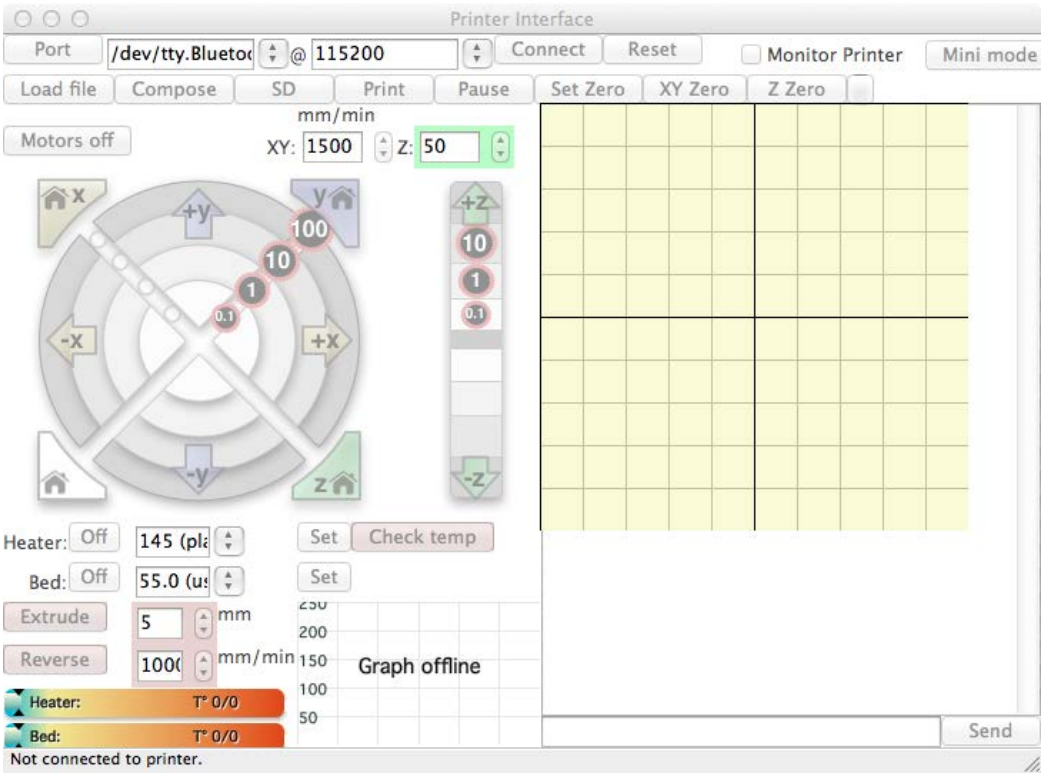

Figure 6.9: *Pronterface - A graphical communications interface for Open Source FDM platforms*

6.1.6 Testing

Testing of the first revision of the Open Multi Material Platform has been focused on verification of the various subsystems. These by priority is the controller firmware, the electronic circuitry, the cartesian system and the extrusion system.

Controller Firmware

The implementation of the controller firmware has been initiated in parallel with the construction of the hardware platform and electronic circuitry, following the V-model software development strategy.[114] This strategy described in figure 6.10 is a method where initial conceptualization and detailing is carried out with an abstraction from verification and integration. Consequently before the realization of the physical manifestation of the FDM platform, an initial firmware revision can be detailed from known requirements, following a downward sequential model in the firmware definition phase. Subsequently moving up through the testing and integration phase where the firmware first is validated in an emulated environment where the interface to individual hardware subsystems such as motors, thermal generators and sensors, and communication module is tested and verified. This allow for writing the firmware without having a platform readily available. Finally the firmware can be tested on the Open FDM platform as an entity, and the development can be wrapped up during general operation and maintenance.

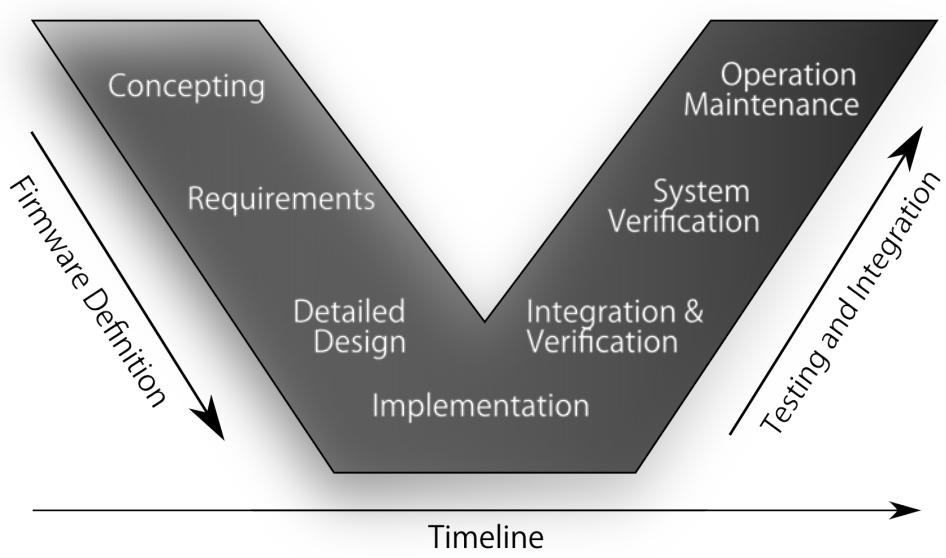

Figure 6.10: *The V-model software development methodology*

The force from using the V-model methodology is that a firmware revision that is close to functional is realized at the same milestone as when the hardware

platform and controller electronics stand ready. The task of testing and verifying the platform as entity thus result in finalizing firmware development as a natural extension of the initial detailing and development phase. What has been supplemented in the firmware during testing is algorithms controlling communication buffering, improvements on algorithms handling cartesian movement and the implementation of lookup-tables for converting raw temperature sensor data to degrees celsius. All these initiatives has resulted in an overall increased platform reliability and operational behavior.

The test routine following the functionality of the controller firmware is the test of the individual electronic subsystems. Here several distinctions are in focus. The main distinctions are signal noise in-between logic integrated circuits, signal noise on host-peripheral communication, noise originating from the power electronics, and finally dissipation of thermal losses of the power electronics. To test and monitor signal noise on host-peripheral communication, the ASCII communication protocol between host and micro controller has been developed so that a checksum can be passed with each command exchanged. When the communication host pass an instruction to the controller electronics, that instruction is parsed by a bitwise XOR of each byte in the instruction, following the ANSI C language. Bitwise XOR is an algorithm that perform a logical excessive OR operation on each bit-pair of two bit sequences. The resulting bit sequence will hold logical ones at each bitwise position where a logical one is found exclusive. The remaining positions will hold logical zeroes. This can be illustrated as:

```
        0010 (decimal 2)
XOR     1010 (decimal 10)
=       1000 (decimal 8)
```

As the instruction is passed from host to the micro controller, the checksum is appended with the instruction. The same bitwise XOR operation is carried out by the micro controller. If the checksums assent, the instruction has been received correctly. If they diverge, it means that one or more of the bytes received has been altered as a result of communication noise. Is the latter the case, the micro controller rise an error to the host. By testing over 112.7 MB of communication, checksum error is received for each $7.51 \text{x} 10^7$ bits (8.95 MB) of communication data, equalling one out of every $3.47 \text{x} 10^5$ instruction. As this frequency is estimated to be remarkably low, an error handling routine in the firmware of the micro controller is used to discard instructions that is misinterpreted, requesting the host to resend the instruction. Hereby noise induced to the electronics has been addressed in the firmware of the micro controller. If noise was a more prevalent issue, this should be addressed outside firmware.

Controller Electronics

Initially, no back-induced noise from the power electronics into the logical traces of the electronics had been detected. However, during operation, a coordinate-drift

was observed. Initially this was thought to be rounding-errors within housekeeping of machine coordinates in the firmware. A closer investigation however proved no such phenomena. By means of signal analysis of the logic level communication between micro controller and motor drivers, it was discovered that noise spikes reaching TTL level on the step-signal pins of the motor drivers, revealed the co-ordinate drift to be a cause of back induced noise from the stepper motor coils. To circumvene this, a series of capacitors functioning as capacitive low-pass filters on the logical supply and signal lines, along with resistors effectively pulling signal levels low on supply lines was birds-nested to the circuit as seen in figure 6.11. These means effectively resolved back-induced noise from motor operation.

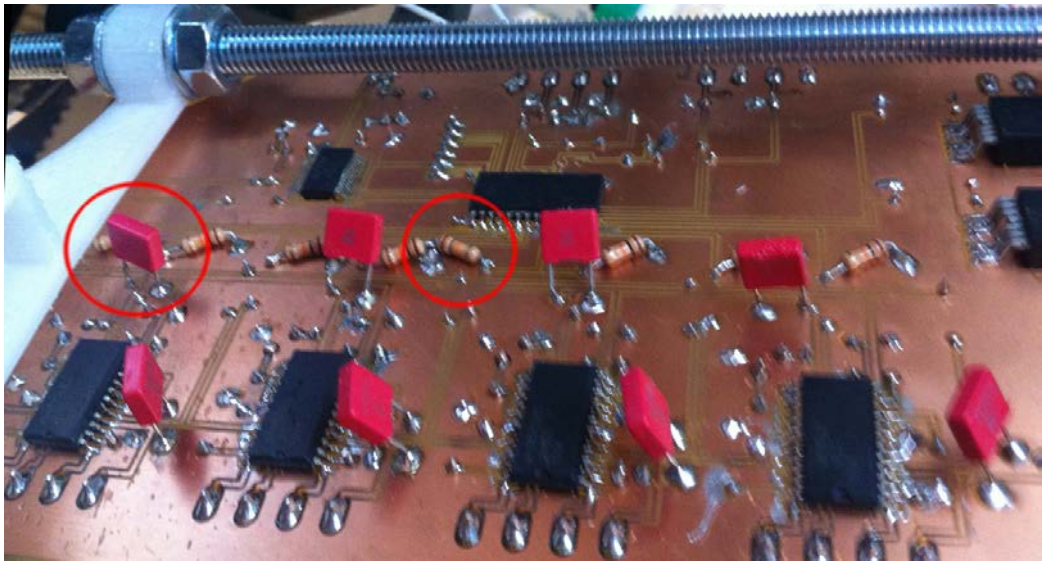

Figure 6.11: *Low-pass filtering supply and signal lines by means of capacitors*

During prolonged operation of the Open FDM platform, it was observed that one or more axis tended to set out. Upon investigation it was proven that this phenomena was due to thermal buildup within the motor driver circuits. The resulting effect is that when the maximum permissible operational temperature of 85 C°degrees is exceeded[111], the heat-protection circuitry within the driver chips set in, and shut down the drivers. To help dissipating heat from these chips, active cooling of the chipset was implemented. As seen on figure 6.12 on the next page, a chipset cooling fan has been press-fit on a bracket to provide sufficient air-flow to dissipate heat that otherwise is built up in the motor drivers. The bracket has been additively manufactured by the machine itself, and on the rear side feature a duct channeling the air-flow over the motor driver chipset, effectively reducing the operational temperature in full-load condition to less than 65 C°degrees.

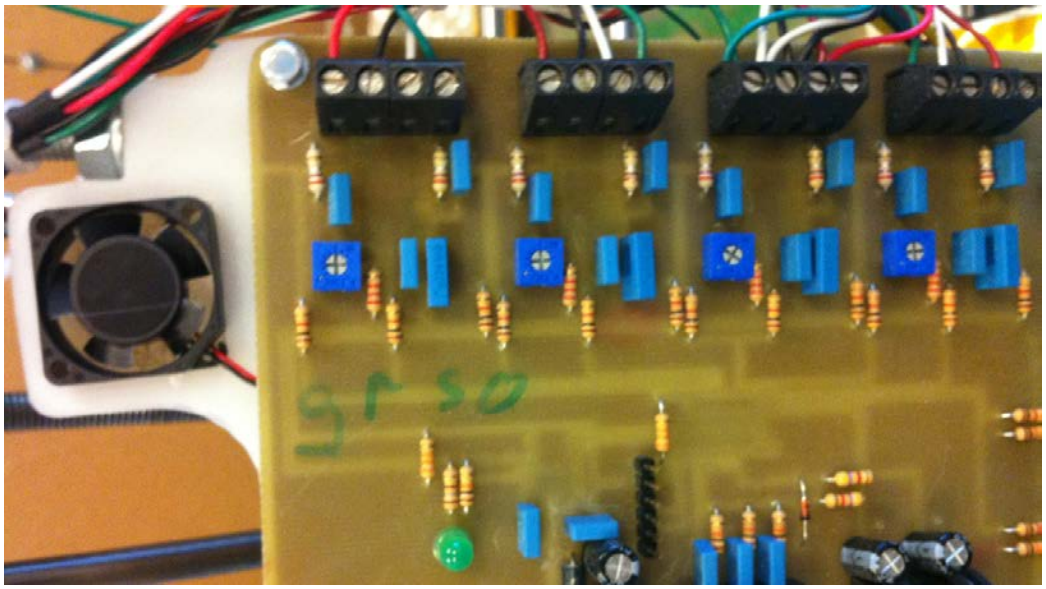

Figure 6.12: *Active cooling of motor driver chipset*

Machine Calibration

With all issues from firmware and electronics corrected, calibration of the cartesian axis of the Open FDM platform was carried out using a micrometer dial gauge to provide calibration parameters to be input to the micro controller. As precise absolute positioning of the cartesian axis of the FDM platform at current level of implementation was not of concern, a 2-step iteratory calibration was found sufficient.

Extrusion tests in PLA

Testing of the thermal extrusion system could now be carried out. ABS and PLA polymer has been tested as processing materials. The tests in the following however will be tests from additive manufacturing of structures in PLA. This because PLA proved easier to visually inspect through magnification. PLA, renowned for its thermal stability, as previously described in section 2.4.1 on page 56. As such PLA impose few challenges during deposition, as the structure that is being built, does not warp or curl off the build-platform as a result from a build-up of stresses from thermal shrinkage, and hence is a suitable polymer for verification of additive manufacturing capabilities of the Open FDM platform. A systematic approach to determine deposition parameters has been carried out, focusing on the material deposition rate in relation to the layer height and the traversing speed of the toolhead. With the optimum build parameters found, using a thermal extruder with an orifice diameter of 0.4mm to deposit PLA polymer, consistent build qualities as shown in figure 6.13 on the next page can be reached.

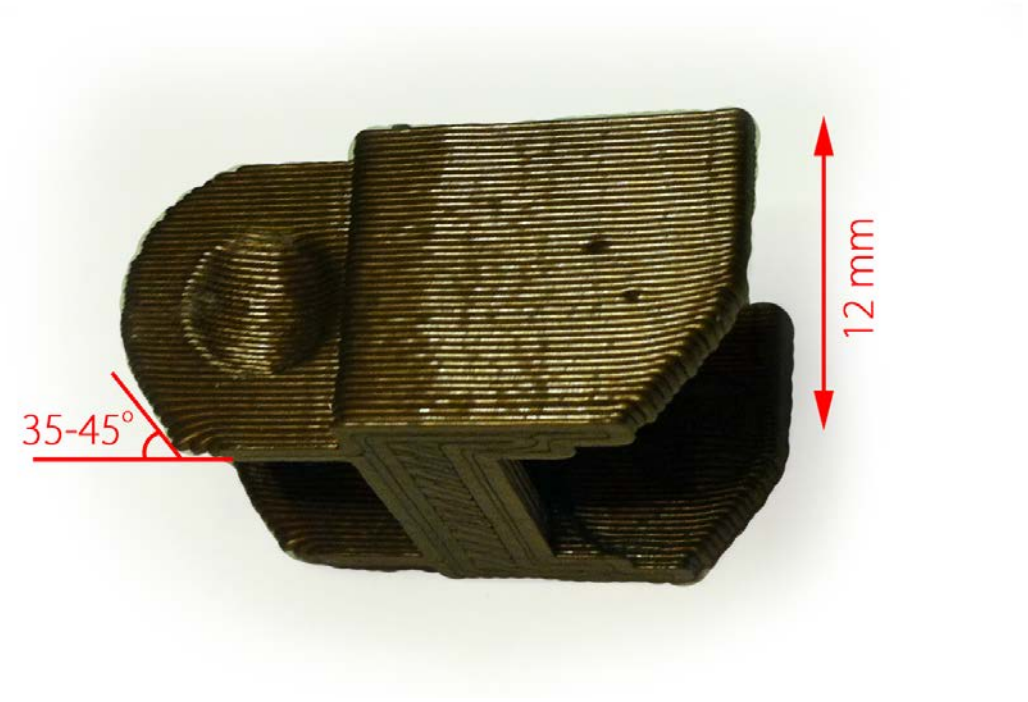

Figure 6.13: *An extruded part in PLA polymer*

The geometry which has been realized, is in a glossy metallic color as the reflective surface yield a high level of details when inspected by means of optical magnification. The geometry has been built with a layer height of 0.3 mm. The extrusion temperature has been 170 C°degrees, and the traverse feed has been 12 mm/s. The geometry is shown as oriented on the build-plate of the FDM platform, photographed from a perspective that allows the very first layer of the part to be inspected. It can be noticed that this first layer is flattened. This as it is the interface between structure and build platform, and as such has been equated by the imprint of the platform to the structure. The three shell-layers of the geometry can be seen tracing the boundary of the first layer of the object. In the core of the first layer, the infill of the structure can be seen as a lined pattern stretching diagonally from boundary to boundary. On the flange to the left, it can be seen that some layers have collapsed in an in-caving manner. This is because the unsupported overhang of the initial layers has been of a magnitude, where there has been no bearing area from the previous layer to hold up the boundary. As the bearing interface changes with the curvature of the geometry, the overhang is less prone to collapse.

At angles exceeding 35-45°, it is common to see the geometry to cave in. The part will form the basis to describe three main process-induced defects to parts

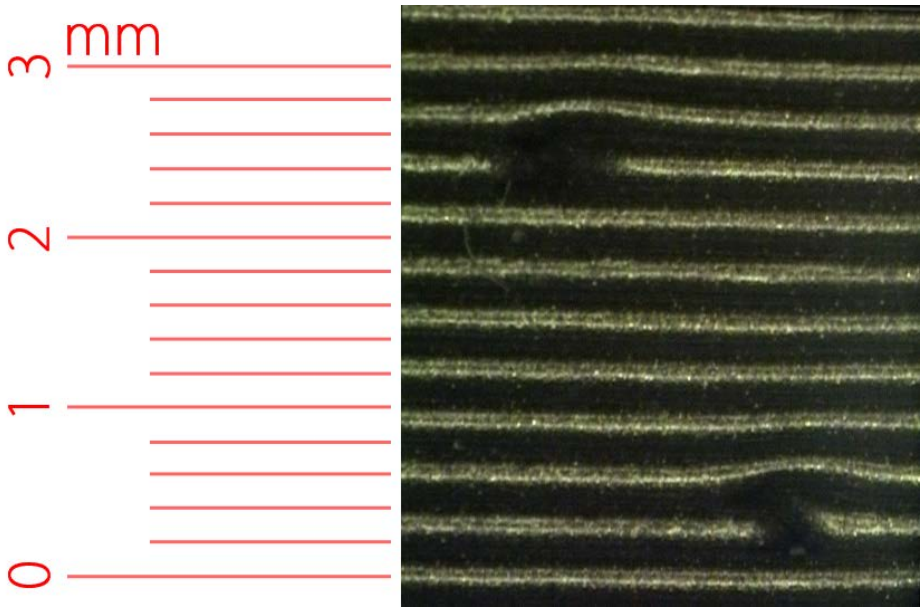

Figure 6.14: *Detailed view of defects formed from layer change*

being manufactured using the FDM principle. Figure 6.15 show a closer detailed view the surface of the geometry, where the uniformity of the layers is clearly evident. It can be observed in the lower right corner that the layers has a tendency to curl upward. This is a result of the geometry having an unsupported overhang. Whereas it could be inspected on the flange of the part in figure 6.13, that the geometry collapsed due to missing overhang, another, yet similar behavior can be observed at times. If the extrusion rate is slightly low in comparison to traversing speed, it can happen that as the extruder orifice is rounding the corner of the geometry, the unsupported strand of filament is being pulled and stretched, herby slightly curling up. This phenomena is hard to prevent, and has been accepted as a process-characteristic for the first generation platform. Two scars can be seen on the surface. A closer view of these can be seen in figure 6.14. These scars are formed after the outer peripheral shell has been deposited, and the extrusion orifice is moved one shell-layer inwards. Several control schemes has been tried to minimize this scarring, yet it has not been possible to completely avoid the effect. Hence this phenomena has also been accepted as a process-characteristic for the first generation platform. Finally, on figure 6.15 on the next page, a small defect can be seen in the upper left corner of the geometry, above the topmost layer. This little defect is where the build-job has finished and the extrusion unit has moved free from the geometry in the z-direction. This scar on the part, upon completion of the build job is as with the other two defects difficult to prevent.

A close study of surface qualities of structures built by polymer extrusion has been undertaken. A test series of $10x10x10mm$ cubes has been built at different

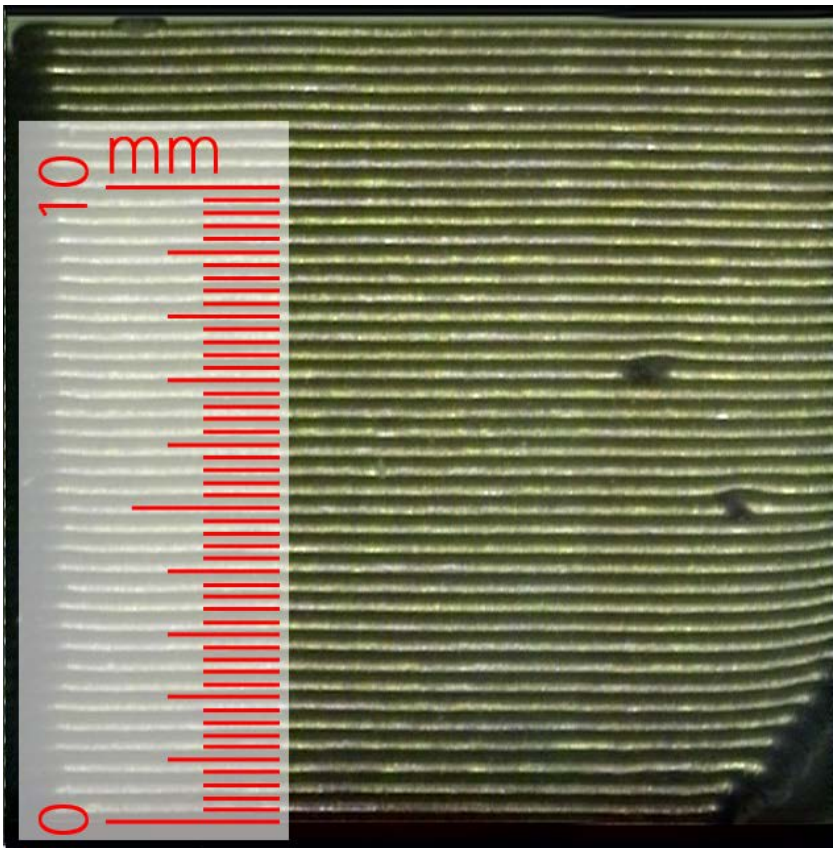

Figure 6.15: *Inspection of layer formation*

build parameters. Well-defined layers of no more than 0.25mm height has been achieved with a 0.4mm nozzle diameter. The main purpose of this parameter-test study is to find the layer height and thus the s stand-off of the nozzle to the previous layer, where it is no longer possible to control the extrude. This as irrespective to the orifice diameter, at infinitesimal stand-off heights, the control of the flow-rate of extrude becomes hyper-critical and uncontrollable as the extrude must likewise be infinitesimal. The cubes from the test series has been measured with an accredited stylus-based 3D profilometer at the metrology section at the Technical University of Denmark. The results yielded that layer-heights down to 0.25 mm the extrude of the boundary of the cubes and hence the definition of the surface-finish of the structures is verycontrollable. This is documented in figure 6.16 on the facing page, showing a 2D surface roughness as well as the raw 3D profile of the surface of the cube in the software ⌜*Scanning Probe Image Metrology*⌟[115]

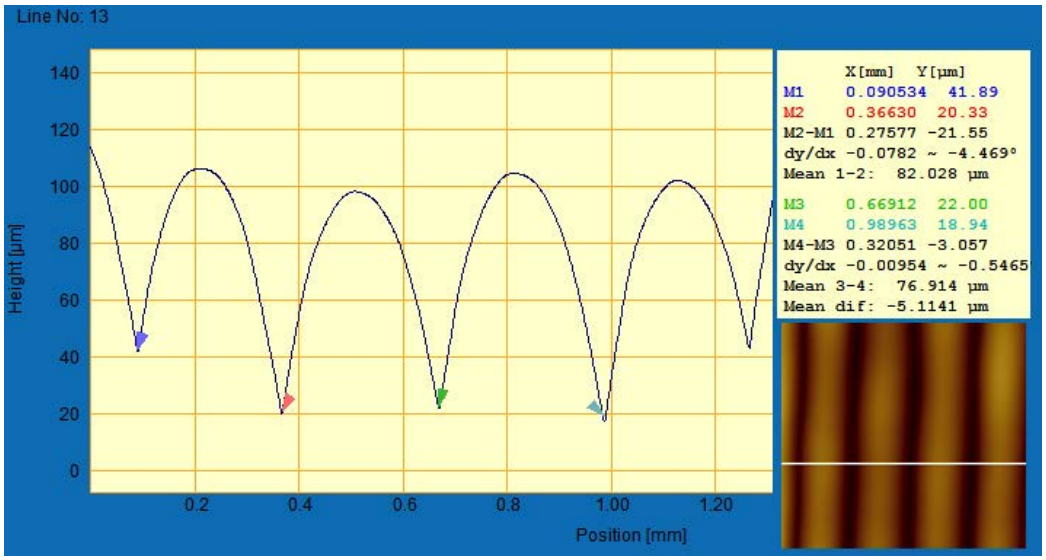

Figure 6.16: *2D and 3D surface roughness analysis of a profile at 0.25mm layer height.*

Factors Influencing Extrusion Speed

The parametric analysis to determine optimum extrusion parameters has additionally yielded a suggested control-scheme for increasing processing speed by halving the layer height of shell deposition while maintaining full layer height while depositing material in the core.[116] A traditional approach to increase vertical resolution of the FDM method has been to decrease the orifice diameter while decreasing the height of each deposited layer. The control scheme allows deposition of the perimeter of each layer to be deposited with half the layer thickness, hereby doubling the level of vertical detail on the surface of the additively manufactured structure. The control scheme has proved to dramatically decrease build time of parts fabricated using the FDM process while not compromising surface quality. Fine layers within FDM extrusion systems is generally considered to be near 0.2mm in height. Stratasys Inc. offer industry-level renowned machines that operate at a minimal layer height of 0.178mm.[117] This is a low layer height in comparison to many other additive manufacturing methods. As described in chapter 2.3.8 on page 53, DLP equipment reach layer heights down to 8 microns. The limited resolution is negatively affecting the potential use of FDM for precision and micro applications. The concern therefore arise that if extrusion based processes proves most promising as the base for a next-gen, multi-material platforms due to the variety of materials that potentially can be used in these machines, then how does this FDM technology become ⌜*ready for micro*⌟? The naive answer will be ⌜*by downscaling the technology*⌟ This as correct at it be, is a part truth. Increased intelligence of tool path generation and control scheme complexity is a method

to reach even higher levels of accuracy. Figure 6.17 show the proposed control scheme. By manufacturing either shell layer but the outmost at full layer height, only to halve the layer height for the outmost boundary layer, a doubling of the level of detail on the surface can be achieved. This without noticeably increasing the manufacturing time of most geometries. This is achieved by extruding from the same orifice diameter as used while extruding the inner boundaries, yet by halving the extrusion rate in relation to the feed rate for the outmost boundary, and tracing the outmost boundary twice.

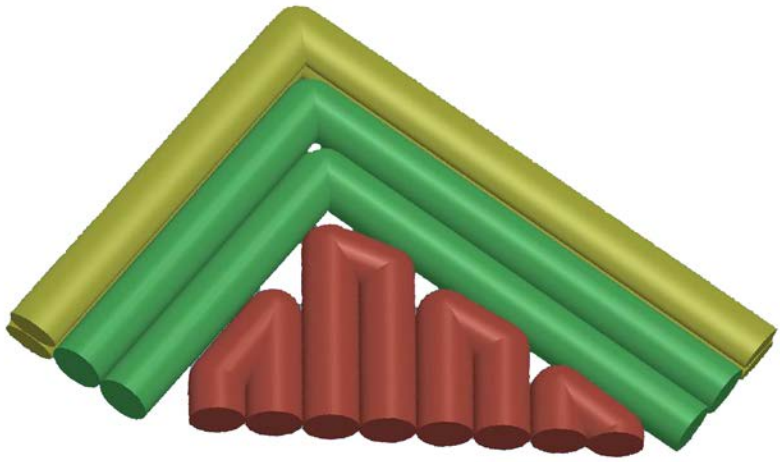

Figure 6.17: *Control scheme for division of shell-layer height while maintaining build-speed*

Using the traditional FDM control scheme where the layer height of the whole layer is halved as a means of increasing the surface quality, a two-fold increase in build time can be expected, as twice the number of layers need to be extruded. Using the proposed control scheme only a second pass of the very outmost boundary is needed to obtain the same reduction in layer height, hereby for most cases reducing the build time. An investigation of the speed-down as a function of layer height has been conducted on a 10x10x10mm cube and can be found on figure 6.18 on the next page.

It can be seen that a subdivision of the border by a factor of two over subdivision of the entire layer result in a constant gain by a magnitude of two. Hence a noticeable doubling of manufacturing process speed can be achieved on the cuboid geometry, over the traditional control scheme. To validate that the boundary subdivision method is a suitable method for increasing surface finish beyond the actual layer thickness, require a study of significant scale to be undertaken in the future.

The speed-down factor of decreasing layer height is just one out of several mechanisms that affect build-times. Another equally important factor is the fill density. It is widely used within FDM extrusion to build parts at varying densities.

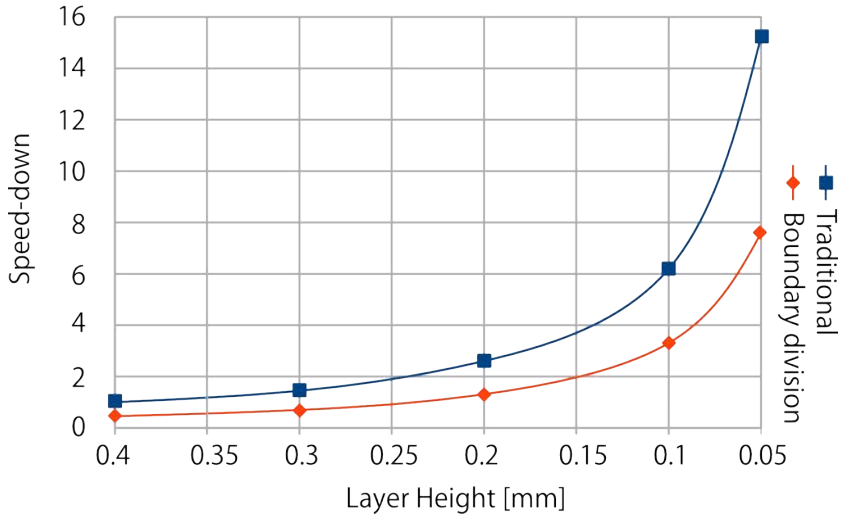

Figure 6.18: *The speed-down of job execution, halving the entire layer height opposed to halving merely the boundary layer*

The density is determined as how much of the core of the structure is comprised of extrude and how much is void. The less dense a structure is, the faster it will build. Once the entire structure has been built, the appearance of the part does not reveal how dense the core is. As such, to illustrate how the core appear on a low-density part, a partial print of a test-cube can be seen in figure 6.19 on the following page. Here a near hollow core is otherwise hidden is revealed.

How the part density affect the build-time has been analyzed by a cross-platform shell-executable script that has been written in Fortran. The script parse a job file, and from the federate and tool-paths given within, calculate the build-time of the job. The script help shed light on the relation between infill and build-time. The relation is highly dependent of the geometry. The build-time of a bulky structure will evidently be affected more by the infill density than a thin-walled shell-like structure. As such the benchmark for a density-analysis is a 10x10x10 cube. Figure 6.20 on the next page demonstrate a relation-graph.

The density analysis has been conducted at two different feed-rates. The first at 12 mm/s whereas the second at 24 mm/s. It can be seen by inter comparison of the two graphs that doubling the federate, lend a halving of job execution time. This is expected. A linear increase in build-time as a function of fill density is also expected. However between 0 and 10% fill density, a divergence is seen. This is caused by the fact that the filling routine disregarding the percentage of infill, pass over the structure in a checkered pattern as seen in the partial print in figure 6.19 on the following page. No matter how many pass over the diagonal that is needed to reach the desired fill density, the extrusion unit needs to trace the boundary,

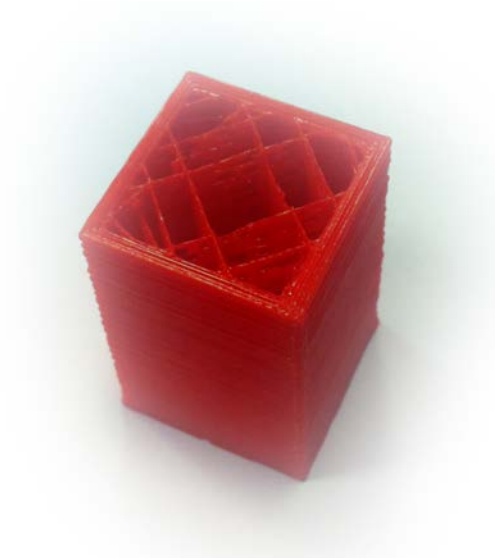

Figure 6.19: *A partial build of a structure with low fill density.*

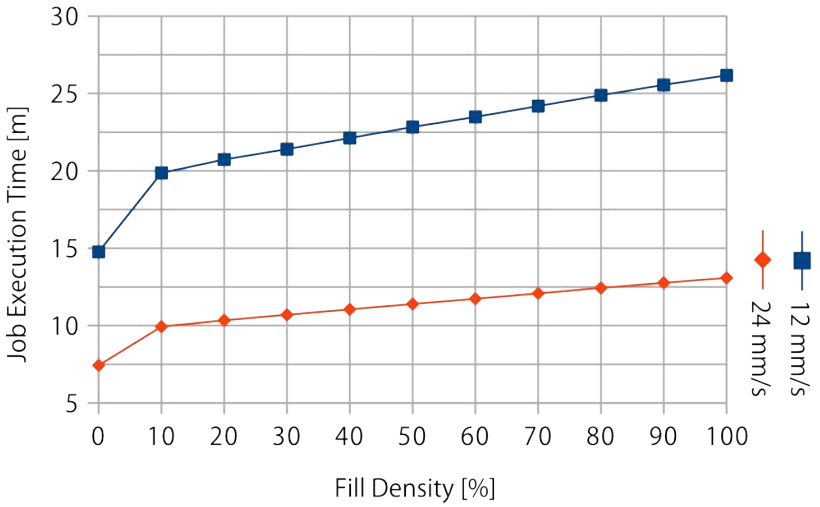

Figure 6.20: *The effect of federate- and density change to the job execution time of a 10x10x10 cube.*

while filling the core of the structure.

Bridging and support

As FDM extrusion does not lend any process-given support to structural overhangs, as it is the case with powder-bed based systems, there will be structures that cannot be built unless support is integrated with the build-job. As already demonstrated with the clip shown in figure 6.13 on page 192, structural overhangs at an angle beyond 35°must be expected to require support. However, certain overhangs can be built completely without support. An example of such structure, a squared frame, can be seen in figure 6.21 on the following page, where the tiles indicate the position of the individual subfigures. Tile 1-2 of the figure show a frame built with a support structure, and the frame after the support structure has been removed. The support structure has been made by adding a grated pattern of pillars onto the CAD model. As can be seen, there is scarring on the bearing-interface from removing the support structure from the overhang. However, the frame has been built without any sagging of the overhanging structure. Case the frame is built without any support whatsoever, the scenario is very different. This can be seen in tile 3. The first several layers of the overhang of the frame fatally collapse. Though subsequent layers stabilize the collapse, it ruin the aesthetic of the structure and most likely render the part unusable. The overhang however, can be built in this particular structure completely without support. As there is a freestanding column on either side, as the first layer of the overhang is to be manufactured, it is possible to span from the one column to the other. This by generating the tool-chains of the first layer of the overhang in a manner so that material is attached to the first column, and then stretched by increasing feed-rate over extrusion-rate as the extrusion unit pass over the overhang. This will stretch the polymer strands, so that these does not sag. Even if slight sagging occur, the strands will contract while cooling, tensing these to form a straight bridge. If this tool-chain scheme is employed, the result is as in frame 4. A slight sagging is seen, however, by optimizing the extrusion-rate over the feed-rate, sagging can be completely avoided.

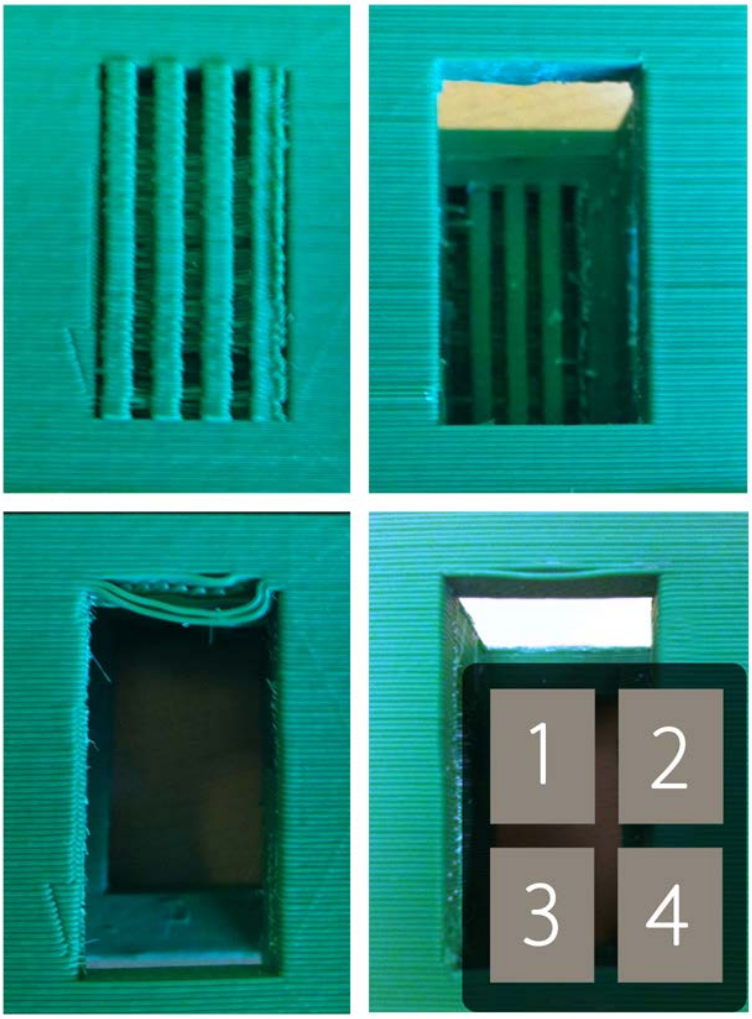

Figure 6.21: *A framed structure built with and without support. The tiled icons indicate numbering order. 1: The structure with support. 2. The structure with support removed. 3. The structure built without support. 4: The structure built without support, accelerating over overhangs.*

6.1.7 Build-speed limitations

All experiments done on the first generation platform has been at very low feedrates in comparison to commercial platforms. Stable extrusion could be be obtained above 12mm/s which as shown by the graph in figure 6.20 on page 198 correlates to less than four cubic centimeter at full density per hour. Build-speed was limited from the extrusion force required to drive the filament through the extrusion unit. If extrusion speed was increased, it was found that the extrusion

drive mechanism would shred the filament instead of pushing it forth. To understand this issue, an examination of the filament drive mechanism and the melt and extrusion mechanism within the extrusion unit was conducted. Figure 6.22 show the filament drive assembly.

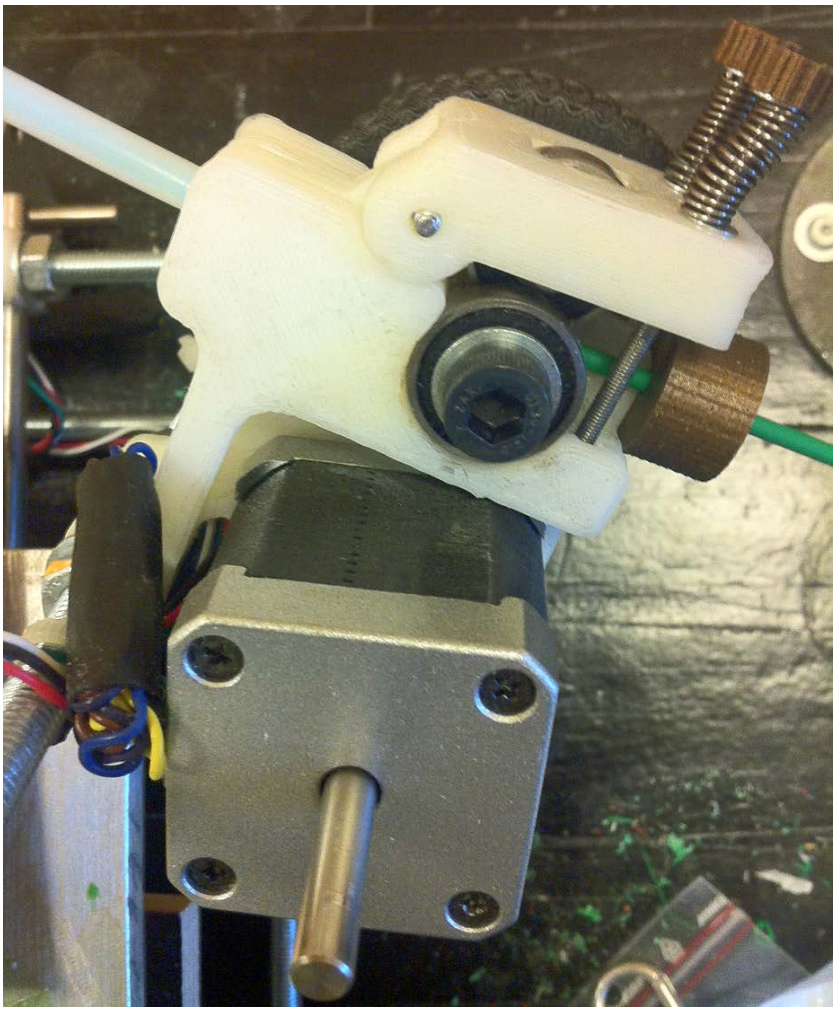

Figure 6.22: *Filament Drive Mechanism: A filament wire (green) is driven by a drive-axle (Allen Headed) with a diagonally hobbed toothing (not visible). An idler bearing hinged, and spring-loaded apply a retaining-force to the filament. The filament is run through a dust-removal cup holding a sponge-filter (gold colored) before entering the mechanism.*

A geared stepper motor drive the filament drive axle, seen in the figure as the Allen headed screw. This axle has a groove with a hobbed diagonal tooth-pattern that engage with the filament wire. Retaining the filament is a hinged, spring-loaded idler bearing. Before the filament enter the drive mechanism it is being run

through a dust-removal device. This is the small gold-colored cup, that holds a sponge filter, that is intended to pick up any foreign particle that otherwise will travel with the filament into the extrusion unit, possibly clogging the nozzle. As the filament exit the drive mechanism, it enters the Bowden cable that links to the carriage and the extrusion unit, not seen in the figure. If the force required to drive the filament wire through the extrusion unit exceed the friction coefficient of the engagement of the drive axle into the filament wire, the wire will slip, and the hobbed teeth of the drive axle will grind the wire. This phenomena can be seen in figure 6.23, where it is visible how the drive axle has shredded the filament. Experimental results where the filament wire was pressed onto a load-cell, the maximum force before the filament start to slip was measured to be 128N. At a filament wire diameter of 3 mm, this correlates to 18MPa of pressure on the melt within the extrusion unit.

Figure 6.23: *Filament Drive Axle and shredded filament wire. The teeth of the drive-axle has ground an indent in the filament.*

In order to understand why such high forces are required to drive the filament through the extrusion unit, an experimental study of the extrusion system was undertaken. The investigation yielded that the reason for the unexpectedly high extrusion force was found in the dynamics of the extrusion unit itself.

Figure 6.24 on the facing page show a schematic view of the extrusion unit. Filament is driven into the insulator barrel at the top, sliding down along the PTFE lining, which function is to reduce friction between the filament and the side-wall

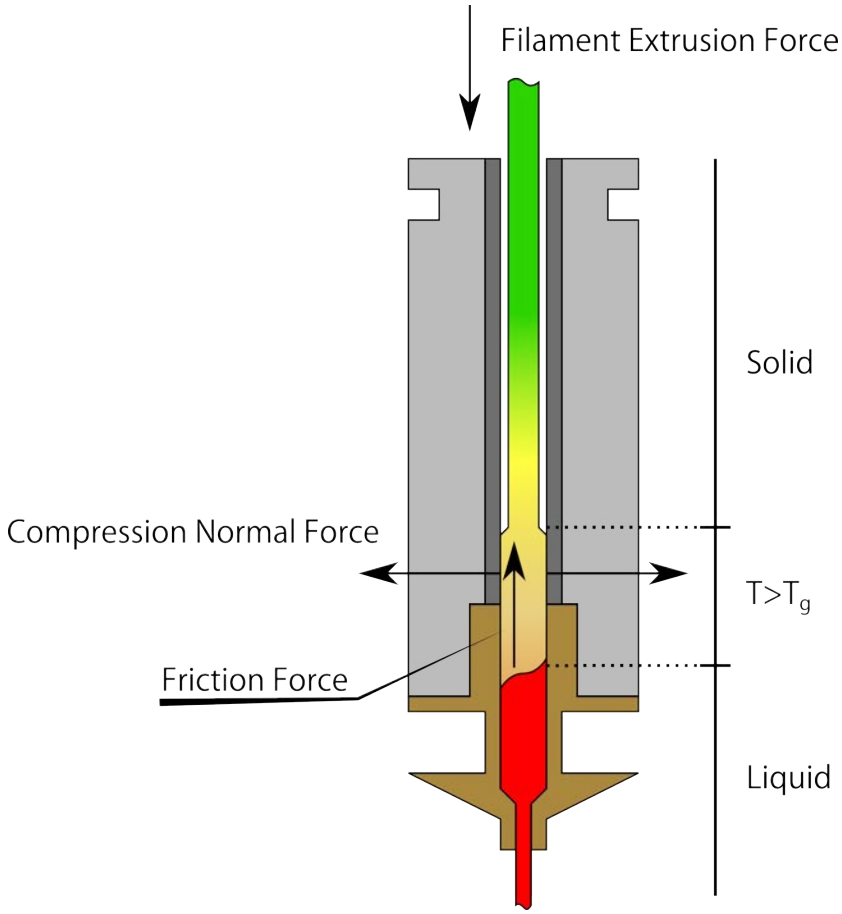

Figure 6.24: *Dynamics of the Extrusion Unit: Heat propagating from the melt up through the filament wire, result in a large zone where the polymer is above its glass transition temperature. Here it is rubbery and expand, Normal forces lend to increased friction and the filament wedge in the extruder barrel.*

of the barrel. As the polymer nears the hot brass nozzle, the temperature of the filament increase. Though the insulator reduce this, heat transfer as thermal conduction however increase the filament temperature above T_g. The filament becomes rubbery and is compressed. This lend to two effects. Advantageous is it that the expansion of the filament form a seal to the side-wall that prevent melt to shoot backward through the barrel, as a film between filament and side-wall. Detrimental is that the high degree of deformation of the rubbery filament at high extrusion rates, and thus the high normal force increase friction between filament and the PTFE lining. However, as PTFE is renowned for its low friction this is counterintuitive. The main contributor to the increased resistance to drive the filament through the extrusion unit is thus linked to the PTFE lining, however not governed by an increase in friction. It is from the fact that the PTFE lining is

compressible. The filament bulge outward, deform the PTFE lining, and as a plug it wedge into the PTFE lining, hereby rendering it impossible drive the filament through.

6.1.8 Conclusions of First Generation Platform

Testing the first generation platform stared with the completion of the development of the firmware and the electronic controller unit following the V-model. Subsequently communication noise was tested to examine its prevalence. Found to be low, a software based checksum algorithm was included. EMF induced noise from the power electronics was found to interfere with the operation of the stepper motor drivers. The result of this was a coordinate-drift within the firmware as the stepper motor drivers interpreted the EMF induced noise as signals from to micro controller unit thus unsanctioned engaged the motors. This issue was solved by filtering out the EMF noise by means of effectively pulling the step- and direction signal lines low by the addition of of pull-down resistors, so that EMF noise would no longer falsely trigger movement. Furthermore the EMF noise itself was addressed by filtering using capacitors to low-pass filer logic supply lines. Subsequently the platform was run in, and a tested by extrusion of PLA polymer. Additive manufacturing of layered parts down to a layer-height of 0.25mm was proven stable. An analysis of structural support and when this can be avoided was carried out. Finally the extrusion speed was assessed, and the mechanism as to why high extrusion rates could not be reached was found, and characterized.

6.2 Second Generation

While the first generation of the Open FDM platform was, providing a reliable platform for extrusion of thermopolymers, several functional issues araised while operating the machine. Furthermore, the first generation platform had no tooling for multi-material deposition. As a result, the platform was revised and formed the base for a second generation machine. The development of this will be described in the following.

6.2.1 Platform Optimization

Whereas noise issues of the controller-system of the first generation platform could be addressed by the addition of resistors and capacitors to the controller board, and communication noise could be addressed by software algorithms, several subsystems needed to undergo changes. The first area of attention was tooling.

6.2.2 Tooling

Extrusion of polymers was successful at low extrusion rates. Due to a design flaw of the extrusion unit, high extrusion rates was never accomplished with stable results. The issues relating to this, caused by thermally induced alterations of mechanical properties of the filament wire, needed to be addressed. This was done by redesigning the extrusion unit. The indirect cause to the low extrusion rate was that the PTFE lining within the insulator barrel became deformed by the expanding filament. The initial solution to the problem was to remove this lining. When extruding ABS polymer, this proved a valid solution for reaching much higher extrusion rates, with PLA however, exhibiting a very low and broad interval between T_g-T_l, expansion and thus high friction between the PLA filament and the PEEK insulator proved to result in similar issues. Extended efforts was put into designing a hybrid-extruder that would allow for efficient extrusion of both PLA and ABS polymers. As a result of this, the PTFE lining was reintroduced. The final extrusion unit design can be seen in figure 6.25.

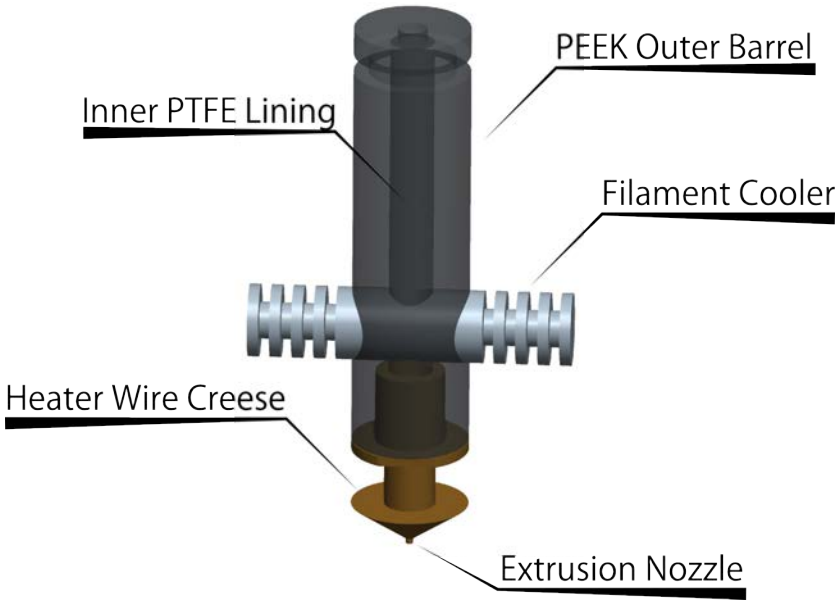

Figure 6.25: *Second Generation Extrusion Unit. A cooling unit will reduce the zone between T_g-T_l.*

What proved an efficient method to avoid extrusion issues, was to introduce a cooling device in close proximity to the heated nozzle. The cooling device efficiently draw out thermal energy from the PEEK insulator barrel, the PTFE lining and the filament wire, to dissipate this to the ambient air. In doing so, the zone where the polymer is above T_g, is moved down to just above the heated nozzle, hence eliminating problems with the filament wedging into the lining, and preventing

extrusion. After the introduction of this extruder design, extrusion tests with PLA polymer was extrusion-rates reaching well beyond the kinematic fast-move limits of the FDM machine.

As the motivation behind constructing an FDM platform is multi-material extrusion, and the platform as such has been proven, development of a multi-material extrusion unit is second in priority over the functional platform. Therefore intent is to include a non-thermal extrusion in the second generation platform. Importunate is that the extrusion unit is derived in a manner that allow for flexibility. Thus the intend of the unit is to allow for extrusion of a variety of materials with the common property that their viscosity at the time of deposition is so low that the materials can be extruded from a ram-type extruder. To allow for fast material-changes, interchange of extruder nozzles, and the ability to preserve and interchange between the existing hot extrusion system and the non thermal system, credence was given to design what best can be detailed as a universal non-thermal extrusion unit for pastes and liquids. The system can be seen in figure 6.26 on the facing page The tool carriage has been extended to allow for the attachment of a yoke that can support a medical syringe. This syringe function as a ram-extruder. The syringe can be filled with any paste or liquid with a viscosity that allow for extrusion. The nozzle diameter can be altered by attaching any commercial needle with an adapter that fit the syringe. The largest orifice obtainable is to run the unit without a needle attachment. The ram of the extruder is the plunger of the syringe. This is shortened in length, to allow for a coupling to attach. The drive mechanism for the ram is the unaltered filament drive mechanism used for thermal extrusion. A PLA or ABS filament wire is driven through the Bowden cable. The Bowden cable connector is removed from the thermal extrusion unit and fixed over the ram of the non-thermal extrusion unit. As filament is driven forth, into the breach of the adapter, the filament will drive the ram downward and extrude the paste or liquid within the syringe. A tool change can be made by detaching the Bowden cable connector, inserting a string with another material, and reset the system. To resume thermal extrusion, the Bowden cable connector is removed from the non-thermal extrusion unit, and repositioned over the thermal extrusion unit.

6.2.3 Electronics

Minor changes to the schematic of the second generation electronics was made in the inclusion of resistors and capacitors to remove the EMF noise that was seen on the first generation board. The main change to the controller electronics between first and second generation, however, was the introduction of another stepper motor driver. The A4982 stepper motor driver. [118] The choice to do so is related to the introduction of the universal extrusion unit. Running the extruder feed motor at half-stepping mode did not provide sufficient resolution to drive the filament wire forth thus advancing the ram of the universal extruder.

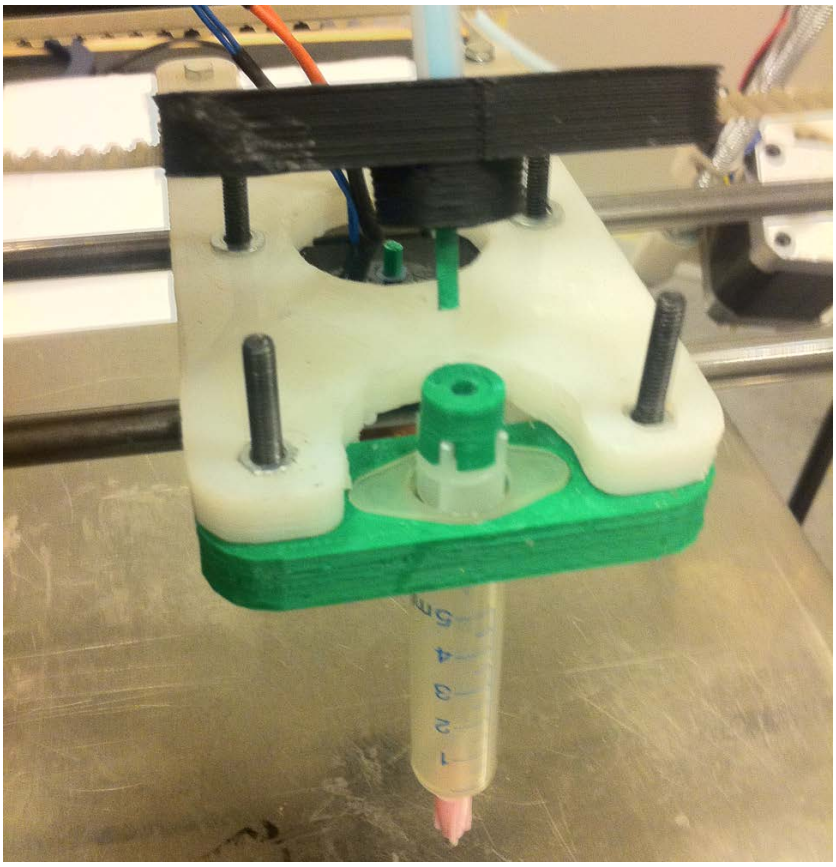

Figure 6.26: *Showing the Universal Extrusion system. The filament drive unit is employed to press on the plunger of a medical syringe held in a yoke.*

The extrude would throb from each step, as the diameter of the extruder ram was greatly increased over the filament diameter. A mechanical solution to this is a viable means of solving the issue, however if solved by driving the filament motor by a micro-stepping control scheme, a generally more smooth motor operation can be achieved over half-stepping. The development of a controller board that employ micro-stepping for all four NC-axis is beneficial not only for the filament drive mechanism, but can allow for all motors on the FDM platform to operate more silent, and reduce vibrations induced to the frame of the machine. As such, solving the extrude drive resolution within the controller board was favorable. The second generation controller board seen in figure 6.27 on the next page distinguish itself from the first generation by many minor minor alterations, and the one primary change, of being fully micro-stepping capable. The upmost wire clamp terminals allow for the four stepper motors to be attached, running in micro-stepping mode. The red capacitors scattered over the controller board are the low-pass noise reduction filters, removing EMF noise from the logic lines to the

logics and the stepper motor driver chips. Four potentiometers allow for limiting the current delivered by the stepper motor drivers to the stepper motors, by means of current chopping. The terminals on the right hand side and bottom of the controller board accommodate power-outputs to heaters and temperature inputs from thermistors. On the left-hand side is the USB connector that establish a communication line to the host computer.

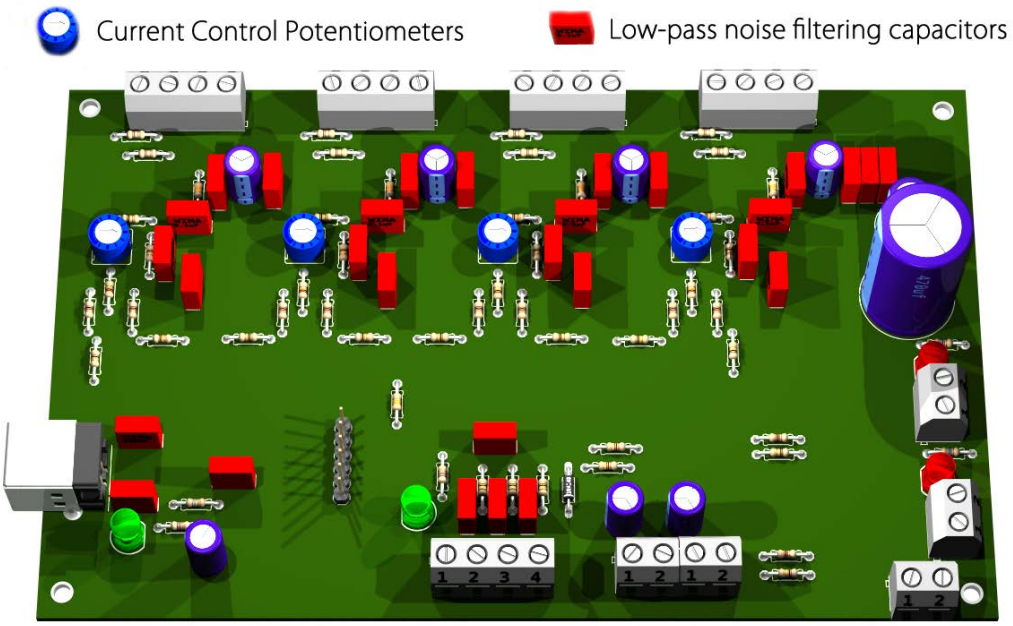

Figure 6.27: *FDM controller electronics, revision 2*

6.2.4 Host software

The first generation host software was entirely comprised by Slic3r, an Open Source tool-path generator, and Pronterface, a serial terminal interface to control and send job-files line-by-line to the FDM platform. This solution lacked the ability to execute multi-material build jobs. This functionality has been achieved by writing a g-code post processor. This post-processer read several job-files, and splice these into a multi-material job. The first generation tool-path generation software also proved during tests the need to handle communication between host and the controller in a more efficient and safe manner. A large amount of redundant data was exchanged between host and controller, and the job-generator could generate code that result in collisions of the extrusion unit to the build-platform.

Hence the G-code post processor that has been developed serve three major purposes. The primary is the ability to merge two or more individual job-files into one multi-material job. The secondary purpose is to enhance instruction execution

speeds by scrubbing the job-files files for redundant data before they are parsed by the G code post processor. The third purpose is to predict and avoid collisions of the extrusion unit to the build platform. The post processor function as shown in figure 6.28

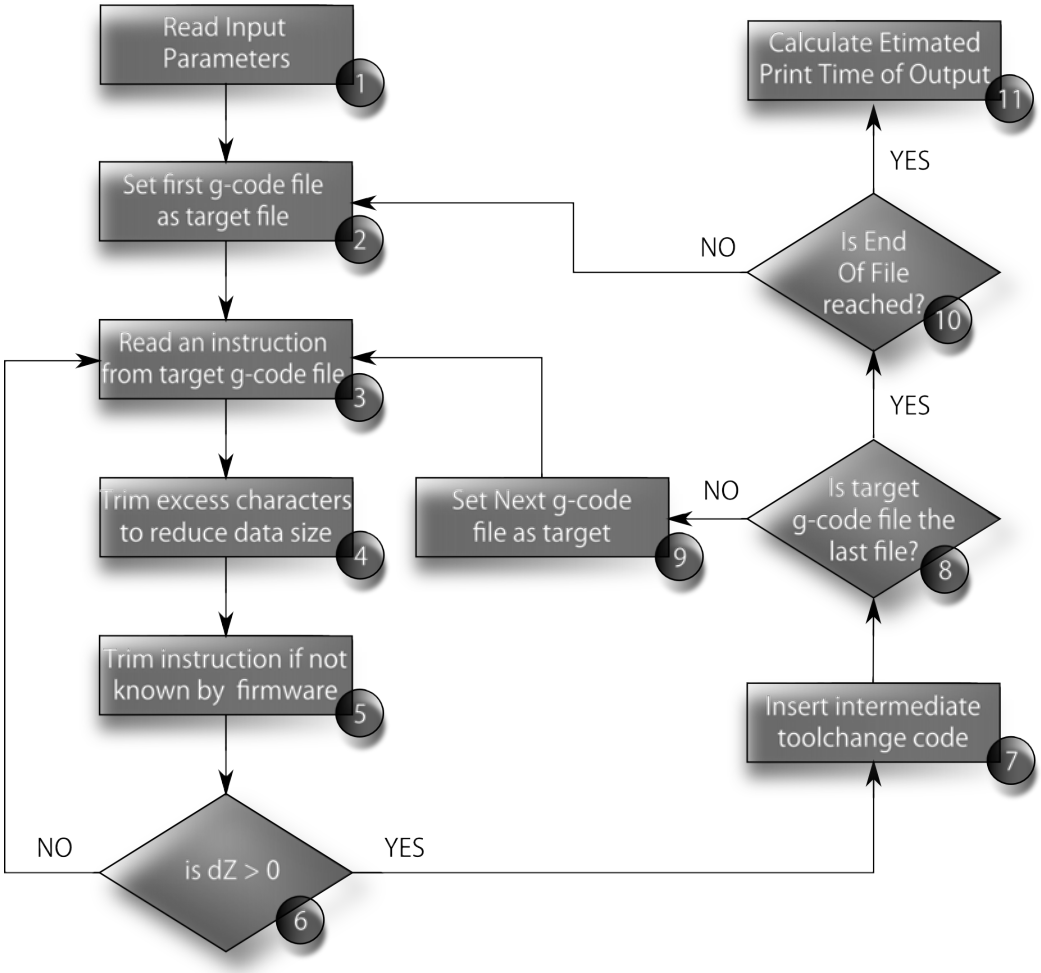

Figure 6.28: *Operational Flow Chart describing the G-code post processor*

The reason that redundant data is sought to be reduced, is because this communication overhead result in a bottle-neck effect. As job-files are generated from 3D structures in the STL format, the de-facto standard used within the field of Additive Manufacturing as described in section 2.2.3 on page 36, the structures are comprised of a triangular mesh. Boundary tool-chains of a build-job are therefore a linear interpolation of the true geometry. It is an interpolation directly linked to the facets that intersect the cut-plane of the layers that the build job is generated from. The higher the facet count, the finer a linear interpolation of curved

geometries. If high surface-detail is to be obtained, and hereby a fine linear interpolation is wanted, a curved boundary is built from a high instruction exchange between host and controller software. This can result in communication to be the significant factor limiting the feederate thus the manufacturing rate.

Short burst of communication data between host and controller is handled within an instruction ring-buffer in the firmware of the controller unit, If a longer burst in communication between host and controller occur, this buffer however can be incidentally emptied or even remain empty if a source STL is highly faceted, and the entire boundary curved. The maximum theoretical allowed communication rate to the controller unit is 460.800 bits/s. However this rate is in practical application limited as most host computers cannot handle serial communication rates above 115.200 bits/s. The most efficient way to decrease communication bandwidth will be to reimplement the communication protocol between the host computer and the controller electronics. At current, this communication is making use of a high-level character based protocol. If a binary protocol was used, this would drastically limit the bandwidth. However this will come at the cost of making it increasingly difficult for the operator to communicate directly with the controller electronics. As such, being an experimental platform, it will dramatically decrease the flexibility of the platform in an a highly experimental environment. Excessive bandwidth losses can however still be limited while maintaining the character based protocol, at fixed bandwidth. The job-generator output a gcode file that is parsed line-by-line to the controller electronics. The generated job file will contain unnecessary information the will result in bandwidth overhead. The cartesian coordinates in the X Y Z and E direction is specified with submicron precision. This is excessive related to the comparably low accuracy of the hardware platform. Furthermore, all four cartesian coordinates are written to the job file irrespectively as to whether the coordinate has changed or not. Hence evenso if movement in just one axis is needed, all four coordinates are written with submicron precision. The G-code post processor scrub the excessive decimals off all four axis and trim away the coodrinates that are not updated. Additional irrelevant information within the job file is scrubbed. This is comments after G-code lines given by the syntax: *command ; comment*. As given from table 6.1 on the facing page the average bandwidth decrease over 112.7 megabytes worth of randomly selected build jobs (10 jobs) has been found to be 20.62%. The third and last purpose of the G code post processor is to implement some safety-means. The feedrate specified to the machine axis are reduced in the output of the G code post processor in case the feedrate is exceeding the machines hardware capabilities. Unknown G code commands that are not implemented in the controller electronics yet generated by the job generator is also scrubbed away, marginally decreasing the filesize of the output file.

Table 6.1: *Depreciated and Weighted G-Code Compression Ratio*

Filename	Original Size (MB)	Scrubbed Size (MB)	Reduction (MB)	Compression Ratio [%]
Yog-Soggoth	5.82	4.65	1.17	79.90
wireholder	0.40	0.28	0.12	70.00
vintagev1	2.24	1.75	0.49	78.13
star_ring_24mm	0.38	0.27	0.11	71.05
standoffs	0.76	0.59	0.17	77.63
pot	11.64	8.54	3.10	73.37
sculpture	51.52	41.47	10.05	80.49
owl_fixed	29.52	23.59	5.93	79.91
lion_solid	10.40	8.32	2.08	80.00

		Depreciated Compression Ratio:	76.70%
Datasize:	112.7 MB	Depreciated Data Compression:	23.30%
		Weighted Compression Ratio:	79,38%
		Weighted Data Reduction	20,62%

6.2.5 Testing

Testing of the second revision of the Open Multi Material Platform has been focused on verification of the ability to handle curved geometries with high polygon-count at high feed-rates. This to incur affirmation to the efforts that has been put into optimizing the ability of the platform to execute instructions at improved rates. Testing of the non-thermal extrusion unit will be carried out, and results from extrusion tests will be shown and elaborated upon.

Table 6.2: *Test geometry 1 - Geometry and Instructions*

Parameter	Value	
Vertices	10842	
Facets	216888	
Height	52.25	mm
Length	29.79	mm
Width	26.86	mm
Feedrate	60	mm/s
Average Boundary Toolpath	0.17	mm
Average Toolpath Execution	352.9	paths/s
Average Command Length	192	bits
Average Bitrate	67764.7	bit/s

High speed extrusion

Two curved geometries has been chosen to illustrate the capabilities of high-speed extrusion. The first geometry is a figurine. It is comprised by 10842 vertices forming 216888 facets. The geometry was built a a federate of 60 mm/s which correlates to an average communication bitrate of the post-processed job-file is 67764.7 bits/s while extruding boundaries. Additional details are available in table 6.2.

Though the average communication bitrate is below the communication rate between host and controller unit @ 115.200 bits/s, consecutive tool-path form tool-chains where the communication rate will be above the capabilities of the system. Here the serial ring-buffer within the firmware guarantee that communication lag will not stall the traveling of the extrusion unit, thus leave the built structure unaffected. The resulting geometry from the build job can be seen in figure 6.29 on page 214

The second test geometry is an organically shaped vase that has been rendered porous by applying a mathematical Voronoi decomposition of the surface to decompose this. The structure is rendered at a height of height of 147mm, counting 37497 vertices forming 75374 facets, and was built at 60 mm/s. The average communication bitrate was 89142.9 bits/s. Additional details are available in table 6.3 on the next page.

Table 6.3: *Test geometry 2 - Geometry and Instructions*

Parameter	Value	
Vertices	37497	
Facets	75374	
Height	147.46	mm
Length	64.88	mm
Width	64.88	mm
Feedrate	60	mm/s
Average Boundary Toolpath	0.14	mm
Average Toolpath Execution	428.6	paths/s
Average Command Length	208	bits
Average Bitrate	89142.9	bit/s

Figure 6.29: *Test geometry 1*

Figure 6.30: *Test geometry 2*

As with the first test geometry, spite the average communication bitrate is below the nitrate limit of 115.200 bits/s, consecutive tool-path form tool-chains where the communication rate will be above the capabilities of the system. As with the first structure, the surface finish of the structure is relying on that the extrusion unit continuously travel at a constant speed over the boundary, thus it is the serial ring-buffer within the firmware must guarantee that communication lag will not stall the extrusion unit. The resulting geometry from the build job can be seen in figure 6.30.

Non-thermal extrusion

Testing of non-thermal extrusion from the universal extrusion nozzle was tested. This was done using polymer-clay as feed material. Polymer clay is malleable, easy to is extrude, and does not alter shape after extrusion. The material was found to be suitable for extruding structures from the syringe, and a demonstration cube was built. This is shown in figure 6.31. The topic of non-thermal and multi material extrusion will be further elaborated in the proceeding chapter.

Figure 6.31: *Test of paste extrusion*

6.3 Conclusion and Discussion on the platform development

An Open and fully customizable FDM based multi material platform was sought to be conceived. The platform was sought to be conceived in a manner so that paramount solicit was on flexibility and on the ability to tinker and alter the platform to conform to a multitude of experiments involving multi-material extrusion. It was the aim that this platform in a efficient manner should it could rise to what challenges may emerge during research within this field. The result of these effort can be seen in figure 6.32. A platform not only capable of extruding a variety of thermo polymers and non-thermal substances, but also a platform that can reproduce and evolve in symbiosis with the operator. It is exactly this ability that was exploit throughout this research project. A first generation platform was built from parts made with a commercial FDM platform. The second generation was

bred by its own predecessor, and emerged as an evolved platform accommodating a multi material extrusion system.

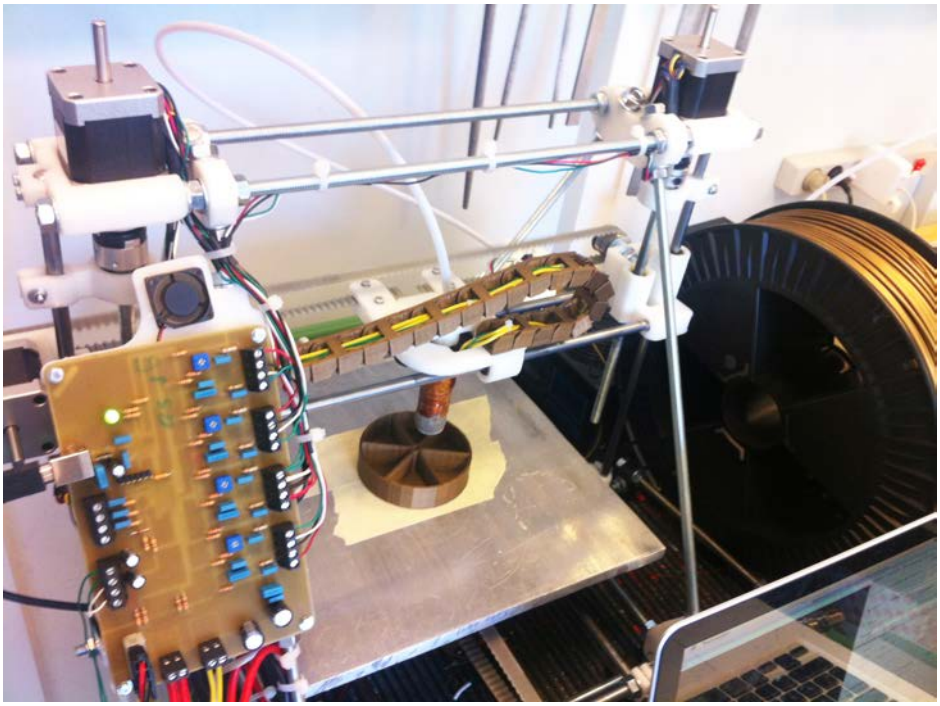

Figure 6.32: *The Open FDM platform under operation*

From a philosophical point of view it indicate that a Darwinian sentiment as addressed in chapter 5.2.8 can be applied to technological evolution, and that the emerge of a true Von Neumann replicator, the self-replicating automaton discussed in section 5 is nearing. There is something bordering to the burlesque if the obsolete term rapid prototyping is used to describe the workflow of the FDM platform development. It could be said that a rapid prototyping machine rapidly made prototype parts to a rapid prototyping machine, that rapidly made prototype parts for a rapid prototyping machine. Truly an indicator of the self-catalyzing nature of reproductive technology.

Left are we with a platform that invite for experiments, that is easily operated, easily customizable, easily repaired and that fuel the desire to push the technology even further. This is exactly what is the aim for the proceeding chapter, where the possibilities within the realm of multi-material manufacturing will be explored.

·⁚Systems Designed for Additive Multi Material Manufacturing. Autonomously manufacture advanced thermo- and electromechanical systems.⁚·

7

Systems for Additive Multi Material Manufacturing

The stimulants for the development of multi-material platforms within additive manufacturing are numerous and have been addressed in section 5.1 on page 146. To empathize why, and how versatile the prospect of multi-material platforms is, a set of subsystems that can be realized by multi-material manufacturing using FDM extrusion has been conceived. Bewilderment caused by being offered the opportunity to operate a multi-material platform is of prevalent contingency. To avoid this, channeling research towards constructivism, an analog of multi-material systems to what is known as traditional standard-elements in mechanical construction has been made. In traditional manufacturing engineering, there are certain mechanical components within the manufacture of a product, that at best will be cumbersome and deficient to attempt to manufacture. These are standard-elements. Ball bearings, nuts, screws, washers, guide-rails and their like. In electronics development an analogy is the components that constitute a circuit. As such, in design of an electronic device, the true development value outside the microchip is that of the circuitry and the layout of the printed circuit board. Not the production of transistors, resistors and capacitors.

It is by the author believed that an effective strategy to conduit acceptance and interest to additive multi material manufacturing technologies, is an evolution of multi material platforms reinforced by the emerge of a variety of complex subsystems constituted by multiple materials, that can be manufactured with the available platform. It is by the author hypothesized that these complex subsystems will play the same role as standard-elements within traditional manufacturing. If these complex subsystems constituted of multiple materials are cataloged in a systems-library that in the coming can be accessed directly within the CAD environment by the designer, then manufactured by the purchase of the processing materials dictated by the specific system, such multi-material subsystems will be the standard elements of the future. To convey the hypothesis of multi-material subsystems as the standard-elements of tomorrow, the gathering of initial content for a systems-library has been manifested as a series of additive manufacturable

sub-systems, described in the following.

7.1 Additive Manufacturing of Battery Cells

Today, batteries by large come in a cylindrical shape of various diameters. Rechargeable batteries of this kind is used in many appliances because they are mass-produced, and readily available as a construction element for the manufacturer. However given their geometrical shape, they do not utilize the allocatable space within many product in an optimum manner. Aside from electrical torches, few products exhibit a shape that advocate the usage of cylindrical battery cells. If however, a battery was regarded as an advance composite material. -A composite comprised of a hard shell, and a core of layered electrochemical pastes that constitute a battery cell- and this ⌜*composite*⌟ was available within the developers CAD library as a material property that could be assigned to any given shape, modeled to occupy any hull within the product, utilization of available blank-space would allow for designing a product with extended battery capacity and hence better service intervals between charges.

Efforts has been put into realizing just this. A battery cell that is additively manufacturable has been realized. A disposable cell-type has been chosen as a base to illustrate the principle, this due to toxicity concerns of common rechargeable cell-types. With an Open FDM extrusion system ready, capable of multi-material job generation and execution by a dual extrusion system comprised of a thermal and a universal non-thermal extrusion unit, a battery cell was modeled in CAD with a shell to be extruded in thermo-polymer and a core constituted by pastes engineered to be extrudable by means of a syringe. The cell, chosen from its wide application as a disposable cell, and its low toxicity is a zinc-carbon cell. A zinc-carbon cell industrially manufactured for general application has the schematic constituents as shown in figure [119, c.8.4.1].

The cell use the zinc casing of the battery as an anode. Manganese Oxide cathode, and Ammonium Chloride as electrolyte. The carbon electrode is used as it is permeable to gasses that otherwise will accumulate within the battery case. As the battery cell discharge, the zinc is oxidized while the manganese oxide is reduced. The overall redox reaction is $Zn + 2MnO_2 \Longrightarrow ZnO \cdot Mn_2O_3$. [119, c.8.2], with an electromotive force of ϵ^0_{cell} = 1.89v. From this, the molar relationship between the chemical constituents can be found, and thus the weight-relation. This is as follows from table 7.1 on the next page.

Second to decide the cell type and deriving the mass relation of the reactants of the cell is to structure an additive manufacturing job that can build the cell. As Carbon is not needed as electrode-material in an experimental cell, deposition of this has not been addressed. MnO_2 as well as NH_4CL is deposited as pastes. The case of the battery is built in thermo-polymer. Deposition of the last reactant, Zinc, was addressed. A suspension of powdered zinc in a gelatin based carrier media

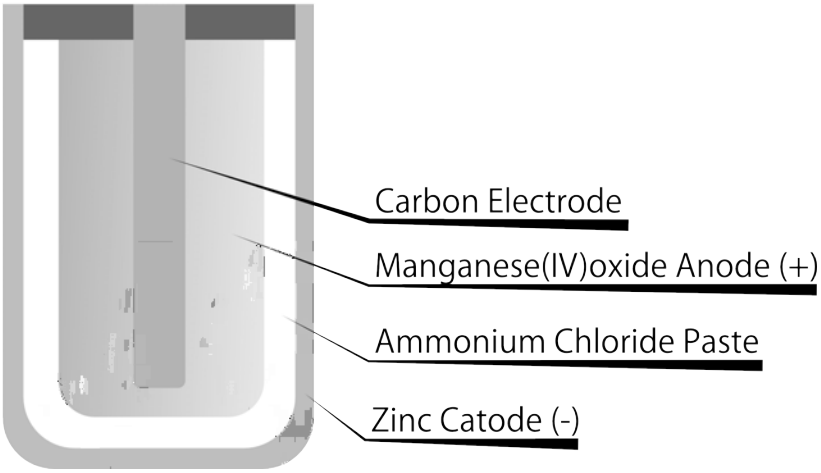

Figure 7.1: *A schematic representation of a Zinc-Carbon cell*

Table 7.1: *Relationship Between Constituents in a ZnC battery cell*

Constituent	Mass
Zn	1.0 g
MnO_2	2.7 g
NH_4CL	1.6 g

proved a reliable method for deposition.

Execution of the build-job can be seen in figure 7.2 on the following page. Here, partially extruded, is a battery cell with an ABS polymer case. In the core of the cell is seen a fill layer of manganese oxide paste. The thermal extruder is about to reposition the extrusion nozzle over the case wall, to seal off the top of the battery. In order to provide a demonstrator, two additively manufactured cells was connected in series as seen in figure 7.3 on the next page was used to drive a light emitting diode.

Several tests of the battery capacity of the additively manufactured battery cells was undertaken, however data was inconclusive and must be backed by a detailed study.

Figure 7.2: *Additive Manufacturing of a battery cell: Showing a partial built, with a partially extruded thermo-polymer based case, and a fill of manganese oxide paste.*

Figure 7.3: *Testing battery cells: Two batteries in series powering a light emitting diode.*

7.2 Additive Manufacturing of Conductors and Resistors

An additive manufacturable battery serve little functional value in an additive manufacturing job, unless the energy of the battery can be harnessed by integrated to other subsystems. Thus, additive manufacturing of conductors to convey electrical current from the battery to the expending subsystem. Electrical conductivity is generally high within metals with silver, copper, gold and aluminum (in order) as the best known conductors. However with melting points from 1064 to 660 C°these metals as pure processing materials are not suitable for additive manufacturing within a multi-material FDM extrusion platform. As such another deposition method of deposition than by melting must be taken. A proposition is to achieve deposition by means of a composite extrusion of fine particles of conductive material in a carrier as a paste. Such pastes are already employed in the industry as conducting adhesives for antistatic protection of circuits to device cases, and as conductive inks for repairing and prototyping of printed circuit boards, and general application for forming conductive circuits.[120] These adhesives and inks are often silver-based and hence expensive to manufacture.

Research has been channeled towards engineering a paste that can be extruded through a syringe, that does not alter shape while setting to a solid, and that is a cheaper alternative to silver based conductive pastes and inks. Copper has been investigated as an alternative. Whereas both copper and silver are comparably good electrical conductors there is a clear reason as to why silver has been preferred over copper for the formulation of conductive inks. Copper is prone to oxidation. Copper as a fine particle powder will passivate from oxidation and as such, powdered copper was from initial experiments proven not conduct electricity. However as the aim is to engineer a paste that set to a solid conductor, the passivated powder of oxidized copper may however still be applicable and prove a tangible candidate for additive manufacturing of conductors, if ingenuity is lent to the engineering of a copper powder based composite. A study was undertaken in order to investigate if a de-oxidation of copper powder could be achieved while the particle was suspended in a carrier to form a paste. The initial idea came from the knowledge that many silicone based sealants cure by release of small quantities of acetic acid. [121] Furthermore these sealants are skin-curing, curing from the skin to the core. [121] The hypothesis is that a strand of silicone rubber with suspended copper particles is deposited to form a track.

The copper particles are oxidized and not conductive. As the strand start to cure, acetic acid is released, and will deoxidize the copper particles, while a non permeable skin is formed preventing re-oxidation. Tests has been conducted using silicon rubber, and polyvinyl acetate as carrier media. Composites of pure copper powder with a average grain size of 20 micrometers, not exceeding 40 micrometers, was suspended in the two carrier media at different concentration levels. As

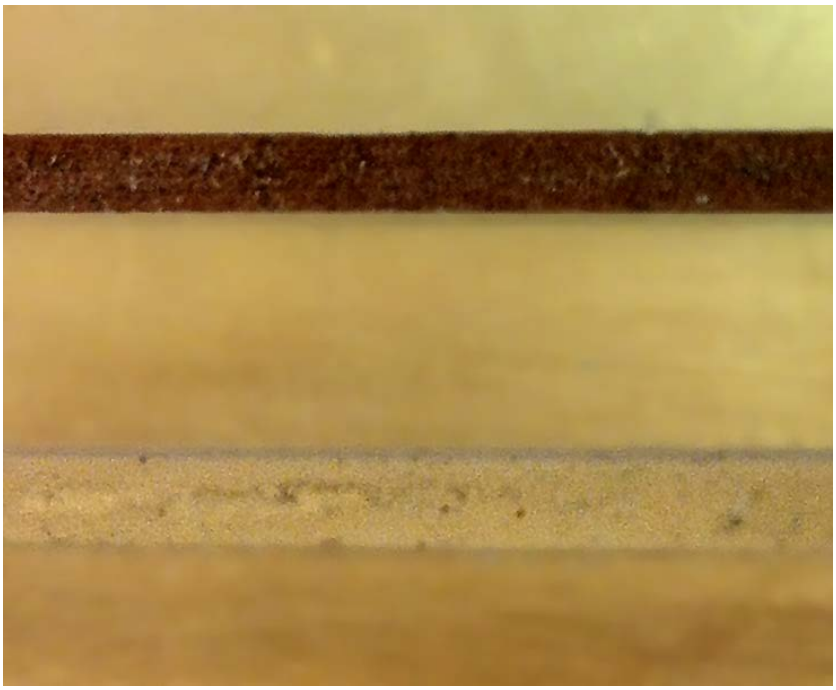

Figure 7.4: *An empty and a spackled groove. Ensuring controlled and repeatable groove cross-sections*

conductivity is governed by the strand-diameter, experiments was designed to ensure repeatable conditions. In order to deposit a well-defined strand of composite material, 2 x 2 x 200 mm grooves was milled in a polycarbonate plate, and the composite was spackled into the grooves, the procedure illustrated in figure. 7.4 Each composite was spackled into 5 grooves, and the conductivity was analyzed over time. A reference track was filled with Field's Metal. Field's Metal is a low-temperature alloy with a melting point of a mere 62 C°degrees comprised of 32% bismuth, 51% indium and 16.5% tin, is of interest due to its low melting point. As such Field's Metal can be extruded by the non-thermal syringe-based deposition unit, detailed in section 6.2.2 on page 205, by melting of the metal before entrapping it within the syringe.

Figure 7.5 on the facing page, display the resistivity of the stands of composite conductors over time. The two graphs display the mean resistivity of five samples of either composite, at 75% copper content. At the point of deposition, where particles are oxidized, the resistivity is in the $M\Omega$ range. Within hours, the resistivity drops to the Ω range, and stabilize. After 2 weeks, the polyvinyl acetate composite start to exhibit an increase in resistivity, followed by the silicone rubber composite after 4 weeks. The mechanism for this is believed to be an oxidation of the copper particles, as a color change observed concurrently with the increase in resistivity.

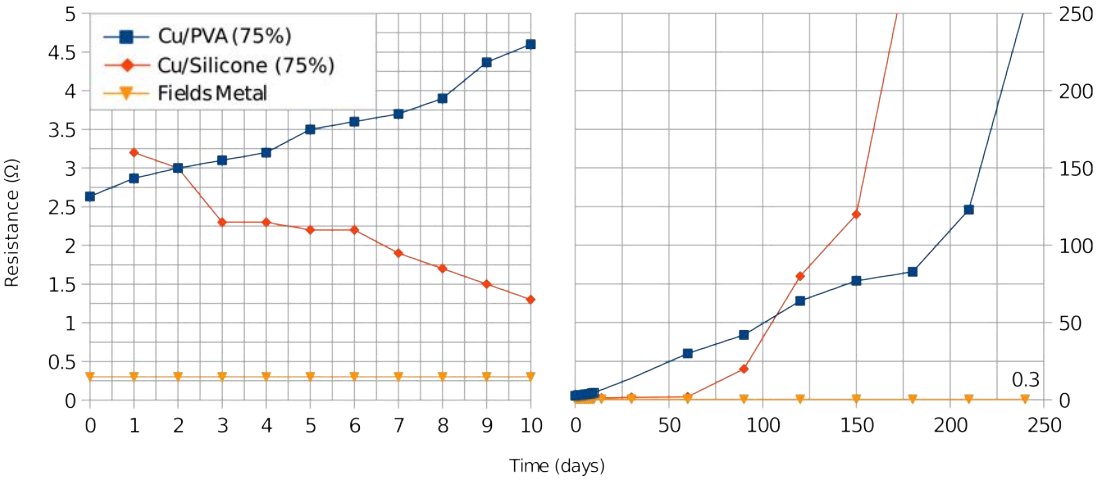

Figure 7.5: *The resistance over time of copper based additive manufacturable conductors of a 2 mm^2 cross section, measuring 200 mm.*

In parallel to the investigation of the engineering of composites for additive manufacturing of conductive tracks, a study of the feasibility of applying the same principe to additively manufacture electrical resistors was undertaken. This by suspending carbon nano particles in polyvinyl acetate. Unlike with the copper based conductors, concerns related to oxidation was not present, and as such, long term stability was expected to be excellent. Figure 7.6 on the next page show the relation between resistance and time. As with the copper composites, an initial drop in resistivity is seen. Unlike the copper composites, however, an initial measurable resistance outside the $M\Omega$ range conceivable. The drop in resistivity is thought to be linked to a contraction of the composite material. A possible explanation is that as matrix material contract under the curing process, more filler grains will get in contact with neighboring grains, forming conductive paths through the composite. Irrespect to the mechanism involved, the resistance of the carbon composite stabilize within one week, and has remained stable in 200 days, up till the day of writing. As indicated by the graph, it is possible to have the resistive paths to stabilize at a broad spectrum of resistance as a function of carbon content. A the length of the resistive path likewise alter the resistance of a resistive strand, it is possibly to span over most common ranges of electrical resistors by change of composition and path length. As such, future additively manufactured circuits can by employing carbon composites have electrical resistors integrated into circuitry simply by forming carbon composite paths.

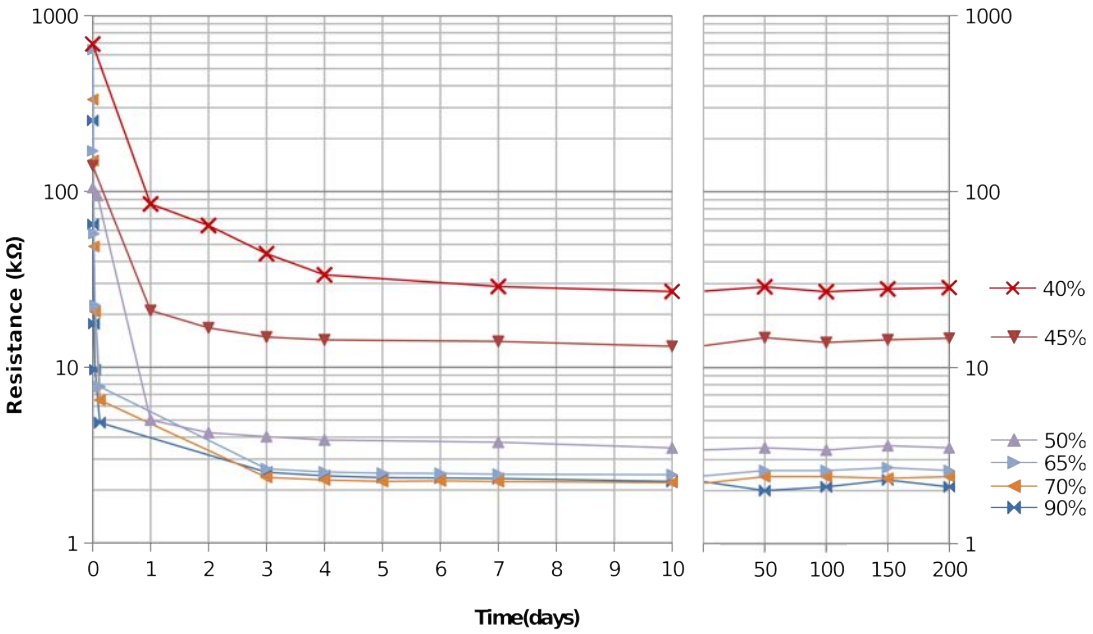

Figure 7.6: *The resistance over time of carbon based additive manufacturable resistors of a 2 mm^2 cross section, measuring 200 mm.*

7.3 Additive Manufacturing of Linear Actuators

Additively manufacturable of actuators has previously been demonstrated by Malone et al.[90] These actuators was based upon electro-active polymers, and while providing fast response times, actuation force is low. A novel proposal is to additively manufacture linear actuation systems by means of phase change materials.

7.3.1 Phase Change Materials

A phase-change material (PCM) is a material that exhibit the least one beneficial behavior during phase change. Examples be PCM with high heat of fusion. Such a material will absorb and release large amounts of energy while undergoing liquid-solid and solid-liquid phase transformation. These materials see application in latent heat storage devices. Here the function of the PCM is to store energy as thermal energy, that can be released ad hog. Research is outspoken in the renewable energy filed using PCMs to store excess energy from sustainable energy sources, such as solar or wind energy. [122] [123] [124]

Energy storage within a PCM, from high heat of fusion is often incident with a large expansion of the material. Methods developed to shape-stabilize PCMs exist, as in many applications the expansion is inexpedient as it set demands to the vessel containing the PCM when it is used as an excess energy storage buffer.[123] [125]

Table 7.2: *Classification of PCMs, and examples of types*

Class	Types
Organic	Parrafins, Fatty Acids
Inorganic	Salt Hydrates, Metallics
Eutectic	Organic-organic, Inorganic-inorganic, Inorganic-organic

Data source: [124][127][128]

[126] However, if the aim not is to store energy within the PCM but harness that the material expand during phase chage, the large expansion can provide sufficient force for motion.

PCM are classified into three basic types, listed in table 7.2. These are organic, inorganic and eutectic. All three types has been investigated as a suitable PCM for harnessing expansion as an actuation force. From this investigation, organic PCM's has excelled as the most promising material. This class exhibit several creditable properties, most prominent their environment friendliness and high phase change expansion.

7.3.2 Characterization of Paraffin Wax as a PCM

The PCM that has garnered most interest for actuation purposes are paraffin wax. Paraffin wax exhibit an precipitant expansion of up to 20% at phase change from solid to liquid. [129] Harnessed in a cylinder, the proposal is to use this thermal expansion to drive linear piston-based actuators similar to hydraulic actuators. By initial system-heating to near-liquid temperatures, and subsequent temperature cycling, expansion and contraction can be controlled. The thermal expansion curve for an expanding paraffin PCM and a material not exhibiting particular behavior at phase change is illustrated by principal graph in figure 7.7 on the next page [129]

The phase change expansion of paraffins are linked to their chemistry. They are straight linked n-alkanes with the generic formula $C_{2n}H_{2n+2}$. Paraffin waxes consist of a mixture of paraffins with varying lengths, normally within the region of of $20 < n < 40$. Chemically paraffin waxes are known to be inert, and their high expansion of up to 20% is, due to a high degree of crystallinity in the solid phase.The crystallinity of paraffin waxes is a result of constituent carbon chains can be packed much closer as a solid than in their disordered formation within the liquid phase. [129] Furthermore, in the liquid phase, dependent on the average length of the paraffin molecules in the range of 60-70C°degrees, paraffin waxes exhibit a low compressibility, which by application as an actuator is relevant as that the volumetric expansion is preserved, even at large loads.[129] The melting temperature of paraffin wax allow for melting, and subsequent deposition by the

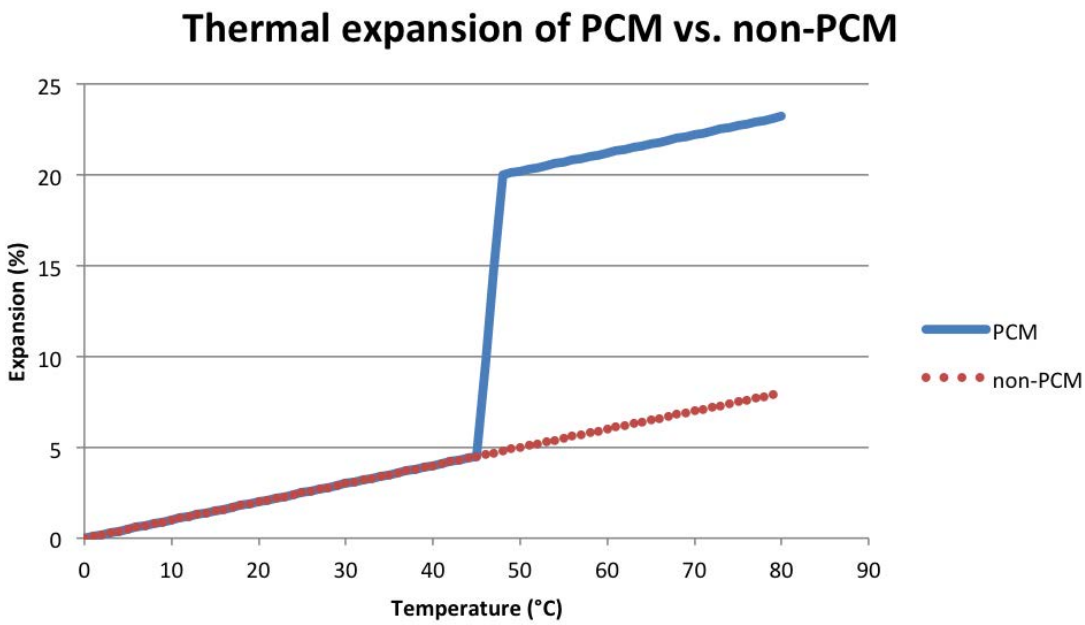

Figure 7.7: *Simplified theoretical thermal expansion of a paraffin base PCM and a material that does not exhibit particular behavior at phase change.*

non-thermal deposition unit of the FDM platform in a liquid form, after which the paraffin following ejection from the syringe will solidify.

7.3.3 Paraffin Actuators

As a part of the analysis of the applicability of additively manufacture paraffin based actuators, an investigation of the performance of paraffin wax employed for PCM actuation was conducted. A test-rig was built to log the work of a wax-driven ram by the expansion of paraffin wax during phase change. The rig, seen in figure 7.8 can accommodate a steel cylinder and let the expanding material drive a piston. The expansion is measured by means of a dial gauge. The force can be calculated from the expansion according to Hookes Law, and springs can be interchanged.The spring and dial gauge is placed on the axis of the expansion.

It was found that the expansion of wax vastly exceed the structural strength of thermo-polymer structures of reasonable dimensions for the manufacture of actuation systems, as described in section 2.4.1 Let alone that extruded structures by FDM manufacturing have a lower structural strength to their injection molded counterparts as described in table 2.1.

As such, no further effort was put into quantify the maximum work that paraffin wax can provide for PCM applications. The behavior of paraffin as a PCM was validated by constant heating of samples in the test rig and as shown in graph 7.9 was characterized. A phase change expansion was noticed up till 11% expan-

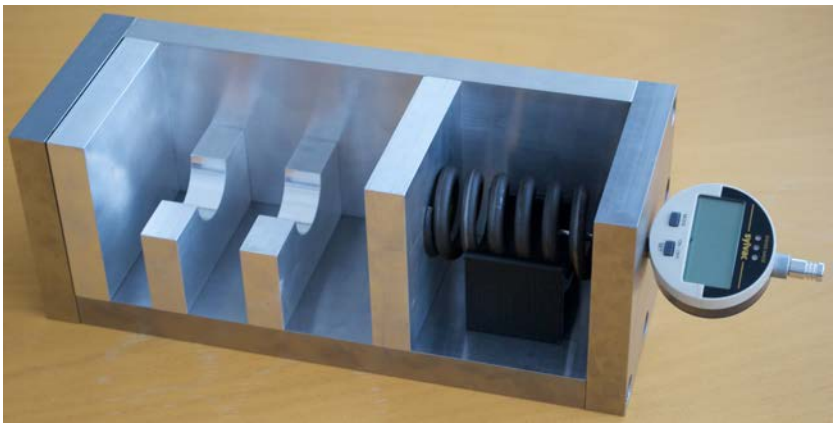

Figure 7.8: *Test-rig for logging the work of a wax-driven ram by the expansion of paraffin wax during phase change.*

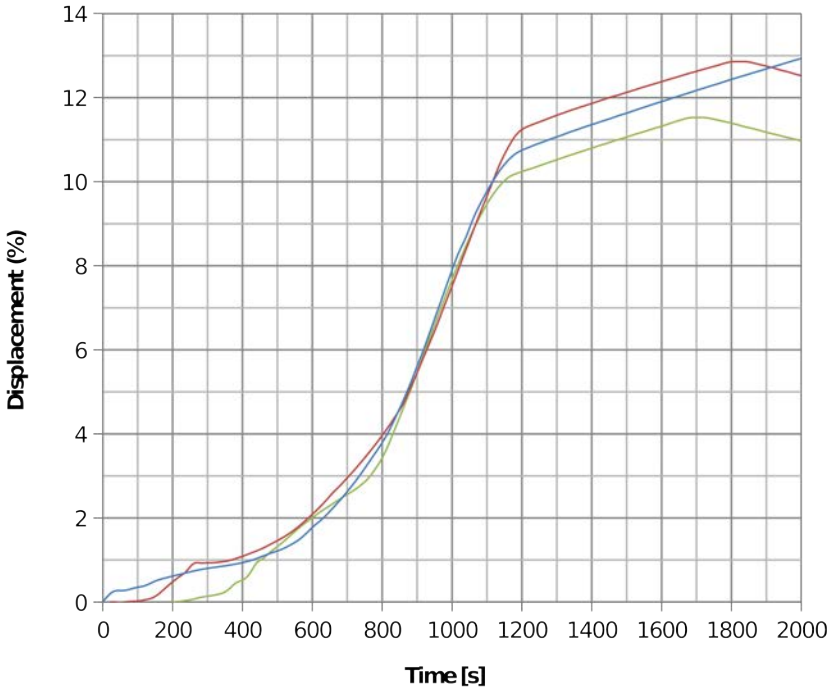

Figure 7.9: *The expansion of paraffin during constant heating.*

sion after which expansion followed a linear growth. Further characterization of paraffin waxes, is but necessary to characterize how paraffin can be utilized for actuation purposes to best extend. Focus was lend to the deposition method by which paraffin was structures can be realized. It was sought to derive a deposition method more advanced but mere deposition of paraffin wax at liquid state into a cavity of an actuator. To construct structures out of paraffin wax by means of

extrusion by controlling melting and solidification.

7.3.4 Paraffin Deposition

As stated in section 7.3.2, paraffin waxes consist of a mixture of paraffins with varying lengths, normally within the region of $20 < n < 40$ Depending on the variance, the paraffin wax will have a melting range from solid through liquid, during which the paraffin wax will change material properties. These following a pattern from Solid $\Longrightarrow$ *Plastic* $\Longrightarrow$ *Semiplastic* $\Longrightarrow$ *Semiliquid* $\Longrightarrow$ *Liquid.* [130, vol. 39 p. 111]

Figure 7.10: *The extrusion of layered structure in paraffin wax. Thermal heating elements are employed to control the palsticity of the wax.*

This allow for a wide array of different deposition schemes. An investigation of these has led to the submission of an article by the author to the Rapid Prototyping Journal from Emerald Group Publishing, that address these different schemes.[131] At liquid state, wax has a viscosity that allow for deposition as an ink. A pen-like deposition method was tested and proven promising. At a semiliquid state, gravity-fed extrusion was tested and proven possible. At semiplastic state, pneumatic controlled extrusion was tested. Initial experiments proved this deposition scheme hard to control. Finally, at plastic state, extrusion by the universal ram extruder

was successful, and shown in figure 7.10 Further investigation into the extrusion of waxes is needed to fully comprehend the mechanisms behind this, and to fully exploit what possibilities the wax offer from its state-based melting behavior.

7.4 Conclusion and Discussion on multi material systems

Multi material manufacturing within the field of additive manufacturing open up for a very creative and different way of thinking product development, manufacturing, and corporate infrastructure. Adressed in section 5.1.3 was how the consumption market of today is governed by mass production in the form of series production. This, however efficient, is a production model that does not accommodate the needs and wishes of the individual customer. Multi-material additive manufacturing may be a step towards a mass production without production of series. With the prospect of decentralized manufacturing of consumer goods, a new era of trade will have a chance to emerge. A Digital trading and manufacturing scenario where products can be traded as virtual products similar to how digital media is traded today. This forecast is but little worth if research in additive manufacturing of multi material systems is not promoted as a relevant field of research. It is in this chapter pledged that bewilderment caused the opportunities that multi material manufacturing may offer is tethered and that research is being channeled towards a constructive cooperative model where additively manufacturable functional subsystems comprised of several materials are catalogued and devout to form a base for a standard-systems library. This systems library could over time grow to an extend where it is applied in the same manner as traditional engineering elements such as ball bearings, nuts, screws, washers, guide-rails, wires, batteries, electrical components and their like are used today. Three possible candidates for such sub-systems has been suggested. An additively manufacturable battery that was realized and proven functional. Conductive and resistive composite materials by which conductors and resistors can be additively manufactured. Finally is suggested a method for additive manufacturable linear actuators by means of phase change materials. These three systems is just a small scratch in the surface of the big domain of possible systems that can be envisioned to be realized using multi material additive manufacturing, and what legacy will be handed over from early research in the field multi material additive manufacturing is yet to be known.

·:*A conclusive twofold summary of what has been achieved, and what is expected from the future of additive manufacturing technologies.*:·

8 Dissertation Summary

A twofold study, highly interdisciplinary in nature and with an abstraction between multi material manufacturing and vision system has been carried out throughout three years of research and within this dissertation documented. As such, there are two distinct areas of focus:

Multi material manufacturing

It is sought to develop a flexible multi material manufacturing platform that will permit fundamental research towards a second generation additive manufacturing system that truly will be a universally applicable manufacturing machine. A desktop sized factory. Not merely the development of such machine is undertaken, also examined is the possibility to additively manufacture complex electromechanical systems, as a step towards being able to autonomously additively manufacture readily functional complex products.

Verification of very complex additively manufactured geometers.

It is a paradox that Additive Manufacturing technologies allow for close-to unrestrained and integral geometrical freedom. Almost any geometry can be manufactured fast, efficiently and cheap. Something that has been missing fundamental capability since the entering of the industrial age. Now, with the geometrical freedom given back to the designer and engineer, a technology stale-mate keep us from benefitting from this freedom. As parts easily can be designed and manufactured beyond the capabilities of all common industrial measurement and verification methods, the designer and engineer is left to design parts that from a geometric metrology point of view possible to verify the tolerances of. A proposal of a method for altering the stale-mate to a check-mate is given. An inline vision system is developed that allow for verification of parts of a complexity that leave the only industrial alternative to the field of CT scanning.

8.0.1 State of development and future expectations

This Ph.D dissertation, ⌜*Additive Manufacturing: Multi Material Processing and Part Quality Control*⌟, deal with Additive Manufacturing technologies which is a common name for a series of processes that are recognized by being computer controlled, highly automated, and manufacture objects by a layered deposition of material. Two areas of particular interest is addressed. They are rooted in two very different areas, yet is intended to fuel the same goal. To help Additive Manufacturing technologies one step closer to becoming the autonomous, digital manufacturing method of tomorrow.

Vision systems

A paradox exist in the field of Additive Manufacturing. The technologies allow for close-to unrestrained and integral geometrical freedom. Almost any geometry can be manufactured fast, efficiently and cheap. Something that has been missing fundamental capability since the entering of the industrial age. Now, with the geometrical freedom given back to the designer and engineer, a technology stale-mate keep us from benefitting from this freedom. Parts can easily be designed and manufactured beyond the capabilities of all common industrial measurement and verification methods, the designer and engineer is left to design parts that from a geometric metrology point of are view possible to verify the tolerances of. A proposal of a method for altering the stale-mate to a check-mate is given. An inline vision system is developed that allow for verification of parts of a complexity that leave the only industrial alternative to the field of CT scanning. The background knowledge to develop such system is synthesized from an analysis of existing additive manufacturing processes and vision systems. The system is implemented and benchmarked throughout the scope of this Ph.D dissertation.

The proposed inline vision system has been put through several tests against several additive manufacturing systems. Till now the system has proven to be up to the task of reconstructing geometries otherwise only possible by CT scanning. The system outcompeted a reference CT scan of a large metal part by to an indisputable degree. The system finally showed promising results when applied indirectly to reconstruct geometries from a DLP system. In general, the system has a potential for being implemented in different AM machines and processes and provides traceable measurements of the complex parts. As the technology of inline layered reconstruction of additively manufactured parts has just been proposed within this thesis, the technology is at a dawning level, and there is an abundance of open questions to be answered and much yet to be investigated. It is impossible but leaving this part of the project open-ended. What is to hope is that future research will tie these ends with the emerge of a fully developed system.

Additive Multi Material Manufacturing

Additive Manufacturing share close family bonds with CNC machine tools. State-of-the-art CNC machine tools of today are multi-axis hybrid machines. A bend of lathes, mills, grinders in one platform. If history repeat itself, hybrid additive manufacturing machines will emerge as the field evolve. It is sought to fuel this, by developing a flexible multi material platform that will permit fundamental research towards a second generation manufacturing system that truly will be a universally applicable manufacturing machine. A desktop sized factory. Not merely the development of such machine is undertaken, also examined is the ability to additively manufacture complex electromechanical systems, as a step towards being able to autonomously additively manufacture readily functional complex products. Based upon a synthesis of the applicability for each industrially accepted additive manufacturing process, the platform deemed most suitable was chosen. The result was an Open and fully customizable FDM based multi material platform. The design solicit flexibility and the ability to alter the platform to conform to a multitude of experiments involving multi-material extrusion. The resultant platform is able to reproduce itself and as such future generations of the platform can efficiently be manifested. Two generations of this platform was realized within the scope of this project.

From a philosophical viewpoint it indicate that a Darwinian sentiment can be applied to technological evolution, and that the emerge of a true Von Neumann replicator, the self-replicating automaton is nearing. There is something bordering to the burlesque if the obsolete term rapid prototyping is used to describe the workflow of the FDM platform development. It could be said that a rapid prototyping machine rapidly made prototype parts to a rapid prototyping machine, that rapidly made prototype parts for a rapid prototyping machine. Truly an indicator of the self-catalyzing nature of reproductive technology. The developed platform invited for experiments from its ease of operation, ease of customization and it fueled the desire to push the multi material technology further.

To empathize why, and how versatile the prospect of multi-material platforms is, a set of subsystems that can be realized by multi-material manufacturing using FDM extrusion has been conceived. A functional battery is built using multi material extrusion. Composites that allow for the additive manufacturing of electrical conductors and resistors are engineered. A proposed method for additive manufacturing of linear actuators is assessed and proved promising. It is proposed that a library of additively manufacturable subsystems are built as a part of a knowledge sharing network. This systems library can over time grow to an extend where it is applied in the same manner as traditional engineering elements such as ball bearings, nuts, screws, washers, guide-rails, wires, batteries, electrical components and their like are used today.

Multi material manufacturing within the field of additive manufacturing open up for a very creative and different way of thinking product development, manufacturing, and corporate infrastructure. Adressed in section 5.1.3 was how the consumption market of today is governed by mass production in the form of series production. This, however efficient, is a production model that does not accommodate the needs and wishes of the individual customer. Multi-material additive manufacturing may be a step towards a mass production without production of series. With the prospect of decentralized manufacturing of consumer goods, a new era of trade will have a chance to emerge. A Digital trading and manufacturing scenario where products can be traded as virtual products similar to how digital media is traded today. This forecast is but little worth if research in additive manufacturing of multi material systems is not promoted as a relevant field of research. It is in this chapter pledged that bewilderment caused the opportunities that multi material manufacturing may offer is tethered and that research is being channeled towards a constructive cooperative model where additively manufacturable functional subsystems comprised of several materials are catalogued and devout to form a base for a standard-systems library. This systems library could over time grow to an extend where it is applied in the same manner as traditional engineering elements such as ball bearings, nuts, screws, washers, guide-rails, wires, batteries, electrical components and their like are used today. Three possible candidates for such sub-systems has been suggested. An additively manufacturable battery that was realized and proven functional. Conductive and resistive composite materials by which conductors and resistors can be additively manufactured. Finally is suggested a method for additive manufacturable linear actuators by means of phase change materials. These three systems is just a small scratch in the surface of the big domain of possible systems that can be envisioned to be realized using multi material additive manufacturing, and what legacy will be handed over from early research in the field multi material additive manufacturing is yet to be known.

Bibliography

[1] Unknown. *Voynich Manuscript*. Beinecke Rare Book and Manuscript Library, Yale University, Early 15th century.

[2] Wohlers Associates. *Wohlers Report 2012 - Additive Manufacturing and 3D Printing State of the Industry Annual Worldwide Progress Report*. Wohlers Associates, 2012.

[3] N C Ferguson. A history of numerically controlled machine tools. *Chartered Machanical Engineer*, September 1978.

[4] G. S. Devere, B. Hargreaves, and D.M. Walker. The dac-1 system. *Datamation*, 12(6):37–47, June 1966.

[5] Rocco Furferi, Lapo Governi, Matteo Palai, and Yary Volpe. From 2d orthographic views to 3d pseudo-wireframe: An automatic procedure. *International Journal of Computer Applications*, 5(6), August 2010.

[6] M. Mäntylä. An introduction to solid modeling. *Computer Science Press, Rockville*, 1988.

[7] Patric Maynard. *Drawing distinctions: the varieties of graphic expression*. Cornell University Press, 2005.

[8] Jim X. Chen. *Guide to Graphics Software Tools*. Springer-Verlag London, 2'nd edition, 2008. ISBN: 978-1-84800-900-4.

[9] Eric Lengyel. *Mathematics for 3D Game Programming and Computer Graphics*. Charles River Media, Hingham, Massachusetts, 2'nd edition, 2004.

[10] Martti Mäntylä, Dana Nau, and Jami Shah. Challenges in feature-based manufacturing research. *Communication Of The ACM*, 39(2):76–84, February 1996.

[11] ASTM International, Subcommittee F42.91. Astm- technical committee f42. *Committee F42 on Additive Manufacturing Technologies*, 2009-2012.

[12] ASTM International, Subcommittee F42.91. Astm f2792 - 12a standard terminology for additive manufacturing technologies,. *ASTM F2792 - 12a*, 2009.

[13] Bill Kennedy. New developments increase rapid prototyping of microscale features. *Micro Manufacturing - Scaled for Micro*, 2(2), June 2009.

[14] C. K. Chua, K. F. Leong, and C. S. Lim. *Rapid Prototyping: Principles and Applications*. World Scientific Publishing Co. Pte. Ltd, 3'rd edition, 2010.

[15] B.J. Gans, P.C. Duineveld, and U.S. Schubert. Inkjet printing of polymers: State of the art and future developments. *Advanced Materials*, 16(3):203–213, February 2004.

[16] Steven Scott Crump. Apparatus and method for creating three-dimensional objects. *US Patent 5121329*, June 1992.

[17] Ed Sells, Zach Smith, Sebastien Bailard, Adrian Bowyer, and Vik Olliver. Reprap: The replicating rapid prototyper maximizing customizability by breeding the means of production. *University of Bath*, April 2010.

[18] Envisiontec GmbH. *3D Bioplotter - Technical Data (4th generation).* Datasheet, March 2011.

[19] Sandia National Laboratories. *Laser Engineered Net Shaping - Manufacturing Technologies.* Sandia Corporation, a Lockheed Martin Company or the United States Department of Energy's National Nuclear Security Administration under contract DE-AC04-94AL85000.

[20] ROBERT P. MUDGE and NICHOLAS R. WALD. Laser engineered net shaping advances additive manufacturing and repair. *Welding Journal*, January 2007.

[21] Objet Ltd. Objet eden, objet.com, September 2012.

[22] Michael Cima, Emanuel Sachs, Tailin Fan, James F. Vredt, Steven P. Michaels, Satbir Khanuja, Alan Lauder, Sang-Joon J. Lee, David Brancazio, Alain Curodeau, and Herald Tuerck. Three-dimensional printing techniques. *US Patent 5387380*, February 1995.

[23] Kenneth Cooper. *Rapid Prototyping Technology: Selection and Application.* CRC Press, 1'st, January 2001.

[24] John Kawola, Scott Harmon, Kevin Lach, Julie Reese, Joe Titlow, and Joe Bortolotti. The wide adoption of color in 3d printing. *Workshop on Rapid Technologies*, September 2009.

[25] Carl R. Deckard. Method and apparatus for produceing parts by selective sintering. *US Patent 4863538*, September 1989.

[26] J.P Kruth, G. Levy, R. Schindel, T. Craeghs, and E. Yasa. Consolidation of polymer powders by selective laser sintering. *Proceedings of the 3rd International Conference on Polymers and Moulds Innovations*, pages 17–19, September 2008.

[27] Terry Wohlers. The world of rapid prototyping. *Published in the Proceedings of the Fourth International Conference On Desktop Manufacturin*, September 1992.

[28] Michael Feygin. Apparatus and method for forming an integral object from laminations. *US Patent 4752352*, 1988.

[29] Charles W. Hull. Apparatus for production of three-dimensional objects by stereolithography. *US Patent 4575330*, March 1986.

[30] Materialize LC. Mammoth stereolithography: Technical specifications. *http://manufacturing.materialise.com/mammoth-stereolithography-technical-specifications*, Last accessed september 2012.

[31] Terry Wohlers. The real cost of rp - what to consider before bringing rp in-house. *Time-Compression Technologies magazine*, March/april 2002.

[32] Patrick Ledda. High dynamic range displays. *Presence: Teleoperators & Virtual Environments - MIT Press*, 16(1):119–122, 2007.

[33] TNO Science and Industry. Datasheet: Improved micro-stereo lithography - faster and more accurate 3d printing. *Document No: Q112007/250*, 2007.

[34] Huntsman Advanced Materials. Araldite digitalis, mass customisation inspired by nature - datasheet. *Huntsman International LCC*, 2008.

[35] RTP Imagineering Plastics. *RTP 2099 X 126211 Z Bio-Based Polylactic Acid (PLA) - datasheet*. RTP Company, 580 East Front Street, Winona, MN 55987, October 2011.

[36] Anders Södergård and Mikael Stolt. Properties of lactic acid based polymers and their correlation with composition. *Progress in Polymer Science*, 27(6):1023–1163, 2002.

[37] Stratasys Inc. White paper: Characterization of material properties, fortus abs-m30. 2011.

[38] Stratasys Inc. White paper: Characterization of material properties, fortus polycarbonate (pc). 2011.

[39] Tim A. Osswald, Erwin Baur, Sigrid Brinkmann, Karl Oberbach, and Ernst Schmachtenberg. *International Plastics Handbook*. Hanser Gardner Publications, 2006.

[40] Andy Extance. White paper: Progess in uv-cured adhesives. *SpecialChem S.A*, September 2009.

[41] M.R Haddon and T.J Smith. The chemistry and applications of uv-cured adhesives. *International Journal of Adhesion and Adhesives*, 11(3):183–186, 1991.

[42] Irem Erel, Ioan Cianga, Ersin Serhatli, and Yusuf Yagci. Synthesis of block copolymers by combination of photoinduced and atom transfer radical polymerization routes. *European Polymer Journal*, 38:1409–1415, 2002.

[43] Jamens V. Crivello. The discovery and development of onium salt cationic photoinitiators. *Journal of Polymer Science: Part A: Polymer Chemistry*, 37:4241–4256, 1999.

[44] W. A Cunningham, R. M. Dunham, and L. L. Antes. Hydration of gypsum plaster. *Industrial and Engineering Chemistry*, 44(10):2402–2408, 1952.

[45] Heiko Hirshmüller, Peter R. Innocent, and Jon Garibaldi. Real-time correlation-based stereo vision with reduced border errors. *International Journal of Computer Vision*, 47:229–246, 2002.

[46] David Bue Pedersen. White paper: Investigation of a method for inline geometrical 3d reconstruction of rapid prototyping parts. *Technical University of Denmark, dept. of Mechanical Engineering.*, 2009.

[47] Andreas Klaus, Mario Sormann, and Konrad Karner. Segment-based stereo matching using belief propagation and a self-adapting dissimilarity measure. *18th International Conference on Pattern Recognition*, 3(15-18), 2006.

[48] Francois Blais. Review of 20 years of range sensor development. *Journal of Electronic Imaging*, 13(1):231–240, January 2004.

[49] J.P. Kruth, M. Bartscher, S. Carmignato, R. Schmitt, L. De Chiffre, and A. Weckenmann. Computed tomography for dimensional metrology. *CIRP Annals - Manufacturing Technology*, 60:821–842, 2011.

[50] Bernd Dammann. White paper: Advanced matlab programming: Computerized tomography. *Technical University of Denmark*, 2010.

[51] Michele Benzi. The early history of matrix iterations: With a focus on the italian contribution. *SIAM Conference on Applied Linear Algebra Monterey Bay – Seaside, California*, October 2009.

[52] The OpenCV developers Team. About OpenCV. *http://opencv.org/about.html*, September 2012.

[53] Computational Vision, California Institute of Technology. Camera Calibration Toolbox for Matlab. *http://vision.caltech.edu/bouguetj/calib_doc*, September 2012.

[54] Janne Heikkilä and Olli Silvén. A four-step camera calibration procedure with implicit image correction. *CVPR'97*, 1997.

[55] C.C. Slama. *Manual of Photogrammetry*. American Society of Photogrammetry, Falls Church, Virginia, 4th edition, 1980.

[56] Irwin Sobel and G Feldman. A 3 x 3 isotropic gradient operator for image processing. *Presented at a talk at the Stanford Artificial Project*, 1968.

[57] James M. Keller, Susan Chen, and Richard M Crownover. Texture description and segmentation through fractal geometry. *Computer Vision, Graphics and Image Processing*, 45:150–166, 1989.

[58] Nobuyuki Otsu. A threshold selection method from gray-level histograms. *IEEE Transactions on Systems, Man, and Cybernetics*, SMC-9(1), January 1979.

[59] C.J. Solomon and T.P. Breckon. *Fundamentals of Digital Image Processing: A Practical Approach with Examples in Matlab*. Wiley-Blackwell, 2010.

[60] A. Marbs and F. Boochs. Investigating the influence of ionizing radiation on standard ccd cameras and a possible impact on photogrammetric measurements. *ISPRS Commission V Symposium Image Engineering and Vision Metrology*, Part 5, September 2006.

[61] GOM - Gesellschaft für Optische Messtechnik mbH. Inspection v7.2 manual - advanced. 2011.

[62] G.T. Herman and H.K Liu. Optimal surface reconstruction from planar contours. *Computer Graphics and Image Processing*, pages 1–121, 1979.

[63] William E. Lorensen and Harvey. E. Cline. Marching cubes: A high resolution 3d surface construction algorithm. *Computer Graphics*, 21(4):163–169, 1987.

[64] http://www.meshlab.org. Meshlab, an open source portable and extensible system for the processing and editing of unstructured 3d triangular meshes. *The Meshlab Project*, 2011.

[65] David Bue Pedersen, Hans N. Hansen, and Jakob Skov Nielsen. Inline monitoring and reverse 3d model reconstruction in additive manufacturing. *The 7th International Workshop on Microfactories, Daejeon, Korea*, October 2010.

[66] H.N Hansen and L. De Chiffre. A combined optical and mechanical reference artefact for coordinate measuring machines. *Annals of the CIRP*, 46(1):467–470, 1997.

[67] Hans N. Hansen, L. De Chiffre, and R. E. Morace. Comparison of coordinate measuring machines using an optomechanical hole plate. *Annals of the CIRP 54/1*, 54(1):479–482, 2005.

[68] Hans N. Hansen and David Bue Pedersen. Absolute 3d geometry reconstruction of complex additive manufactured parts using layered mesh generation. *Proceedings of AEPR'11, 16th European Forum on Rapid Prototyping and Manufacturing*, June 2011.

[69] D. Donatello. Metrological vaidation of 3d scanners. *Thesis, Deptartment of Mechanical Engineering, Technical University of Denmark*, 2010.

[70] Julia F. Barrett and Nicholas Keat. Artifacts in ct: Recognition and avoidance. *Radiographics: The Journal of Continuing Medical Education in Radiology*, September 2004.

[71] Ulrik V. Andersen, David Bue Pedersen, Hans N. Hansen, and Jakob Skov Nielsen. In-process 3d geometry reconstruction of objects produced by direct light projection. *Journal of Manufacturing Technologies*, Submitted: November 2012.

[72] Envisiontec GmbH. Technical data: Perfactory sxga w/erm mini mult lens. May 2008.

[73] Evan Malone. Factories at home: Promoting innovation and the future of personal fabrication. *EuroMold Conference Concentrates on the Factory of the Future*, 2008.

[74] P.L. Travers and R. Stevenson. Mary poppins. Motion Picture, August 1964.

[75] K. Eric Drexler. *Engines of Creation: The Coming Era of Nanotechnology.* Doubleday, 1986.

[76] John Von on Neumann. *Theory of Self-Reproducing Automata.* University of Illinois Press, 1966.

[77] Umberto Pesavento. An implementation of von neumann's self-reproducing machine. *Artificial Life (MIT Press) 2 (4)*, pages 337–354, 1995.

[78] Vicki Glaser. Tissue engineering revenues rise. *Genetic Engineering and Biotechnology News*, 32(13), July 2012.

[79] Peter X. Ma and Jennifer Elisseeff, editors. *Scaffolds in Tissue Engineering.* CRC Press, 1 edition, August 2005.

[80] Shoufeng Yang, Kah-Fai Leong, Zhaohui Du, and Chee-Kai Chua. The design of scaffolds for use in tissue engineering part i. traditional factors. *Tissue Engineering*, 7(6), 2001.

[81] I Zein., D.W. Hutmacher, K. C. Tan, and S.H Teoh. Fused deposition modelling of novel scaffold architectures for tissue engineering applications. *Biomaterials*, 23(4):1169–1185, February 2002.

[82] Jordan S. Miller, Kelly R. Stevens, Michael T. Yang, Brendon M. Baker, Duc-Huy T. Nguyen, Daniel M. Cohen, Esteban Toro, Alice A. Chen, Peter A. Galie, Xiang Yu, Ritika Chaturvedi, Sangeeta N. Bhatia, and Christopher S. Chen. Rapid casting of patterned vascular networks for perfusable engineered three-dimensional tissues. *Nature Materials*, 11:768–774, 2012.

[83] Peter Kareiva et al. Domesticated nature: Shaping landscapes and ecosystems for human welfare. *Science*, 216:1866–1869, June 2007.

[84] International Steel Statistic Bureau. Global overview. *http://www.issb.co.uk/global.html*, September 2012.

[85] David Bue Pedersen. Development of an open rapid prototyping platform. Master's thesis, Technical University of Denmark, June 2009.

[86] Envisiontec GmbH. *NanoCure RC25 Tough, Stiff, High temperature Nanocomposite resin for Perfactory and Vanquish Systems*. Datasheet, 2007.

[87] A.M. Ivanova, S.P. Kotova, N.L. Kupriyanov, A.L. Petrov, E.Yu.Tarasova, and I.V. Shishkovskii. Physical characteristics of selective laser sintering of metal - polymer powder composites. *Quantum Electronics*, 28(5):420–425, 1998.

[88] Chunze Yan, Yusheng Shi, Jingsong Yang, and Jinhui Liu. Preparation and selectivelasersintering of nylon-12 coated metal powders and post processing. *Journal of Materials Processing Technology*, 209(17):5785–5792, August 2009.

[89] Scott J. Hollister. Porous scaffold design for tissue engineering. *Nature Materials*, 4:518–524, 2005.

[90] Evan Malone and Hod Lipson. Solid freeform fabrication for autonomous manufacturing of complete mobile robots. *Robosphere04*, 2004.

[91] S. Masurtschak and R.A.Harris. Enabling techniques for secure fibre positioning in ultrasonic consolidation for the production of smart material structures. *SPIE*, 7981, March 2011.

[92] 3D systems. Rapid prototyping 3d printer, 3d systems, September 2012.

[93] E.C. Kinzel, X. Xu, and W.J Chappell. Selective laser sintering of multilayer, multimaterial circuit components. *Microwave Symposium Digest, 2006. IEEE MTT-S International*, pages 1788–1791, June 2006.

[94] http://www.solido3d.com Solido Ltd. http://www.solido3d.com, september 2012.

[95] Urban Harrison. Method and apparatus for producting free-form products. *US Patent 2008/0220111 A1*, September 2008.

[96] Evan Malone and Hod Lipson. Fab@home: the personal desktop fabricator kit. *Rapid Prototyping Journal*, 13(4):245–255, 2007.

[97] H. Richard. 3-way quick-fit extruder and colour blending nozzle. *http://richrap.com/?p=121*, August 2012.

[98] H. Richard. Universal paste extruder - ceramic, food and real chocolate 3d printing... *http://richrap.blogspot.co.uk/2012/04/universal-paste-extruder-ceramic-food.html*, April 2012.

[99] University of Twente. Pwdr - http://pwdr.github.com/usermanual.html, September 2012.

[100] Kevin Hawkinson. Personal 3D Printer rev.3 Beta - http://tech.groups.yahoo.com/group/diy_3d_printing_and_fabrication, September 2012.

[101] Angela E Douglas. *The Symbiotic Habit*. New Jersey: Princeton University Press, 2010.

[102] Brian Evans. *Practical 3D Printers: The Science and Art of 3D Printing*. Apress, 1'th edition, August 2012.

[103] National Electrical Manufacturers Association. Ansi/nema mg 1-2011: Standards for motors and generators. *The Association of Electrical Equipment and Medical Imaging Manufacturers*, 2011.

[104] The Reprap Project. Prusa mendel assembly, 2005-2012.

[105] Mark Balch. *Complete Digital Design: A Comprehensive Guide to Digital Electronics and Computer System Architecture*. McGraw-Hill Professional, 2003.

[106] Microchip Inc. Pic18f2525/2620/4525/4620 data sheet 28/40/44-pin enhanced flash microcontrollers with 10-bit a/d and nanowatt technology. *Document no. DS39626E*, 2008.

[107] Mark Curtin and Paul O'Brien. Phase-locked loops for high-frequency receivers and transmitters - part 1 to part 3. *Analog Dialogue*, 1999.

[108] Future Technology Devices International Ltd. Ft232r usb uart ic datasheet version 2.10, clearance no.: Ftdi# 38. FT_000053, 2010.

[109] Robert Lacoste. Pid control without math. *Circuit Cellar*, 221, December 2008.

[110] V. V. Athani. *Stepper Motors - Fundamentals, Applications and Design.* New Age International Publishers, 1997, 2005.

[111] Allegro MicroSystems Inc. *A3982 - DMOS Stepper Motor Driver with Translator*, document no. 26184.28c edition, 2005-2008.

[112] Internal Rectifier. Irf1324s-7ppbf hexfet power mosfet. *Document no. PD-97263B*, 2010.

[113] Alessandro Ranellucci. Slic3r - a g-code generator for 3d printers, September 2012.

[114] H. Cotterman K Forsberg, H. Mooz. *Visualizing Project Managemen.* John Wiley and Sons, NY, 3rd edition, 2005.

[115] Image Metrology A/S. Datasheet: Spip - the de-facto standard for nano- and micro scale image processing and 3d visualization. *http://www.imagemet.com*, page September, 2012.

[116] David Bue Pedersen, Hans N. Hansen, and Jakob Rasmussen. A method for doubling vertical resolution in fused deposition modeling. *4M association*, October 2012.

[117] Stratasys Inc. Stratasys, dimension series specification brochure. *http://www.dimensionprinting.com/pdfs/prodspecsfam/DimensionBrochure.pdf*, March 2012.

[118] Allegro MicroSystems Inc. *A4982 - DMOS Microstepping Driver with Translator And Overcurrent Protection*, document no. 4982-ds rev. 4 edition, 2008-2012.

[119] D. Linden and T.B Reddy. *Handbook of Batteries.* Mc-Graw Hill, 3'rd edition, 2002.

[120] J. Perelaer, B. J de Gans, and U. S. Schubert. Ink-jet printing and microwave sintering of conductive silver tracks. *Advanced Materials*, 18(16):2101–2104, 2006.

[121] J. Comyn, J. Day, and S. J. Shaw. Kinetics of moisture cure of silicone sealants. *The Journal of Adhesion*, 66(1-4):289–301, 1998.

[122] Yuichi Hamada, Wataru Ohtsu, and Jun Fukai. Thermal response in thermal energy storage material around heat transfer tubes: Effect of additives on heat transfer rates. *Solar Energy*, 75(4), 2003.

[123] H.Inaba and P.Tu. Evaluaton of thermophysical characteristics on shape-stabalized paraffin as a solid-liquid phase change material. *Heat and Mass Transfer*, 32, 1997.

[124] M. Kenisarin and K. Mahkamov. Solar energy storage using phace change materials. *Renewable and Sustainable Energy Reviews*, 11(9):1912–1965, 2007.

[125] Weilong Wang, Xiaoxi Yang, Yutang Fang, Jing Ding, and Jinyue Yan. Enhanced thermal conductivity and thermal performance of form-stable composite phase change materials by using beta-aluminium nitride. *Applied Energy*, 86(7-8):1196–1200, 2008.

[126] Yinping Zhang, Jianhong Ding, Xin Wang, Rui Yang, and Kumping Lin. Influence of additive on thermal conductivity of shape-stabilized phase change material. *Solar energy materials and solar cells*, 90(11):1692–1702, 2005.

[127] Atul Sharma, V.V Tyagi, C.R. Chen, and D. Buddhi. Review on thermal energy storage with phase change materials and applications. *Renewable and Sustainable Energy Reviews*, 13(2):318–345, 2009.

[128] B Zalba, J.M. Marin, L.F Cabeza, and H. Mehling. Review on thermal energy storage with phase change materials, heat transfer analysis and applications. *Applied Thermal Engineering*, 23(3):251–283, 2003.

[129] Roger Bodén. *Ph.d thesis: Microactuators for Powerful Pumps*. PhD thesis, Acta Universitatis Upsaliensis, Uppsala, 2008.

[130] *Ullmann's Encyclopedia of Industrial Chemistry*, volume 39. Wiley-VCH, John Wiley and Sons, April 2012.

[131] H. N. Hansen, D B Pedersen, and G D'angelo. Towards multi material additive manufacturing in fused deposition modeling. *Rapid Prototyping Journal*, Submitted 2012.